CHEMICAL REVIEWS

pubs.acs.org/CR

Review

Biomaterials for Bioprinting Microvasculature

Ryan W. Barrs,[‖] Jia Jia,[‖] Sophia E. Silver, Michael Yost, and Ying Mei*

Cite This: *Chem. Rev.* 2020, 120, 10887−10949

Read Online

ABSTRACT: Microvasculature functions at the tissue and cell level, regulating local mass exchange of oxygen and nutrient-rich blood. While there has been considerable success in the biofabrication of large- and small-vessel replacements, functional microvasculature has been particularly challenging to engineer due to its size and complexity. Recently, three-dimensional bioprinting has expanded the possibilities of fabricating sophisticated microvascular systems by enabling precise spatiotemporal placement of cells and biomaterials based on computer-aided design. However, there are still significant challenges facing the development of printable biomaterials that promote robust formation and controlled 3D organization of microvascular networks. This review provides a thorough examination and critical evaluation of contemporary biomaterials and their specific roles in bioprinting microvasculature. We first provide an overview of bioprinting methods and techniques that enable the fabrication of microvessels. We then offer an in-depth critical analysis on the use of hydrogel bioinks for printing microvascularized constructs within the framework of current bioprinting modalities. We end with a review of recent applications of bioprinted microvasculature for disease modeling, drug testing, and tissue engineering, and conclude with an outlook on the challenges facing the evolution of biomaterials design for bioprinting microvasculature with physiological complexity.

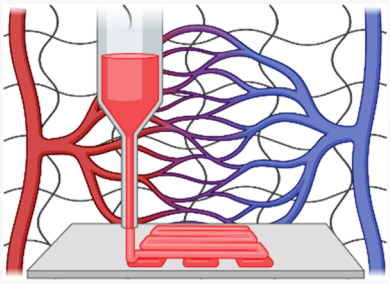

CONTENTS

Special Issue: 3D Printing for Biomaterials

Received: January 13, 2020
Published: September 1, 2020

https://dx.doi.org/10.1021/acs.chemrev.0c00027
Chem. Rev. 2020, 120, 10887−10949

1. INTRODUCTION

The human cardiovascular system consists of a sophisticated hierarchical network of blood and lymphatic vessels that conduct fluids to and from tissues and organs.[1,2] Each level of this hierarchy plays a distinct role in maintaining homeostasis throughout the body. Larger vessels like arteries and veins are responsible for transporting large volumes of blood between organ systems. Following Murray's Law, large blood vessels branch into progressively smaller vessels to control local blood pressure and volumetric flow to the tissues and cells within each organ system.[3,4] Capillaries are the smallest and most densely distributed vessels in the cardiovascular system and have a specialized role in directly exchanging fluid with cells deep within tissues. The exact distribution and orientation of microvasculature is influenced by the metabolic activity of the given tissue.[5] While large and small vessels have specialized roles, they operate in unison to efficiently maintain homeostasis throughout the body.

The anatomy of large vessels differs from that of small vessels.[6] Large vessels (i.e., arteries and veins) have three layers: an inner layer composed of endothelium, a middle layer composed of smooth muscle, elastic tissue, and collagen fibers, and an outer layer composed of elastic tissue and collagen fibers.[7] The percentage of elastic tissue in arteries is much higher than those in veins because arteries conduct blood at higher pressures.[8] Small vessels (i.e., arterioles, venules, capillaries) are much narrower and thinner than arteries and veins. Arterioles and venules have thin layers of smooth muscle and fibrous tissue, respectively.[7] Capillaries are the smallest vessels in the body and are only one cell layer thick to allow for fluid permeability and mass exchange. The cell types within large and small vessels also differ slightly. Arteries, arterioles, and veins are composed of endothelial cells (ECs), smooth muscle cells (SMCs), and pericytes.[9] Venules are usually made up of ECs and pericytes, along with SMCs, which have distinct characteristics compared to SMCs derived from arteries.[10−12] Capillaries are composed of a single layer of ECs and some pericytes for stabilization.[13] The large vessels are mainly responsible for mass transport, while the small vessels, especially capillaries, are involved in multiple biological processes, including mass exchange, immune response, lymphocyte migration, and homing, etc.[1,2,13] The varied structures and functions of blood vessels exemplify their remarkable complexity.

Engineering the complexity of microvasculature has been a key obstacle in the field of tissue engineering since its inception.[14,15] Diffusion of oxygen and nutrients within tissues is effectively limited to 100−200 μm. Therefore, engineered tissues larger than these dimensions require endogenous microvasculature for proper nutrient delivery and survival in vivo.[15−18] Numerous biofabrication methods have been developed to create vascular networks in vitro, which generally involve microfluidics-based molding techniques.[19−23] In addition, controlled delivery of proangiogenic factors like VEGF within biomaterials (e.g., hydrogel scaffolds) has also been a popular strategy to promote vascularization.[24,25] Despite the significant progress made with these techniques, they generally lack the spatiotemporal precision and control required to replicate the physiological complexity and function of 3D vascular networks.

To address this challenge, 3D bioprinting has emerged as a powerful means of fabricating vascularized tissues with structural complexity unattainable by traditional fabrication methods.[26−32] The ultimate ambition for the bioprinting field is to resolve the organ donor shortage by creating patient-specific, transplantable replacement tissues and organs in the lab.[33−36] However, while there has been success in creating large and small-diameter vessels using bioprinting approaches, fabricating functional microvasculature in constructs of human scale is still an unmet need and a key hurdle in the clinical translation of bioprinted tissues and organs. Biomaterials play a central role in the bioprinting process and serve as writing materials, or "bioinks", for printing the desired tissue construct. Therefore, the development of biomaterials for bioprinting microvasculature is a key driving force in the evolution of the field.

There have been essentially two approaches to using biomaterials for bioprinting microvasculature: indirect and direct. Indirect approaches employ sacrificial bioinks to print hollow tubes that can conduct fluid within a tissue construct (Figure 1A). Sacrificial, or "fugitive", bioinks can be printed as

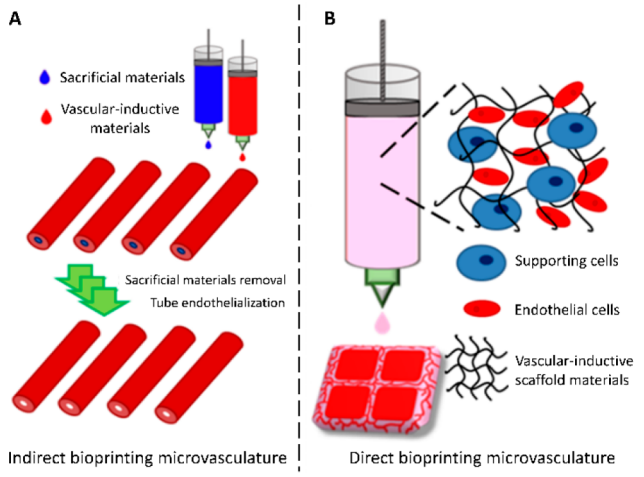

Figure 1. Bioprinting microvasculature. Indirect and direct approaches employ biomaterials in different manners to fabricate microvessels.

solid filaments during printing then removed after printing to leave behind hollow channels that can be perfused and endothelialized. While indirect approaches could theoretically be used to print capillary networks, the resolution of most indirect bioprinting platforms (>100 μm) does not approach that of capillaries (5−10 μm). Alternatively, direct approaches exclude the use of sacrificial materials and employ vascular-inductive bioinks containing endothelial cells to guide their self-assembly into capillary networks after printing via cell−cell

https://dx.doi.org/10.1021/acs.chemrev.0c00027
Chem. Rev. 2020, 120, 10887−10949

and cell−matrix interactions (Figure 1B). Because this strategy leverages cells, scaffolds, and signaling molecules to assemble vasculature endogenously, it is more suitable for promoting the formation of smaller vessels (e.g., capillaries) than indirect bioprinting.[37] However, there is a limited availability of proangiogenic biomaterials with high printability for direct bioprinting. Indirect and direct approaches for bioprinting microvasculature will be further discussed in section 3.

In this article, we will review and discuss the use of biomaterials for bioprinting microvasculature. Before we begin, it is first necessary to define microvasculature in the context of this review. A universally accepted definition of microvasculature is unclear, as it may vary between disciplines. For example, a surgeon may define microvasculature differently than an engineer. The medical definition of microvasculature is "the part of the circulatory system made up of minute vessels (such as venules or capillaries) that average less than 300 μm in diameter". However, reports from the engineering community have described vessels larger than 300 μm as microvasculature, with or without a lining of ECs.[38−40] In the bioprinting field, there has been limited consideration given specifically to microvasculature. A search for "microvascular bioprinting" in the PubMed database yields 17 results. In contrast, "vascular bioprinting" yields close to 300 results. While microvascularization has been achieved in numerous vascular bioprinting platforms, there have been limited efforts to intentionally design biomaterials for bioprinting microvessels/capillaries. Therefore, in the interest of breadth, we define microvasculature through an engineering lens. Bioprinted microvasculature satisfying the following criteria was considered for this review: (1) The diameter of the microvessel(s) are around or smaller than 500 μm with preference given to the latter; (2) the microvessels conduct fluid with or without a lining of ECs; (3) endothelial "cords" or primitive networks without lumens are also included because they may precede the formation of more patent microvessels.

Because the selection and utilization of these biomaterials rely on an understanding of biological mechanisms underlying blood vessel development, section 2 will offer a brief introduction of the fundamental biology of microvessel formation (i.e., angiogenesis and vasculogenesis), including the roles for growth factors, supporting cell types, and ECM. Because the selection of biomaterials also depends on the requirements of the specific technique it will be applied in, section 3 will review techniques for bioprinting microvessels and their associated printability considerations for biomaterials. Section 4 will critically review the current landscape of biomaterials and bioinks used for bioprinting microvasculature. We categorize bioinks based on the source of the scaffold materials, which include naturally derived and synthetic hydrogels. Section 5 will review recent applications of bioprinted microvessels for in vitro disease modeling, drug testing, tissue engineering, and regenerative medicine therapies. We end with an outlook on future challenges facing the development of biomaterials for bioprinting microvasculature.

2. BIOLOGICAL MECHANISMS OF MICROVASCULATURE FORMATION

2.1. General Introduction of Vessel Formation

Microvessel formation is mediated through highly sophisticated biological mechanisms. Several different models of vessel formation and remodeling are shown in Figure 2.[41] Among these, angiogenesis and vasculogenesis are the most extensively studied.[41,42] There are significant distinctions between these two models during organogenesis. Vasculogenesis gives rise to the primitive vascular plexus during embryonic development through the differentiation and growth of mesodermal-derived hemangioblasts.[43,44] Vasculogenesis also occurs in adults via differentiation of endothelial progenitor cells into ECs. Angiogenesis is characterized by endothelial sprouting and tube formation from pre-existing vessels.[45] Angiogenesis and vasculogenesis have been extensively studied and utilized in tissue engineering and regenerative medicine strategies for therapeutic vascularization.[41,42] Therefore, the following sections will provide some background on the biological mechanisms driving these processes.

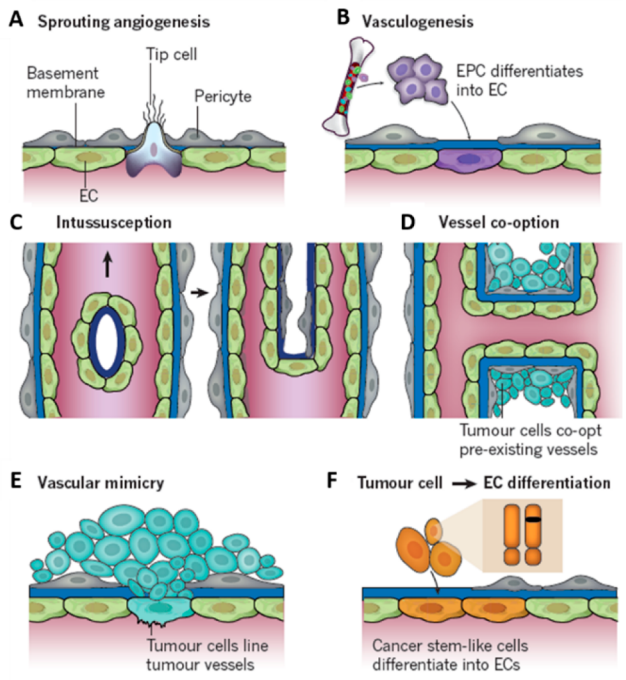

Figure 2. Models of vessel formation. The several known models of blood vessel formation under physiological and pathological conditions. (A−C) Vessel generation under normal conditions: (A) sprouting angiogenesis, (B) vasculogenesis−endothelial progenitors differentiate into ECs and supporting cells to forming vessels, (C) intussusception−vessel splitting into two new vessels. (D−F) Vessel generation in the tumoral environment: (D) vessel co-option induced by tumor cells, (E) vascular mimicry−tumor vessels can be lined by tumor cells along with normal ECs, (F) tumor cell to EC differentiation−tumor vessels can also be lined by the tumoral differentiated ECs. Reproduced with permission from ref 41. Copyright 2016 Springer Nature.

2.1.1. Angiogenesis. Angiogenesis is the process of new blood vessel formation from pre-existing vessels.[42] In addition to physiological conditions, angiogenesis is associated with multiple pathological conditions (e.g., atherosclerosis, chronic inflammation, and cancer). Significant progress has been made in revealing the underlying mechanisms of angiogenesis.[46] Numerous comprehensive reviews about angiogenesis can be found in refs 41,42,47. Therefore, the following sections provide a brief introduction of the current consensus of angiogenesis mechanisms. In addition, the effects of growth factors, cell sources, and ECM will also be reviewed.

https://dx.doi.org/10.1021/acs.chemrev.0c00027
Chem. Rev. 2020, 120, 10887−10949

There are two distinct mechanisms of angiogenesis: sprouting angiogenesis and intussusception. During sprouting angiogenesis, growth factors such as vascular endothelial growth factor (VEGF), angiopoietin-2 (Ang2), and fibroblast growth factor (FGF) trigger proangiogenic gene activation in quiescent vessels. Pericytes detach from the vessels, proteases break down basement membrane, and cell−cell junctions loosen to facilitate sprouting from the vessel wall. A subtype of ECs called "tip cells" migrate along the chemokine gradient and establish the path of the new sprouting vessel (Figure 2A). The neighboring cells of the tip cells, "stalk cells", support the tip cells invading into remodeled ECM and pericytes help stabilize the integrity of the nascent vasculature. During intussusception (Figure 2C), interstitial cellular columns insert into the lumen of pre-existing vessels. Further expansion and growth of these inserted columns lead to vessel branching, eventually causing the remodeling of the vascular networks.[45]

2.1.2. Vasculogenesis. Vasculogenesis is initiated by angioblasts during embryonic development to form the primitive capillary plexus.[42] In adults, vasculogenesis occurs via migration and differentiation of endothelial progenitor cells (EPCs) from bone marrow into mature ECs (Figure 2B). While vasculogenesis is mostly referred to in a developmental context, vasculogenesis has also been reported in cultures of mature ECs and supporting cells (e.g., pericytes and fibroblasts).[48−51] In the tissue engineering field especially, vasculogenesis is used loosely to describe de novo formation of vascular networks from dissociated suspensions of endothelial cells. Some of these models can be found in Table 1.

2.2. The Roles of Growth Factors

As described above, sprouting angiogenesis is initiated by proangiogenic signaling molecules (e.g., growth factors). These signals control and direct vessel development during angiogenesis.[41,42] Physiologically, these signals are released by cells under hypoxia[52] and include but are not limited to platelet derived growth factor (PDGF), vascular endothelial growth factor (VEGF), fibroblast growth factor (FGF), transforming growth factor β (TGF-β), angiopoietins, epithelial growth factor (EGF), and insulin-like growth factor (IGF). We refer readers to refs 41,53. for comprehensive reviews about these factors. Here, we will give a glance at each category and their role in vascular morphogenesis.

Table 1. Models of Vasculogenesis[a]

EC types	supporting cell types	media supplements	culture time	ref
HUVEC	pericytes	M-199 with SCF, IL-3 and SDF	3 days	49
	none	EBM with FBS, VEGF and FGF	3 days	55
	adipose stromal cells	IMEM/F12, VEGF, BCGF, EGF	50 days	56
	mesenchymal stem cells	EGM-2	7 days	57
	foreskin fibroblasts	EGM-2	7 days	50
	dermal fibroblasts	EGM-2	7 days	51
HDMEC	none	EGM2-MV	20 days	58
BOEC	pericytes	M-199 with SCF, IL-3 and SDF, HEPES saline	5 days	48
EPC	lung fibroblasts	EGM-2	7 days	59

[a]EC = endothelial cell; HUVEC = human umbilical vein endothelial cell; SCF = stem cell factor; IL = interleukin; SDF = stromal cell-derived factor; EBM = endothelial cell growth basal medium; FBS = fetal bovine serum; VEGF = vascular endothelial growth factor; FGF = fibroblast growth factor; BCGF = B-cell growth factor; EGF = epidermal growth factor; EGM = endothelial growth medium; HDMEC = human dermal microvascular endothelial cell; MV = microvascular; BOEC = blood outgrowth endothelial cell; EPC = endothelial progenitor cell.

2.2.1. PDGF Family. The most well-studied members of the PDGF family are PDGF-A and PDGF-B, which are encoded by the PDGF gene. They can form three different forms of dimers, PDGF-AA, PDGF-AB, and PDGF-BB. Recent publications have discovered additional PDGF genes and proteins, PDGF-C and PDGF-D.[54]

PDGFs play a critical role during development.[60] Although the current understanding of the functions of PDGFs in physiological and pathological conditions remains incomplete, emerging literature shows a correlation between the altered expression levels of PDGFs and the pathological/regeneration progression of blood vessels.[61] Several PDGF-targeted therapies have been developed. Especially, recombinant human PDGF-BB based therapy has been utilized clinically as a wound-healing therapy for diabetic ulcers.[62,63]

There are three known types of PDGF receptors: PDGFR-$\alpha\alpha$, PDGFR-$\alpha\beta$, and PDGFR-$\beta\beta$. PDGFR activation can affect a variety of signaling pathways (e.g., Ras-MAPK, PI3K, and PLC-γ). As a result, the activation of PDGFRs is highly involved in many types of organogenesis, including vascular development. In addition to supporting the fundamental functions of ECs (e.g., survival and proliferation), PDGFs also play critical roles in the function of multiple supporting cell types, such as pericytes[64] and SMCs.[65] Specifically, PDGF-B targets PDGFR-β as a paracrine signaling mechanism between ECs and perivascular cells.[66] Studies have also shown that PDGF-B/PDGFRβ signaling is responsible for the recruitment of pericytes[61] and vascular smooth muscle cells.[67]

PDGF is also an important molecular mediator of vasculogenesis. The PDGF family functions as a major mitogen for many mesenchymal/neuroectodermal originating cells. PDGFs also have chemo-attractive properties during multiple tissue remodeling processes, such as wound healing, bone formation, and the development of various organs.[68]

In summary, the PDGF family has significant roles in angiogenesis and vasculogenesis, especially for mural cell recruitment and vessel stabilization. The following section will introduce VEGF, which is closely related to the PDGF family, as a detailed example.

2.2.2. VEGF Family. VEGF is the most well-studied and one of the most critical signaling molecules for angiogenesis. VEGF has several isoforms, including $VEGF_{121}$, $VEGF_{145}$, $VEGF_{165}$, and $VEGF_{189}$. Some isoforms are matrix-bound while others are soluble. Each isoform plays a distinct role in promoting angiogenesis.[69] There are three primary receptors for these VEGF isoforms: VEGFR1 (Flt-1), VEGFR2 (Flk-1 or KDR), and VEGFR3 (Flt-4). Targeting to these different receptors can lead to different effects during angiogenesis. For instance, VEGFR2 (Flk-1 or KDR) is thought to be the primary receptor for EC proliferation and migration, while VEGFR1 (Flt-1) is believed to be an important modulator during vessel development through the VEGF signaling

https://dx.doi.org/10.1021/acs.chemrev.0c00027
Chem. Rev. 2020, 120, 10887−10949

pathway.[70,71] VEGF is usually required for angiogenesis in vitro, which can be either exogenously introduced or locally secreted by cells.[69] VEGF gradients control filopodia extension and tip cell migration for endothelial sprouting during angiogenesis as well as vessel permeability.[72−74]

Interestingly, positive VEGF gradients trigger endothelial cell sprouting while negative gradients inhibit it.[75] Furthermore, it has been reported that different forms of VEGF, either enzyme-releasable or permanently immobilized, contribute to the formation of enlarged or branching vessels, respectively.[76] VEGF also plays a substantial role in vasculogenesis, promoting angioblast differentiation from hemangioblasts[77−80] and EPC differentiation into ECs via binding of VEGFR2.[81]

Overall, VEGF is a central mediator of neovascularization. We refer readers to ref 82 for a more detailed discussion on the biology of VEGF and its receptors.

2.2.3. FGF Family. FGFs belong to another important protein family for angiogenesis. Among them, basic fibroblast growth factor (bFGF or FGF-2) was the first identified molecule claimed to have "angiogenic effects".[83] To date, there are around 20 different FGF isoforms discovered in the FGF family. FGF-1 and FGF-2 are the most studied molecules.[84] The correspondent receptors for FGFs are FGFR-1, -2, -3, and -4.

Molecular biology studies have demonstrated the activation of different FGF receptors leads to distinct functions. For instance, FGFR-1 has been shown as a critical receptor for vascular development during embryonic stages.[85] During vasculogenesis, FGF can synergize with VEGF to influence angioblast differentiation or EPC differentiation to ECs.[77,78,81] Inactivation of the gene encoding FGFR-3 causes abnormalities in mouse skeletal development.[86] Furthermore, several angiogenesis-related pathways are activated by FGFR-1-mediated signaling pathways, such as Ras, PI3K, and PLC pathways, which leads to survival, proliferation, and migration of ECs and supporting cells.[87−90] FGFs have high binding affinity to heparan sulfate proteoglycans (HSPGs), making HSPGs function as a reservoir of FGFs, mediating the local concentration and gradient of FGFs. Inspired by this, several biomaterials systems have incorporated HSPGs to sequester and prolong the delivery of FGFs for angiogenesis.[91−93] We refer readers to ref 94 for a detailed review of the biology and therapeutic potential of the FGF family.

2.2.4. TGF-β Family. The transforming growth factor-beta (TGF-β) family is composed of more than 30 different isoforms.[95] TGF-β1 is the most studied among them. TGF-β is secreted in an inactivated form, which forms a large latent complex (LLC). The LLC can be activated by integrin $\alpha_v\beta_6$ and $\alpha_v\beta_8$ subunits by multiple cell types through different mechanisms.[96−98] In ECs, active TGF-β binds to its receptor and promotes the phosphorylation and activation of type I TGF-β receptor (ALK-1). The signal is transduced through Smad1/5/8 and enhances the secretion of angiogenic factors, such as ID1 or IL1.[99]

TGF-β regulates angiogenesis in a context-dependent manner. For instance, angiogenesis is enhanced at a low expression level of TGF-β but inhibited at a high level of expression.[100,101] They hypoxic condition of tissues can augment the concentration and effects of TGF-β.[102,103] TGF-β can control angiogenesis through different mechanisms. For instance, TGF-β manipulates its targeted receptors (ALK1 and ALK5) to switch between two different signaling cascades, which lead to varied levels of vessel remodeling and maturation.[104] Furthermore, TGF-β is capable of changing the expression level and altering the function of other angiogenic factors like VEGF.[105,106] TGF-β also has significant roles during pathological angiogenesis.[107]

TGF-β also has multiple distinct roles during vasculogenesis. It can induce EC differentiation while also inhibiting endothelial tube formation.[104] It enhances VEGF synthesis by MSCs but inhibits the proliferation of the vascular supporting cell types.[108,109] TGF-β signaling is reviewed in detail in ref 95.

2.2.5. Angiopoietin Family. Angiopoietins and Tie signaling play important roles in vascular morphogenesis, homeostasis, and remodeling.[110,111] The angiopoietin (Ang) family includes four different isomers, Ang1, Ang2, Ang3, and Ang4.[112] Ang1 and Ang2 were initially recognized as agonistic and antagonistic ligands for the Tie2 receptor, respectively.[113,114] Ang3 and Ang4 were subsequently discovered as human and mouse orthologues of Ang1 and Ang2.[112] In general, the Ang/Tie system controls sprouting angiogenesis, vascular remodeling, EC activation, and mural cell recruitment.[111] Recent studies revealed that Ang/Tie system is also involved in regulation of lymphatic system development,[115] lymphangiogenesis,[116] inflammation,[117] and even tumor development.[118]

During Ang/Tie signaling cascades, Ang1 and Ang2 have distinct roles. In quiescent endothelium, pericytes release Ang1 to promote EC survival and vessel stabilization.[119] During angiogenesis, matrix-bound Ang1 mediates EC migration and adhesion while Ang2 behaves as a competitive antagonist against Ang1 for the Tie2 receptor and promotes pericyte dissociation and vascular permeability to allow tip cells to sprout and respond to angiogenic cues.[120] However, the relationship of Ang1 and Ang2 to vessel development is more complicated than "binary opposition". Ang2 regulates vessel formation and regression through Tie2 signaling in a context-dependent manner. As mentioned above, Ang2 is released during EC activation and potentially performs as a stimulator of Tie2 signaling in activated endothelium.[121] However, it also maintains quiescent endothelium by balancing the activities of Ang/Tie signaling.[122]

The Ang/Tie system plays a critical role in maintaining vessel integrity through pericyte recruitment, as severe defects in recruitment of pericytes in Ang-1 and Tie-2 deficient mice have been observed, leading to edema and localized hemorrhage.[123] While the exact mechanisms involved in Ang/Tie-mediated SMC recruitment are not fully understood, Ang1 has been shown to enhance EC-stimulated SMC migration by a mechanism involving up-regulation of endothelial-derived heparin binding EGF-like growth factor (HB-EGF), which is a known effector of SMC migration and recruitment via ErbB1 and ErbB2 receptors.[124]

Angiopoietins also perform as cofactors to regulate vessel development and remodeling. There are multiple reports that demonstrated the synergistic effects between angiopoietins and VEGF.[118,125,126] In the absence of VEGF, Ang2 induces EC apoptosis and vessel regression. In the presence of VEGF, Ang2 promotes EC migration, proliferation, and vessel sprouting in tandem with VEGF.[125] The ratio between VEGF and Ang2 also governs vessel development. For instance, Oshima and co-workers showed that a higher ratio of Ang2 to VEGF causes vessel regression while low ratio of Ang2 to VEGF leads to angiogenesis.[126,127] In addition to VEGF, angiopoietins also cooperate with cytokines such as

https://dx.doi.org/10.1021/acs.chemrev.0c00027
Chem. Rev. 2020, 120, 10887−10949

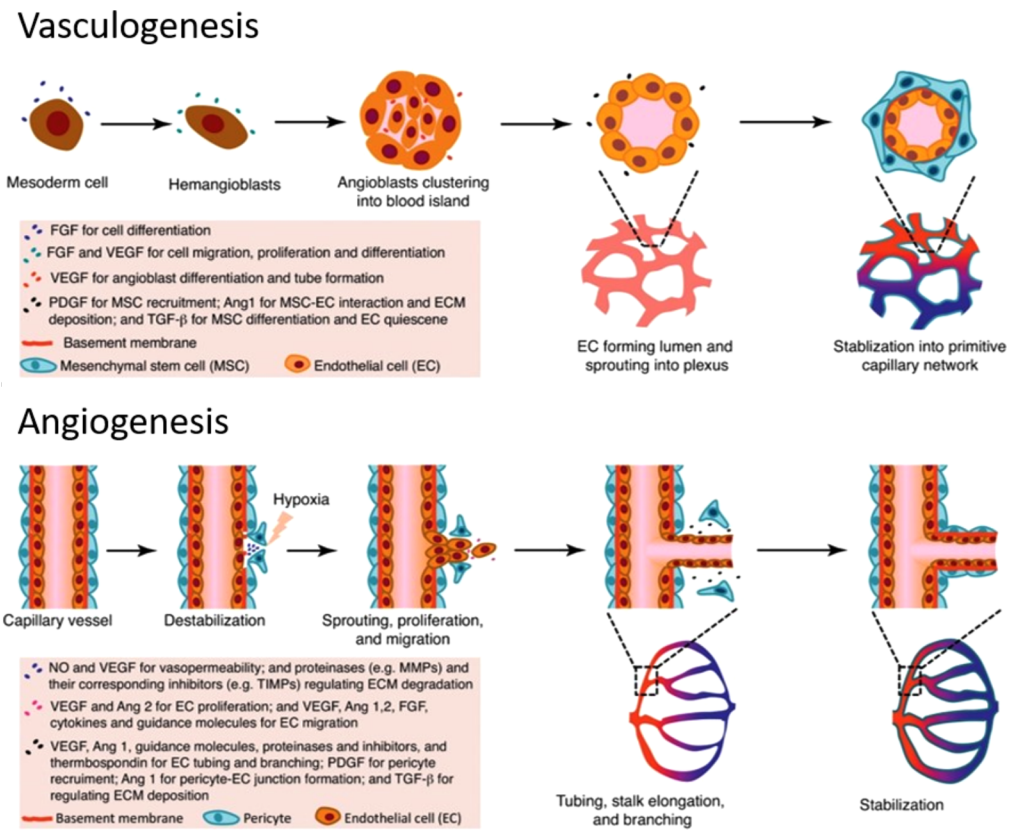

Figure 3. Roles of growth factors in neovascularization. Spatiotemporal regulation from various growth factors, cytokines, and enzymes orchestrates vasculogenesis, to form a primitive capillary network. Angiogenesis occurs with an existing capillary network and forms neovessels through sequential processes regulated by growth factors, cytokines, and guidance molecules. Extracellular matrix degradation, endothelial cell migration, stalk elongation, and vascular stabilization are regulated by different proteinases and their corresponding inhibitors. Adapted with permission from ref 155. Copyright 2017 Elsevier.

TNF-α[117] and IL-6.[128] For more detailed information about angiopoietins and Tie signaling for vessel development, we refer readers to a detailed review in ref 111.

2.2.6. Other Molecules. Other growth factors, such as BMP, EGF, and IGF, have shown vasculogenic and angiogenic potential. However, effects of most of these factors are mediated through supporting cell types instead of ECs. For instance, it was confirmed that EGF would stimulate A431 cells (a cell type in human epidermoid carcinoma) to secrete VEGFs and promote HUVEC migration.[129] Further information about these molecules can be found in refs 130−132.

In addition to growth factors, cytokines are also reported to promote angiogenesis. The activation of IL-8 not only promotes EC proliferation, but it also enhances MMP-2 and MMP-9 secretion in ECs.[133,134] Stromal cell derived factor-1 (SDF-1) has been shown to synergize with VEGF to promote angiogenesis.[135] SDF-1 is also a potent homing factor that promotes mobilization of endothelial progenitor cells to sites of vascular injury via binding of its receptor CXCR4.[136] Growth-regulated peptide-α/growth-regulated oncogene-1 has also been shown to induce EC proliferation.[137]

We have provided an overview of growth factors that are known to be important molecules in vessel development through vasculogenesis and angiogenesis. The general interactions of these factors during neovascularization are represented in Figure 3.

2.3. Cell Sources

2.3.1. Endothelial Cells. Endothelial cells (ECs) are the primary cell type that make up the inner lining of blood vessels.[138] Currently, there are a variety of EC subtypes used for vascular biology research.[139] For organ-on-chip models and translational applications, human-derived ECs are especially favorable. The selection of ECs for specific fabrication purposes is critical because differences have been shown in the expressions of both surface marker and RNA profiles of ECs derived from different tissues.[140] In addition, it has been shown that there are differences in EC cell type between large vessel endothelium and small vessel endothelium.[141] We will provide a background on three common EC types used for tissue engineering: human umbilical vein endothelial cells (HUVECs), human microvascular endothelial cells (HMVECs), and induced pluripotent stem cell-derived endothelial cells (iPSC-ECs).

2.3.1.1. Human Umbilical Cord Vein Endothelial Cells (HUVECs). HUVECs are derived from the endothelium of veins from the umbilical cord and are the most popular model endothelial cell type used to study vascular function and pathology. Because the umbilical cord is usually discarded as medical waste, HUVECs are an economical and abundant source of human ECs. Early passage HUVECs present EC markers like CD31 (PECAM-1), von Willebrand factor (vWF) as well as most receptors for growth factors, cytokines, and vascular signaling molecules.[142−144] HUVECs can easily be distinguished from vascular progenitor cells because they are

https://dx.doi.org/10.1021/acs.chemrev.0c00027
Chem. Rev. 2020, 120, 10887−10949

negative for the expression of vascular progenitor markers, such as CD133.[145] HUVECs can form both large and small blood vessels in vitro.[146−148] HUVECs are also widely used in a variety of engineering applications, including tissue fabrication (bioprinting) and organ-on-a-chip.[149,150] However, because HUVECs are derived from large veins, they may not fully recapitulate native microvessels like arterioles and capillaries. Further discussion of the potential of HUVECs for microvascular tissue engineering can be found in references.[151,152]

2.3.1.2. Human Microvascular Endothelial Cells (HMVECs). HMVECs can be derived from human microvessels in multiple different types of tissues. On the basis of their original organs, HMVEC could be further categorized into several subtypes, including human adipose-derived microvascular endothelial cells (from adipose tissue), human liver sinusoidal microvascular endothelial cells (from liver), and human cardiac microvascular endothelial cells (from cardiac tissues), etc. Although derived from different tissues, these ECs share common markers, such as vWF and CD31 as well as being LDL uptake positive.[151] HMVECs can be incorporated with parenchymal cell types from their tissue of origin to mimic the tissue-specific vascular microenvironment.[153,154] Because they originate from microvessels, HMVECs inherently have excellent potential for forming microvasculature in engineered tissues.

2.3.1.3. Induced Pluripotent Stem Cell Derived Endothelial Cells (iPSC-ECs). Induced pluripotent stem cell-derived ECs are an autologous source of ECs and have been obtained through multiple differentiation methods from several different cell lines.[156−159] The markers of iPSC-ECs are CD31, CD34, and VEGFR. They respond to shear stress and can form tubular networks on Matrigel.[156−159] In addition, they respond to inflammatory stimulus (e.g., IL-1β, TNF-α, and lipopolysaccharide).[158,160] These characteristics of iPSC-ECs in immune, transport, hematological, and mechanical response qualifies them as a valuable autologous alternative to primary ECs. iPSC-ECs have been used in various applications, including the fabrication of patient-specific vasculature in vitro for disease modeling and precision medicine.[161] However, ECs isolated from a particular organ could lose their organ-specific features once they depart from their native environment.[162] In addition, the relatively complicated differentiation protocols from iPSC to EC have greatly hindered the further use of iPSC-ECs.

2.3.2. Endothelial Progenitor Cells (EPCs). Endothelial progenitor cells (EPCs) were first identified in human peripheral blood based on shared antigens with hematopoietic stem cells (HSCs).[163] EPCs were found to differentiate into endothelial cells and contribute to neovascularization in adults, similar to the paradigm of vasculogenesis previously thought to be restricted to embryonic vascular development.[42,164] The capacity of EPCs to augment collateral vessel growth to sites of ischemia has made them a popular cell source for therapeutic vascularization and vascular tissue engineering.[165,166] Some studies have even shown EPCs to outperform vascular-derived ECs in forming vascular networks in vitro and in vivo.[167−169] One of the most studied EPC types, circulating EPCs, will be further discussed in the following section.

2.3.2.1. Circulating EPCs (cEPCs). Circulating EPCs (cEPCs) were the first of several types of EPCs initially discovered from blood.[170] They are generally two subtypes based on their origin, hematopoietic EPCs and nonhematopoietic EPCs.[165,166] Hematopoietic EPCs are derived from hematopoietic stem cells, which originate from bone marrow.[171] Nonhematopoietic EPCs, based on their nomenclature, are not derived from HSCs but are instead believed to derive from organ or tissue-derived EPCs, including blood cells.[172,173] Because of the heterogeneity of these two subtypes, there is no consensus on the general phenotype, surface markers, and stable origins for cEPCs.

Hematopoietic EPCs were originally identified through $CD34^+$ cells from peripheral blood, and they were probably the earliest portion of cEPCs which were proven to contribute to the treatment of ischemic diseases in vivo by neovascularization.[163] In subsequent studies, markers for these EPCs were suggested as $CD34^+/CD133^+/VEGFR2^+$, which was supported by the correlations between this EPCs phenotype and cardiovascular conditions through clinical observations.[163,174] Although these markers are still widely utilized for EPC sorting, a series of additional markers were also recommended, including CD45, CD105, CD106, CD117, and CD144.[175] Meanwhile, some characteristics, such as the uptake of acetylated low-density lipoproteins and activated aldehyde dehydrogenase, were also suggested as coevidences of the phenotype of these EPCs.[176] Additionally, some populations of hematopoietic EPCs were also observed to present many similar characteristics with monocytic cells, such as uptake of lectin and acetylated low-density lipoproteins, as well as expressing monocytic marker, CD14.[177] Because of these similarities, these EPCs were called "early EPCs" (eEPCs) in some studies.[177−180]

Nonhematopoietic EPCs, were believed to derive from nonhematopoietic tissue and vessel walls were one of the most possible sources.[172,173] The heterogeneity among isolated nonhematopoietic EPCs has led to little consensus on the typical general marker(s) for isolating nonhematopoietic EPCs. Importantly, nonhematopoietic EPCs have demonstrated less proliferative capacity and progressive senescence during culture, making them less suitable for clinical applications.[181]

The unique functions of hematopoietic and nonhematopoietic EPCs are complex and still not fully understood. It is generally agreed upon that these two cell types can differentiate into endothelial lineages and secrete and respond to angiogenic/vasculogenic factors for paracrine effects.[169,180,182−184] Recently, subpopulations of EPCs known as endothelial colony forming cells (ECFCs) and endothelial out-growth cells (EOCs) have received additional attention because of their unique functions and good potential for clinical therapies.[169,178,185]

2.3.2.2. Endothelial Colony Forming Cells (ECFCs) and Endothelial Outgrowth Cells (EOCs). ECFCs were initially discovered through an endothelial colony formation assay, which was developed with the purpose of clearly distinguishing EPCs and HSCs for precisely sorting EPC phenotype.[186−188] Similarly, EOCs were reported through another type of endothelial colony formation assay system.[178,185]

The subcategorical definition of ECFCs in the EPC family is still debated. It is suggested that ECFCs are hematopoietic EPCs because they initially were isolated from blood-derived mononuclear cells and they exhibit some classical hematopoietic markers, such as CD34 or CD133.[185] However, because of the heterogeneity of ECFCs, the defined markers for these cells are still under development, and the most widely used protocols have employed the markers $CD146^+/CD45^-/CD133^-$, which suggested that these cells originated from

https://dx.doi.org/10.1021/acs.chemrev.0c00027
Chem. Rev. 2020, 120, 10887−10949

vessel walls rather than bone marrow.[189] More recently studies even recommended a unique profile of "$CD45^-/CD34^+/CD31^{low}$" because it could generate pure endothelial populations.[173]

Compared to ECFCs, EOCs are most likely categorized as one type of nonhematopoietic EPCs because they cannot be placed into any classic hematopoietic related cell types due to the undetermined origin.[165] In addition, the major approach to obtain EOCs still relies on the endothelial colony formation assay system.

Both ECFCs and EOCs exhibit the capacity to differentiate into endothelial lineages and directly contribute to the de novo vessel formation.[181,190] Cell populations which can secrete angiogenic/vasculogenic factors have also been discovered in ECFCs and EOCs, which would offer the paracrine effects for neovascularization.[183,190] ECFCs display robust proliferative potential, form capillary networks in vivo, and functionally anastomose with host vasculature in vivo, making them a strong cell source for vascular tissue engineering and regeneration.[191]

2.3.3. Supporting Cell Types. *2.3.3.1. Pericytes.* Mural cells (e.g., pericytes) play an important role in the regulation of vascular dynamics both in embryonic and adult stages.[192] Pericytes support ECs through not only physically wrapping around them but also by modulating ECs through paracrine effects.[193] In addition to stabilizing established vessels, pericytes also provide mechanical support, manage the diameter of vessels, and remodel the vascular ECM microenvironment.[194−196] Furthermore, recent publications have demonstrated that pericytes also regulate the permeability of vessels and the barrier function in blood−brain barrier system.[194,197]

2.3.3.2. Mesenchymal Stem Cells (MSCs). Mesenchymal stem cells are multipotent stem cells with potential for osteo-, chondro-, adipo-, and myogenic differentiation.[198,199] MSCs are defined by their multilineage potential and ability to self-renew, along with expression of several cell-surface markers, including CD44, CD73, CD105, and CD90, and lack of endothelial or hematopoietic cell-surface markers such as CD45 and CD34.[200,201] MSCs are typically harvested from bone marrow or adipose tissue but can also be obtained through isolation from umbilical cord or placenta.[200]

MSCs play an important role in angiogenesis and the development of vascular networks. Paracrine effects are one mechanism through which MSCs promote blood vessel formation. MSCs produce and secrete several growth factors and vesicles that enable cell communication and the regulation of vascular development.[202] Additionally, MSCs have been recognized as perivascular progenitor cells and have the ability to differentiate into vascular phenotypes such as smooth muscle and endothelial cells.[203,204] Furthermore, there are many links between MSCs and pericytes, including cell-surface markers and functions such as stabilizing endothelial cells and secretion of pro-angiogenic growth factors.[198,205,206] Importantly, MSCs have been shown to have antithrombogenic effects when incorporated into vascular grafts.[207] Accordingly, MSCs have been widely used in tissue engineering strategies to facilitate the generation of functional vasculature. Taken together, the autologous availability, low immunogenicity, multilineage potential, and proangiogenic characteristics of MSCs make them excellent supporting cell types in therapeutic angiogenesis and vascular tissue engineering, as reviewed in ref 208.

2.3.3.3. Fibroblasts. Fibroblasts are an important and widely used supporting cell type for vascular studies. Their main function is to secrete ECM scaffold proteins like collagen to reinforce ECM mechanical properties and promote vascular network and lumen formation.[209,210] More information about the topic of ECM secreted by fibroblasts for angiogenesis can be found in ref 209. Fibroblasts also release numerous proangiogenic paracrine factors for the modulation of angiogenesis.[211]

2.3.3.4. Vascular Smooth Muscle Cells (vSMCs). In mature vessels, vascular smooth muscle cells are responsible for contraction and regulating blood pressure. During embryonic vascular development, vSMCs have a high proliferation rate and produce a large number of ECM components for blood vessel wall assembly.[212] In addition, vSMCs still hold a remarkable plasticity in mature animals.[213] A detailed review of the features of vSMCs can be found in ref 214.

2.4. The Role of Extracellular Matrix

The ECM plays a central role in vascular morphogenesis. In the quiescent state, there is a dense basement membrane surrounding blood vessels, which is mainly composed by type IV collagen and laminin proteins. In addition to serving as physical scaffolds, they also maintain blood vessel homeostasis through cell-ECM signaling. During angiogenesis, the basement membrane is degraded by proteases (e.g., MMPs) secreted by the cells activated by angiogenic stimuli (e.g., hypoxia, growth factors). This disrupts the basement membrane and exposes the sprouting ECs to the interstitial ECM to facilitate their proliferation and migration. Glycoproteins in the interstitial ECM, such as fibronectin, collagen, and laminin, directly engage cell surface integrins to support vessel formation. It has been demonstrated that different types of integrin activation can promote distinct orientation and density of nascent blood vessels.[215] The interstitial ECM is also rich in proteoglycans and glycosaminoglycans (GAGs), which can bind to angiogenic growth factors (e.g., VEGF and FGF) and sequester their release in a precise spatiotemporal manner for vessel patterning. Overall, the ECM functions as a dynamic biomolecular scaffold to guide and support neovascularization.[216] A general relationship between the ECM and ECs during angiogenesis is illustrated in Figure 4.

3. BIOPRINTING TECHNIQUES AND BIOMATERIALS CONSIDERATIONS FOR BIOPRINTING MICROVASCULATURE

There have been numerous techniques developed for bioprinting microvasculature. Although not the focus of this review, we feel it is important to have a basic understanding of these techniques, as each have unique requirements for printability and therefore require distinct biomaterials properties. A basic understanding of the different bioprinting techniques will provide the reader with necessary context before analyzing biomaterials for bioprinting in section 4.

Each modality has unique advantages and disadvantages for bioprinting microvasculature in terms of speed and resolution. Bioprinting techniques are commonly categorized as droplet-based bioprinting (DBB), extrusion-based bioprinting (EBB), and light-assisted bioprinting (LAB). Numerous in-depth review articles have been published detailing these modalities and their applications in bioprinting.[32,36,218,219] Here we focus on bioprinting platforms in the context of bioprinting microvasculature. In each section, we will provide a brief

https://dx.doi.org/10.1021/acs.chemrev.0c00027
Chem. Rev. 2020, 120, 10887−10949

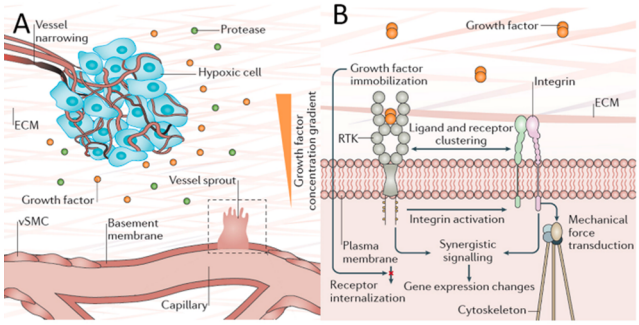

Figure 4. ECM microenvironment during angiogenesis. (A) Angiogenesis can be triggered by vessel narrowing induced hypoxia. The hypoxic cells secrete proteases to degrade ECM, altering the physical and chemical properties of ECM. The cells also secrete growth factors, which are sequestered by proteoglycans to create a chemokine gradient. Meanwhile, surrounding capillaries sense these changes and initiate multiple responses, such as vessel sprouting. (B) Sprouting endothelial cells simultaneously adhere to surrounding ECM via integrins while sensing sequestered growth factors through cell surface receptor tyrosine kinases. Concerted growth factor and integrin activation drive synergistic angiogenic signaling toward restoring blood flow to hypoxic cells. Reproduced with permission from ref 217. Copyright 2016 Springer Nature.

introduction to the bioprinting techniques, their associated biomaterials requirements for printability, and applications in vascular tissue engineering before critically analyzing and comparing their suitability for bioprinting microvasculature.

3.1. Droplet-Based Bioprinting

Droplet-based bioprinting, or DBB, is an approach that involves the serial deposition of droplets of biomaterials and/or cells in precisely defined 2D or 3D arrangements. Like commercial inkjet printers that propel droplets of ink onto paper to reproduce a digital image, inkjet bioprinters propel droplets of "bioinks" onto a bioprinting substrate, sometimes referred to as "biopaper". Bioinks are formulations of biomaterials and/or cells that serve as the writing material for bioprinting and are discussed further in section 4. The resolution of droplet-based bioprinting is generally around 50–300 μm, making it suitable for printing microvasculature. Capillary network formation in DBB approaches relies on self-assembly of ECs in the printed bioink. Therefore, proangiogenic bioinks or biopaper substrates are ideal to promote microvascularization after printing. DBB can be further categorized into inkjet bioprinting, acoustic-droplet-ejection bioprinting, and microvalve bioprinting, depending on the means of droplet formation. For more details on DBB techniques, we refer readers to a comprehensive review of droplet-based bioprinting in ref 220.

In general, bioinks for droplet-based bioprinting must have a low viscosity (<10 mPa s) as it becomes increasingly difficult to generate droplets in high viscosity bioinks, which may cause clogging at the nozzle orifice. Cell density also affects droplet formation, with higher densities leading to increased droplet size, decreased droplet velocity, and increased breakup time.[221] To preserve the integrity of the printed structure, it is ideal to use biomaterials that can be rapidly cross-linked to form a solid hydrogel after deposition. This can be accomplished by printing bioinks into a liquid solution containing cross-linker, applying cross-linker solution to the printed bioink through another nozzle or by mist or by using photopolymerization for photosensitive biomaterials. There are numerous biomaterials that can be cross-linked instantaneously via physical or chemical methods, which will be discussed further in section 4. To bioprint microvasculature using DBB methods, it is imperative to consider the proangiogenic features of both the bioink and the printing substrate. The properties of the bioink and substrate should be complementary in promoting both high printability and rapid self-assembly of endothelial cells into functional vascular networks during culture. Benning and others recently conducted a side-by-side comparison of conventional hydrogel bioinks and found that collagen and fibrin were most suitable for inkjet bioprinting of endothelial cells as they best supported HUVEC proliferation in 2D and sprouting from HUVEC spheroids after 3D printing.[222]

DBB techniques are valuable tools for microvascularized tissue engineering due to their high resolution, precision, and cytocompatibility. Biomaterials, cells, and other biologics may be deposited with great spatiotemporal control in droplets that are nano- or picoliters in volume. Boland's group pioneered the modification of commercial inkjet printers for direct droplet-based bioprinting of microvasculature. The first demonstration used a modified Hewlett-Packard (HP) inkjet printer to deposit bovine aortic endothelial cells and smooth muscle cells onto Matrigel and collagen, respectively.[223] The cells remained highly viable after 3 days of culture. Nakamura and others also demonstrated an electrostatically driven inkjet system that was highly biocompatible with endothelial cells.[224] To generate 3D tube-like constructs, Boland's group suspended rat smooth muscle cells in an alginate hydrogel bioink for layer-by-layer printing in a $CaCl_2$-containing bath.[225] The cells remained viable after 2 weeks of culture and, interestingly, exhibited vasoreactivity to a vasoconstricting agonist endothelin-1. A later study demonstrated that endothelial cells could adhere to the pores of the alginate-based printed vascular structures.[226] Boland's group has applied their inkjet bioprinting platform to fabricate microvascularized bilayer skin grafts to treat full-thickness wounds in mice.[227] Compared to a commercial skin graft, the bioprinted graft promoted wound contraction and formation of healthy, vascularized skin with both dermal and epidermal layers of normal thicknesses. In another study, Atala's group used an inkjet bioprinter to create complex 3D heterogeneous constructs[228] and showed that the bioprinted structures significantly improved functional vascularization and bone tissue formation in vivo compared to manually seeded scaffolds. Three-dimensional vascular tube-like structures with bifurcations have also been fabricated by valve-based printing of alginate bioinks layer-by-layer into a $CaCl_2$-containing bath.[226,229] These studies demonstrate the capabilities of DBB techniques to position multiple cell types in user-defined arrangements with excellent precision and viability, leading to enhanced vascularization and overall function of the tissue construct. The accessibility, affordability, and mobility of droplet-based bioprinters is also very advantageous for translational applications of DBB in microvascularized tissue engineering. Accordingly, recent studies have modified droplet-based bioprinters for in situ bioprinting of cell-laden hydrogels for skin tissue regeneration in small and large animal models.[230,231] Lastly, inkjet bioprinting is uniquely advantageous for printing microvasculature as it was recently revealed that thermal inkjet bioprinting triggers activation of the VEGF pathway in human microvascular ECs, as illustrated in Figure 5.[232]

Despite the advantages of DBB, there are still important concerns associated with these approaches. One major concern

https://dx.doi.org/10.1021/acs.chemrev.0c00027
Chem. Rev. 2020, 120, 10887–10949

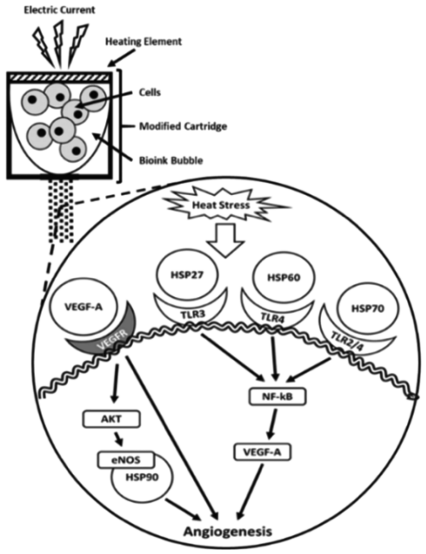

Figure 5. Thermal inkjet bioprinting triggers the activation of the VEGF pathway. The schematic illustration shows how heat from the printing process causes cellular heat stress leading to various pathways in which extracellular heat-shock proteins play an angiogenic role. Reproduced with permission from ref 232. Copyright 2019 IOP Publishing Ltd.

for droplet-based bioprinting is the hydration of printed cells. Because printed droplets are quite small, they may evaporate quickly during the printing process, leaving cells dehydrated. Therefore, the printing substrate should have a high-water content to keep cells within the droplets hydrated. Furthermore, the small droplet sizes generated by DBB methods makes scaling the production of larger tissues or organs a serious challenge. Conventional DBB strategies are mostly limited to 2D structures because the discontinuous droplets may be mechanically unstable when printed in multiple layers.[233] Therefore, DBB may be most suitable for bioprinting microvasculature within 2D patches (i.e., skin or cardiac) for tissue engineering or for patterning chemokine gradients onto a 2D surface to study endothelial cell behavior. DBB methods are also relatively slow because the bioinks are printed drop-by-drop, although the throughput of DBB methods can be massively improved with multinozzle and multimaterial printheads.[234,235] Finally, the low viscosity required of bioinks for printing with DBB reduces the versality of these techniques and the breadth of compatible biomaterial formulations. Therefore, novel bioinks containing biomaterials that are both printable and proangiogenic should be emphasized for DBB applications.

3.2. Extrusion-Based Bioprinting

Extrusion-based bioprinting, or EBB, uses pneumatic-, piston-, or solenoid-driven actuators to extrude bioinks through a nozzle onto a printing substrate. EBB is a widely used approach due to its accessibility, compatibility with high viscosity bioinks, and fast multilayer printing times. In EBB approaches, cylindrical bioink filaments can be printed layer-by-layer to form a lattice-like macroporous construct. The continuous extrusion of cylindrical filaments allows larger 3D constructs to be printed with superior mechanical integrity compared to DBB. However, shear stress-induced cell death is more of a concern with EBB due to higher pressures generated at the nozzle during extrusion.[236] In addition, EBB techniques generally have the lowest resolution of the bioprinting platforms with a minimum feature size above 100 μm, making them less suitable for fabricating capillary-like structures.[237]

EBB approaches have been widely utilized for bioprinting vascular constructs. Because of resolution limitations, generation of capillary networks in the printed structures using EBB approaches mostly relies on vasculogenesis and angiogenesis within the filaments after printing, while large vessel-like channels can be printed directly or indirectly.[238−242] Most studies have used EBB techniques to rapidly fabricate large channels first, followed by endothelization to form functional vasculature. There have also been demonstrations that achieved formation of capillary networks through angiogenesis from the larger parent vessels during culture.[243,244] Vascular networks printed using EBB have been shown to improve mass transport and diffusion within the printed construct.[243] In addition to capillary formation, several supporting cell types have also been incorporated into EBB platforms to improve vessel stabilization and maturation, including but not limited to pericytes, smooth muscle cells, and fibroblasts.[245−247] For instance, Ma's group has incorporated mouse fibroblasts into bioprinted hollow constructs and demonstrated good viability of the fibroblasts after 7 days' culture.[247] Zhang and others employed human coronary artery smooth muscle cells (HCASMCs) and human bone marrow-derived mesenchymal stem cells (hMSCs) to facilitate 3D small-diameter vasculature formation.[248] Furthermore, there are also demonstrations using tissue spheroids rather than single cells as building blocks for EBB.[249] Overall, EBB techniques are among the most popular for vascular bioprinting due to their capacity to rapidly print tubular structures and multilayer constructs, as well as their accommodation of a wide range of bioinks. For a comprehensive analysis of current advances in EBB, we refer readers to a detailed review by Ozbolat and Hospodiuk in ref 250.

Coaxial extrusion is a popular type of EBB approach for printing microvasculature. Coaxial nozzles are composed of an inner and outer compartment, allowing simultaneous extrusion of a bioink and a cross-linker solution in a core−shell fashion for rapid gelling at the dispensing head. The immediate cross-linking at the nozzle orifice in coaxial systems enables printing accuracy to be decoupled from bioink rheological behavior[251] and allows for the fabrication of multilayer constructs with low viscosity bioinks.[149] Hollow tubular fibers or bulk fibers can be printed by extruding cross-linking solution in either the core or shell compartment, respectively (Figure 6). The core−shell element of coaxial extrusion is a powerful feature, as it allows for rapid fabrication of perfusable tubular constructs with one nozzle. Further, different biomaterials and cells can be incorporated into the core and shell compartments to generate heterogeneous tubular structures. For instance, Liu and others used a custom Dual Ink coaxial bioprinter to fabricate vascularized pancreatic constructs.[252] Islets were housed in the core compartment and were surrounded by EPCs or regulatory T cells in the shell compartment. The coaxial positioning of these cell types improved vascularization of the construct while providing immunoisolation to the islets. Coaxial bioprinting systems also enable user-defined control over the sizes of printed channels by adjusting nozzle size and geometry as well as extrusion settings (i.e., pressure/flow rate) of inner and outer compartments based on the requirements of the applications.[247] For example, Millik and others used customized coaxial nozzles of varying diameters and extrusion

https://dx.doi.org/10.1021/acs.chemrev.0c00027
Chem. Rev. 2020, 120, 10887−10949

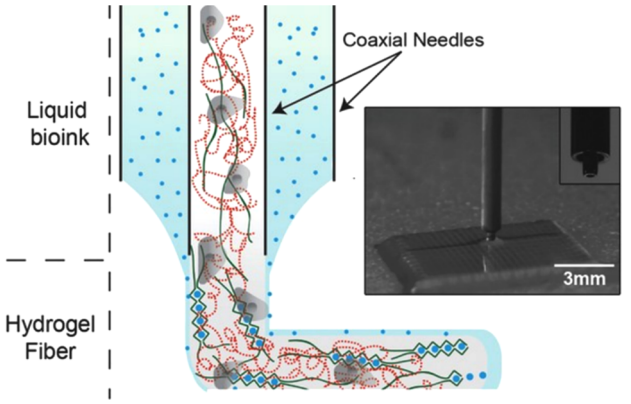

Figure 6. Coaxial extrusion-based bioprinting. Solid or hollow hydrogel fibers can be printed with a coaxial nozzle depending on which axis (core or shell) the hydrogel and cross-linker are extruded through. Reproduced with permission from ref 255. Copyright 2015 John Wiley and Sons.

conditions to generate perfusable hydrogel tubes with different cross-sectional geometries.[253] The shape and orientation of the printed vasculature can also be managed through computer-aided design and the 3D printing process. Along with the aforementioned studies, there have been multiple coaxial bioprinting systems developed for printing smooth and continuous lumens in any predesigned length, confirming the power of this technology.[247,254]

To further improve the heterogeneity of extrusion-based techniques, microfluidics-assisted multimaterial EBB systems have been developed. These are necessary for printing heterogeneous constructs with tunable features that mimic the spatial complexity of human tissues at the microscale.[256,257] Most multimaterial EBB systems to date have used multiple syringes to sequentially print bioinks one at a time. This is relatively low-throughput and requires the nozzles to be carefully calibrated. The frequent start-and-stop of flow between extrusion can also introduce defects and discontinuity in the extrudate. Extruding multiple materials from one nozzle can increase the throughput and allow for the fabrication of

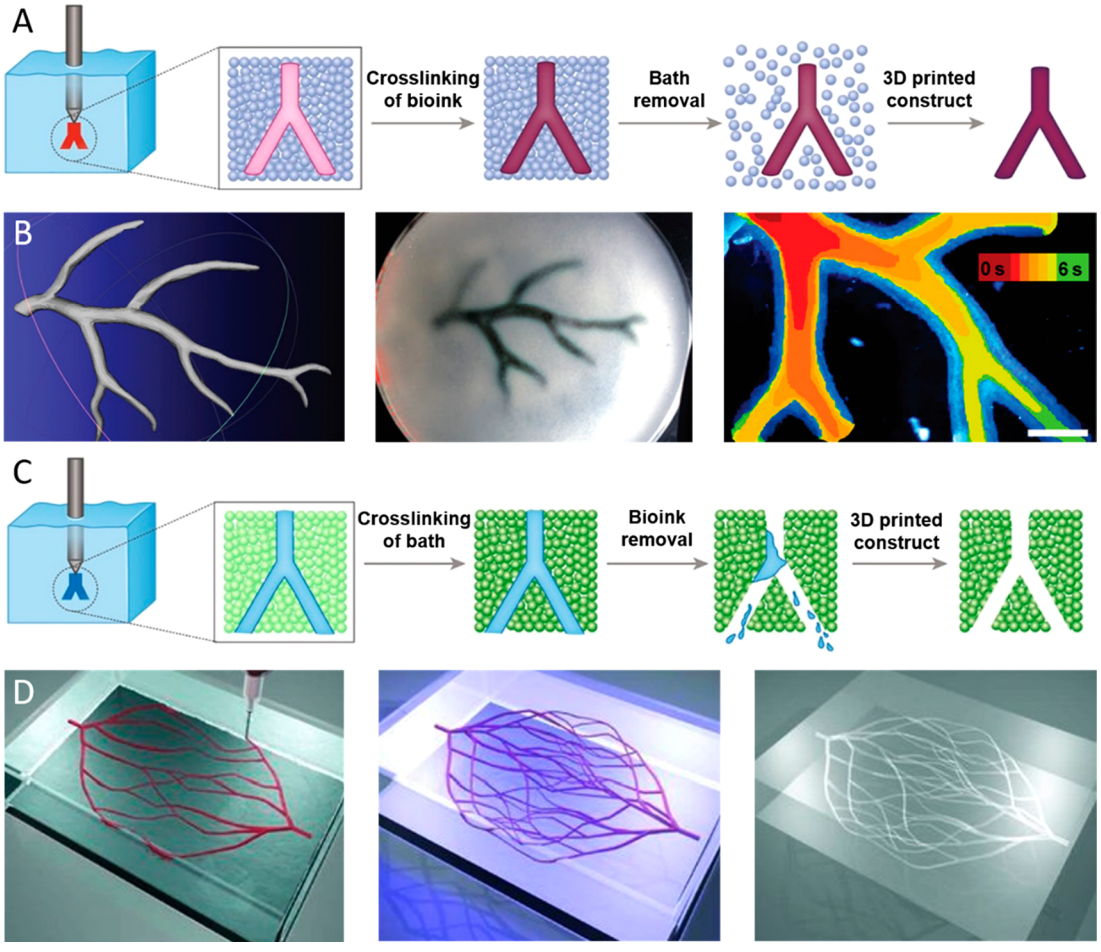

Figure 7. Embedded 3D bioprinting of vascular structures. (A) Approach for directly bioprinting vascular structures within a supportive bath based on cross-linking of the bioink and removal of the supportive bath after printing. Adapted with permission from ref 268. Copyright 2019 Elsevier Ltd. under the terms of the Creative Commons (CC BY 4.0) License https://creativecommons.org/licenses/by/4.0/. (B) Example of perfusable vasculature printed in a sacrificial gelatin support bath using an alginate bioink. Reproduced from ref 269. Copyright 2015 American Association for the Advancement of Science under the terms of the Creative Commons (CC BY 4.0) License https://creativecommons.org/licenses/by/4.0/. (C) Approach for indirectly bioprinting vascular structures within a supportive bath based on cross-linking of the bath materials (i.e., by UV exposure) and removal of the sacrificial bioink after printing. Adapted from ref 268. Copyright 2019 Elsevier Ltd. under the terms of the Creative Commons (CC BY 4.0) License https://creativecommons.org/licenses/by/4.0/. (D) Example of perfusable microvascular networks embedded within a photopolymerized Pluronic F127-diacrylate matrix using a sacrificial Pluronic F127 bioink. Reproduced from ref 241. Copyright 2011 Wiley-VCH.

https://dx.doi.org/10.1021/acs.chemrev.0c00027
Chem. Rev. 2020, 120, 10887−10949

structures with encoded composition and variable properties along the print path.[258] To this end, Hardin and others developed microfluidic printheads that could seamlessly switch between two viscoelastic PDMS bioinks "on-the-fly" during printing.[259] To switch between inks during printing, syringe B is compressed while syringe A is simultaneously decompressed. This results in a rapid pressure change that permits flow from syringe B while prohibiting flow from syringe A. The timing of this switch may be precisely controlled for programmable microscale properties in the printed construct. Active mixing printheads have also been developed for controlled blending of two bioinks in one nozzle immediately before extrusion.[260] Khademhosseini's group recently developed a method to rapidly dispense up to 7 bioinks in one nozzle by bundling several capillary extrusion tips into one dispenser housing and independently programming the flow of each bioink.[261] These approaches offer exciting potential to rapidly multiplex different biomaterials and cells within an engineered tissue to enhance its biomimicry.

3.3. Embedded 3D Bioprinting

In most EBB systems, bioinks are directly written onto substrates in open air without supports. This limits the complexity of printed structures and can lead to gravity-induced sagging during the printing process, especially when using soft hydrogel bioinks (<100 kPa). Embedded 3D printing addresses this problem by printing directly into a physical support matrix to prop up the extrudate during printing. This allows for omnidirectional extrusion within the support matrix and minimizes gravity-induced sagging. The hydrated support matrix also helps maintain cell viability during printing by providing an aqueous environment with tight control over pH, temperature, and sterility. During embedded printing, the nozzle generates void space in its wake as it moves through the support matrix. Ideally, the support matrix should exhibit shear-thinning and self-healing viscoplastic properties to accommodate nozzle translation and fill the void space to maintain support of the extrudate.[262] Thixotropic hydrogels, which yield to higher loads and fully recover afterward, are ideal support matrices for embedded 3D printing. Jennifer Lewis's group first developed embedded 3D bioprinting for fabricating acellular microvascular networks within a Pluronic F127 support matrix.[241] This platform has also been used for soft robotics applications[263] and to embed strain sensors into elastomeric hydrogels.[264] Since then, several other embedded 3D bioprinting platforms have emerged with more biocompatible support matrices.

Granular hydrogels are an excellent support medium for embedded 3D bioprinting.[265,266] Granular microgels "jam" to form solid-like matrices at low shear strains but can yield locally to high shear strains. After the strain is removed, granular hydrogels recover back to their solid-like "jammed" state. More details on the properties of granular hydrogels can be found in a review by Riley and others.[267] During embedded printing, granular gels exhibit thixotropic properties, fluidizing around the nozzle then quickly recovering around the extrudate.[266] The tip speed and flow rate can be adjusted to tailor the diameter of the extruded filaments. Intricate hierarchical networks containing hollow tubes with diameters of 100 μm have been printed in granular support mediums.[266] One approach for fabricating vascular structures using embedded 3D bioprinting involves directly embedding a bioink within a sacrificial support bath (Figure 7A), as demonstrated by Hinton and others[269] with an alginate bioink and calcium-containing granular gelatin hydrogel support bath (Figure 7B). Once the bioink is cross-linked inside the matrix, the bath may be removed and the printed construct retrieved. Another approach relies on embedding a sacrificial bioink within a polymerizable support matrix to indirectly pattern a perfusable microvascular network (Figure 7C). After cross-linking the support matrix around the sacrificial bioink, the bioink can be removed to leave behind a biomimetic vascular network, as demonstrated by Wu and others[241] using a sacrificial Pluronic F127 bioink and photopolymerizable Pluronic F127−diacrylate support matrix (Figure 7D). These different approaches allow for the use of a variety of different biomaterials as the bioink and support matrix to fabricate tissue- and organ-specific constructs with perfusable microvasculature.

Several conventional hydrogel bioinks, including poly(ethylene glycol) (PEG), hyaluronic acid (HA), and alginate can be used as biomaterials for bioprinting in granular matrices.[266] Likewise, numerous different biomaterials can serve as the granular medium. In FRESH bioprinting (freeform reversible embedding of suspended hydrogels), developed by Feinberg and others, granular gelatin microparticles are used as the supporting medium (discussed further in section 4.1.1.3.).[269,270] In "GHost writing", developed by Burdick and others, hyaluronic acid hydrogels modified for supramolecular host−guest interactions are used as the supporting medium (discussed further in section 4.1.2.4.).[271] SWIFT bioprinting (sacrificial writing into functional tissue), developed by Lewis and others, uses sacrificial bioinks written into support matrices composed of dense compactions of cellular aggregates or organ building blocks (discussed further in section 3.5) to fabricate tissues with physiological cell density.[272]

As a relatively emergent approach, 3D embedded bioprinting has shown great promise for its application in microvascularized tissue engineering. Free-standing biological structures have been fabricated with impressive complexity in vitro using embedded bioprinting techniques, including models of the heart,[269,272,273] brain,[270] cardiac patches,[273] and perfusable vascular structures with biomimetic features.[244,265,271,274,275] Several of these studies have demonstrated physiological cell- and tissue-level function within the printed structures, making them applicable for in vitro drug testing and vascular modeling. Further studies are necessary to demonstrate biocompatibility and organ-level functions of these structures to fully realize their potential as replacements for human tissues and organs.

3.4. Light-Assisted Bioprinting

Light-assisted bioprinting, also known as laser-assisted bioprinting or LAB, uses light energy to manipulate cells and photoreactive biomaterials in 2D, 3D, and recently in 4D, based on a digital design. Laser-assisted techniques are arguably the most suitable for bioprinting microvasculature as they have exceptionally high resolution, with feature sizes less than 10 μm.[276] Accordingly, LAB techniques have been used for many tissue engineering applications, including bone,[277,278] skin,[279,280] and cardiac[281] regeneration, as well as in vitro models of microvasculature for lab-on-a-chip studies.[282] Tissue engineering applications using LAB are reviewed in detail in refs 283−286. Light-assisted methods can be categorized into laser-assisted direct writing, laser-based

https://dx.doi.org/10.1021/acs.chemrev.0c00027
Chem. Rev. 2020, 120, 10887−10949

stereolithography, and projection-based stereolithography. While the principles of these methods are discussed in detail elsewhere,[284,287] we will review and analyze LAB techniques for printing microvasculature and their associated biomaterials considerations.

3.4.1. Laser-Assisted Direct Writing. Laser-assisted direct-write approaches can be additive or subtractive. Laser-induced forward transfer (LIFT) is a common laser-assisted additive technique that uses laser energy to deposit cells and biomaterials directly onto substrates with high resolution and reproducibility.[284,287] LIFT setups are typically composed of a pulsed laser source (e.g., Nd:YAG crystal laser), a print ribbon coated in cell-laden bioink, and a collector substrate or biopaper on a motorized stage. When the ribbon is irradiated with laser energy, heat and pressure are generated and a droplet of bioink is ejected onto the collector substrate. To protect cells and biological materials from damaging laser exposure during LIFT, an energy-absorbing layer (e.g., metal or biopolymer) can be placed between the print ribbon and the bioink.[288,289] Droplet volume during LIFT is dependent upon laser pulse energy and repetition, and the energy needed for droplet formation depends on the rheological properties of the bioink and the cell density used.[290] LIFT principles and physical parameters are discussed in detail in ref 291.

Various cell types can be printed with high viability (>95%) using LIFT because it is a noncontact approach.[292] ECs have been printed with nearly 100% viability using biological laser printing (BioLP).[288] In a more recent study, Wu and Ringeisen used BioLP to print HUVECs into capillary-scale branch/stem structures resembling the complex vein networks of a leaf. Bioinks used in LIFT typically have low material concentration and low viscosity (1−300 mPa·s) to facilitate droplet formation, but they can accommodate relatively high cell densities (up to 60 million cells/mL). For example, 1 wt % alginate has been used as a bioink for printing ECs via LIFT.[293] The bioink had a viscosity of 100 mPa·s and, depending on the laser energy, could be printed in droplets around 50 μm in diameter. The viscosity increased 20% when ECs were incorporated at 40 million cells/mL. To promote capillary network formation after printing, proangiogenic biomaterials like Matrigel and collagen can be used as collector substrates.[278,281,293,294] Kérourédan and others have optimized LIFT parameters for bioprinting ECs onto collagen biopaper (Figure 8).[278]

Subtractive laser-assisted techniques are also powerful platforms for direct writing of capillary networks (Figure 9).[295] These approaches mostly rely on photoablation, where focalized high-intensity pulsed lasers cause local ablation of material to etch patterned networks. Nano- or femto-second pulsed lasers have energies of around 80−150 mW and 500−900 mW, respectively, which are enough to break covalent bonds.[296] Early work used laser-assisted direct writing to etch microfluidic mixers and artificial capillary networks onto 2D silicon and Pyrex surfaces.[297,298] Photodegradation techniques commonly employ synthetic hydrogels because they can easily be modified with photolabile functional groups for tuning of their chemical and physical properties.[299] These hydrogel systems are discussed further in section 4.2.1. The main advantage of laser-assisted direct writing is the simplicity of generating perfusable capillary-scale networks without involving the complex steps necessary for removing sacrificial materials in indirect bioprinting approaches. The main drawback of laser-assisted direct writing techniques is that they are relatively slow and become slower with increasing vessel size. Higher intensity lasers can be used to ablate larger channels, but this comes at the expense of increased cell death near the laser and compromising the structural integrity of the bulk construct. Therefore, photoablation techniques are only practical for fabricating submillimeter-scale vasculature in cellularized hydrogels. For true multiscale vascular bioprinting, laser-assisted direct writing would need to be combined in tandem with a complementary approach capable of printing larger vessels.

Because of their relative simplicity, laser-assisted direct writing techniques have been widely used to bioprint

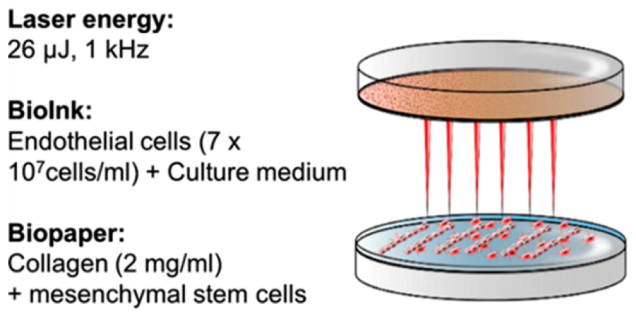

Figure 8. LIFT bioprinting of endothelial cells. Schematic illustration shows optimal parameters for LIFT bioprinting of endothelial cells. Reproduced with permission from ref 278. Copyright 2019 Springer Nature.

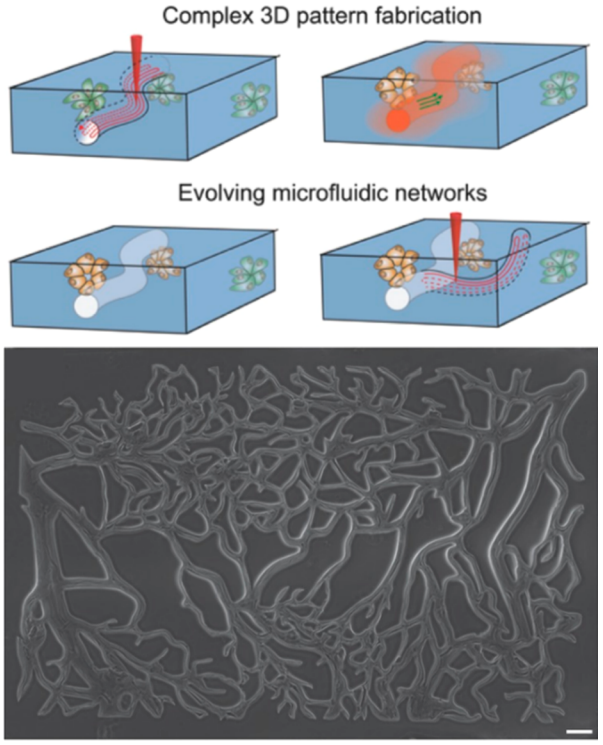

Figure 9. Direct writing of microvasculature using laser-assisted direct writing. Schematic illustration of microvascular patterning within a cell-laden hydrogel using a focalized pulsed laser and an example of patterned microvasculature using this technique. Scale bar = 100 μm. Adapted with permission from ref 300. Copyright 2016 John Wiley and Sons.

https://dx.doi.org/10.1021/acs.chemrev.0c00027
Chem. Rev. 2020, 120, 10887−10949

microvasculature for tissue engineering applications. In a recent study, an LAB bioprinter was developed for in situ patterning of endothelial cells into a mouse calvaria bone defect.[277] When printed onto a collagen substrate containing human MSCs and VEGF, the printed cells self-assembled into organized vascular networks that contributed to improved vascularization and bone regeneration compared to randomly seeded endothelial cells, providing evidence of the clinical applicability of LAB. In another study, LIFT was used to pattern human stem cells and endothelial cells in a defined pattern on a polyester urethane urea (PEUU) cardiac patch.[281] The patches were cultured in vitro before being transplanted to infarcted rat hearts, where the LIFT-printed patches improved cardiac functional recovery, capillary density, and functional anastomosis with host vasculature compared to patches with randomly seeded cells. Laser-assisted direct writing has also been used to fabricate skin substitutes by patterning keratinocytes and fibroblasts onto Matriderm, a commercial dermal substitute composed of collagen and elastin.[279] The substitutes formed skin-like structures in vitro and promoted blood vessel migration toward the printed cells in vivo when transplanted to a dorsal skin fold chamber in mice. These studies demonstrate the versatility and translational potential of laser-assisted direct writing approaches. However, they are mainly limited to engineering planar tissue constructs.

3.4.2. Laser-Based Stereolithography. The stereolithography apparatus (SLA) is the most popular 3D laser-assisted fabrication modality. There are two main types of SLA: laser-based and projection-based. Laser-based SLA utilizes raster scanning of a focused UV or near-UV laser to cross-link a photopolymerizable resin based on a digital CAD model. Laser-based SLA is a bottom-up approach as each layer is polymerized point-by-point. Each cured layer is lowered on a stage in the *Z*-direction for printing of the next layer and the process is repeated, eventually yielding a 3D object. The CAD models for stereolithography can be derived from 3D drawings (e.g., in PowerPoint slides) or from magnetic resonance imaging (MRI) and computed tomography (CT) scans. Micro-CT scans of corrosion casts can be used for generating CAD models of microvasculature.[301] We refer readers to a review by Melchels, Feijen, and Grijpma in ref 302 for details about the principles of the SLA method.

Biomaterials used in laser-based additive manufacturing methods like SLA must be photo-cross-linkable. They should behave as a liquid in the printing reservoir and rapidly solidify when illuminated with light. There are numerous photo-cross-linkable hydrogels and photoinitiators that are suitable for SLA, and they are discussed in detail in ref 286. Synthetic polymers like PEG and PVA and natural polymers like gelatin and hyaluronic acid can be modified with photoreactive acrylate/methacrylate groups for printing with SLA.[285] The mechanical properties of constructs printed with SLA can be tailored by varying material concentration, composition, laser exposure time, and laser intensity. To print live cells via SLA, biomaterials should be hydrophilic and cross-linked under mild conditions. Synthetic photopolymerizable polymers can be modified with cell-adhesive RGD peptides and growth factor-sequestering heparan sulfate proteins to enhance their bioactivity.[303] Several water-soluble photoinitiators have been identified as cytocompatible in UV and visible light-based systems.[304,305] A more comprehensive discussion on materials and additives for stereolithography can be found in ref 306.

Stereolithography has proven useful in many biomedical applications, including vascular bioprinting and tissue engineering. Early studies leveraged SLA for rapidly prototyping patient-specific anatomical models using data from imaging modalities like MRI and CT. For example, life-size patient-specific models of aortic aneurysms[211] and other arterial pathologies[307] have been fabricated from CT data using SLA to help surgeons plan individual procedures, design novel stent grafts, and study physiologically accurate flow dynamics in the altered anatomy. These studies paved the way for using SLA to fabricate cellularized constructs out of photoreactive biomaterials for vascular tissue engineering.

While SLA approaches have traditionally relied on single-photon UV absorption, two-photon photopolymerization (TPP), or multiphoton polymerization, it has been used as a more precise alternative to single-photon polymerization as TPP excitation is highly localized to a small focal volume, enabling nanoscale resolution.[283,308−310] Far-red laser light is often used for TPP, which is relatively safe for cell culture. Accordingly, cell-laden constructs have been printed with high viability using TPP.[308] Remarkably, vascular structures with lumen diameters <20 μm have been printed using TPP.[311] However, the lumens collapsed once they reached 4 μm, indicating a lower threshold for vascular dimensions in TPP methods. Emerging applications of TPP include bioactive site-selective protein modification of biomaterials to guide cell morphogenesis.[312−314] In an early study, TPP was used to micropattern RGDS, an adhesive ligand, in PEG hydrogels to guide 3D fibroblast migration, demonstrating the capacity of TPP to guide tissue regeneration at the microscale.[315] For vascular tissue engineering, DeForest's group has pioneered the use of multiphoton polymerization and photoablation for laser-based direct writing of capillary networks in cell-laden hydrogels.[316] In a recent study, they used multiphoton photoablation to engineer 5−10 μm channels in collagen hydrogels to model biophysical and biomolecular interactions of malaria-infected erythrocytes in human capillaries.[317] As evidenced by these studies, the unprecedented resolution of TPP methods holds great promise for engineering capillaries with physiological scale and function within biocompatible hydrogels. The main disadvantages of TPP techniques are their relatively slow speed and short penetration depth, which may be restricted to small constructs (~1 mm thick), limiting the scalability of TPP approaches. Complementary techniques with more robust fabrication capacities (e.g., extrusion-based methods) would likely need to be applied in parallel with multiphoton polymerization to produce multiscale features within human-scale scaffolds.

The emerging development of 3D holography bioprinting shows promise to significantly accelerate print times for multiphoton approaches.[318] This technology has been pioneered by Prellis Biologics. Holographic bioprinting essentially combines the precision of multiphoton polymerization with the speed of projection-based stereolithography, effectively decoupling speed from resolution. A holographic projection is cast onto a photocurable substrate to simultaneously cross-link multiple voxels at once with submicron resolution. The holograms are projected as a series of images at high speeds (up to 300 Hz) to print structures within a 3D field of view without the need for a moving stage. Objects can also be printed inside structures that have already been printed using this method. While the technology is proprietary, Prellis Biologics has developed a holographic bioprinter in collabo-

https://dx.doi.org/10.1021/acs.chemrev.0c00027
Chem. Rev. 2020, 120, 10887−10949

ration with CellINK to offer commercial products that enable 3D cell culture in microvascular networks.

3.4.3. Projection-Based Stereolithography. Projection-based stereolithography is often preferred over traditional laser-based lithography as it provides much faster build times. While laser-based SLA approaches polymerize hydrogels point-by-point, projection-based SLA techniques are top-down approaches that cross-link planes of photocurable material at once according to a digital image. Shaochen Chen's research group pioneered the use of projection-based stereolithography for rapidly fabricating complex 3D microenvironments.[319] In their approach, known as dynamic optical projection stereolithography (DOPsL), a digital micromirror device (DMD) and an objective lens are used to project UV light in a 2D image across a plane of a photocurable solution. The DMD contains an array of mirrors that can be flipped to either reflect light or not and can be continuously switched within microseconds, allowing for a dynamic "maskless" projection of custom digital images. A 3D image obtained by CT can be divided into 2D slices and used as projections for rapidly prototyping the scanned object layer-by-layer.

Perfusable multiscale vascular networks can be patterned within photoreactive hydrogels using projection-based stereolithography (Figure 10).[320] These hierarchical networks mimic

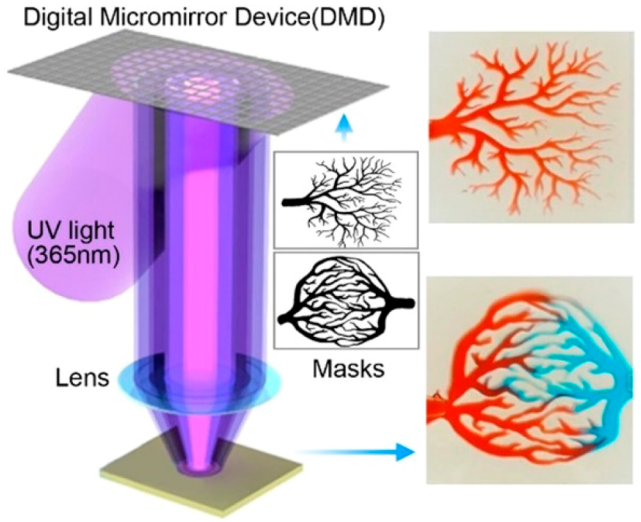

Figure 10. Projection-based stereolithography for patterning microvasculature. Perfusable capillary-scale networks can be patterned into photoreactive hydrogels via user-defined photomasks. Reproduced with permission from ref 320. Copyright 2018 American Chemical Society.

physiological vasculature, with millimeter- and micrometer-scale vessels forming continuous vascular trees and capillary networks. Projection-based SLA allows for these different vessels sizes to be fabricated concurrent with each other layer-by-layer, offering unprecedented speed and complexity for advanced vascular tissue engineering. Accordingly, Chen's group has applied projection-based SLA to fabricate prevascularized tissues with complex microarchitecture.[321] Their study showed that hierarchical vascular networks could be patterned directly into cell-laden hydrogels using projection SLA and that these prevascularized constructs significantly improved vascularization and anastomosis when implanted in vivo. In the future, projection-based SLA could be utilized to engineer complex microvascular networks within tissue-specific constructs, such as cardiac or liver, to enhance their biological relevance in vitro and improve engraftment in vivo.[322] Furthermore, proangiogenic growth factors such as VEGF and PDGF could be embedded within the tissue-specific architectures for controlled release to promote vascular morphogenesis, as demonstrated by Wang and others.[323]

Most SLA techniques rely on ultraviolet (UV) light as an energy source. This is problematic because exposure to UV light can cause DNA damage-induced cell death by apoptosis.[324] Next-generation lithography methods are turning to visible light cross-linking for better biocompatibility and clinical translation potential. To this end, visible light-sensitive photoinitiators like eosin Y have been incorporated into hydrogel mixtures of PEG and GelMA for printing highly viable cells.[325,326] Grigoryan and others recently identified tartrazine (yellow food coloring), curcumin (from turmeric), and anthocyanin (from blueberries) as nontoxic additives that could absorb visible light for projection-based stereolithography bioprinting.[327] Tartrazine was identified as the best candidate because it is FDA approved and could easily be washed out of the printed construct. This allowed for the fabrication of intravascular topologies of unprecedented complexity within biocompatible hydrogels, offering promise for clinical applications of projection SLA in vascular tissue engineering.

3.5. Scaffold-Free Bioprinting

Scaffold-free bioprinting, as the name suggests, excludes the use of biomaterials as scaffolding material in the bioink formulation. Instead, dense populations of cells are forcibly aggregated together and produce their own ECM to support their shape. As opposed to traditional scaffold-based "cells-in-gels" approaches, scaffold-free approaches allow the use of much higher cell densities that approach physiological levels. Cell−cell interactions are much more prevalent in these systems because cells are not separated by scaffold materials, and the cell aggregates, or spheroids, can quickly fuse to form tissue/organ building blocks. There are numerous methods for generating spheroids for scaffold-free bioprinting, with hanging-drop[328] and micromolding[329] being the most common. Although the generation of spheroids itself does not involve exogenous biomaterials, spheroids are often printed within hydrogels to support their arrangement into 3D constructs. This is because spheroids by themselves have poor printability and cannot be bioprinted into a freeform 3D structure without collapse. Direct embedding of spheroids into hydrogels has been demonstrated in droplet-based, extrusion-based, and recently laser-assisted LIFT bioprinting approaches.

Some of the first bioprinting platforms for vascularized tissue fabrication utilized 3D cell aggregates. The self-assembling capacity of spheroid microtissues has made them attractive "building blocks" for vascular tissue engineering. Gentile et al. developed hollow vascular spheroids by treating E8.5 mouse allantois-derived spheroids with VEGF.[330] This method yielded uniluminal spheroids with distinctive inner and outer layers of ECs and SMCs, respectively. These spheroids can fuse to form even larger vascular microtissues while still retaining their hollow core.[331] Vascularized macrotissues can also be fabricated by "coating" spheroids with ECs. During culture, endothelial cell-coated microtissues fuse to form macrotissues with endogenous vasculature.[332] Importantly, human endothelial cell-based vascular spheroids can form robust blood and lymphatic vasculature after in vivo implantation.[333] In a recent

https://dx.doi.org/10.1021/acs.chemrev.0c00027
Chem. Rev. 2020, 120, 10887−10949

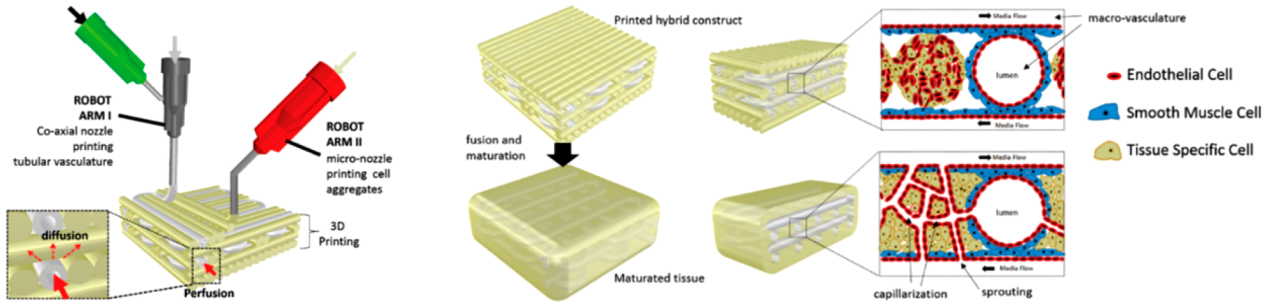

Figure 11. Multiscale vascularized constructs printed with tissue strands. Hollow vascular networks can be printed in tandem with tissue-specific aggregate strands to provide mechanical support and media perfusion. Endothelial cells within tissue strands self-organize and create capillary networks that functionally anastomose with adjacent vascular networks under perfusion. Reproduced with permission from ref 341. Copyright 2014 American Society of Mechanical Engineers.

study, Pattanaik and others found that prevascularized endothelial-fibroblast aggregates can anastomose with host vasculature in as little as 6−12 h, which could enable high viability postimplantation.[334]

While early studies demonstrated impressive engineering of vascularized micro- and macrotissues, their architectural complexity was mostly limited to spherical shapes or patches. To address this, scaffold-free bioinks were adapted for 3D bioprinting. Forgacs and others have made pioneering advances in the field of scaffold-free biofabrication. In their foundational work, Jakab and others established mathematical and experimental models of spheroid fusion to demonstrate their potential as building units for bioprinting.[335] They manually printed aggregates of Chinese hamster ovary (CHO) cells (∼500 μm diameter) into collagen hydrogels in ring and tube-like structures and modeled their fusion into the printed shape. In a later study, aggregates of embryonic cardiac cells and ECs were used to print vascularized cardiac constructs.[336] Interestingly, the ECs migrated to the boundaries between spheroids and lined the void space between them. To print the aggregates, they were placed in a glass capillary so that spheroids were densely packed at the tip and could be deposited sequentially into a collagen I substrate. In another study, Tan and others printed ring-shaped molds with alginate and then deposited spheroids composed of ECs and SMCs (1:1 ratio).[337] The spheroids fused to form toroid-shaped tissue units and secreted endogenous collagen during in vitro culture. Alternatively, cell aggregates can be suspended in alginate-based bioink and printed onto a moving stage in a $CaCl_2$ bath to fabricate zigzag cellular tubes with the need for supports..[338]

Precisely controlling the placement of individual spheroids can be challenging. Spheroid fusion is closely dependent on their packing density[339] and inconsistent placement of spheroids may lead to inhomogeneous fusion.[30] To address this, spheroids have been prefused into solid cylinders overnight before the printing process. The fusion of cylindrical tissues units is faster and more continuous at a large scale compared to spherical units.[340] These "tissue strands" can be printed into vessel-like structures and subsequently fuse into a large vascular tube.[249]

Ozbolat's research group first proposed the concept of bioprinting tissue strands along with vascular channels to promote multiscale vascularization of tissue constructs (Figure 11).[341] A hybrid approach with a multiarm bioprinter could be used for coaxial dispensing of hollow alginate microfibers in tandem with endothelialized tissue strands. Perfusion of the vasculature during culture would theoretically drive angiogenesis in the tissue strands, eventually establishing perfusable microvasculature throughout the tissue. While this has not been demonstrated experimentally, chondrocyte-laden tissue strands have been used to print cartilage patches.[342]

Cell aggregate-based bioinks are promising tools for bioprinting vascularized tissues with clinically relevant cell densities. However, the high costs and laborious cell culture needed to generate the required number of spheroids for scaffold-free bioprinting is a major obstacle to translation. To address this, De Moor and others have developed a platform for high-throughput fabrication of prevascularized spheroids with controlled size and high yield using agarose micromolds (Figure 12A).[343] Combining HUVECs with fibroblasts and

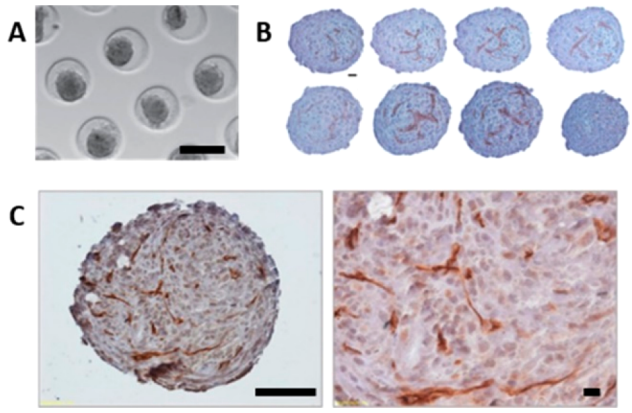

Figure 12. Prevascularized spheroids for scaffold-free bioprinting. (A) Fabrication of spheroids by gravity-induced aggregation in agarose microwells (scale bar = 200 μm). (B) Sequential sections of two large HUVEC/HFF/ADSC fused spheroids (scale bar = 20 μm). (C) Capillary-like network formation in fused constructs composed of HUVEC/HFF/ADSC spheroids. Overview scale bar = 100 μm (left), 40× objective magnification scale bar = 20 μm (right). Adapted with permission from ref 343. Copyright 2018 IOP Publishing Ltd.

ADSCs improved capillary formation within the spheroids (Figure 12B). The spheroids were also able to fuse into large constructs and produce robust endogenous capillary networks (Figure 12C). This platform could be a promising approach to regulate the production of a high number of vascularized microtissues for bioprinting capillarized macrotissues.

Besides being used as writing materials, cellular aggregates can also be used as granular support materials. Sacrificial writing into living tissue, or SWIFT, is a recently developed

https://dx.doi.org/10.1021/acs.chemrev.0c00027
Chem. Rev. 2020, 120, 10887−10949

technique based on the principle of embedded 3D bioprinting. Instead of a self-healing hydrogel support medium, dense compactions of organ building blocks (OBBs) cured in a thermoresponsive Matrigel/collagen matrix are used to support the embedding and subsequent perfusion of a sacrificial gelatin bioink. Jennifer Lewis's group developed the SWIFT method to print elaborate perfusable constructs of physiological cell density ($\sim 10^8$ cells/mL).[272] The OBBs may be embryoid bodies, organoids, or other cellular aggregates, depending on the desired application. OBBs could be produced using iPSC-derived cells for fabricating patient-specific constructs. The OBB-based matrices effectively behave as a self-healing, viscoplastic matrix, yielding to nozzle translation and recovering in its wake to support 3D embedding. Hundreds of thousands of OBBs could be incorporated into a SWIFT construct, improving upon typical "cells-in-gels" approaches where cell densities are 1−2 orders of magnitude lower than that in native tissues. Depending on print speed, filaments between 400 and 1000 μm in diameter could be embedded. This enabled fabrication of multiscale hierarchical networks within embryoid body (EB) support matrices. Attempts at endothelializing SWIFT constructs with HUVECs resulted in incomplete lining of the sacrificial channels, although some VE cadherin-positive monolayers were observed. Such dense constructs may contract significantly during culture as the dense populations of OBBs remodel their environment, which may impact the stability of embedded vasculature. Spatiotemporal patterning of OBBs in SWIFT constructs would also be a beneficial improvement, as the current version only allows for homogeneous casting of the OBB matrix into a mold.

There have been few studies focusing on microvascularization within scaffold-free systems. Going forward, it is crucial that bioprinted scaffold-free tissues and organs have hierarchical branched vascular networks that span the scale of macro- and microvasculature.[344,345] Cell aggregates can be densely compacted and their endogenous ECM can inhibit diffusion of nutrients to cells in the middle of the spheroid. This can lead to a necrotic core if vasculature is not established. Future studies should focus on the formation of functional microvascular networks within macro-assemblies of scaffold-free vascular building units to realize the scalability of these approaches.

We have presented a necessary background on the large variety of techniques available for bioprinting microvasculature, along with their unique advantages and disadvantages. We feel that this provides the reader with necessary context and knowledge to understand the state-of-the-art in bioprinting approaches for vascular tissue engineering and biofabrication. In the next section, we will turn our focus toward a comprehensive analysis of the role of biomaterials within the various printing techniques for bioprinting microvasculature.

4. BIOMATERIALS FOR BIOPRINTING MICROVASCULATURE

The "raw materials" of bioprinting are formulations of printable biomaterials known as "bioinks". Hydrogels are the most common biomaterials used for bioprinting as they mimic the physical properties of native ECM. Hydrogels can be processed for additive manufacturing by tailoring the nature of their gelation, cross-linking, and polymer composition.[346,347] Hydrogels can be further categorized as natural or synthetic, depending on their source. Hydrogels can also be blended into hybrid formulations to customize their properties.

In this section, natural and synthetic hydrogel bioinks for bioprinting microvasculature will be thoroughly reviewed. In each section, we will critically analyze and discuss the advantages and disadvantages of each platform. The structure and composition of each material will be introduced before focusing on their applications in vascular tissue engineering and bioprinting microvasculature. Hydrogel blends will be reviewed in sections corresponding to their base material. Each section will include critical discussion and outlook on the application of the respective hydrogel in bioprinting microvasculature. For this review, we focused on hydrogel bioinks that have had at least some application in vascularized bioprinting, with preference given to those that considered angiogenesis and capillary-scale microvascularization. Both in vitro and in vivo formation of microvasculature in printed bioinks were considered. There are many more hydrogels available for tissue engineering applications that are not discussed here because they have not been established in vascularized bioprinting platforms. We refer readers to refs 286,346,348,349 for more comprehensive reviews of hydrogels for tissue engineering. In general, bioinks that are highly printable, biocompatible, and form functional microvascular networks are considered ideal for bioprinting microvasculature Figure 13.

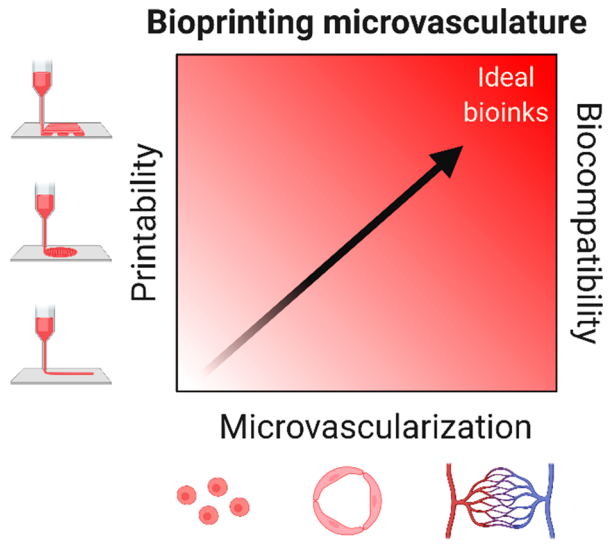

Figure 13. Ideal bioinks for bioprinting microvasculature. Created with BioRender.com.

4.1. Naturally Derived Hydrogel Bioinks

Naturally derived hydrogels originate from a biological source, which may be mammalian or nonmammalian. Naturally derived biomaterials are often isolated by extraction via solvents or enzymatic digestion. The preparations of natural hydrogels are reviewed in ref 350. Naturally derived hydrogels are favored for their biocompatibility, and some are inherently proangiogenic. Naturally derived hydrogels are widely used in tissue engineering applications[351] and can be processed for bioprinting in numerous techniques as reviewed in ref 352. Naturally derived hydrogels can be further categorized as protein-based or polysaccharide-based. Here we review protein-based and polysaccharide-based hydrogel bioinks that have been used for bioprinting microvasculature. Only those hydrogels that have been applied in bioprinting micro-

https://dx.doi.org/10.1021/acs.chemrev.0c00027
Chem. Rev. 2020, 120, 10887−10949

vasculature will be reviewed, but we acknowledge that other naturally derived hydrogels not included in this review are also suitable for bioprinting (e.g., chitosan, silk fibroin).

4.1.1. Protein-Based Hydrogels. *4.1.1.1. Collagen.* Collagen is the primary structural component of mammalian ECM and is essential for tissue formation and homeostasis. There have been 29 different types of collagen proteins identified, with type I being the most abundant. Types I, II, III, V, and XI can form fibers. Collagen IV forms a sheet and is the main scaffold component of the basement membrane that surrounds and stabilizes blood vessels.[353] Collagen has a triple helical structure with three alpha polypeptide chains composed of thousands of amino acids based on the repeating Gly-X-Y motif.[354,355] The chains form stable fibers via hydrogen and covalent bonds. Collagen-based biomaterials are widely utilized in biomedical research and tissue engineering applications and have been reviewed extensively in ref 356.

Collagen I hydrogels are excellent biomaterials for therapeutic vascularization as they provide an ideal microenvironment for angiogenesis. Collagen hydrogels can be derived from multiple animal sources, with the most common being bovine. Previous studies have shown that collagen I may stimulate angiogenesis by binding endothelial cell-surface integrins $\alpha_1\beta_1$ and $\alpha_2\beta_2$ via the GFPGER sequence of the collagen fibril.[357,358] Endothelial cells are able to degrade and invade collagen matrices via MMPs to establish vascular networks.[359] Collagen I activates Src and Rho to initiate capillary morphogenesis in ECs.[360] This leads to disruption of VE-cadherin and basement membrane proteins to drive sprouting in the surrounding matrix followed by maturation of the newly formed network Figure 14. The proangiogenic

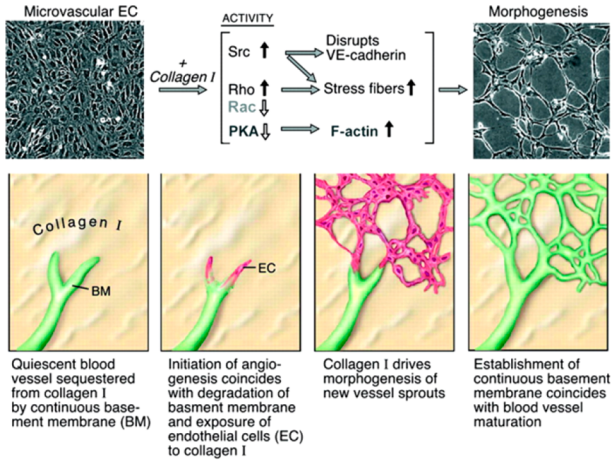

Figure 14. Influence of collagen I signaling on capillary morphogenesis in vitro. Collagen type I activates Src and Rho and suppresses Rac and PKA through β1 integrins. This results in induction of actin stress fibers, disruption of VE-cadherin, and formation of precapillary cords. Degradation of basement membrane and exposure of activated and proliferating ECs to collagen type I initiates morphogenesis of new capillary sprouts. Adapted with permission from ref 364. Copyright 2005 Wolters Kluwer Health.

capacity of collagen biomaterials depends on numerous factors, including polymer concentration and cross-linking.[361,362] Rigid collagen gels promote the formation of thick and sparsely distributed microvessel networks while softer collagen hydrogels promote thinner, more dense networks.[363] Collagen gels with low matrix density (0.7 mg/mL) cannot support endothelial cell adhesion and migration, while collagen gels that are too dense (>3 mg/mL) inhibit migration and sprout formation. Collagen hydrogels with intermediate matrix density (1.2−1.9 mg/mL) promote long, stable sprout formation by balancing endothelial cell proliferation and migration.[363]

Collagen has been used in EBB, DBB, and LAB approaches. The printability of collagen bioinks mostly depends on their storage and loss moduli before and after printing.[365] Collagen solutions at concentrations of 0.5−1.5% exhibit shear-thinning properties.[366] The moduli and gelation kinetics of collagen hydrogels are dependent on temperature and pH, with the storage modulus peaking around a pH of 8 at 37 °C (Figure 15A,B).[365] Gelation of collagen is optimal at 37 °C and a pH

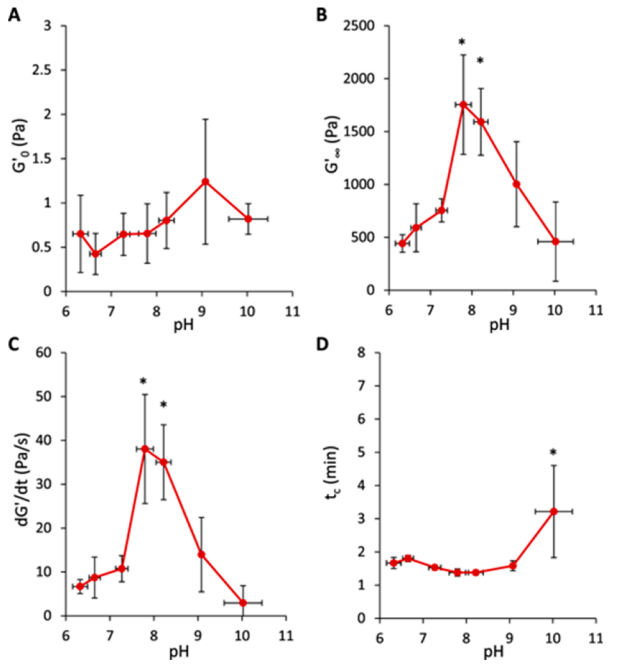

Figure 15. Rheological properties of collagen bioinks before, during, and after gelation at 37 °C. (A) Storage modulus (G') of bioink at 4 °C before gelation. (B) G' of bioink after complete gelation at 37 °C. (C) Maximum growth rate of G' after increasing temperature to 37 °C. (D) Crossover time of G' and G'' after increasing temperature to 37 °C. * indicates significant difference ($p < 0.05$) compared to pH 7.0−7.5. Reproduced with permission from ref 365. Copyright 2017 IOP Publishing Ltd.

of 8 (Figure 15C). In general, the physical cross-linking of collagen I is slow, which is unfavorable for extrusion-based bioprinting. The slow gelation results in spreading across the substrate upon deposition, which lowers the printing resolution. Gelation of collagen I at 37 °C can take several minutes. This can be quantified by the crossover time where the storage modulus (G') becomes greater than the loss modulus (G'') (Figure 15D). High cell densities can increase the gelation time of collagen,[367] and the cells may sediment before gelation is complete, leading to an inhomogeneous suspension.[218] This makes collagen-only bioinks generally unsuitable for extrusion-based 3D bioprinting. A stronger material like polycaprolactone can be used as a "framework" to support multilayer deposition of collagen-only bioinks.[368]

The printability of collagen bioinks can be improved by blending with fast-gelling materials or by using alternative

https://dx.doi.org/10.1021/acs.chemrev.0c00027
Chem. Rev. 2020, 120, 10887−10949

cross-linking mechanisms. Cross-linking reagents like EDC/NHS[369] and glutaraldehyde (GA)[370] have been used to improve the viscosity and mechanical properties of collagen, but these reagents are cytotoxic and not suitable for bioprinting live cells. Instead, cytocompatible cross-linking reagents like genipin[371] and tannic acid (TA)[372] can be used to improve the printability of collagen for EBB. Importantly, cells remain highly viable when using these reagents. Cross-linking collagen with tannic acid improves its stability by lowering its sensitivity to collagenase.[373] Recently, tannic acid cross-linked collagen bioinks were used in core/shell EBB to print a freestanding intestinal villi structure with an endogenous capillary network.[374]

Collagen bioinks have been used in a newly developed EBB technique termed "pre-set extrusion". With this method, multiple bioinks can be printed simultaneously in a predefined shape through a single nozzle.[375] Bioinks are placed into a precursor cartridge with a specific configuration and then attached to the printing nozzle. The bioinks can then be extruded into filaments containing the design of the cartridge. Printing ECs (20 million cells/mL) and hepatic cells (30 million cells/mL) in separate collagen bioinks preset in a hepatic lobule design resulted in cell viability and proliferation that were similar to a "mixed" or homogeneous design. Notably, HepG2 cells showed the indication of the improved functionality in the preset design, as evidenced by higher expression of the CYP3A4 enzyme following rifampicin exposure. Therefore, interactions between vascular and parenchymal cells in heterogeneous printed structures are different than those in homogeneous structures and may promote more organotypic function.

For DBB, collagen I has been blended with alginate to enable instantaneous cross-linking and prevent spreading after printing.[376] After the collagen had time to fully cross-link, alginate could be chelated to leave behind a pure collagen hydrogel. This improved the shape fidelity of printed collagen, but some collapse of the droplet was still evident. To address this problem, Gettler and others used a superhydrophobic surface to preserve droplet morphology while printing adipose-derived stromal vascular fraction (SVF) cell-laden spheroids with a collagen I bioink.[377] Droplets were immobilized on a hydrophobic coating of polydimethylsiloxane (PDMS) modified with hexamethyldisilazane. Spheroid morphology was preserved using this method and SVF cells remained highly viable after 14 days in static and dynamic culture. Angiogenic sprouting phenotypes were also observed. Colocalization of endothelial-specific lectin *Griffonia simplicifolia* (GS-1) and alpha smooth muscle actin (α-SMA) indicated the formation of stabilized capillary networks.

Using collagen I as a "biopaper", or printing substrate, a capillary-like network can be patterned by laser-assisted bioprinting.[278] Kerouredan et al. patterned endothelial progenitor cells onto an MSC-containing collagen hydrogel substrate (2 mg/mL) using LIFT and then overlaid it with a collagen hydrogel after printing to study subsequent microvascular network formation. Network formation depended on cell density, with higher densities (70 million cells/mL) yielding the most extensive network formation. In a follow-up study, Kérourédan et al. used LIFT for in situ micropatterning of HUVECs and stem cells from the apical papilla (SCAPs) directly onto mouse calvaria bone defects.[277] A layer of collagen substrate was first spread across the defect before cells were printed either randomly or in ring-shaped, disc-shaped, or crossed-circle-shaped designs, generating a vascularized network to promote bone regeneration. Interestingly, the extent of vascularization differed among designs. The crossed circle shape significantly enhanced vascular network formation and bone regeneration after two months. This in vivo printing platform could possibly bypass the need for an in vitro construction and maturation phase, which would shorten the time to patient bedside.

Collagen was recently used to bioprint compartments of the human heart using an embedded 3D bioprinting technique. Utilizing an updated version of FRESH (freeform reversible embedding of suspended hydrogels) bioprinting, organ-level anatomical structures were printed, including a trileaflet heart valve, multiscale vasculature, and a neonatal-scale human heart.[269] Unmodified collagen was printed as an aqueous, acidified solution into a pH 7.4 buffered granular support bath of monodisperse gelatin microparticles. Upon deposition, the collagen rapidly neutralized and gelled to form a filament, exhibiting excellent gelation kinetics. Compared to casted collagen gels, FRESH-bioprinted collagen gels loaded with VEGF promoted more extensive in vivo microvascularization. The collagen bioink used in this study was loaded into the printing reservoir as an acidic solution (pH = 3.5), which is cytotoxic. Therefore, this collagen bioink could not be seeded with cells before printing. Nevertheless, this study is a major step forward for vascularized organ bioprinting and greatly improves the printability of collagen bioinks for embedded 3D bioprinting.

Laser-based direct writing has been used for in situ patterning of capillary networks in collagen hydrogels.[300] Early work by Liu and others established an optimal collagen concentration for substrate patterning and cell viability as well as a laser fluence threshold for ablation in collagen hydrogels.[378] Hribar and others have used a near-infrared femtosecond laser to pattern microvascular networks in cell-laden collagen hydrogels.[379] Gold nanorods were mixed into the hydrogel to help convert laser energy to heat and stimulate thermal denaturation of the surrounding collagen matrix. Interestingly, ECs suspended in the collagen matrix migrated toward the etched microchannels and elongated adjacent to the hollow tube structures. However, perfusion of the patterned channels was not assessed. The authors noted a trade-off between cell viability and laser power, with higher laser energy (>150 mW) causing significant cell death and complete denaturation of the bottom of the collagen hydrogel where the NIR makes first contact. In a recent study by Brandenberg and Lutolf, a focalized pulsed laser was used to etch hollow microchannels in a collagen matrix. The authors first established feasible dimensions for the gel as well as the geometry of microfluidic networks that could be fabricated using photoablation (Figure 16A). Importantly, microchannels well below 100 μm in diameter could be patterned with their approach. The patterned microchannels (~50 μm) could then be seeded with HUVECs by microfluidic perfusion. Within 5 days, a confluent layer of HUVECs expressing CD31 and VE-cadherin was established within the channels (Figure 16B). This approach was also compatible with other naturally derived hydrogels such as agarose, gelatin, and Matrigel. While this direct writing approach can fabricate true capillary-scale microchannels, it is only feasible in millimeter-scale constructs, limiting the scalability of the technique. Nevertheless, laser-based direct writing is a promising strategy for fabricating intricate capillary-scale networks in collagen hydrogels that

https://dx.doi.org/10.1021/acs.chemrev.0c00027
Chem. Rev. 2020, 120, 10887−10949

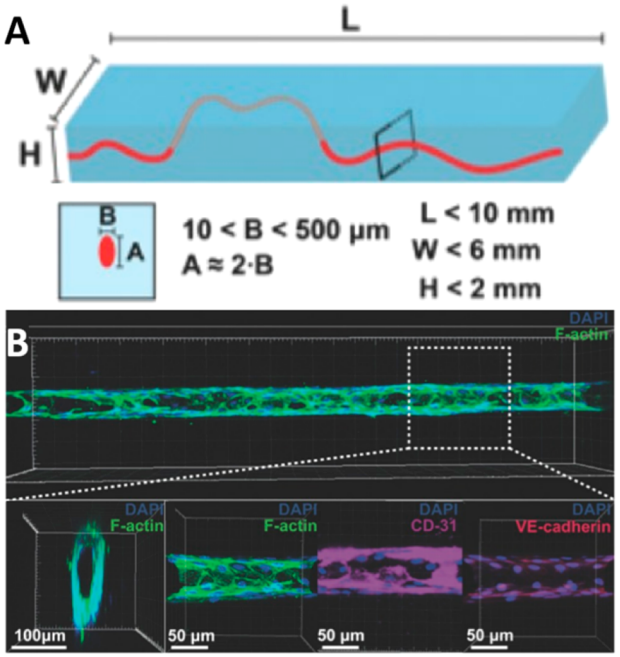

Figure 16. In situ patterning of microvasculature in collagen hydrogels with laser-assisted direct writing. (A) Schematic representation of the gel size range and microfluidic network geometry that can be processed. (B) Confocal 3D reconstruction of a hollow endothelial cell tube (HUVECs) formed in collagen type I. Adapted with permission from ref 300. Copyright 2016 John Wiley and Sons.

could not otherwise be achieved with other printing techniques. However, the intense heat generated during photoablation raises concerns about cell viability and structural integrity with these techniques. Therefore, the laser energy and writing speed must be carefully optimized to prevent significant cell death.

Collagen shows great promise as a biomaterial for bioprinting microvasculature but still faces some challenges. The limiting factor in collagen bioinks is their relatively low printability, which makes it difficult to print at capillary-scale resolution. Blending with other materials or chemical modification of collagen is currently needed to improve its printability. Laser-assisted approaches may be necessary to achieve high resolution bioprinting with collagen.[300] Collagen can be modified with methacrylate groups to be rendered photo-cross-linkable, making it feasible to print collagen via SLA approaches.[380] However, this has not yet been demonstrated. Developing novel collagen bioinks for SLA could enable high-resolution free-form fabrication and may be a promising avenue for printing microvasculature with collagen bioinks going forward. Another major obstacle is that collagen I hydrogels contract significantly (up to 50% of their initial surface area) during culture, which may compromise the intended geometry of printed constructs.[381] Mitigating this contraction is an important consideration when printing collagen-based constructs. Cross-linking collagen with succinimidyl glutarate polyethylene glycol (PEG-SG), for example, can help preserve the initial surface area of collagen hydrogels.[381] In addition, the exact composition of collagen is not well understood and can vary depending on its source and processing conditions. This lack of characterization affects the regulation of collagen biomaterial properties and raises concerns about the reproducibility of its bioactivity. Further characterization of collagen is necessary to understand its function and to tailor its printability and vasculogenic properties. As mentioned earlier, collagen sourced from bovine skin is commonly used in tissue engineering and bioprinting. Because this is a xenogenic source that carries the risk of pathogen transfer, the use of bovine collagen is not suitable for clinical translation. Bacterial engineered recombinant collagen may be a better alternative as its composition can be regulated and it poses less risk of immunotoxicity.[382] Overall, there is currently a limited availability of collagen blend bioinks tailored specifically for printing microvasculature. Leveraging the proangiogenic properties of collagen in printable bioink formulations could enable robust fabrication of 3D microvascular networks for in vitro and in vivo applications.

4.1.1.2. Fibrin. Fibrin is the main matrix component of blood clots. Thrombin-mediated proteolysis of cryptic binding sties in soluble fibrinogen proteins results in polymerization of fibrin monomers. The fibrin matrix is covalently cross-linked and stabilized by transglutaminase factor XIIIa in the coagulation cascade.[383,384] Fibrin has been widely used as a biomaterial for wound healing applications and is FDA-approved as a surgical adhesive.[385] Fibrin networks form relatively soft viscoelastic hydrogels but exhibit shear stiffening properties under high strains due to the stretching of fibrin monomers.[386] The exact properties of fibrin gels depend on the nature of their polymerization, which is influenced by thrombin concentration, salt concentration, factor XIII concentration, and pH.[387]

Fibrin bead assays have been used extensively as a model to study the fundamentals of angiogenic sprouting.[146] HUVECs sprout from microcarrier beads when cocultured with fibroblasts in fibrin gels (Figure 17A). The microporous and

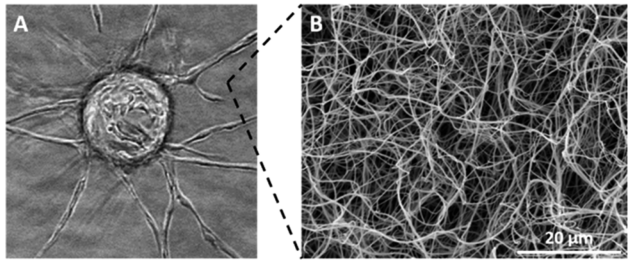

Figure 17. Angiogenic sprouting in fibrin gels. (A) Angiogenic sprouting from a HUVEC-coated bead embedded in fibrin in the presence of skin fibroblasts. (B) Scanning electron micrograph of polymerized fibrin network. (A) Reproduced with permission from ref 146. Copyright 2003 Elsevier Ltd. (B) Reproduced with permission from ref 395. Copyright 2009 The Royal Society.

nanofibrous topography of fibrin networks is conducive to cell adhesion and migration (Figure 17B). Fibrinogen binds integrin $\alpha_V\beta_3$,[388] which is required for angiogenesis.[389] Cytoskeletal changes via integrin binding and Rho signaling regulate capillary sprouting and lumen formation in fibrin gels.[390] Growth factors like FGF-2 and VEGF can bind fibrinogen to regulate endothelial cell proliferation and heparins stabilize and retain these factors within the fibrin matrix.[391,392] Prevascularization of fibrin-based constructs is known to accelerate anastomosis with host vasculature after transplantation.[393] Fibrin-based biomaterials for tissue engineering have been reviewed in ref 394.

Fibrin-only bioinks generally have poor printability. Fibrin gels have poor mechanical integrity and degrade rapidly during

https://dx.doi.org/10.1021/acs.chemrev.0c00027
Chem. Rev. 2020, 120, 10887−10949

culture. Furthermore, fibrin can take several minutes to fully polymerize.[396] Solutions of fibrinogen and thrombin must be kept separate until the moment of printing. These solutions generally have very low viscosity and are therefore suitable only for droplet-based bioprinting. Droplets of thrombin cross-linker solution can be printed onto a fibrinogen substrate to print a 2D fibrin construct.[396,397] An early study by Cui and Boland determined optimal conditions for printing human microvasculature with fibrin via thermal inkjet bioprinting.[396] Solutions of thrombin, $CaCl_2$, and HMVECs were printed drop-by-drop onto a fibrinogen substrate to form cell-laden fibrin lattice structures (Figure 18A). Printed fibers were less

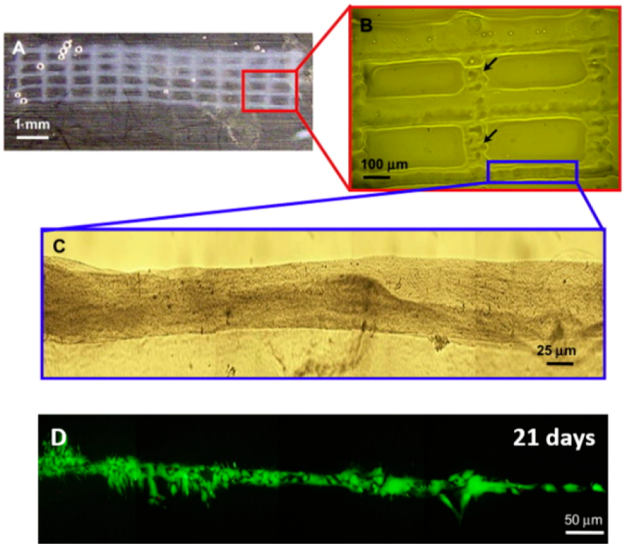

Figure 18. Printed human microvasculature in fibrin scaffold. (A) Printed fibrin scaffold using modified HP Deskjet 500 thermal inkjet printer. (B) Shape of printed fibrin scaffold after printing. (C) Individual printed fiber. (D) Printed microvasculature after 21 days. Reproduced with permission from ref 396. Copyright 2009 Elsevier Ltd.

than 100 μm in diameter but had some minor deformations (Figure 18B,C). The HMVECs proliferated and formed multicellular networks over 21 days (Figure 18D).[396] These networks were quite immature, however, and this platform was limited to 2D printing.

For 3D extrusion-based bioprinting, fibrin can be blended with more printable biomaterials and/or printed within a support scaffold material. Piard and others developed a bioink blend of fibrin (5 wt %) and gelatin (5%) to print an osteon-like scaffold containing an inner region of HUVECs and an outer region of hMSCs. Printing these discrete cellular regions led to significantly enhanced neovascularization in vivo compared to casted controls.[398] However, blending with gelatin can lead to significant mass loss during culture due to the melting and dissolution of gelatin.

Although fibrin is a favorable proangiogenic material, it is far from an ideal bioink. Therefore, fibrin is usually blended with more printable biomaterials. Fibrin bioinks can be used when angiogenesis is desired after bioprinting, but they are not suitable as the major bulk material of the printed construct because they degrade rapidly. Fibrin-only bioinks have poor shape fidelity and have mostly been used for droplet-based bioprinting of 2D tissues like skin[231] or cardiac patches.[399] Solid freeform extrusion of fibrin hydrogels is difficult due to the need to keep fibrinogen and thrombin solutions separated until after deposition. While it has not yet been explored, fibrinogen and thrombin could possibly be printed in coaxial nozzles for instantaneous cross-linking upon extrusion. Granular mediums are also a promising platform for fabricating 3D structures with poorly printable materials like fibrin.[270] To overcome the rapid degradation of fibrin, fibrinolytic inhibition via addition of aprotinin and tranexamic acid can be used to slow proteolysis.[400] The use of recombinant fibrinogen and thrombin is ideal to prevent immunogenicity of fibrin hydrogels and enable clinical translation of fibrin bioinks.[401]

4.1.1.3. Gelatin. Gelatin is a mixture of polypeptides formed from denatured collagen. Gelatin is thermoresponsive and forms a hydrogel below 37 °C by aggregation of gelatin monomers through hydrogen bonding. At temperatures higher than 37 °C, the monomers dissociate and gelatin melts, returning to a liquid state. Gelatin hydrogels contain adhesive peptide sequences like Arg-Gly-Asp (RGD) as well as protease-sensitive sites,[402,403] making it a useful biomaterial for tissue engineering and regenerative medicine.[404,405]

Human microvascular endothelial cells can form capillary networks on 2D surfaces of micropatterned gelatin.[405] Unmodified gelatin dissolves completely after 24 h of incubation[406] but can be cross-linked with glutaraldehyde to slow its degradation. Glutaraldehyde is cytotoxic, though, and should be avoided when using live cells. Phenolic hydroxyl groups can be added to gelatin for enzymatic cross-linking and tailoring of its proteolytic degradability, but this requires the presence of potentially cytotoxic hydrogen peroxide and horseradish peroxidase for cross-linking.[406] Alternatively, gelatin can be enzymatically cross-linked with microbial transglutaminase (mTG), although the gelation time is quite slow.[407] Sacrificial poly(*N*-isopropylacrylamide) (PNIPAM) microfibers have recently been incorporated into mTG-cross-linked gelatin hydrogels for developing 3D microvascular networks. At room temperature, the PNIPAM fibers melt and can be washed out to leave behind perfusable microchannels <100 μm. Refinement of this platform for 3D printing could be further explored.

Because of its fast melting at normal incubation temperatures (37 °C), gelatin is used mostly as a sacrificial bioink. Lee and others have extruded HUVEC-laden sacrificial gelatin tubes within layers of collagen to yield perfusable channels.[408] HUVECs were able to line the channel and sprout into the surrounding collagen matrix via angiogenesis. Perfusion of 10 μm fluorescent microbeads confirmed the presence of luminal structures within these capillary sprouts. In another study, the same group printed an endothelial cell-laden fibrin hydrogel bioink between sacrificial gelatin channels to generate robust multiscale vasculature in a thick collagen matrix (Figure 19).[243] Large sacrificial channels (lumen size of ~1 mm) were first printed with gelatin on top of a bottom layer of collagen. A fibrin hydrogel bioink seeded with endothelial cells and fibroblasts was then printed between the gelatin channels and followed by a top layer of collagen. The gelatin was melted and perfused with endothelial cells to form large vascular channels. During culture, capillary networks formed within the fibrin hydrogel and then connected to the large channels by sprouting angiogenesis (Figure 19A). By day 14, the microvascular bed in the fibrin hydrogel functionally connected to parent vascular channels and could be perfused. The presence of the capillary network increased the overall diffusional permeability of the construct compared to without

https://dx.doi.org/10.1021/acs.chemrev.0c00027
Chem. Rev. 2020, 120, 10887−10949

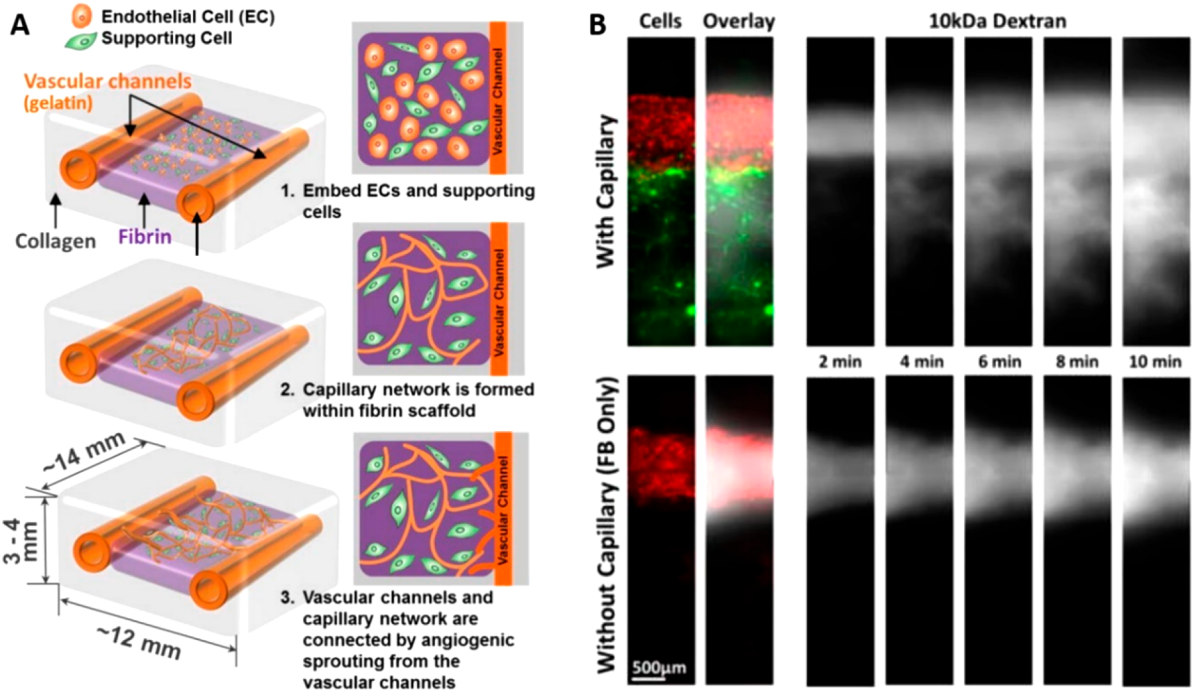

Figure 19. Functional multiscale vasculature generated by combining direct and indirect bioprinting. (A) Schematics of the growth and maturation process of bioprinted multiscale vascular system. Perfusable endothelialized vessels are patterned within collagen using sacrificial gelatin bioink. Perfusion of the channels promotes angiogenic sprouting and capillary network formation within the adjacent cell-laden fibrin gel. (B) Diffusion of 10 kDa Dextran is enhanced with capillary networks compared to without. Adapted with permission from ref 243. Copyright 2014 Springer Nature.

the capillaries (Figure 19B). This platform demonstrated the power of combining direct and indirect approaches to fabricate thick tissues with functional multiscale vascular structures down to the capillary scale.

In the FRESH bioprinting method developed by the Feinberg Lab, granular gelatin microgels have been used as sacrificial support mediums for embedded 3D bioprinting of vascular structures.[269,270,274] After printing, the gelatin matrix can easily be liquified at 37 °C and the embedded structure can be removed without any loss of structural integrity. In the first version of FRESH published in 2015, granular gelatin slurries were created by mechanical blending of a gelatin block gel in a commercial blender. The microparticles formed with this approach were relatively large (65 μm), polydisperse, and amorphous, which lead to irregular shapes and sizes of extruded filaments and limited the printing resolution of collagen to 200 μm.[270] An updated version of FRESH, published in a 2019 study, used a coacervation technique to produce smaller (25 μm), monodisperse, and spherical gelatin microparticles.[269] This greatly improved the printing resolution to as low as 20 μm.

In general, gelatin is a versatile biomaterial for bioprinting microvasculature. The biocompatibility and thermoreversibility of gelatin hydrogels makes them ideal sacrificial bioinks to pattern vascular networks within 3D constructs. However, because gelatin is commonly printed using droplet-based or extrusion-based techniques, its resolution is limited to >100 μm, which is larger than the dimension of capillaries. Therefore, gelatin must be printed with complementary biomaterials to induce capillary sprouting. Also, the thermosensitive gelation property of gelatin requires a cautious regulation on temperature during bioprinting. This may limit the application of gelatin within other biomaterial systems that have conflicting thermogelation requirements with gelatin.

4.1.1.4. Gelatin Methacryloyl (GelMA). Modification with methacrylamide and methacrylate groups is the most popular strategy to improve the stability of bioprinted gelatin. GelMA is a semisynthetic hydrogel as it is based on a naturally derived material but contains synthetic functional groups. Methacrylation enables covalent cross-linking of gelatin macromers by photopolymerization in the presence of a photoinitiator (Figure 20A,B).[409,410] Depending on their degree of methacrylation and gel concentration, GelMA hydrogels can be tuned for user-defined mechanical properties (Figure 20C).[409] GelMA hydrogels have been used in a wide range of tissue engineering applications, including bone, cartilage, and cardiac tissues.[411] Because GelMA hydrogels retain RGD sequences, they promote endothelial cell adhesion and

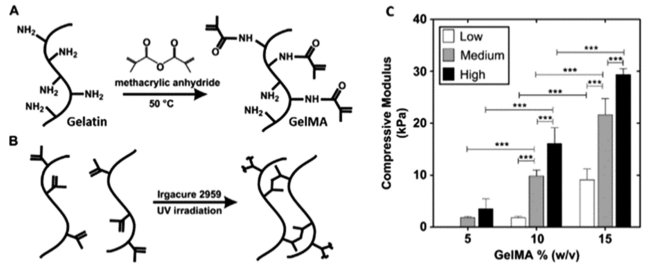

Figure 20. Synthesis and characterization of methacrylated gelatin. (A) Gelatin macromers containing primary amine groups are reacted with methacrylic anhydride (MA) to add methacrylate pendant groups. (B) Methacrylated gelatin is cross-linked using UV irradiation in the presence of a photoinitiator to yield a covalently cross-linked hydrogel. (C) Compressive modulus for 5%, 10%, and 15% (w/v) GelMA at low (~20%), medium (~50%), and high (~80%) degrees of methacrylation. Adapted with permission from ref 414. Copyright 2010 Elsevier Ltd.

https://dx.doi.org/10.1021/acs.chemrev.0c00027
Chem. Rev. 2020, 120, 10887−10949

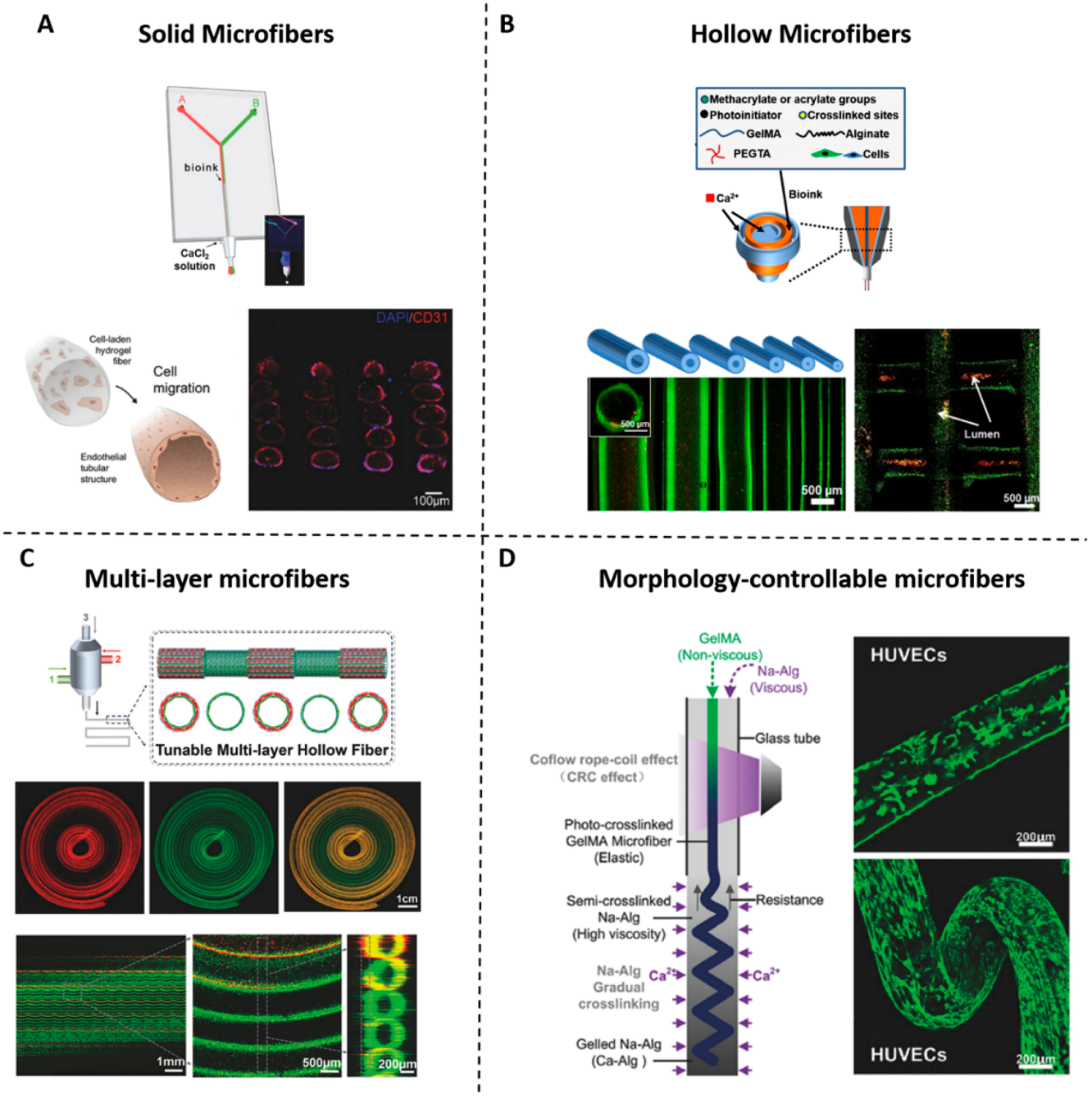

Figure 21. Bioprinting microvessels with GelMA/alginate bioinks. Several coaxial systems have been developed to bioprint (A) hollow, (B) solid, (C) morphology-controllable, and (D) multilayer hollow GelMA/alginate microfibers. (A) Adapted with permission from ref 149. Copyright 2016 John Wiley and Sons. (B) Adapted with permission from ref 417. Copyright 2016 Elsevier Ltd. (C) Adapted with permission from ref 147. Copyright 2018 John Wiley and Sons. (D) Adapted with permission from ref 416. Copyright 2018 John Wiley and Sons.

microvascular network formation.[410,412−414] The bioactivity and tunability of GelMA makes it an excellent bioink candidate for direct bioprinting of microvasculature.

Khademhosseini's research group has made pioneering efforts in developing GelMA bioinks for bioprinting. Their early efforts optimized GelMA bioinks for direct-write bioprinting of hepatocytes.[238] Because GelMA prepolymer solutions have very low viscosity, the bioinks were prepolymerized in the printing nozzle and extruded as solid filaments. This method was limited by the requirement of relatively high concentration bioinks that would be too stiff to accommodate vascular morphogenesis. In more recent studies, GelMA has been blended with alginate and printed using the coaxial extrusion technique to produce complex microfibers. These include solid, hollow, morphology-controllable, and multilayer microfibers (Figure 21).

A printable low-viscosity bioink was developed by blending GelMA with alginate and using a coaxial microfluidic printing head to extrude calcium chloride cross-linker in the outer shell.[255] The alginate immediately cross-linked upon extrusion and preserved the cylindrical fiber structure, preventing the collapse of the otherwise slow-gelling GelMA. This microfluidic approach allows for either bioink to be printed one at a time or both to be printed simultaneously in a Janus structure.

https://dx.doi.org/10.1021/acs.chemrev.0c00027
Chem. Rev. 2020, 120, 10887−10949

After printing, the GelMA can be cross-linked by UV exposure and the alginate washed out. HUVECs can be incorporated into GelMA/alginate bioinks and printed with good viability, depending on the UV exposure time. Remarkably, encapsulated HUVECs can migrate to the periphery of the bioprinted fibers after 10 days of culture, self-assembling into tubular structures (Figure 21A,B).[415]

In another study using a multichannel coaxial nozzle, hollow GelMA/alginate microfibers were digitally tuned "on-the-fly" by varying flow rates of the bioinks in the channels (Figure 21C).[147] In this study, Pi and others developed a "GAP" bioink blend of alginate, GelMA, and eight-arm poly(ethylene glycol) (PEG) acrylate with tripentaerythritol core (PEGOA) to print single- and double-layer hollow microfibers.[147] PEGOA allowed for UV-induced covalent cross-linking of the fibers after printing and improved the mechanical properties of the bioink compared to GelMA/alginate bioinks without PEGOA. The layered microfibers have been continuously tuned during printing by controlling the flow rates of $CaCl_2$ cross-linker in the core nozzle with the bioinks in the inner and outer shell nozzles. These microfibers have been directly embedded with ECs and SMCs, which exhibited high viability and formed CD31+ and α-SMA+ networks over 14 days.

Most traditional coaxial systems are only capable of producing cylindrical filaments with no control over their morphology, which limits the complexity of these methods. A novel coaxial bioprinting method was developed by Shao and others to generate morphology-controlled GelMA microfibers that resemble small-diameter blood vessels (Figure 21D).[416] On the basis of the "liquid-rope-coil effect," straight, wavy, and helical GelMA microfibers were printed within a progressively cross-linked alginate matrix. The GelMA bioink in the core was cross-linked via UV light exposure at the nozzle while sodium alginate in the shell was ionically cross-linked upon printing into a Ca^{2+}-containing bath. The flow rate of sodium alginate has been varied to tailor the diameters of straight and helical fibers, and some straight fibers had diameters below 100 μm. HUVECs directly encapsulated within the microfibers were viable, proliferative, and migrated to the periphery of the fiber during in vitro culture, forming a continuous lumen in both the straight and helical fibers. Microfibers generated in this study were not immediately perfusable, however the GelMA could theoretically be degraded from the core to leave a hollow endothelialized channel. While this platform enables more versatility in directly bioprinting microvasculature, it is mostly limited to fiber-shaped tissues like muscle fibers, nerve fibers, and blood vessels.

While coaxial nozzles are limited to the number of bioinks that can be extruded at one time, custom bioprinting nozzles have been developed to print multiple bioinks in one step. Liu and others developed a multimaterial EBB platform that could extrude seven different GelMA bioinks in a continuous, programmable fashion through a single nozzle.[261] GelMA bioinks containing different human cell types (HDFs, HUVECs, HepG2, and hMSCs) were used in this platform to create a heterogeneous heart-like structure and vascularized tissue construct. All four cell types were viable after 7 days, but vascular morphogenesis was not reported. Nevertheless, this platform could greatly increase the throughput of fabricating heterogeneous vascularized constructs.

Though GelMA contains cell-adhesive RGD sites, its vascular activity can be further enhanced through bioconjugation. For example, VEGF can be chemically immobilized to GelMA via EDC/NHS coupling chemistry (Figure 22A).[418] The GelMA+VEGF bioink significantly improved vascular

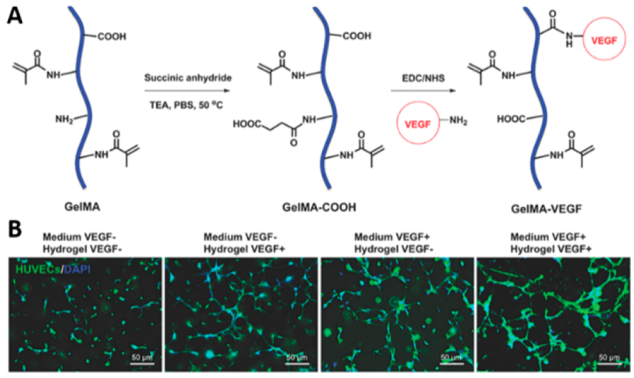

Figure 22. VEGF-conjugated GelMA bioink. (A) Schematic for the preparation of −COOH modified GelMA and chemical conjugation of VEGF. (B) Endothelial cell sprouting inside VEGF-conjugated and nonconjugated bioprinted GelMA hydrogels. Adapted with permission from ref 418. Copyright 2017 John Wiley and Sons.

morphogenesis compared to native GelMA after 5 days (Figure 22B). The bioink was applied in fabricating a pyramidal structure containing different amounts of VEGF in radial layers to create a graded vasculogenic niche. A soft GelMA bioink with low methacrylation was printed in the middle of the construct and degraded during culture to form a hollow channel within the structure. HUVECs and MSCs were able to line the channel after perfusion, forming hollow vascular lumens around 500 μm in diameter. However, angiogenic sprouting from the parent vessel into the surrounding GelMA +VEGF matrix was not demonstrated. GelMA with low methacrylation is also a poor sacrificial material, as it took 3 days to fully degrade before the channel could be perfused.

For more defined control over vascular morphogenesis in GelMA hydrogels, VEGF-mimetic peptides can be conjugated to the polymer backbone. The VEGF-mimetic "QK" peptide developed by D'Andrea and others can bind VEGFR-2 and stimulate angiogenesis.[419] Covalently immobilizing an acrylated QK peptide onto GelMA (Figure 23A) can enhance microvascular network formation (Figure 23B).[420] Cui and

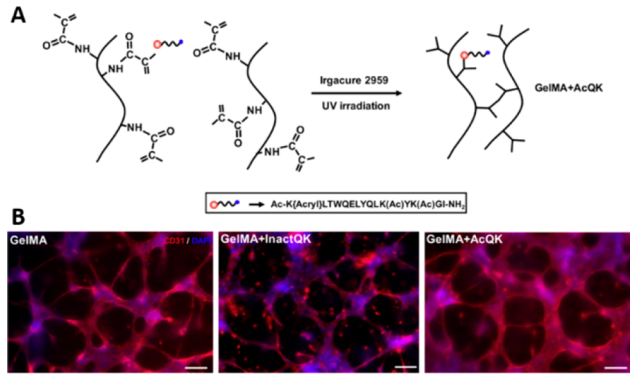

Figure 23. VEGF-peptide functionalized GelMA enhances microvascularization. (A) Synthesis of GelMA covalently immobilized with acrylated QK VEGF-mimetic peptide. (B) GelMA+AcQK hydrogels enhanced formation of tubular networks compared to unmodified GelMA. Scale bars = 100 μm. Adapted with permission from ref 420. Copyright 2017 Elsevier Ltd.

https://dx.doi.org/10.1021/acs.chemrev.0c00027
Chem. Rev. 2020, 120, 10887−10949

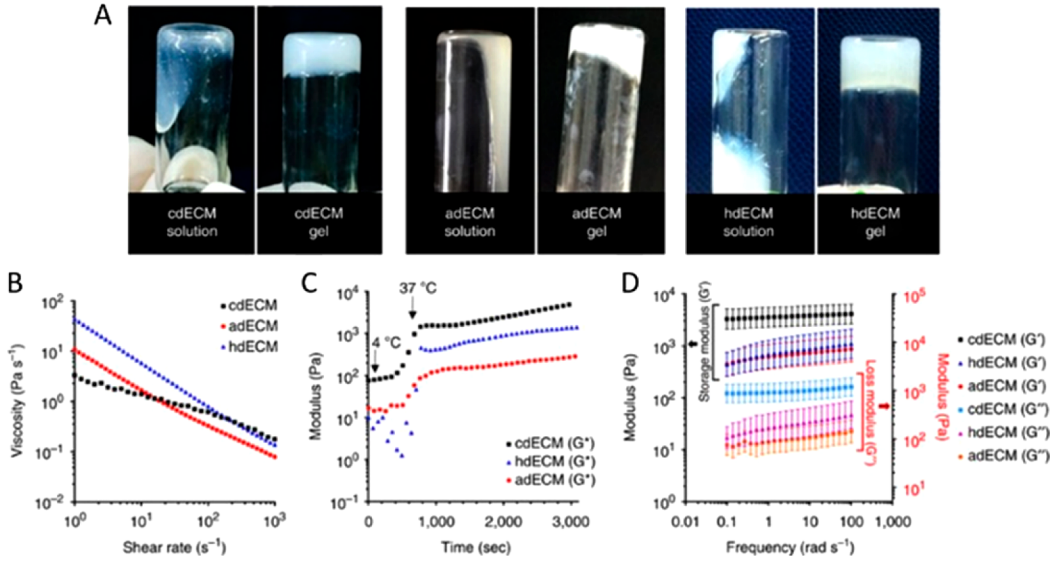

Figure 24. Rheological behavior of tissue-specific dECM bioinks. (A) Sol−gel transition of dECM pregels prepared from cartilage dECM (cdECM), heart dECM (hdECM), and adipose dECM (adECM). (B−D) Rheological properties of the dECM pregels, (B) viscosity at 15 °C, (C) gelation kinetics from 4 to 37 °C, and (D) dynamic modulus at varying frequency at 37 °C. Reproduced with permission from ref 432. Copyright 2014 Springer Nature.

others developed a catechol-functionalized GelMA (GelMA/C) bioink with an immobilized VEGF-mimetic peptide to coaxially print small-diameter vasculature along with a sacrificial HUVEC-laden Pluronic F127 slurry.[421] Catechol groups can be cross-linked rapidly in the presence of a trace amount of sodium periodate ($NaIO_4$) and adhere strongly to tissue surfaces. The fugitive slurry contained $NaIO_4$, which rapidly cross-linked the GelMA/C bioink after extrusion.[248] The VEGF peptide-functionalized GelMA/C bioink enhanced vasculature development in vitro and, after in vivo implantation, anastomosed with host vasculature and promoted capillary invasion from host tissue after 6 weeks. The use of synthetic biomimetic peptides is encouraged as they can be used to engineer chemically defined hydrogels tailored for specific cell engagement.[422] The stiffness of GelMA can also be varied to mimic the unique properties of a tissue-specific niche. Soft GelMA hydrogels promote vasculogenesis and capillary-like network formation of human dermal microvascular endothelial cells (HDMECs), while stiffer GelMA matrices can support osteogenesis and bone matrix formation by hASCs.[423] GelMA-collagen blend bioinks have been developed for droplet-based bioprinting of hMSCs and HUVECs to support capillary network and lumen formation after 14 days.[424] Blending 2.8% or 4% GelMA with 0.208% or 0.16% collagen I, respectively, leads to a bioink blend with shear-thinning properties and a higher elastic modulus. The main disadvantage to using GelMA as a bioink material is the need to use UV light exposure for cross-linking. UV light causes base damage in DNA, and while most studies have reported decent cell viability (>75%), cytotoxicity and mutagenesis are still a concern when using UV-cross-linked materials.[324] The scaling up of bioprinted tissues using GelMA will require longer UV exposures to fully cross-link the entire construct, which could compromise the viability of the encapsulated cells. Visible light cross-linkable gelatin using photoinitiators like eosin Y or Rose Bengal may be a more biocompatible alternative.[425,426] However, current visible light photoinitiators take much longer to polymerize than UV-sensitive photoinitiators.

4.1.1.5. Decellularized ECM. The extracellular matrix is nature's scaffolding material. Cell−ECM interactions are critical for vascular morphogenesis.[364] Native ECM is highly complex and its composition varies across different tissues and even regionally within the same tissue. Conventional hydrogels cannot entirely replicate the structure and function of ECM, limiting their capacity to direct cell behavior. To address these limitations, extracellular matrix can be harvested through a tissue biopsy and decellularized to leave behind just the ECM scaffolding. This yields an ideal biological template that can either be reseeded with autologous cells or processed for other tissue engineering applications as a biomaterial.

There have been many decellularization protocols developed for tissues and whole organs, with the exact methods being dependent on tissue density, geometry, and intended application. In general, decellularization protocols involve physical and chemical agents for lysing cells before rinsing them out of the tissue to leave behind pure ECM. An overview of tissue and whole organ decellularization and their applications in regenerative medicine can be found in refs 427−429. While most of the ECM proteins and gross architecture can be preserved, decellularization protocols always result in some loss of ECM surface structure and composition. Microvasculature and other microscale features of native ECM are particularly difficult to preserve during decellularization.[428,430,431] Therefore, seeding decellularized ECM scaffolds with endothelial cells often results in incomplete microvascularization. Inadequate microvasculature is a major source of failure for decellularized organ transplants, as leaky vessels and exposed ECM cause edema and blood coagulation.[430,431]

Decellularized ECM can be processed for bioprinting to build vascularized tissues from the bottom-up. These bioinks possess proangiogenic ECM proteins and growth factors that many conventional hydrogels lack unless supplemented exogenously. Even then, conventional hydrogel bioinks provide a matrix that mimics broad aspects of soft tissue, while dECM bioinks sourced from specific tissues can more accurately

https://dx.doi.org/10.1021/acs.chemrev.0c00027
Chem. Rev. 2020, 120, 10887−10949

recapitulate the ECM content of that tissue. For example, lyophilized dECM from adipose, cartilage, and heart tissues have been used to print tissue-specific analogues. After decellularization, the dECM was converted into a powder and solubilized into pregel solutions that were liquid below 10 °C and gels above 37 °C (Figure 24A). Interestingly, the rheological properties of the dECM bioinks varied across tissue sources (Figure 24B−D). The dECM bioinks supported long-term cell viability 14 days after printing.[432] While structural elements of the dECM were lost during conversion to a powder, the tissue-specific bioinks still promoted lineage differentiation and structural maturation of human tissue-derived mesenchymal stem cells. However, the bioinks had to be kept below 15 °C while printing to prevent gelation, which may compromise cell viability during long printing sessions. Also, the slow physical gelation of the dECM bioink prevented it from being printed in multiple layers without a PCL support scaffold.

The mechanical properties of dECM bioinks can be tailored by incorporating photosensitive cross-linking agents. For example, vitamin B2-induced UVA cross-linking can be used to increase the mechanical strength and stability of dECM bioinks.[433] Incorporating various PEG-based cross-linkers (linear, four-arm, and eight-arm) can also be used for fine-tuning the mechanical properties of dECM-based bioinks.[434] Methacrylate groups have been added to kidney-derived dECM (KdECM) bioinks for covalent photo-cross-linking.[435] This allowed for tunable stiffness before and after printing and KdECMMA hydrogels were significantly more stable in culture compared to nonmethacrylated KdECM.

The capacity of dECM to promote vascular morphogenesis depends on its source. Interestingly, human dermal microvascular endothelial cells (hDMVECs) secrete significantly more proangiogenic factors and express more angiogenesis-related genes when cultured on dECM derived from vascularized tissues (e.g., tracheal mucosa) compared to avascular tissues (e.g., cornea).[436] Therefore, it may be best to source dECM bioinks from tissues that are naturally vascularized because their composition would provide microenvironmental cues of vascular niches. Accordingly, dECM bioinks derived from vascular tissue (i.e., aorta) have been developed to treat ischemic disease[437] and volumetric muscle loss.[438] Gao et al. used a hybrid bioink of vascular-derived dECM (VdECM) and alginate to print tubular "bio-blood-vessels". The hybrid bioink provided a suitable environment for proliferation, differentiation, and neovascularization of EPCs, and the dual ionic and thermal cross-linking gave the bioink good printability. Loading the bioink with PLGA microparticles for controlled release of atorvastatin, a proangiogenic drug, significantly enhanced functional recovery, capillary density, and arteriole density in a murine hindlimb ischemia model.[437] Cho et al. used a VdECM bioink and granular gelatin support bath to 3D print a prevascularized muscle construct that improved vascularization, innervation, and functional recovery in a rat model of volumetric muscle loss.[438] Coaxial printing of the bioinks led to more robust $CD31^+$ networks along the fibers in vitro compared to if the bioinks were homogeneously mixed. Therefore, using the coaxial technique to compartmentalize different bioinks improved their overall performance, highlighting the synergy between method and material to enhance the spatial organization and biomimicry of printed vascularized tissues.

Vascular-derived dECM (VdECM) bioink was further utilized in another study to coaxially bioprint freestanding, perfusable, and functional microvessels. VdECM was combined with alginate in the shell, while Ca^{2+}-containing Pluronic F127 (CPF1−27) was printed in the core (Figure 25A).[439]

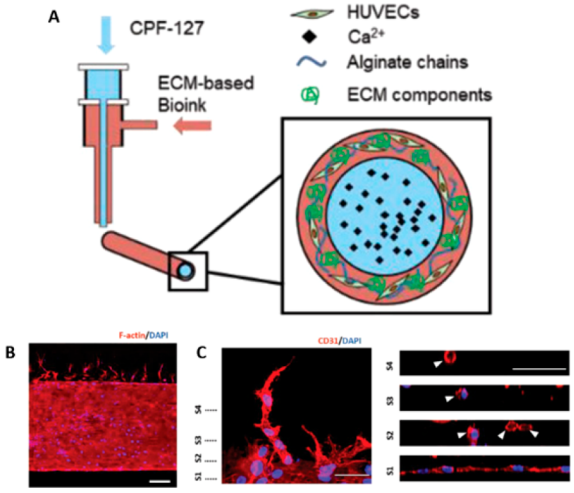

Figure 25. Coaxial bioprinting functional microvasculature with vascular-derived dECM bioinks. (A) Coaxial cell-printed vessels using HUVECs-laden VdECM/alginate hybrid bioink. (B,C) Angiogenic capillary sprouting of microvessels into collagen hydrogel containing proangiogenic growth factors [scale bars: 200 μm (B) and 50 μm (C)]. Adapted with permission from ref 439. Copyright 2018 John Wiley and Sons.

CPF-127 preserved the patency of the microchannels while simultaneously cross-linking alginate in the VdECM-containing bioink. Pluronic F127 and poloxamer bioinks are discussed further in section 4.2.2. The diameter of the printed vessels depended on the needle size, with 25G nozzles capable of printing channels with a diameter around 250 μm. When HUVECs were printed within the channel, they formed a stable monolayer after a week in culture. A collagen hydrogel with or without growth factors (VEGF and bFGF) was cast around the endothelialized vessels to model angiogenic sprouting from the parent vessel toward a chemokine gradient. Endothelial cells from the main channel only sprouted into collagen containing growth factors (Figure 25B,C), eventually forming lumenized capillaries by day 3.

While decellularized ECM offers unique advantages over other natural hydrogels in terms of biomimicry, it is often sourced nonautologously. This poses a threat of immune response or pathogen transfer in humans if the ECM is not processed thoroughly. For example, alpha gal antigen, which is a carbohydrate found in mammals and not primates, was found remaining in porcine-derived dECM even after aggressive decellularization.[440] In contrast, autologous dECM from human omentum tissue did not stain positive for alpha gal antigen and elicited a lower immune response compared to xenogenic and allogenic dECM, highlighting source-dependent differences in biocompatibility of dECM. Moreover, human omentum dECM hydrogels could efficiently reprogram patient-derived iPSCs into multiple lineages, including endothelial cells, demonstrating that ECM from omentum, which is a highly vascularized tissue, possesses requisite physical and biochemical cues to generate personalized

https://dx.doi.org/10.1021/acs.chemrev.0c00027
Chem. Rev. 2020, 120, 10887−10949

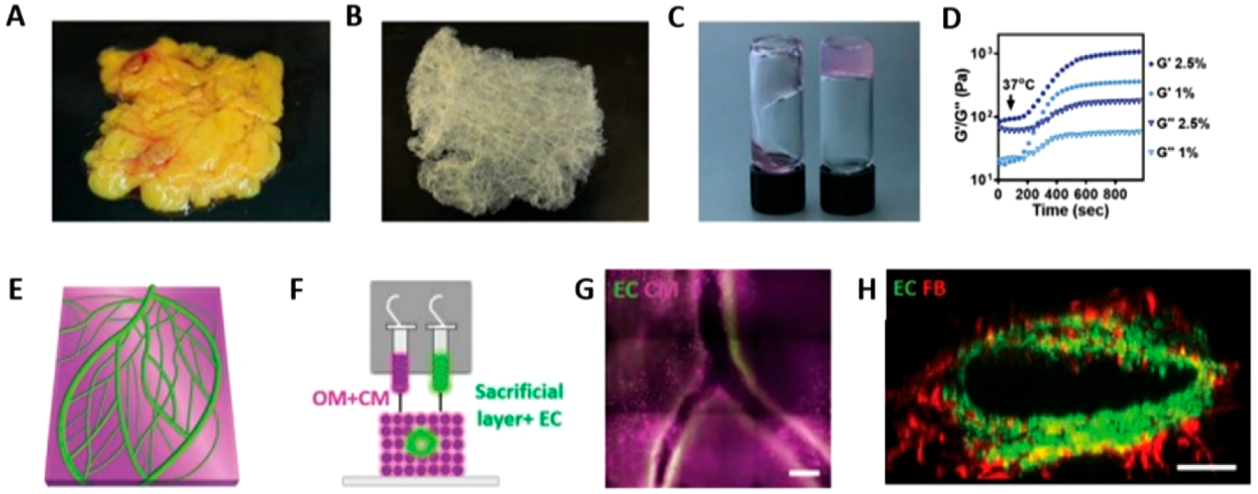

Figure 26. Personalized dECM bioinks for autologous bioprinting of microvascularized constructs. (A,B) Human omentum tissue (A) before and (B) after decellularization. (C) dECM hydrogel at room temperature (left) and after gelation at 37 °C (right). (D) Rheological characterization of 1% w/v and 2.5% w/v omentum hydrogels, exhibiting gelation at 37 °C. (E) 3D model of a vascularized cardiac patch. (F) Concept of printing vascularized, patient-specific cardiac tissue with distinct cellular bioinks. (G) Patient-specific cardiac patch printed with blood vessels (CD31 in green) embedded within cardiac tissue (actinin in pink). (H) Cross-section of a single lumen, showing the interaction of GFP-expressing ECs and RFP-expressing fibroblasts. Adapted with permission from ref 273. Copyright 2019 Wiley-VCH, under the terms of the Creative Commons (CC BY 4.0) License https://creativecommons.org/licenses/by/4.0.

hydrogels for engineering autologous vascularized tissue replacements.

Noor and others converted dECM from patient-derived human omentum tissue into a personalized bioink to bioprint personalized cardiac patches and perfusable heart-like structures.[273] Omentum biopsies could be decellularized and converted into concentrated aqueous solutions (1−2.5% w/v) that were thermoresponsive, forming a weak gel at room temperature and increasing in storage modulus upon incubation at 37 °C (Figure 26A−D). Microvascularized cardiac patches were fabricated using cardiomyocyte-laden omentum bioink and a sacrificial gelatin bioink containing ECs (Figure 26E,F). The ECs adhered to the surrounding omentum matrix during incubation (Figure 26G) and the gelatin could be evacuated, leaving behind viable endothelial cell-lined channels around 300 μm in diameter (Figure 26H). Spreading and vascular morphogenesis of the ECs was not demonstrated, however. Using a granular support bath made of gelatin microparticles and xanthan-gum supplemented culture medium, the omentum dECM bioink was then used to print a perfusable small-scale bifurcated blood vessel and vascularized heart-like structure with discrete ventricle compartments. The printed vasculature in this application was relatively large, and incorporation of smaller microvasculature would be needed to enable the viability and function of such thick tissues.

Overall, dECM bioinks offer unique advantages over conventional hydrogel bioinks. They better recapitulate the biochemical and microenvironmental properties of native ECM compared to conventional hydrogels, making dECM bioinks an attractive biomaterial for supporting vascular morphogenesis. The extrudability of dECM bioinks can be improved by blending with fast-gelling materials like alginate or using a support scaffold like PCL or granular support medium for embedded 3D bioprinting. For printing vascularized tissues and organs, ECM derived from tissues that are naturally vascularized (i.e., omentum) may be suitable for providing a proangiogenic microenvironment to ECs. The greatest promise of dECM bioink platforms is the possibility of printing fully autologous, personalized tissue and organ replacements. Recent work from Tal Dvir's research group has provided proof for this concept, but microvasculature will need to be more of a focus in future studies. Current dECM bioinks have mostly been developed for extrusion-based bioprinting, which has limitations in resolution. Future efforts could explore photo-cross-linkable dECM bioinks for high-resolution printing via SLA. Improvements in decellularization methods are also necessary to preserve more of the ECM components that are lost during the decellularization process. Preservation of these ECM components through the refinement of decellularization protocols can further improve the bioactivity of dECM bioinks.

This section has reviewed protein-based naturally derived hydrogels for bioprinting microvasculature. These hydrogels are summarized in Table 2. In the following section, we will review naturally derived polysaccharide-based hydrogels and their applications in bioprinting microvasculature.

4.1.2. Polysaccharide-Based Hydrogels. *4.1.2.1. Agarose.* Agarose is a linear polysaccharide composed of repeating units of agarobiose, a disaccharide of D-galactose and 3,6-anhydro-l-galactopyranose. Agarose gelation is thermoreversible, with gelation typically occurring between 30 and 40 °C and melting between 80 and 90 °C. These properties depend on agarose concentration, molecular weight, and number of side groups.[441] Aqueous agarose solutions undergo a three-stage gelation process: induction, gelation, and pseudoequilibrium.[442] At its gelation point, agarose molecules form helical structures by electrostatic interactions and hydrogen bonding between oxygen and hydrogen in the side groups.[443] The self-gelling feature of agarose makes it easy to use and highly biocompatible because potentially toxic cross-linking agents are not needed. Therefore, agarose-based biomaterials have been used for tissue engineering and regenerative medicine.[444]

As a bioink, agarose is most suitable for extrusion-based bioprinting due to its viscoelasticity and shear-thinning properties at high concentrations, but concentrations below 4% may be suitable for DBB if printing temperatures are

https://dx.doi.org/10.1021/acs.chemrev.0c00027
Chem. Rev. 2020, 120, 10887−10949

Table 2. Protein-Based Hydrogel Bioinks for Bioprinting Microvasculature[a,b]

biomaterial	bioink formulation	concentration	printing approach	technique	cell type	cross-linking	printed structures	capillary formation?	ref
collagen	collagen I	4% w/v	direct	EBB	HUVECs	chemical	capillary region of intestinal villi model	yes	374
	collagen I	3 mg/mL	direct	EBB	stromal vascular fraction cells	physical	SVF cell-laden collagen spheroid	yes	377
	collagen I + VEGF + fibronectin	in vitro: 24 mg/mL in vivo: collagen I: 12 mg/mL VEGF: 100 ng/mL fibronectin: 60 μg/mL	Indirect	embedded 3D bioprinting	n/a	physical	in vitro: Multiscale vasculature of human heart in vivo: microporous scaffold	yes	269
	collagen I	3 wt %	direct	EBB	EA.hy926 endothelial cells	physical	hepatic lobule structure	yes	375
	collagen I + gold nanorods	collagen I: 0.4% w/v gold nanorods: 6×10^{-10} M	direct	LAB	bEnd.3 endothelial cells	physical	3D microfluidic networks	yes	379
	collagen I	0.4% w/v	direct	LAB	perfused with HUVEC suspension	physical	in situ patterned microfluidic networks	yes	300
fibrin	thrombin + $CaCl_2$	thrombin: 50 U/mL $CaCl_2$: 80 mM	direct	DBB	HMVECs	enzymatic	lattice structure	yes	396
	fibrinogen/gelatin blend	fibrinogen: 10% w/v gelatin: 5% w/v	direct	EBB	in vitro: HUVECs in vivo: RAECs	enzymatic	osteon-like scaffold	yes	398
gelatin	gelatin	10 wt %	indirect	EBB	HUVECs	physical	perfusable vascular channel within collagen hydrogel	yes	408
	gelatin	15 wt %	indirect	EBB	perfused with HUVEC suspension	physical	perfusable vascular networks within OBB matrix	no	272
gelatin methacryloyl (GelMA)	GelMA/alginate	GelMA: 4.5% w/v alginate: 4% w/v	direct	EBB	HUVECs	chemical and physical	heterogeneous vascularized 3D construct	no	149
	GelMA/alginate/PEGTA	GelMA: 7% w/v alginate: 3% w/v PEGTA: 2% w/v	direct	EBB	HUVECs and MSCs	chemical and physical	perfusable vascular constructs	no	417
	GelMA + sodium alginate	GelMA: 5% w/v alginate: 2% w/v	direct	EBB	HUVECs	chemical and physical	morpholog-controllable microfibers	no	416
	VEGF-functionalized GelMA	5−10% w/v	direct	EBB	HUVECs and hMSCs	chemical	vascularized bone tissue construct	yes	418
	VEGF peptide- functionalized GelMA/Catechol + Pluronic F127 and sodium periodate ($NaIO_4$)	GelMA: 20% w/v pluronic F127:30% w/v $NaIO_4$: 23.4 nM	direct	EBB	HUVECs and HCASMCs	oxidative and physical	small-diameter vasculature with smooth muscle and endothelium	yes	248

https://dx.doi.org/10.1021/acs.chemrev.0c00027
Chem. Rev. 2020, 120, 10887−10949

Table 2. continued

biomaterial	bioink formulation	concentration	printing approach	technique	cell type	cross-linking	printed structures	capillary formation?	ref
	GelMA/collagen	GelMA: 2.8% or 4.0% w/v collagen: 0.16% or 0.208% w/v		DBB	HUVECs and hMSCs	physical and chemical	proangiogenic hydrogel structures	yes	424
	GelMA	15% w/v	direct	LAB	HUVECs	chemical	hemisphere structures	yes	319
dECM	vascular dECM (VdECM)/alginate+ atorvastati-loaded PLGA microspheres		direct	EBB	EPCs	physical	"bio-blood- vessel" constructs	yes	437
	vascular dECM (vdECM) + skeletal muscle dECM (mdECM)		direct	embedded 3D bioprinting	HUVECs	physical	vascularized muscle fibers	yes	438
	VdECM/alginate		direct	EBB	HUVECs	physical	freestanding vascular tubes	yes	439
	omentum dECM + gelatin sacrificial ink		indirect	embedded 3D bioprinting	iPSC-ECs and HNDFs	physical	vascularized cardiac patch and heart-like structures	no	273
	heart or liver dECM/GelMA		direct	LAB	n/a	chemical	hierarchical branched vascular structure	yes	322

[a]n/a = not applicable. [b]EBB = extrusion-based bioprinting; SVF = stromal vascular fraction; LAB = light-assisted bioprinting; DBB = droplet-based bioprinting; RAEC = rat aortic endothelial cell; OBB = organ building blocks; PEGTA = poly(-ethylene glycol)-tetra-acrylate; LAP = lithium phenyl-2,4,6-trimethylbenzoylphosphinate; HCASMC = human coronary artery smooth muscle cell; dECM = decellularized extracellular matrix; HNDF = normal human dermal fibroblasts.

maintained above 37 °C to prevent clogging.[222] Low concentration agarose bioinks spread across the substrate and have poor integrity after extrusion but can be blended with alginate for better printability.[445] Agarose has also been used as a bioink for LIFT bioprinting.[446] Agarose hydrogels have suitable swelling and degradation properties for bioprinting and can provide structural support to 3D printed constructs.[222]

Agarose rods have been used as a bioprinting template to indirectly pattern microchannels ranging from 250 to 500 μm in diameter within casted methacrylated gelatin (GelMA) hydrogels (Figure 27). The microchannels were perfusable and

Figure 27. Bioprinted agarose microchannels. Agarose hydrogel fibers (green) with diameters ranging from 250 to 500 μm could be printed and cast in a GelMA hydrogel before being removed and perfused with fluorescent beads (pink) or endothelial cells. Reproduced with permission from ref 239. Copyright 2015 Royal Society of Chemistry.

could be seeded with ECs that adhered and spread along the GelMA surface. After the GelMA hydrogel was cross-linked, the agarose rods had to be physically removed, making this approach only feasible for microchannels with simple geometries. Otherwise, physical removal of biomaterials would disrupt the shape and integrity of the printed structure, especially for delicate capillary-scale microvasculature.

While agarose is biocompatible, agarose hydrogels do not readily support endothelial cell adhesion.[447] Therefore, agarose has been blended with other biomaterials that are cell-adhesive (e.g., Matrigel, collagen).[448] Agarose−collagen blend bioinks can support adhesion and spreading of human umbilical artery smooth muscle cells.[449] In agarose−collagen blend bioinks, agarose provides long-term mechanical stability in culture while collagen provides microenvironmental cues for vasculogenesis. Kreimendahl and others found that blending 0.5% agarose with 0.5% collagen supported HUVEC assembly into capillary-like networks after 14 days without significantly affecting the printability of agarose.[450] Blending agarose and collagen led to a significantly altered shear modulus compared to pure agarose or collagen and the shear modulus of AGR0.5COLL0.5 bioinks increased with increasing temperature. The microvascular networks contained lumens from around 5 to 30 μm in diameter, and HUVECs were found to spread alongside collagen fibrils. This provides a promising platform to directly print microvasculature with agarose-based bioinks.

Besides blending, agarose may also be chemically modified for innate vasculogenic properties. Carboxylation of the agarose backbone can switch the secondary structure of agarose hydrogels from α-helix to β-sheet.[451] Carboxylation diminishes hydrogen bonding between polymer chains and leads to less helical−helical interactions, resulting in softer hydrogels. The degree of carboxylation can be varied to tailor the mechanical properties of agarose hydrogels. Modifying soft, carboxylated agarose with RGD peptides led to apical polarization in HUVECs and lumen formation around 50−100 μm. RGD-functionalized carboxylated agarose (60%)

https://dx.doi.org/10.1021/acs.chemrev.0c00027
Chem. Rev. 2020, 120, 10887−10949

matched the stiffness of fibrin clots (~0.5 kPa) and, upon injection, stimulated angiogenesis, capillary stabilization, and recruitment of $CD11b^+$ myeloid and $CD11b^+/CD115^+$ monocytes in vivo.[452] Carboxylated agarose was recently shown to be extrudable and possess shear-thinning properties depending on the degree of carboxylation.[452] MSCs had higher viability when printed with carboxylated agarose bioinks compared to native agarose.[453] However, the ability of this emergent material to promote microvascularization in a bioprinted construct has yet to be shown.

Hollow channels with diameters less than 200 μm have been fabricated within photolabile agarose hydrogels to guide neural cell migration,[454] but this technique has not been explored for vascular engineering. Further optimization of laser-assisted bioprinting approaches with agarose could enable high-resolution patterning of microvascular channels for endothelial cell growth within mechanically stable agarose-based hydrogels.

Overall, agarose-based bioinks are mostly used for improving the mechanical integrity of printed structures due to their stability at physiological temperatures. For direct bioprinting of microvasculature, agarose must be blended with bioactive materials or chemically modified with adhesive motifs. Indirect bioprinting of small-diameter vascular channels has been accomplished with agarose-based bioinks, but capillary-scale microvasculature remains a challenge. More systematic studies are needed to optimize agarose-based bioinks for high-resolution printing of microvasculature.

4.1.2.2. Alginate. Alginate is a naturally derived anionic polysaccharide commercially obtained from brown algae (*Phaeophyceae*) and is structurally characterized as an unbranched linear copolymer of (1,4)-linked β-D-mannuronate (M) and α-L-guluronate (G) residues. Carboxylate groups in the G-blocks of alginate can be ionically cross-linked via divalent cations like Ca^{2+}, Ba^{2+}, Mg^{2+}, and Sr^{2+} in an "egg-box" model as proposed by Morris et al.[455] The properties of alginate hydrogels depend on the molecular weight and ratio of M and G blocks in the polymer chain, which vary depending on the source of the alginate.[456] We refer readers to a review by Lee and Mooney in ref 457 for more details on the properties of alginate.

Alginate has been extensively used as a bioink and can be adapted for several printing modalities, including DBB, EBB, and LAB, as reviewed in ref 458. The rheological behavior of alginate solutions for bioprinting have been studied in detail.[459] Alginate possess several features that are favorable for bioprinting. Alginate has excellent gelation kinetics and can be cross-linked instantly in the presence of divalent cations (e.g., calcium chloride). Sodium alginate is shear-thinning,[459,460] which reduces the shear stresses experienced by cells in alginate bioinks. The degradation profiles of alginate hydrogels can be tailored by periodate oxidation of uronic acid residues[461] or by gamma irradiation to modify alginate's molecular weight distribution.[462] The viscosity of alginate bioinks mainly depends on alginate concentration, molecular weight, cell density, temperature, and pH. Our lab has systematically evaluated oxidized alginate bioinks for printability and cytocompatibility in droplet-based bioprinting (Figure 28).[463]

Xu and others have printed multiple cell types into complex heterogeneous tissue constructs containing microvascular networks using inkjet bioprinting.[228] The cell types included human amniotic fluid-derived stem cells (hAFSCs), canine smooth muscle cells (dSMCs), and bovine aortic endothelial cells (bECs). Each cell type was suspended in a solution of calcium chloride ($CaCl_2$) before being printed in a "pie" shape onto an alginate/collagen printing substrate. The cells have been printed in discrete regions and promoted tissue vascularization after 2 weeks of subcutaneous implantation in mice. Importantly, printing cells in a specific pattern improved vascularization compared to manually seeded cells.

Oxidized alginate bioink selection

Ox. \ Conc.	2	5	8	10	15	20
0	-	+	+	-	-	-
1	-	-	+	+	-	-
3	-	-	+	+	-	-
5	-	-	-	+	+	-
10	-	-	-	-	+	+

Figure 28. Printable alginate bioink formulations for droplet-based bioprinting. Summary table of the preferable range of alginate bioink formulations with high printability (green) based on three important printability criteria: homogeneous cell suspension, high printing resolution, and high cell viability. Reproduced with permission from ref 463. Copyright 2014 Elsevier Ltd.

For extrusion-based bioprinting, Khalil and Sun were the first to explore a "fabrication window" for bioprinting viable ECs using alginate bioinks.[464] Low wt % alginate bioinks best support endothelial cell viability, but these hydrogels suffer from poor printability and mechanical stability during culture. Alginate can be cross-linked before printing to enable better shape fidelity after extrusion, but this may lead to deformities in printed constructs. To address this, alginate has been mixed with gelatin to improve its printability because gelatin is slightly viscous at room temperature.[465] Gao and others have recently taken a systematic approach to optimize alginate–gelatin composite bioinks for solid freeform extrusion.[466] Their study identified an important role for the loss tangent (G''/G') in balancing printability and cytocompatibility.

Coaxial bioprinting systems have become the most popular modality for printing vascularized constructs with alginate bioinks. Alginate is the most widely used biomaterial for coaxial bioprinting because it can be rapidly cross-linked with calcium chloride upon extrusion. Calcium chloride cross-linker solutions in the core or shell can allow for the extrusion of hollow or solid alginate microfibers. Alginate is often blended with proangiogenic biomaterials for coaxial bioprinting of vascularized constructs.

Besides coaxial extrusion, alginate bioinks have recently been utilized in embedded 3D bioprinting approaches. By including calcium chloride in the support matrix, alginate bioinks can be cross-linked rapidly during embedding. Cell-laden alginate bioinks have been printed with high resolution in Ca^{2+}-containing gelatin supports via FRESH bioprinting.[269,270] Wang and others recently used alginate as a sacrificial bioink to embed 3D vascular networks within prepolymers of agarose/gelatin and GelMA hydrogels.[467] The alginate cross-linked within the Ca^{2+}-loaded prepolymer, leaving behind a channel that could be washed out after solidifying the prepolymer (Figure 29A). While hierarchical networks were fabricated with this approach (Figure 29B,C), the smallest

https://dx.doi.org/10.1021/acs.chemrev.0c00027
Chem. Rev. 2020, 120, 10887−10949

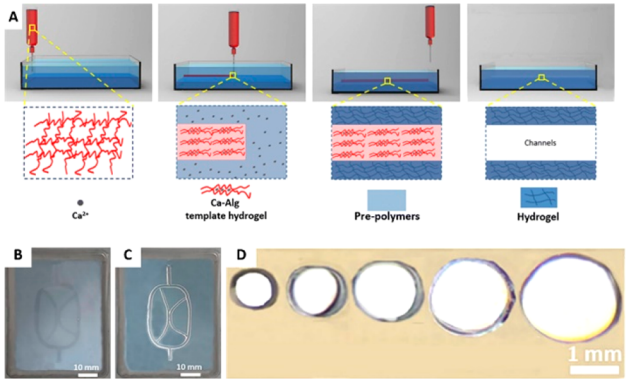

Figure 29. Patterning vascular networks in a prepolymer support matrix with sacrificial alginate bioink. (A) Schematic of fabricating patterned vascular networks by direct writing alginate bioink inside the prepolymer of hydrogels. (B) Patterned templates and (C) hollow microchannels printed with sacrificial alginate within a GelMA support matrix. (D) Cross sections of microchannels with varying diameters fabricated with the direct writing approach. Reproduced with permission from ref 467. Copyright 2019 Springer Nature.

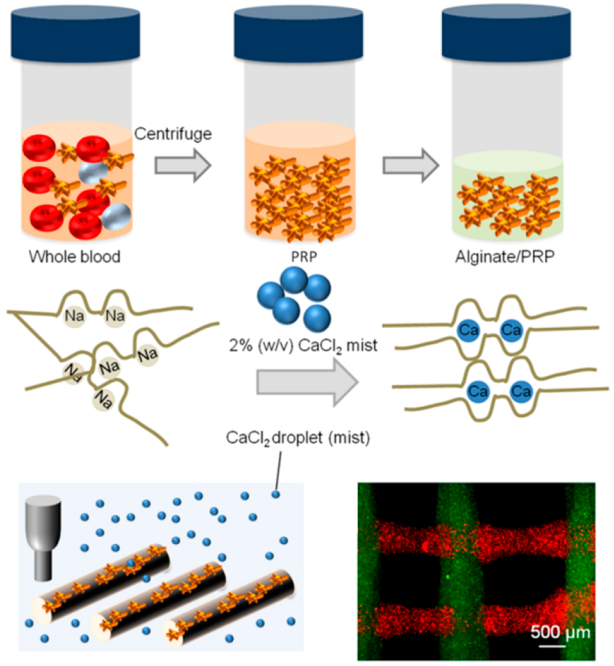

Figure 30. Alginate-based bioink with autologous growth factors. Platelet-rich plasma (PRP) is incorporated within alginate to form the bioink and can be bioprinted to form a scaffold embedded with autologous growth factors. Adapted with permission from ref 470. Copyright 2018 John Wiley and Sons.

diameter channel was around 400 μm, which is much larger than capillaries (Figure 29D). Therefore, the prepolymer support matrix would need to encourage angiogenesis from the parent channels for adequate microvascularization of the construct.

While alginate hydrogels are highly printable, bare alginate is bioinert and does not support vascular morphogenesis. Therefore, there have been numerous approaches to improving the bioactivity of alginate. Alginate bioinks can be loaded with proangiogenic growth factors to stimulate vascularization and controlled release from alginate improves the potency of VEGF when compared to adding it directly to bulk media.[468] Laponite, a synthetic clay, has been blended with alginate to improve its printability and enable sustained release of growth factors.[469] Faramarzi and others have developed patient-specific alginate-based bioinks by incorporating platelet-rich plasma (PRP) as an autologous source of angiogenic growth factors (Figure 30).[470] The alginate/PRP bioink enhanced vascular network formation with HUVECs in vitro compared to native alginate, but this was only demonstrated in 2D. Branched vascular structures were also printed with the alginate/PRP bioink, but multilayer 3D organization of microvascular networks was not demonstrated. Nevertheless, using autologously sourced growth factors could broadly improve the translational potential of proangiogenic bioinks.

Besides growth factor supplementation, alginate can be modified with synthetic bioactive peptides like RGD to support cell adhesion. Injectable RGD−alginate hydrogels have been shown to promote endothelial cell adhesion and proliferation in vitro and angiogenesis in vivo.[471,472] Torres and others found that injectable RGD-alginate microgels with higher M-to-G ratios can guide vascular morphogenesis in vitro and promote anastomosis with host vasculature in vivo due to lower cross-link density in the alginate matrix.[473] The applications of proangiogenic alginate hydrogels in bioprinting have not been fully realized. RGD−alginate hydrogels could be useful for bioprinting microvasculature, and their printability should be evaluated along with other peptide-modified alginates in future studies. This should be relatively straightforward, as certain material properties required for injection are also in agreement with extrusion (i.e., shear-thinning).

Overall, the printability and biocompatibility of alginate hydrogels make them an excellent biomaterial for bioprinting. The rapid gelation of alginate allows one to essentially blend their hydrogel of choice with alginate for improved gelation and shape fidelity during printing. However, alginate bioinks are mostly suitable for extrusion-based systems where resolutions below 100 μm are rarely achieved, necessitating angiogenesis in the construct after printing to generate microvasculature. New developments in photoreactive alginate may enable printing structures less than 100 μm using techniques like stereolithography.[474] While there have been many studies using growth factors or bioactive peptides to promote angiogenesis in alginate-based hydrogels, their potential for bioprinting microvasculature has not been explored. Future investigations should evaluate the printability of peptide-functionalized alginate hydrogels to expand the design space of vasculogenic and angiogenic alginate bioinks.

4.1.2.3. Carbohydrate Glass. Carbohydrate glass is formed by the solidification of melted sugar and sugar-alcohol solutions upon cooling. Isomalt, a sugar-alcohol commonly used in culinary applications, is the most common form of carbohydrate glass used for bioprinting. Sugar glass is an ideal sacrificial material because it is highly printable, water-soluble, and biocompatible. Furthermore, carbohydrate glass is cheap and readily available. Nanoscale glass fibers can be produced via melt-spinning sugar (cotton candy). These fibers have been embedded in PDMS to create a sacrificial microvascular network similar in size and density to capillaries.[475] Sugar glasses can also be extruded as filaments if kept above their glass-transition temperature during printing. The filaments cool rapidly upon extrusion at room temperature and form stiff, brittle filaments. Because of their rapid curing, sugar glass

https://dx.doi.org/10.1021/acs.chemrev.0c00027
Chem. Rev. 2020, 120, 10887−10949

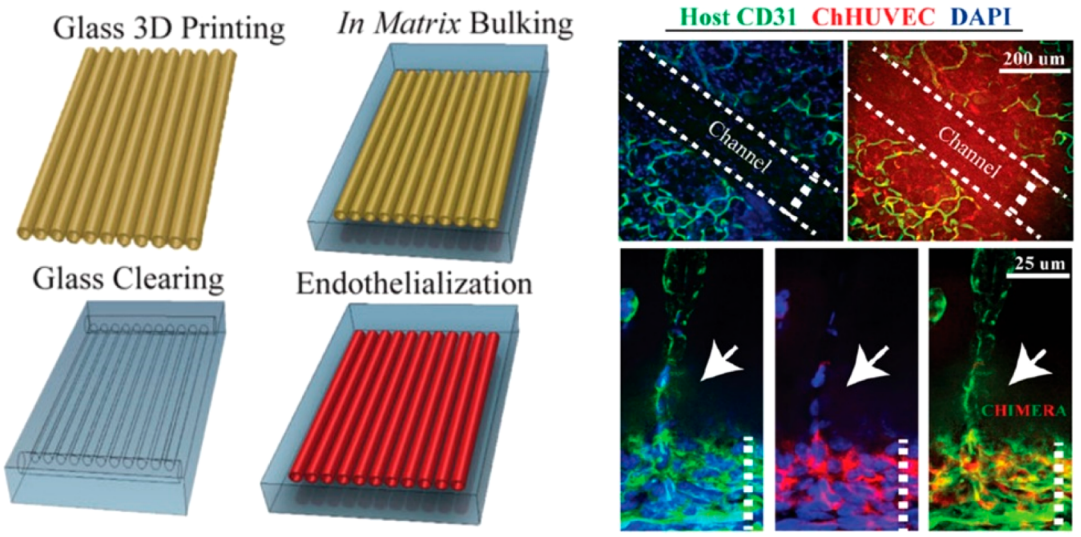

Figure 31. Bioprinting microvasculature with carbohydrate glass. Hydrogels can be cast around sacrificial glass networks and implanted to functionally anastomose with host microvasculature, forming chimeric vessels. Adapted with permission from ref 478. Copyright 2017 Springer Nature.

filaments can be precisely printed as freestanding structures using model-guided design.[476,477]

In their seminal work, Chen and others used a sacrificial network of carbohydrate glass to pattern vascular networks within cell-laden hydrogels.[242] Depending on nozzle travel speed, filaments between 200 and 1000 μm could be extruded and a variety of ECM biomaterials could be cast around the networks. The channels can be dissolved within minutes, leaving behind perfusable vascular networks within the construct. Importantly, perfusion of the networks with HUVECs led to endothelialized channels that exhibited angiogenic sprouting from the main channel into the bulk fibrin hydrogel. In a subsequent in vivo study, 3D printed carbohydrate glass networks within a fibrin bulk matrix (10 mg/mL) promoted angiogenesis and integration with host vasculature (Figure 31).[478] This improved perfusion in animal models of hind limb ischemia and myocardial infarction. A disadvantage of these approaches was that the bulk ECM could only be cast homogeneously instead of 3D printed, inhibiting precise placement of cells and ECM around the sacrificial network.

A related study investigating surgical anastomosis of vascular networks made by sacrificial sugar glass determined that the networks could withstand pulsatile flow as evidenced by Doppler perfusion in a hindlimb ischemic model.[479] However, this was only confirmed up to 3 h postimplantation. Vascularization of the surrounding PDMS bulk matrix was not demonstrated, likely due to the inability of PDMS to support cell adhesion and migration. More biocompatible hydrogels like alginate can be cast around sugar glass filaments loaded with calcium chloride.[480]

Overall, carbohydrate glass is an excellent fugitive material for indirectly patterning vascular networks within biocompatible hydrogels. To date, applications of carbohydrate glass in printing microvasculature have mostly used simple cylindrical structures >100 μm. Below these diameters, sugar glass is quite fragile and may break during casting. Future work should develop sugar glass formulations for printing smaller, more intricate microvascular networks that remain intact during fabrication. Furthermore, temporospatial printing of cell-laden hydrogels around sacrificial glass networks would be a more biomimetic approach to printing microvascularized matrices than homogeneous hydrogel casting. Concerns about hyperglycemic response of suspended cells to the concentrated sugar solutions should also be addressed.

4.1.2.4. Hyaluronic Acid. Hyaluronic acid (HA), or hyaluronan, is a nonsulfated glycosaminoglycan found ubiquitously in human ECM. It helps maintain the structure and fluid homeostasis in loose connective tissues.[481] HA can influence cell morphogenesis by directly binding the cell surface hyaluronan receptor CD44, as well as other receptors.[482] Furthermore, HA is highly hydrophilic and forms hydrated networks that permit intercellular signaling.[483] The polymer structure of HA is a linear polysaccharide composed of repeating units of a disaccharide, β-1,4-D-glucuronic acid−β-1,3-*N*-acetyl-D-glucosamine. The molecular weight of HA ranges from 10^3 to 10^4 kDa depending on the source. Low molecular weight HA oligosaccharides stimulate endothelial cell proliferation, migration, and angiogenesis by binding CD44 receptors expressed by ECs.[484] In physiological conditions, HA proteins take on an expanded random coil conformation and entangle to form continuous hydrated networks. Their conformation can be further influenced by HA-binding proteins known as hyaladherins.[485]

Physical gelation of HA yields fragile hydrogel networks that rapidly degrade. Therefore, many alternative cross-linking strategies have been developed to improve the stability of HA hydrogels, as reviewed in refs 486 and 487. The carboxylic acid and *N*-acetyl groups of HA can be targeted for chemical modification by various chemistries. Methacrylated HA (MeHA), developed by Burdick and others, has been widely used to generate photopolymerizable HA hydrogels with tunable mechanical and degradation properties.[488] MeHA hydrogels have been used to support self-renewal and differentiation of hESCs.[489] Bioactive peptides like RGD can be conjugated to acrylated hyaluronic acid (AHA) for further control over cellular adhesion and migration in HA-based hydrogels.[490,491] Gerecht's research group has pioneered the development of HA hydrogels to engineer microvascular networks from pluripotent stem cells in vitro (Figure 32). We

https://dx.doi.org/10.1021/acs.chemrev.0c00027
Chem. Rev. 2020, 120, 10887−10949

refer readers to refs 492−496 for more about hyaluronic acid hydrogels and their applications in engineering microvasculature.

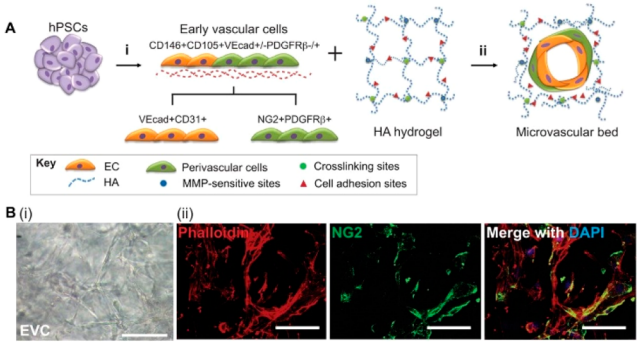

Figure 32. Engineered vascular network from pluripotent stem cells within a hyaluronic acid hydrogel matrix. (A) Human pluripotent stem cells (PSCs) differentiate into early vascular cells that can mature into functional endothelial cells (i) and perivascular cells (ii) when placed within a designer synthetic hyaluronic acid (HA) hydrogel. (B) PSC-derived EVCs self-assemble into networks in HA hydrogels (i) and form hollow capillary structures stabilized by NG2+ perivascular cells (ii). Reproduced with permission from ref 496. Copyright 2014 Company of Biologists.

Cross-linking HA with acrylated synthetic polymers can improve its rheological properties and suitability for bioprinting.[497,498] Methacrylated collagen has also been combined with thiolated HA to develop a hybrid bioink for 3D bioprinting liver microenvironments.[499] Vessel-like constructs have been bioprinted with extrudable MeHA and GelMA blend bioinks in a two-step UV cross-linking approach.[500] Tetracylated PEG can be added to these blends to further improve their mechanical properties after printing.[501] However, these bioinks have been limited to large-diameter vessel constructs.

The Burdick laboratory has developed HA bioinks based on guest−host supramolecular chemistry for embedded 3D bioprinting.[271] Adamantane (Ad, guest) and β-cyclodextrin (CD, host) can be conjugated to HA and physically cross-link to form shear-thinning and self-healing hydrogels. This allows for shear-thinning guest−host HA bioinks to be printed directly into self-healing guest−host HA hydrogel matrices in a technique known as "GHost writing". During nozzle translation, Ad-HA and CD-HA interactions are disrupted but quickly recover to solidify around the extruded material in the wake of the nozzle. Microfibers with diameters as low as 35 μm can be printed with this method, depending on the nozzle size. Guest−host HA hydrogel bioinks can either be used as sacrificial or stabilized bioinks depending on their chemical modifications (Figure 33). Primary modification with guest and host functionalities yields a sacrificial bioinks, while secondary modification with methacrylate groups allows for

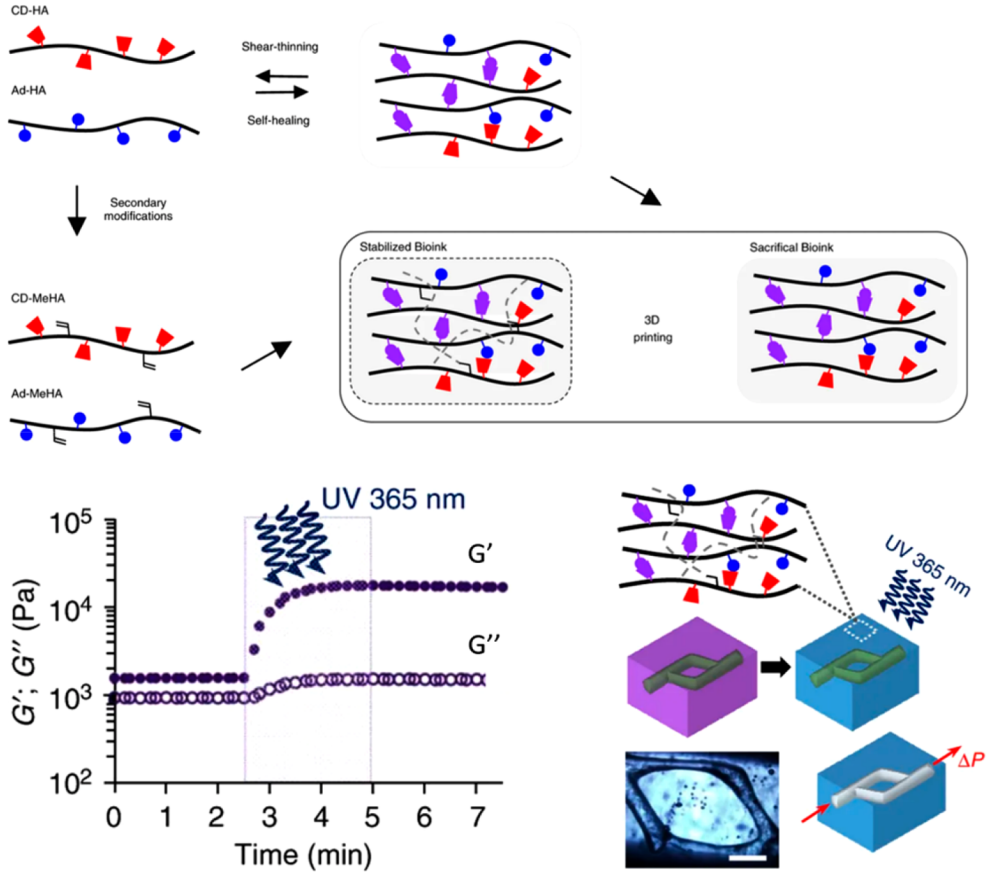

Figure 33. Bioprinting microvasculature with supramolecular guest−host hyaluronic acid bioinks. Physically cross-linked guest−host HA hydrogels can serve as sacrificial bioinks, while methacrylated guest−host HA hydrogels can be covalently cross-linked by UV to form a mechanically stabilized bioink. Sacrificial guest−host HA bioinks can be embedded within stabilized guest−host MeHA hydrogels to fabricate a perfusable network (scale bar = 500 μm). Adapted with permission from ref 502. Copyright 2017 Spring Nature.

https://dx.doi.org/10.1021/acs.chemrev.0c00027
Chem. Rev. 2020, 120, 10887−10949

Table 3. Polysaccharide-Based Hydrogel Bioinks for Bioprinting Microvasculature[a,b]

biomaterial	bioink formulation	concentration	printing approach	technique	cell type	cross-linking	printed structures	capillary formation?	ref
agarose	agarose	2−8 wt %	indirect	EBB	perfused with HUVEC suspension	physical	microchannels in GelMA matrix	no	517
	agarose and collagen	agarose: 0.5 wt % collagen: 0.5 wt %	direct	DBB	HUVECs and HDFs	physical	hydrogel column	yes	450
alginate	alginate	0.8 wt %	Indirect	DBB	n/a	physical	Bifurcation model with 90 μm channel	yes	376
	alginate	1.5 wt %	direct	EBB	Rat heart endothelial cells	physical	3D lattice construct with viable ECs	no	464
	alginate	1−3 wt %	indirect	embedded 3D bioprinting	perfused with HUVEC suspension	physical	patterned vascular networks in agarose/gelatin and GelMA hydrogels	no	467
	alginate + $CaCl_2$ + platelet-rich plasma	alginate: 1% w/v $CaCl_2$: 0.025% w/v plasma: 50 U	direct	EBB	HUVECs	physical	branching vascular structure	no	470
carbohydrate glass	sugar glass maintained at 165 °C	25 g glucose + 53 g sucrose + 10 g dextran in 50 mL water	combined	EBB	perfused with HUVEC suspension	physical	patterned vascular networks in multiple hydrogel matrices	yes	242
	sugar glass maintained at 155 °C	100 g isomalt + 10 g dextran in 60 mL water	indirect	EBB	perfused with HUVEC suspension	physical	patterned vascular networks in a fibrin hydrogel	yes	478
	sugar glass	n/a	Indirect	EBB	n/a	physical	patterned vascular networks in a PDMS hydrogel	yes	479
	sugar glass + $CaCl_2$ maintained at 110 °C	3% w/v	indirect	EBB	n/a	physical	patterned vascular networks in an alginate hydrogel	no	480
hyaluronic acid (HA)	Ad-HA and CD- HA	Ad-HA: 4 wt % CD-HA: 4 wt %	indirect	embedded 3D bioprinting	perfused with HUVEC suspension	chemical and physical	endothelialized microchannels in cell-degradable HA support hydrogels	yes	244
	GMHA/gelMA	GMHA: 2% w/v GelMA: 5% w/v	direct	LAB	HUVECs and ADSCs	chemical	vascularized hepatic model	yes	503
	HA/GelMA	HA: 1% w/v GelMA: 2.5% w/v	direct	LAB	HUVECs and 10T1/2 cells	chemical	prevascularized tissue constructs with complex 3D microarchitecture	yes	504

[a]n/a = not applicable. [b]HDF = human dermal fibroblast; Ad = adamantane; CD = cyclodextrin; GMHA = glycidyl methacrylate-HA.

https://dx.doi.org/10.1021/acs.chemrev.0c00027
Chem. Rev. 2020, 120, 10887−10949

stabilization bioink stabilization after printing. Accordingly, perfusable microchannels can be fabricated by printing sacrificial guest−host HA bioinks within stabilized HA bioinks. These channels can last up to 30 days in culture, depending on the degree of methacrylation.[502] Incorporating RGD peptides and protease-degradable cross-linkers into the support hydrogel for GHost writing can support robust capillary sprouting from parent channels.[244] GHost writing with HA bioinks represents an outstanding emergent method to print high-resolution microvasculature with HA hydrogels.

Because methacrylated HA is photoreactive, it can also be printed using laser-assisted methods, which offer better resolution. Glycidal methacrylate-hyaluronic acid (GMHA) and GelMA bioinks have been used to print an iPSC-derived vascularized hepatic lobule model with DLP-SLA.[503] This method used an interesting approach whereby digital masks were applied in a two-step sequential manner to print a first layer of hiPSC-derived hepatic cells in 5% (w/v) GelMA followed by a layer of endothelial and mesenchymal supporting cells (HUVECs and ADSCs) in 2.5% GelMA and 1% GMHA. The HUVECs formed microvascular networks after 7 days of culture, and the triculture model significantly enhanced liver-specific gene expression and functions in 3D. In another study, Zhu and others used DLP-based microscale continuous optical bioprinting (μCOB) to create prevascularized constructs containing a "base" layer of HepG2 cells in 5% (w/v) GelMA and a "vascular" layer of HUVECs and 10T1/2 cells in 2.5% GelMA and 1% HA.[504] Lithium phenyl-2,4,6-trimethylbenzoylphosphinate (LAP) was used as a cytocompatible photoinitiator. By using different digital masks, heterogeneous vascularized constructs could be printed with gradient channel widths regionally controlled biomaterials properties. Encapsulated HUVECs formed lumen-like structures and microvascular networks after 1 week of in vitro culture. Furthermore, the prevascularized networks could functionally anastomose with murine host vasculature after two-week subcutaneous implantation. Nonprevascularized constructs were shown to integrate poorly with host vasculature.

The versatility and biocompatibility of hyaluronic acid makes it a useful biomaterial for bioprinting microvasculature. The mechanical and bioactive properties of HA hydrogels can be finely tuned through various chemical methods, making HA an excellent canvas biomaterial for engineering "semi-synthetic" bioinks with highly controllable microenvironments. There have been impressive platforms developed recently to promote human microvascular network formation in engineered HA hydrogels.[494] These platforms can potentially be adapted for the development of bioinks with highly defined proangiogenic microenvironments.

This section has reviewed polysaccharide-based naturally derived hydrogels for bioprinting microvasculature. These hydrogels are summarized in Table 3. Synthetic hydrogels will be reviewed in the following section along with their applications in bioprinting microvasculature.

4.2. Synthetic Hydrogel Bioinks

Synthetic hydrogels are based on hydrated networks of polymers synthesized using chemical methods. The chemical and physical properties of synthetic polymers can be tightly controlled depending on the monomers used and the nature of their cross-linking. Synthetic hydrogels are known for their inability to support cell adhesion but can be functionalized with bioactive peptides for cell-mediated adhesion and degradation.[505,506] This makes synthetic hydrogels excellent canvas materials for user-defined functionalities. Synthetic hydrogels are highly printable because their physicochemical properties can be tailored to meet the printability requirements of a given technique. In this section, we will review common synthetic hydrogel bioinks applied in bioprinting microvasculature.

4.2.1. Poly(ethylene glycol) (PEG). Poly(ethylene) glycol, or PEG, is a popular synthetic biomaterial for a variety of biomedical applications. PEG is a linear polyether compound and is favored for its hydrophilicity and resistance to protein and cell adsorption. PEG is generally biocompatible and elicits minimal immune response, although there is some emerging evidence demonstrating anti-PEG antibodies produced in rodents.[507] PEG is often modified with diacrylate (DA) or methacrylate (MA) groups for free-radical polymerization. This affords PEG hydrogels with highly tunable and defined mechanical properties. Importantly, PEG is nontoxic and other biomaterials that have limited tunability can be "PEGylated" or cross-linked with PEG monomers to tailor their physical properties.

PEG hydrogels do not possess cell attachment sites and are nonbiodegradable. Therefore, various strategies have been developed to engineer PEG hydrogels with proangiogenic properties. Growth factors like VEGF, bFGF, and PDGF as well as proangiogenic signaling ligands like EphrinA1 can be covalently bound to PEGDA hydrogels to promote EC migration and tubulogenesis.[508−510] Protease-sensitive degradation sites can also be engineered into multiarm PEG matrices for cell-mediated matrix remodeling and self-assembly into vascular networks Figure 34.[511−513] Interestingly,

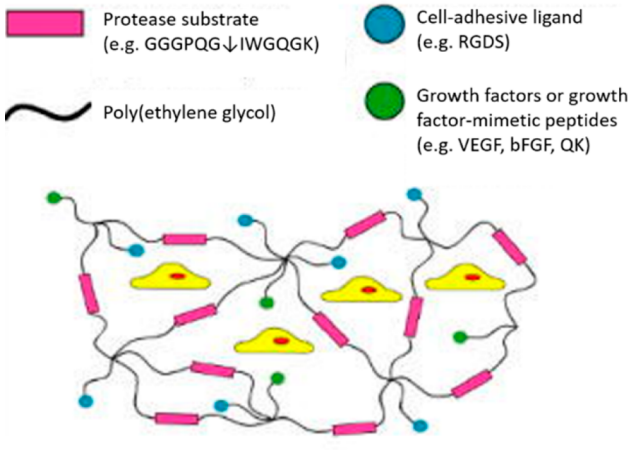

Figure 34. Schematic of proteolytically degradable PEG hydrogels to promote vascular morphogenesis. The ↓ represents an MMP-cleavable site. Adapted with permission from ref 513. Copyright 2010 Elsevier Ltd.

conjugating the VEGF-mimetic peptide QK to PEG hydrogels significantly enhances vascular morphogenesis compared to PEG-VEGF or VEGF alone.[514] Multiarm PEGs offer numerous sites for conjugating different bioactive substrates, enabling the engineering of complex proangiogenic microenvironments within PEG hydrogels.

PEG hydrogels have been used in various bioprinting approaches. For EBB, PEGs are mostly used to tune the mechanical integrity of extrudable bioinks. Multiarm PEGs can

https://dx.doi.org/10.1021/acs.chemrev.0c00027
Chem. Rev. 2020, 120, 10887−10949

increase the shear modulus of hydrogel bioinks due to higher cross-linking density. Co-cross-linking multiarm PEGs with thiolated hyaluronic acid and gelatin can enable 3D printing of vessel-like constructs that support cell viability for up to 4 weeks.[501] Adding four-armed PEG acrylate (PEG-4A) to methacrylated gelatin and methacrylated hyaluronic acid cryogels improved their mechanical properties and supported capillary network formation in a coculture of ADSCs and HUVECs.[515]

In a microfluidics-assisted bioprinting approach, bioinks containing PEG monoacrylate-fibrinogen (PF) and alginate were used to print multicellular lattice constructs of varying geometries.[516] The role of alginate was to immediately cross-link the bioink to preserve its shape during printing, while PF could be covalently cross-linked after printing for long-term stability as well as promoting cell attachment. Alginate could be removed by EDTA after printing, leaving behind pure PF fibers around 100 μm in diameter. After 7 days, especially in Janus constructs, HUVECs migrated to the periphery of the fibers and formed vascular-like tubes with lumens around 150 μm. These vascular networks were able to anastomose with host vasculature in mice after subcutaneous implantation for 15 days.

Most of the studies using PEG biomaterials employ cross-linking methods that require UV exposure. More biocompatible cross-linking strategies are necessary to maximize cell viability in PEGylated hydrogels. Rutz et al. have developed a PEGX toolkit to manipulate the properties of PEG-based bioinks before and after printing (Figure 35).[256] In the PEGX method, PEG is functionalized with reactive groups on both ends which represent the "X". PEGX can then be used to cross-link a variety of polymers with a diverse selection of chemical methods. The mechanical properties of the resulting gel can be tuned depending on the concentration of PEGX as well as its molecular weight and display of functional groups. For cell-encapsulating PEGX bioinks, cytocompatible cross-linking chemistries like click chemistry and Michael-type additions can be used. In a recent study, Rutz and others used Thiol Michael type addition and tetrazine-norbornene click chemistry to tailor post printing mechanical properties and cell viability in gelatin-based bioinks.[518] HUVECs can be printed using the PEGX method, but vascular morphogenesis has not been demonstrated. Nevertheless, PEGX bioinks could offer great flexibility in expanding the printability of otherwise poorly printable hydrogels like gelatin. It would be interesting to investigate vascular morphogenesis in PEGX systems that place more consideration on angiogenesis in the future. For example, protease-sensitive proangiogenic PEG hydrogels like those described in the previous paragraph could theoretically be developed into a bioink for direct bioprinting of microvasculature with the PEGX method.

Most PEG hydrogels are modified for UV-based cross-linking, which makes them amenable to laser-assisted bioprinting approaches. Zhang and others have patterned biomimetic 3D capillary structures in PEGDA hydrogels using projection-based stereolithography.[319] In a more recent study, Grigoryan et al. fabricated vascular structures with unprecedented complexity in PEGDA hydrogels using a custom projection stereolithography apparatus for tissue engineering (SLATE). These structures included entangled multivascular networks with intravascular features that mimic the sophistication of in vivo vasculature. A voxel resolution of 50 μm was achieved using cytocompatible tartrazine as a photoabsorber.

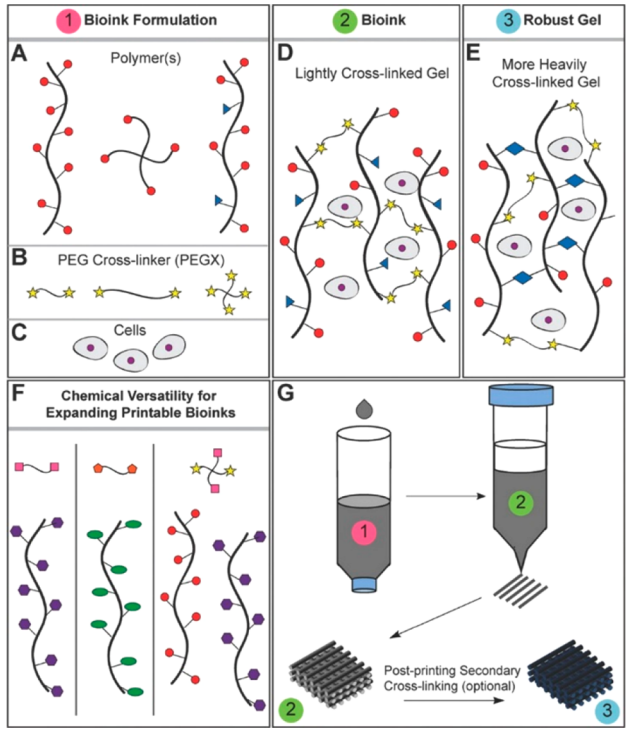

Figure 35. PEGX method for tuning bioink printability. (A) Polymer or polymer mixtures can be linear (e.g., gelatin), branched (e.g., four-arm PEG amine), or multifunctional (e.g., gelatin methacrylate). (B) PEGX can be linear or multiarm and can be various chain lengths. (C) Cells can be optionally incorporated by (D) mixing with polymers and PEGX to form the bioink. (E) Secondary cross-linking can increase mechanical robustness after printing. (F) By changing the reactive groups of PEGX, polymers of other functional groups may be cross-linked. (G) Printing process of PEGX bioink method and corresponding phase. Reproduced with permission from ref 256. Copyright 2015 John Wiley and Sons.

Furthermore, the vascular networks could be endothelialized and incorporated into a hydrogel carrier to support engraftment of hepatic aggregates in nude mice. Though the networks generated with this approach were highly sophisticated in form, their lumen diameter was above 100 μm and therefore did not recapitulate capillaries. The 20% (w/v) PEGDA hydrogel formulation would also be much too stiff to promote angiogenesis from the parent vascular network. It is unclear whether the light blocking additives would allow for the fabrication of patent capillary-like networks. Incorporation of the identified light blockers into a more proangiogenic hydrogel may facilitate the formation of capillary networks in vitro and in vivo using this approach.

PEG hydrogels are useful biomaterials for direct writing via LAB. Culver and others used two-photon laser scanning lithography to pattern immobilized bioactive peptides in a PEG scaffold.[519] In this study, acrylated PEG was functionalized with a matrix metalloproteinase peptide (GGPQGIWGQGK, abbreviated PQ) for cell-mediated degradation and an RGDS peptide for cell adhesion. Both peptides were acrylate-terminated, and a photoinitiator was incorporated into the PEG matrix so that, upon excitation with a tightly focused two-photon laser, site-specific immobilization could take place via addition polymerization. Unbound peptides could then be washed away, leaving behind a precisely organized 3D pattern of immobilized biomolecules with features as small as 5 μm in

https://dx.doi.org/10.1021/acs.chemrev.0c00027
Chem. Rev. 2020, 120, 10887−10949

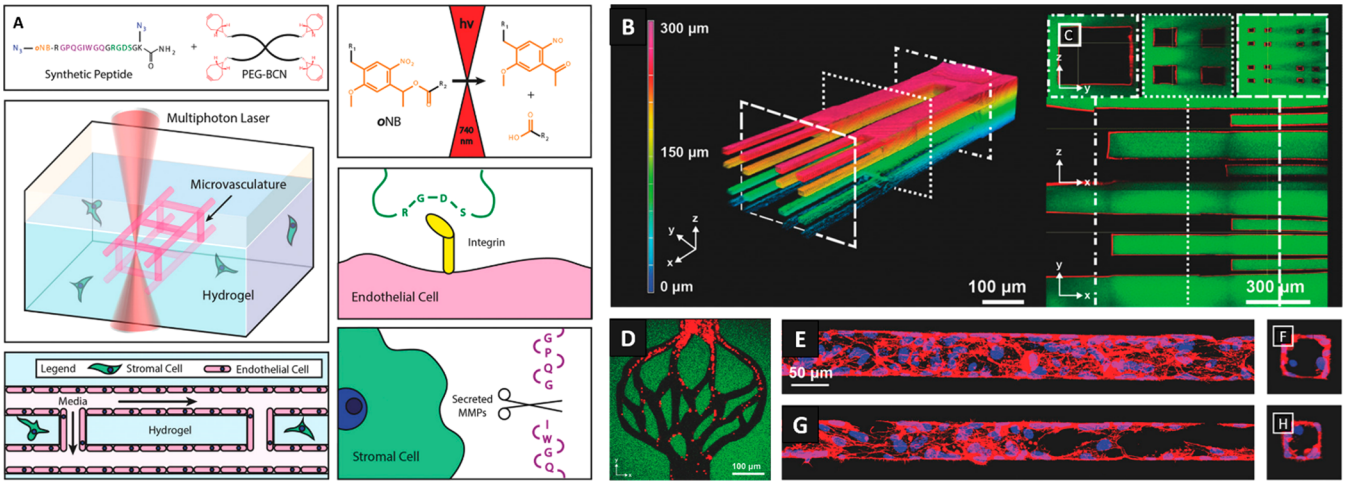

Figure 36. Direct writing microvasculature in functionalized PEG hydrogels. (A) Multiphoton excitation induces localized degradation via oNB photocleavage, resulting in microchannel (pink) generation in the presence of embedded stromal cells (green). (B) A fabricated 3D hierarchical vascular network comprised of one 300 μm × 300 μm channel branching into four 100 μm × 100 μm channels and then terminating in 16 channels, each with 25 μm × 25 μm cross-section. (C) Cross-sectional views of the branched microvascular network indicate patent vascular lumens. (D) Biomimetic capillary networks can be created with user-defined geometrical control within the hydrogel. Endothelialization of (E,F) 60 μm × 60 μm and (G,H) 45 μm × 45 μm (width × height) channels was achieved. Adapted with permission from ref 316. Copyright 2017 John Wiley and Sons.

the axial direction. This strategy was used to pattern biomimetic features derived from various tissues (e.g., cerebral cortex capillaries) that could be used to pattern the organization and tubule structures of HUVECs.

In a more recent study, Brandenberg and Lutolf used focalized short-pulsed lasers for in situ bioprinting of microfluidic networks in 3D cellularized PEG and collagen hydrogels.[300] Protease-sensitive and integrin-binding peptides were functionalized onto the PEG hydrogel to promote cell-mediated degradability in the bulk hydrogel. Importantly, cells as close as 20 μm away from the pulsed laser were still viable, highlighting the cytocompatibility of this technique. However, the use of photoablation with high-intensity lasers still raises concerns over structural integrity as it induces nonspecific chemical bond photolysis and microcavitation. To address this, Arakawa and others used a multiphoton laser with cytocompatible wavelength and intensity for 4D patterning of microvasculature and cell-instructive ligand presentation in PEG hydrogels (Figure 36).[316] In this study, a diazide-modified synthetic peptide was used to cross-link a PEG-tetrabicyclononyne hydrogel via strain-promoted azide−alkyne cycloaddition (SPACC). The synthetic peptide contained a photodegradable *ortho*-nitrobenzyl linker (oNB) that could be degraded by pulsed near-infrared light to generate multiscale vascular networks as small as 10 μm in diameter. This circumvents the use of high-intensity laser for photoablation, which is potentially harmful to cells. The synthetic peptide cross-linker also contained RGD and protease-cleavable sequences to promote cell adhesion and remodeling of the hydrogel matrix (Figure 36A). Perfusable, hierarchical 3D vascular networks ranging from 300 to 25 μm in diameter were patterned within the hydrogel (Figure 36B,C) as well as biomimetic capillary structures (Figure 36D). Endothelialization of patterned microchannels with cross sections of 60 μm × 60 μm (Figure 36E,F) and 45 μm × 45 μm was obtained after perfusion with HUVECs, which is currently the smallest endothelialized synthetic vessel generated within a cytocompatible biomaterial (Figure 36G,H).[316] These channels can be fabricated in the presence of stromal cells to fabricate multicellular tissues with multiscale vasculature, highlighting the potential of this approach to produce functional, heterogeneous, capillarized tissues.

4.2.2. Poloxamers. Poloxamers, commonly known by their trade name Pluronics, are triblock copolymers composed of hydrophilic poly(ethylene oxide) and hydrophobic poly(propylene oxide) in linear alternating PEO−PPO−PEO blocks. Gelation of poloxamers is thermoreversible, and they form micellar liquids below their sol−gel point (~20 °C) and gels at physiological temperature via physical aggregation of micelles.[520] The exact sol−gel point of poloxamers depends on polymer concentration, with higher concentrations having lower sol−gel temperatures.[521] Poloxamers have commonly been used as a controlled release vehicle for hydrophobic drugs.[522] They have also been used as a wound dressing.[523] Poloxamer 407, or Pluronic F-127, is a poloxamer that is FDA-approved for use in humans and is the most commonly used poloxamer biomaterial.

While Pluronics are generally cytocompatible, they are not ideal for cell encapsulation. Concentrations starting at 10% (w/w) have significant negative effects on cell viability.[524] This is problematic, as the minimum concentration of Pluronic F127 needed to form a gel in mammalian cell culture medium is 14%.[525] Encapsulation of HMVECs in 15.6% (w/w) F127 gels led to complete cell death in 5 days.[524] Membrane-stabilizing agents (hydrocortisone, glucose, and glycerol) can rescue cell viability in F127 gels, but may have inadvertent effects on cell function.

Poloxamers are frequently used as sacrificial bioinks due to their thermoreversible gelation. Jennifer Lewis's group has made major contributions to bioprinting perfusable vascular networks using Pluronic F127 bioinks.[241] In their foundational work, they used Pluronics to pattern omnidirectional microvascular networks within a physical hydrogel.[241] Photopolymerizable diacrylate-functionalized Pluronic F127 was used as a fluid reservoir to fill in voids created in the physical F127 gel substrate by nozzle translation. Nozzle size and

https://dx.doi.org/10.1021/acs.chemrev.0c00027
Chem. Rev. 2020, 120, 10887−10949

printing pressure could be varied to create channels as small as 150 μm in diameter that could be perfused after UV curing of Pluronic F127-diacrylate from the fluid reservoir. In a subsequent study, Kolesky and others used Pluronic F127 to pattern fugitive channels within vascularized heterogeneous cell-laden GelMA hydrogels.[526] In a later report, Kolesky used Pluronic F127 to pattern perfusable vascular networks within constructs several millimeters thick.[148] In this study, a multilayer vascular lattice was first printed with Pluronic F127 "vascular ink" and a gelatin "cell ink". Then, a GelMA/fibrin hydrogel was cast around the lattice. The fugitive Pluronic bioink was washed out and the open channels were seeded with HUVECs to form an endothelialized channel around 200 μm in diameter after 2 days (Figure 37). The

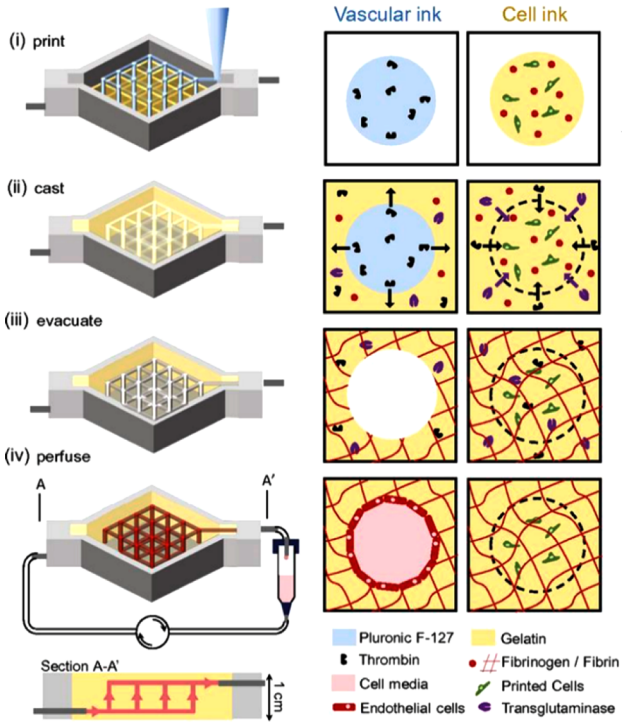

Figure 37. Microvascularized 3D tissue fabrication with Pluronic F127 fugitive bioinks. (i) Fugitive (vascular) ink, which contains pluronic and thrombin, and cell-laden inks, which contain gelatin, fibrinogen, and cells, are printed within a 3D perfusion chip. (ii) ECM material, which contains gelatin, fibrinogen, cells, thrombin, and TG, is then cast over the printed inks. After casting, thrombin induces fibrinogen cleavage and rapid polymerization into fibrin in both the cast matrix, and through diffusion, in the printed cell ink. Similarly, TG diffuses from the molten casting matrix and slowly cross-links the gelatin and fibrin. (iii) Upon cooling, the fugitive ink liquefies and is evacuated, leaving behind a pervasive vascular network, which is (iv) endothelialized and perfused via an external pump. Reproduced with permission from ref 148. Copyright 2016 National Academy of Sciences.

networks could be perfused and support the viability of cells throughout the large construct. However, angiogenic sprouting from parent channels was not demonstrated, even after 45 days of perfusion. Furthermore, casting of the bulk hydrogel around the sacrificial network limits heterogeneity of the final construct. In another study, Millik et al. used coaxial extrusion of unmodified Pluronic F127 in the core and Pluronic F127-bisurethane methacrylate (F127-BUM) in the shell to fabricate hollow tubes with diameters as low as 150 μm.[253] Adding collagen to the F127-BUM bioink enabled cell adhesion to the luminal surfaces of the tubes and promoted monolayer formation during in vitro culture.

The previously mentioned studies did not demonstrate sprouting of ECs from the main channels and therefore did not recreate proper hierarchical vascular networks with microchannels <100 μm. This is mostly due to the resolution limits imposed by extrusion. To integrate capillary-scale networks, Jacoby and others fused a dense "fluff" of melt-spun shellac microfibers (5−500 um) with networks of manually extruded Pluronic F127.[527] After sacrificing the materials, ECs and SMCs could be perfused throughout, self-assembling into hierarchical structures resembling arterioles, venules, and a capillary bed. This study demonstrated how sacrificial networks printed with poloxamers can be complemented by alternative biofabrication approaches to integrate capillary-scale features.

Poloxamer bioinks are highly printable and can be used to fabricate sacrificial vascular networks with excellent shape fidelity. However, poloxamers are currently only suitable for extrusion-based bioprinting, which is limited in resolution as has been previously discussed. Therefore, bioprinting capillary networks with sacrificial poloxamer bioinks is not currently feasible. However, patterned vasculature printed with poloxamer bioinks can be surrounded by proangiogenic hydrogels to promote capillary sprouting from the fugitive network. Another drawback of using poloxamer bioinks is the need to use subphysiological temperatures to liquefy and evacuate the sacrificial poloxamer network.

In this section, we have reviewed synthetic hydrogels for bioprinting microvasculature. Synthetic hydrogel bioinks for bioprinting microvasculature are summarized in Table 4.

We have now critically analyzed the biomaterials currently available for bioprinting microvasculature. We have focused on individual biomaterials (and blends) in each section and how they are formulated into printable bioinks for fabricating microchannels and microvascular networks in vitro and in vivo. Sections 3 and 4 have provided a thorough analysis of techniques and biomaterials used to bioprint microvasculature. An important aspect of these technologies that has not yet been discussed yet is how they are applied. In the next section, we review how bioprinted microvasculature can be applied for disease modeling and drug testing as well as tissue engineering and regenerative medicine.

5. APPLICATIONS OF BIOPRINTED MICROVASCULATURE

Applications of bioprinting microvasculature have improved the quality and scope of existing disease modeling and tissue regeneration methods. In this section, we begin by providing examples of pathophysiological models of several tissue types that incorporate bioprinted microvasculature and move to examples of bioprinted microvasculature for tissue engineered constructs intended for regenerative therapies. In our discussions, we include the advantages of incorporating microvasculature and how microvascular structures can improve the biomimicry and efficacy of constructs intended for disease modeling, drug testing, and regeneration strategies.

5.1. Bioprinting Microvasculature for in Vitro Disease Modeling and Drug Testing

Conventional in vitro tissue models have until recently remained in the realm of 2D structures and microfluidic devices. These models have proven to be useful in the

https://dx.doi.org/10.1021/acs.chemrev.0c00027
Chem. Rev. 2020, 120, 10887−10949

Table 4. Synthetic Hydrogel Bioinks for Bioprinting Microvasculature[a]

biomaterial	bioink formulation	concentration	printing approach	technique	cell type	cross-linking	printed structures	capillary formation?	ref
poly(ethylene glycol) (PEG)	PEG monoacrylate- fibrinogen/alginate	PEG: 1% w/v alginate: 4% w/v	direct	EBB	HUVECs and iPSC-CMs	chemical and physical	vascularized heart tissue	yes	516
	PEGDA	20% wt	direct	LAB	perfused with HUVEC-collagen slurry	chemical	multivascular networks and intravascular topologies	yes	327
	acrylate-PEG functionalized with MMP- sensitive and cell-adhesive peptides	7.5% w/v	direct	LAB	HUVECs and $10T_{1/2}$ fibroblasts	chemical	biomimetic 3D patterning of bioactive molecules	yes	519
	eight-arm PEG containing FXIIIa substrate peptides, MMP-sensitive peptides, and integrin- binding peptides	n/a	direct	LAB	n/a	enzymatic	in situ patterned microfluidic networks	yes	300
	PEG-tetraBCN	7% w/v	direct	LAB	perfused with HUVEC suspension	chemical	multicellular vascularized engineered Tissues	yes	316
poloxamers	Pluronic F127 fugitive ink	23% w/v	indirect	embedded 3D bioprinting	n/a	chemical	omnidirectionally printed 3D microvascular networks	yes	241
	Pluronic F127 fugitive ink co-printed with GelMA cell inks	40% w/v	combined	EBB	perfused with HUVEC suspension	chemical	3D vascularized, heterogeneous cell-laden tissue constructs	no	526
	Pluronic F127 fugitive ink + thrombin printed with fibrinogen-gelatin cell ink	Pluronic F127: 38% w/v thrombin: 100 U/mL	combined	EBB	perfused with HUVEC suspension	enzymatic	3D thick vascularized tissues	no	148

[a] n/a = not applicable.

https://dx.doi.org/10.1021/acs.chemrev.0c00027
Chem. Rev. 2020, 120, 10887−10949

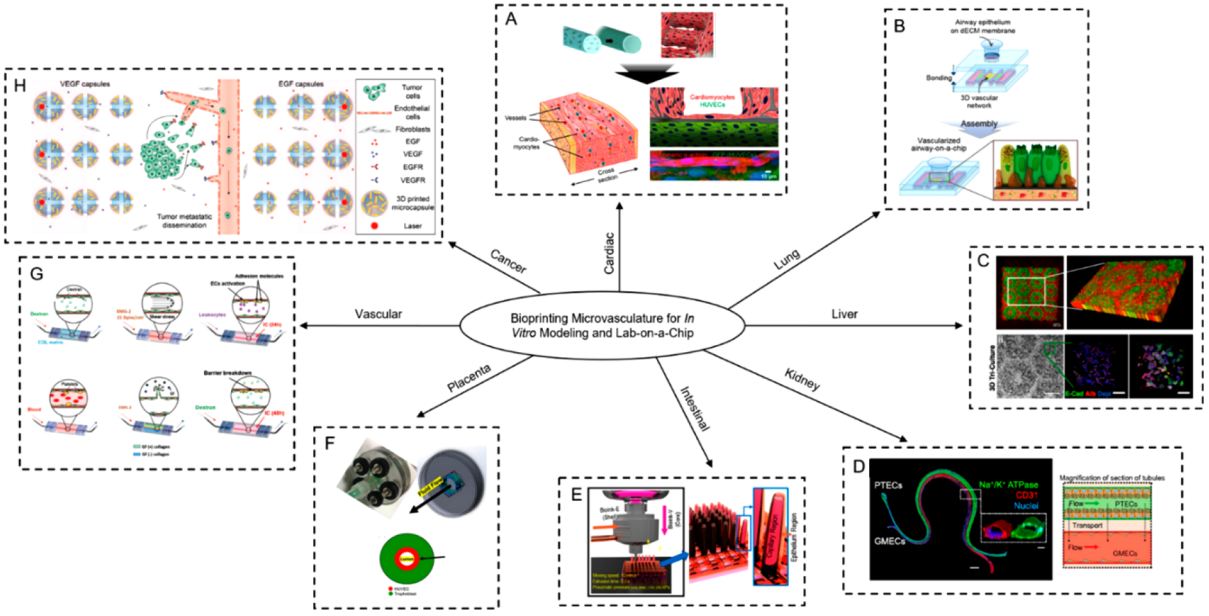

Figure 38. Applications of bioprinting microvasculature for disease modeling and drug testing. (A) Cardiac applications include encapsulating HUVECs inside bioprinted microfibers to create confluent epithelial layers and seeding the scaffold with cardiomyocytes to create an endothelialized myocardial tissue. Adapted with permission from ref 539. Copyright 2016 Elsevier Ltd. (B) Vascularized airway-on-a-chip models were fabricated from a 3D vascular network and an airway epithelium. Adapted with permission from ref 436. Copyright 2018 IOP Publishing Ltd. (C) Liver modeling has included triculture bioprinted models of liver lobules. Adapted with permission from ref 503. Copyright 2016 National Academy of Sciences. (D) Bioprinted kidney models have relied on interactions between proximal tubule epithelial cells (PTECs) and glomerular microvascular endothelial cells (GMECs) to examine renal reabsorption. Adapted with permission from ref 546. Copyright 2016 National Academy of Sciences. (E) Intestinal model applications have included bioprinted structures that consist of an epithelial layer and a capillary region to simulate the villi of the intestine. Adapted with permission from ref 374. Copyright 2018 American Chemical Society. (F) Applications of bioprinting microvasculature have been used in placental modeling to gain insights into preeclampsia and other reproductive diseases. Adapted with permission from ref 547. Copyright 2019 John Wiley and Sons. (G) Various vascular parameters can be simulated with bioprinted microvascular models. Adapted with permission from ref 439. Copyright 2018 John Wiley and Sons. (H) Bioprinted tumor models can be used to examine tumor metastasis. Adapted with permission from ref 548. Copyright 2019 John Wiley and Sons.

collection of inexpensive data but fall short in recapitulating complex and physiologically relevant tissues. Three-dimensional structures, however, can better represent in vivo environments in which there are complex interactions, such as those between cells, growth factors, and the extracellular matrix.[528] Additionally, traditional microengineering methods have limitations in the use of multiple cell types and ECM environments in unique spatial arrangements that mimic in vivo conditions.[529] Bioprinting can be used to position biomaterials and cells in precise positions while maintaining control over various spatiotemporal elements in the 3D structures.[36] Therefore, bioprinting is an enticing technique for applications in in vitro disease modeling and drug testing studies.

The current unmet need to develop effective in vitro models for various pathologies lies in the fact that animal models are inadequate in representing human diseases.[530] Additionally, existing disease models such as 2D cell culture and macroscale hydrogels do not sufficiently recapitulate pathophysiological conditions.[531] The bioprinted tissue-specific 3D models can facilitate drug testing. Approximately 25% of all drugs that are withdrawn from clinical trials are attributed to toxicity and pharmacokinetics.[532] The development of in vitro models that better mimic in vivo conditions is essential to advance drug development and testing.[533] One significant feature that can be introduced to the advanced 3D tissue models for drug testing is microvasculature; a vascularized component in models will permit the biomimetic transportation of nutrients, oxygen, and drugs throughout the construct.[534] To date, various bioprinted constructs for pathophysiological modeling and drug testing have been developed to introduce microvasculature and simulate the conditions of cardiac, lung, liver, kidney, intestinal, placental, vascular, and cancer tissues. These are summarized in Figure 38 and will be reviewed in the follow sections.

5.1.1. Cardiac Tissue Model. The myocardial tissue of the heart is made of cardiomyocytes that are uniquely aligned to exhibit electrical and mechanical functions necessary for contraction of the heart.[535] The creation of cardiac tissue models is met with several challenges. In terms of constructing physiologically relevant cardiac models, spatial control over cardiomyocytes and the 3D architecture is necessary to completely recapitulate aspects of native myocardium such as signal propagation and cardiomyocyte contraction.[536] Additionally, to create thick constructs for cardiac tissue models, it is necessary to introduce microvasculature to promote nutrient diffusion and waste removal throughout the models.[537] To meet these challenges, bioprinting has proven to be a useful technique to both implement microvasculature and mimic the organization of native cardiac tissue.[36,538]

In one study, Zhang et. al created multilayer microfibrous structures utilizing bioprinted microvasculature to model cardiac tissues (Figure 38A).[539] The group used neonatal rat cardiomyocytes seeded onto a bioprinted endothelialized microfibrous scaffold. The subsequent endothelialized myocardial structure demonstrated uniform beating that lasted up to at least 2 weeks while undergoing perfusion culture. This

https://dx.doi.org/10.1021/acs.chemrev.0c00027
Chem. Rev. 2020, 120, 10887−10949

bioprinting approach to cardiac modeling serves several advantages, including control of scaffold parameters, the ability to create scaffolds with multiple cell types, and further applications of the endothelialized structures outside the study of cardiac tissues. Furthermore, the model can be translated to human studies in a step toward personalized medicine using a hiPSC-derived cardiomyocyte (hiPSC-CM) model, which was proven by using hiPSC-CMs as the source of cardiomyocytes rather than neonatal rat cardiomyocytes. The model in this case demonstrated uniform and synchronized beating, much like the prototype with the neonatal rat cardiomyocytes.

Studies on the effects of drugs on cardiovascular functions are of high priority due to the fact that cardiac safety is the leading cause for the discontinuation of drugs.[540] Zhang et al. additionally used their endothelial myocardial model described above to test the toxicity of several drugs by combining their microfibrous model with a bioreactor.[539] The group found that their model was able to predict cardiovascular drug toxicity, as proven by dose-dependent responses when treated with the anticancer drug doxorubicin. Following exposure to doxorubicin, both the beating rate of cardiomyocytes the secretion of vWF by ECs decreased. The response to doxorubicin, which has known cardiovascular toxicity effects,[541] demonstrates that their model shows promise for testing potential cardiotoxicity of other drugs. Furthermore, their model demonstrates potential in the field of personalized medicine because hiPSC-CMs seeded onto the scaffolds showed dose-dependent responses to doxorubicin.

5.1.2. Lung Tissue Model. Blood is oxygenated via respiration and diffusion of inhaled air from the lung alveoli to the pulmonary capillaries.[542] Capillary networks make up a large portion of the lungs, with ECs covering a surface area of approximately 130 m^2.[543] In lung models, it is important that both the lung tissue and the endothelial networks are recapitulated due to the close association between the alveoli and capillary networks in the diffusion of oxygen and removal of carbon dioxide.[544] In vitro lung modeling has consisted of simulations of the alveolar and capillary interface on microfluidic devices[544] that simulate breathing conditions through cyclic positive and negative pressure loops.[545] Bioprinting has emerged as a useful tool for creating improved and more tunable 3D airway models, specifically through their advanced simulation of the interface between alveolar and capillary tissues.[436,545]

A vascularized airway-on-a-chip model was made through a bioprinted dECM bioink laden with ECs and lung fibroblasts (Figure 38B).[436] The construct included a vascular platform consisting of bioprinted ECs that organized into an interconnected vascular network after 7 days. In the model, endothelial cell orientation was responsive to shear stress and inflammatory mediators. Additionally, the model was able to recapitulate the epithelium−blood interaction of the physiological airway. Park et al. also applied their lung model for disease modeling.[436] In this system, they utilized their bioprinted airway-on-a-chip to create an asthmatic airway epithelium model that responded with increased mucus secretion. Furthermore, they used their bioprinted design to create an asthma exacerbation model to mimic environmental exposures that contribute to chronic inflammation.[436]

5.1.3. Liver Tissue Model. The major purpose of the liver is detoxification and metabolism of foreign substances.[549] Recapitulation of native liver functions by engineered models relies heavily on facilitating proper interactions between hepatocytes and supporting cell structures. Because these interactions rely on 3D assembly of the cell types, bioprinting is a useful tool in engineering liver models.[503] In the native liver, microvasculature is necessary for the execution of detoxification; therefore, liver models can become more physiologically relevant when microvasculature is included. Several studies have demonstrated that bioprinting can aid in the incorporation of microvasculature to fabricate advanced liver models.[534,550]

Through controlling the placement of hiPSC-derived hepatic progenitor cells (hiPSC-HPCs) in culture with HUVECs and adipose-derived stem cells, hepatic lobule constructs have been fabricated (Figure 38C).[503] The inclusion of controlled geometries and materials and multiple cell types through bioprinting led to enhanced function of the hiPSC-HPCs. Furthermore, this bioprinted model was specifically advanced because it was created with hiPSC-derived hepatic cells and, therefore, makes strides toward applications as a patient-specific model.

Drug testing in liver models with microvasculature is of specific importance due to the role the liver plays in the breakdown of drugs and the fact that liver damage caused by drug toxicity is a major concern in drug development.[549] Bioprinting has been implemented to create 3D liver tissue chips capable of high-throughput drug testing by sandwiching a layer of HepG2 cells between two layers of HUVECs.[550] In another study, Massa et al. used bioprinting of microvasculature to study drug toxicity in a liver model.[534] The group printed microchannels by printing a sacrificial agarose fiber in a cell-laden GelMA hydrogel and then seeding the channel with ECs, creating endothelialized microchannels within a 3D liver model. They applied this technique to drug toxicity screening and showed that the implementation of the microvascular channel within the liver model delayed the permeability of molecules into the construct and demonstrated a protective role, both of which are physiologically relevant characteristics of the microvasculature in the liver. Additionally, the incorporation of the endothelialized channel led to higher viability of the HepG2/C3A cells.

5.1.4. Kidney Tissue Model. The kidney serves the important role in the human body of filtering solutes in the blood through the interactions between renal compartments and a vascular network.[551] Because of the precise structural interaction requirements of kidneys, 3D models are helpful in recapitulating kidney functions. For instance, 3D printing of microfluidic chambers has been used in conjugation with kidney organoids to facilitate the formation of vascular networks.[551] Furthermore, 3D bioprinting of microvasculature with endothelial cell-laden bioinks within renal constructs has emerged as an attractive technology for disease modeling and regenerating kidney functions.[552]

To improve upon current kidney-on-chip models that do not have substantial 3D architecture, Lin et al. made use of bioprinting microvasculature to study renal reabsorption in 3D kidney proximal tubule model (Figure 38D).[546] Using a fugitive ink, they created ∼200 μm channels seeded with glomerular microvascular endothelial cells to create a microvascular structure adjacent to a 3D bioprinted kidney epithelium. Proximal tubule epithelial cells printed along the microvascular structures demonstrated selective uptake of albumin and reabsorption rates of glucose that could be compared to in vivo values. Additionally, they demonstrated

https://dx.doi.org/10.1021/acs.chemrev.0c00027
Chem. Rev. 2020, 120, 10887−10949

that their bioprinting model could be used to study diabetes through the induction of hyperglycemic conditions.

5.1.5. Intestinal Tissue Model. The functions of the human intestine include digestion of ingested foods, nutrient absorption, and pathogen defense.[553,554] To facilitate these functions, a complex structure is found in intestinal tissue.[554] Intestines are made of multiple cell types along with symbiotic microbes that come together to create a 3D structure consisting of villi and crypts.[555] Therefore, to model intestinal tissue, 3D constructs are needed to provide more accurate recapitulations of physiological conditions. Specifically, there is a need for models that have control of geometry and architecture, which can be achieved through bioprinting.

For proper function of the intestine, capillary systems are vital. The vessels serve the purpose of absorption and transportation of nutrients and drugs that come into contact with the intestinal epithelium.[556] Therefore, physiologically relevant intestinal models and gut-on-a-chip models have benefited from the introduction of microvasculature, specifically through bioprinting.[374] In an application in which a shell of colon epithelial cells and a vascular core of HUVECs were printed to create an intestinal villi model, Kim et al. conducted simulation of the epithelial barrier function of the intestine (Figure 38E).[374] This was achieved by measuring permeability and glucose absorption. Permeability and glucose uptake were highest in the structures printed with the vascular network, indicating that the vascularization created by bioprinting play a large role in the reproduction of the physiology of the human intestine.

5.1.6. Placental Tissue Model. The female reproductive system is unique in the fact that the development of new blood vessels does not follow the typical pattern of being in a quiescent state as is the case throughout almost all tissues in the adult human body. In the female reproductive system, angiogenesis occurs regularly and cyclically during the menstrual cycle and to maintain pregnancy.[557] Additionally, vascular remodeling is an important aspect in preparation for embryo implantation and placentation.[558]

The placenta is vital in providing nutrients to a developing fetus. Understanding the physiology of the human placenta is necessary to realize the source of pregnancy complications.[559] The placenta is developed in part from trophoblasts that provide nutrients to the early fetus, and understanding the interactions between trophoblasts and ECs can provide insight into irregular trophoblast invasion that can lead to pregnancy complications.[547] Current in vitro models have not been able to examine trophoblasts and ECs. However, bioprinting using GelMA hydrogels laden with HUVECs and HTR8 extravillous trophoblasts allowed Kuo et al. to create a placental model capable of examining trophoblast−endothelium interactions (Figure 38F).[547] HUVECs printed in the model demonstrated outgrowth and network formation that was later impaired by the incorporation of trophoblasts. The direct coculture of HUVECs and trophoblasts in a dynamic environment showed that this placenta model could be used to help researchers in their understanding of the interactions between trophoblasts and the endothelium, which shows potential for gaining insights concerning preeclampsia and other human reproductive pathologies.

5.1.7. Vascular Model. The endothelium of blood vessels in the body serve as the primary interface between blood and tissues and serves an important function in controlling the movement of nutrients and soluble factors in the blood.[560] Modeling of the vascular endothelium is important in understanding various pathologies, including tissue overgrowth and cancer and other vascular abnormalities that occur in the cardiovascular, neurovascular, and musculoskeletal system.[561] Several fabrication techniques have been used for modeling various vascular parameters and creating vascular systems. For instance, standard photolithography methods have been used to model vascular properties that become abnormal during disease states while recapitulating physiologically relevant properties of the endothelial barrier such as intimal stiffness, self-deposition of the basement membrane, and self-healing of the endothelial barrier.[562] Additionally, 3D printing has been used to create a template within a GelMA hydrogel construct containing $10T_{1/2}$ cells and a lining of ECs.[563] Bioprinting, however, has demonstrated the ability to improve techniques in vascular modeling due to the capacity to create structures with different cell types and materials and overcome the challenge of fabricating complex vascular models that exists in current free-standing microfluidic models.[561]

Using bioprinted microvasculature on the scale of ∼500 μm, Gao et al. modeled various vascular parameters (Figure 38G).[439] In this model, they were able to observe permeability, antiplatelet adhesive effects, response to shear stress, and microvessel sprouting. Following formation of their bioprinted vascular model, Gao et al. modeled pathological changes in response to airway inflammatory stimulation.

In silico modeling has also shown potential in the applications of bioprinting microvasculature.[339,564] In two studies, Wang and colleagues modeled the fusion of cell aggregates in the bioprinting of several tissue architectures. The group simulated layer-by-layer deposition of scaffold-free cell spheroids to fabricate various tissue geometries, including a bifurcated vascular junction. Through their model, they showed that computer-aided design tools can be used to gain insight into the bioprinting process and ideally be implemented for use in bioprinting vascular networks.[339] In a second study, the group looked at the fusion of cell spheroids to fabricate vascular networks through kinetic Monte Carlo simulations.[564] They relied on parameters pertaining to cell−cell and cell−medium interactions to create a model to simulate the fusion and cell sorting that would occur during bioprinting of vascular networks.[564]

5.1.8. Cancer Model. Effective recapitulation of the tumor microenvironment, including chemical and biophysical cues, is necessary for the fabrication of cancer models.[531] 3D bioprinting has been used to fabricate spatially precise and complex constructs with the structures necessary for mimicking tumor environments.[565] One particular structure that should be introduced in cancer models is microvasculature due to the critical roles it plays in tumor survival and metastasis.[566]

To study glioblastoma (GBM) and the roles angiogenesis plays in the development of GBM, Wang et al. developed a tumor model consisted of bioprinted glioma stem cells.[567] Glioma stem cells were printed into a grid structure with porous channels using an alginate−gelatin−fibrinogen hydrogel. The stem cells formed tubular networks across the pores and expressed higher amounts of angiogenesis-related genes versus those from the suspension culture. This observation demonstrates that the 3D bioprinted structure recapitulates the tumor microenvironment more closely and has the potential to be used for the study of the roles glioma stem cells play in tumor angiogenesis. Furthermore, these bioprinted models could be used in research for antitumor angiogenesis therapies.

https://dx.doi.org/10.1021/acs.chemrev.0c00027
Chem. Rev. 2020, 120, 10887−10949

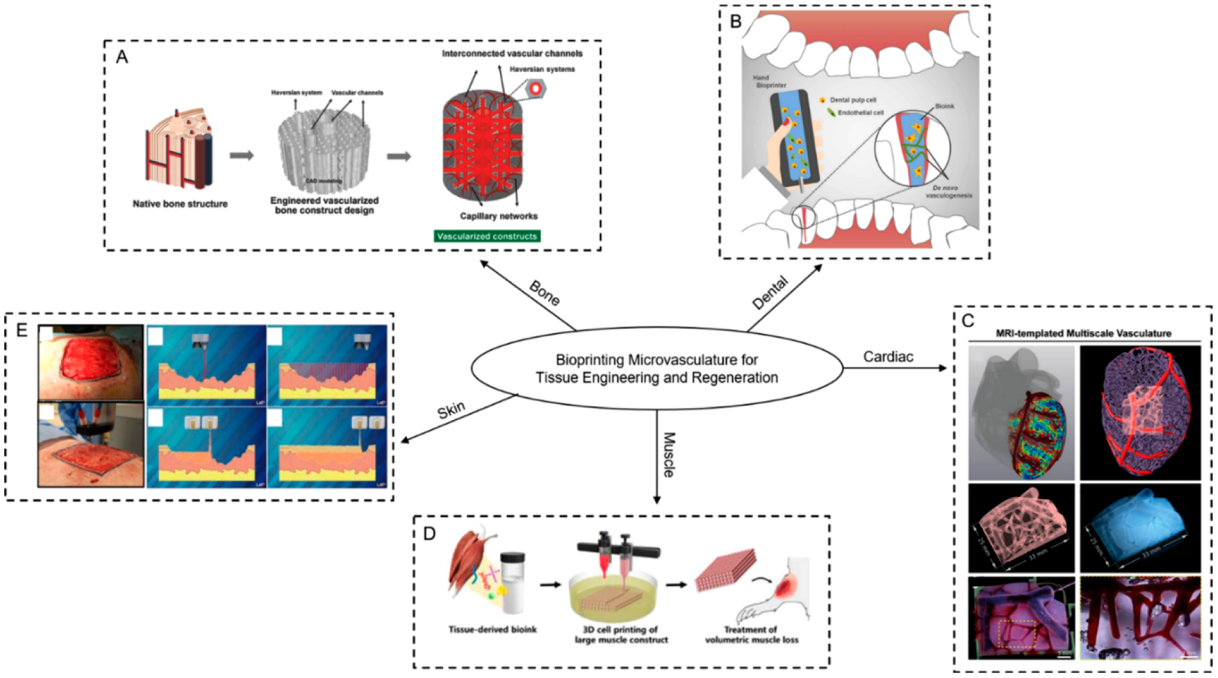

Figure 39. Applications of bioprinting microvasculature for tissue engineering and regeneration. (A) Bone applications have included bioprinting of biphasic vascularized bone constructs. Adapted with permission from ref 579. Copyright 2016 John Wiley and Sons. (B) In situ hand-held bioprinting has been used to engineer prevascularized dental pulp. Adapted with permission from ref 580. Copyright 2019 Taylor and Francis. (C) Patient-specific coronary vasculature has been recapitulated with bioprinting of multiscale vascular structures. Adapted with permission from ref 269. Copyright 2019 American Association for the Advancement of Science. (D) Muscle constructs have been fabricated through bioprinting for treatment and repair of volumetric muscle loss. Adapted with permission from ref 438. Copyright 2019 Elsevier Ltd. (E) Applications for skin engineering and regeneration have consisted of in situ methods for wound repair. Adapted with permission from ref 230. Copyright 2019 Springer Nature, under the terms of the Creative Commons (CC BY 4.0) License https://creativecommons.org/licenses/by/4.0/.

Bioprinting was also used by Meng et al. to build vascularized tumor constructs to study characteristics of the tumor microenvironment in metastasis (Figure 38H).[548] In this study, bioprinting was especially useful in manipulating chemical gradients as well as the placement of cell types, including tumor cells, stromal cells, and infused vascular cells. The metastatic tumor models consisted of a primary tumor cell droplet, endothelialized microchannel, a fibroblast-laden hydrogel to serve as the stroma, and release capsules serving as gradients of chemotactic agents. The models were capable of recapitulating mechanisms of tumor spreading and were additionally used for anticancer drug screening.

5.2. Bioprinting Microvasculature for Tissue Engineering and Regeneration

With the ultimate goal of engineering whole replacement tissue and organs, microvasculature is an essential step in ensuring nutrient diffusion in complex and large-scale tissue.[568] Additionally, microvasculature play a critical role for proper vascular integration of therapeutic tissue engineered constructs in vivo.[569] Various challenges persist in the fields of tissue engineering and regenerative medicine in terms of the implementation and engineering of microvasculature. These include facilitating proangiogenic interactions between cells and 3D matrices,[570] creating hierarchical vascular architectures that meet diffusion requirements, fabricating capillary-size vasculature,[569] achieving functional anastomosis in vivo.[569,571] Importantly, bioprinting have demonstrated the ability to conquer many of these challenges and advance tissue engineered structures through the introduction of microvasculature. In this section, we will review and evaluate different microvascularized tissue models created by bioprinting. These models are summarized in Figure 39.

5.2.1. Bone Tissue. Bone tissue is comprised of bone matrix and vascularized tissue that serve several functions in the body, including providing structural support, protecting internal organs, and holding cells responsible for hematopoiesis with marrow.[572] The vascular network within bone is especially important in supplying nutrients to cells within the bone matrix and removing waste.[573] Additionally, microvasculature is necessary for providing bone with hormones, growth factors, and neurotransmitters, as well as controlling hematopoiesis.[574] Proper bone function relies on interactions between both vascularized and bone matrix regions of bone tissue. Therefore, it is vital that both regions are recapitulated in tissue engineered constructs. Bioprinting has demonstrated potential in printing multielement bone structures.[575] For example, bioprinting has been used to position HUVEC spheroids and calcium phosphate into GelMA hydrogels create constructs that have an osteogenic outer layer and angiogenic inner layer.[576] Furthermore, bioprinting of microvasculature can be applied to fabricate vascularized grafts, which is one of the largest challenges facing fabrication of constructs for the treatment of large bone defects.[398]

Bioprinting 3D structures for bone tissue engineering has been implemented to induce prevascularization of bone constructs. For instance, sequential seeding of hSMCs followed by HUVECs on porous 3D-printed hyperelastic bone (HB) scaffolds promoted the formation of vascular structures across 3D-printed fibers of the HB scaffolds.[577] HUVECs cultured on these scaffolds expressed large amounts of endothelial cell-related genes and microscale tube-like structures were seen in

https://dx.doi.org/10.1021/acs.chemrev.0c00027
Chem. Rev. 2020, 120, 10887−10949

HB scaffolds with pores up to 1000 μm.[577] Additionally, seeding of HUVECs and MSCs onto 3D printed scaffolds of calcium phosphate cement and alginate−gellan gum preloaded with VEGF promoted the formation of tubular networks.[578] When implanted into bone defects in rat femurs, the printed scaffolds promoted infiltration of microvasculature into the wound area.[578]

Utilization of bioinks laden with ECs has also proven to be effective in bone tissue engineering and regeneration. Bone-like 3D structures have been created through bioprinting of cylindrical rods with two different GelMA bioinks to create osteogenic and vasculogenic niches.[418] This approach to fabricating bone-like structures shows promise in applications such as the treatment of large bone defects. Printing of HUVEC-laden hydrogels has also proven useful in bioprinting hybrid scaffolds that consist of bioprinted microvasculature.[150] Through printing a HUVEC-laden gel into the pores of a PDACS/PCL scaffold laden with Wharton's jelly mesenchymal stem cells (WJMSCs), both osteogenesis and angiogenesis can be enhanced. Although they did not show any in vivo application of the bioprinted scaffold, the proof of promotion of both angiogenesis and osteogenesis demonstrates that their methods hold potential in future regeneration of bone defects.

Biphasic bioprinted structures have also been used to mimic the native osteons of cortical bone.[398] Cortical bone consists of osteons in which osteogenic cell types are organized into lamellae and vasculogenic cell types create branched Haversian systems that run through the centers of the lamellae throughout the cortical bone.[572] Piard et al. used bioprinting of microvasculature to recapitulate the osteogenic and angiogenic potential of cortical bone osteons to enhance neovascularization.[398] The group recreated the Haversian canals of cortical bone using a HUVEC-laden bioink printed in the center of a fibrin bioink containing hMSCs and demonstrated the angiogenic potential of the scaffolds through in vivo studies, proving the potential use of biphasic osteon-mimicking scaffolds for vascularized bone tissue engineering. An additional application of bioprinted microvasculature has been conducted to recapitulate the complex, hierarchical architecture of bone through printing a soft organic bioink into a hard, mineral structure (Figure 39A).[579] The structure itself promoted the ECs within the GelMA hydrogels to form capillary-like networks with lumen-like channels. When functionalized with VEGF- and BMP2-mimetic peptides, enhanced angiogenic and osteogenic potential was observed. Furthermore, dynamic culture of the constructs in which the vascular channels were under shear stress improved the formation of vascular lumen. The structure shows potential of clinical translation and therapeutic bone regeneration.

Methods of in situ bioprinting to pattern ECs for prevascularization have been used to promote bone regeneration. As shown by Kerouredan et al., bone regeneration was enhanced depending on the pattern in which the ECs were printed into calvaria bone defects. Bone regeneration was evaluated based on the percentage of bone formation, and the authors concluded that the prevascularization due to bioprinting corresponded with printing pattern, in that they observed enhanced bone regeneration when the ECs were patterned in disc and crossed circle patterns.[277]

5.2.2. Dental Tissue. The tooth and supporting tissue include the periodontium, dentin−dental pulp complex, tooth root, blood vessels, and nerves. The interactions between the complex architecture of teeth and their supporting tissues is necessary for functions performed by teeth such as speech, chewing, and aid in digestive functions.[581] Without complete recapitulation of these tissue elements, tooth regeneration will not be possible. Microvasculature is especially important in the engineering of dental pulp due to its high levels of vascularization and the supporting vasculature of teeth.[582] Bioprinting can be implemented to control the architecture of tooth tissues and promote synergistic activity of the various elements within dental tissues.

Duarte Campos et al. created a novel bioprinting strategy that utilized the bioprinting of microvasculature to aid in the engineering of dental pulp tissue (Figure 39B).[580] Their design included a hand-held bioprinter that would print an agarose and collagen type I hydrogel bioink directly into the tooth root canal. The bioink induced the formation of hollow vascular tubes by HUVECs inside the ink. Their design holds promise in future clinical application for dental pulp regeneration.

5.2.3. Cardiac Tissue. Cardiovascular disease is the leading cause of death worldwide and accounts for approximately one-third of deaths in the United States.[583] Therefore, there is a large need for therapeutic strategies to maintain heart function. Because of the low regenerative capacity of the heart, there is a pressing need for research in cardiac tissue engineering and regenerative medicine.[584] The purpose of cardiac tissue engineering is to stabilize areas of the heart through revascularization and restoration of function.[585] Although there are several elements important in cardiac tissue engineering, microvasculature is vital in regeneration of cardiac tissue. The average intercapillary distance in myocardial tissue is approximately 20 μm, which is often not recapitulated with tissue engineered constructs that span several hundred μm to several mm.[586] Additionally, microvasculature is necessary for transportation of nutrients to keep both cells in engineered constructs and native cells viable. Therefore, vessel architecture must be imposed on tissue engineered structures.[586]

Sacrificial methods for the bioprinting of microvasculature have been implemented to create microvasculature in cardiac constructs. One method involves application of the SWIFT method for the fabrication of cardiac tissue.[272] Using a support bath of iPSC-derived cardiac organ building blocks, a perfused branching architecture could be printed into the tissue, yielding high viability and sarcomeric structure development in the cardiac tissue. These printing methods were then used to recapitulate patient-specific cardiac structures, including a segment of the left anterior descending artery.[272] Additionally, using patient left ventricle data from CT images, several mm thick structures consisting of two bioinks, one with cardiomyocytes and the other of a sacrificial ink containing ECs and fibroblasts, were used to bioprint microvasculature.[273] Incorporation of microvasculature, as demonstrated in these applications, allowed the bioprinted structures to be several millimeters thick, which shows the potential for this technology to be applied to clinically relevant cardiac patches.[273] In another technique, ECs were preorganized to create a vascularized cardiac patch through seeding of ECs in patterned channels.[478] The patches were useful in promoting anastomosis of native vessels in the host through paths created in vitro. Given the limitation of resolution of sacrificial printing, other methods must be implemented to make smaller scale capillary-like structures.

An improvement on the use of sacrificial bioprinting for the introduction of microvasculature in tissue engineered cardiac structures included a sacrificially printed branched channel

https://dx.doi.org/10.1021/acs.chemrev.0c00027
Chem. Rev. 2020, 120, 10887−10949

networks used in conjunction with an oriented microporous scaffold.[587] The pores within the structures allowed for elongation of cardiomyocytes and confluent seeding of ECs that were perfused through the channels. Additionally, the pores allowed for migration of ECs, which could facilitate the formation of microvascular networks.[587]

Using endothelial cell-laden bioinks, significant strides in bioprinting microvasculature have been made.[149,478,585] For example, microfluidic techniques can be coupled with bioprinting to create multiple-cell type tissue constructs for cardiac tissue engineering. Bioinks laden with ECs have been printed to create a prevascular structure that supports synchronous beating of cardiomyocytes seeded on top of the construct.[149] Cardiac patches have been constructed by bioprinting a methacrylated collagen hydrogel laden with human coronary artery endothelial cells, as shown by Izadifar et al.[585] To create the implant framework, alginate was printed into a calcium chloride bath, followed by the removal of calcium chloride and the printing of the cell-laden hydrogel. In the three-layer patch, which consisted of the alginate framework and cell-laden MeCol gel, lumen-like structures were formed by the ECs.

Several developing techniques in bioprinting have emerged to have large potential in advancing bioprinting microvasculature for cardiac applications. FRESH 3D bioprinting has demonstrated the potential to print small-scale vessels (Figure 39C).[269] Feinberg and colleagues printed multiscale vasculature based on MRI-derived CAD models that contained vascular structures patent at ∼100 μm. Additionally, their technology demonstrated the ability to print organ-scale structures. Their proof-of-concept models exhibit the potential for future applications in which FRESH 3D bioprinting can be used for introducing microvasculature in tissue engineered constructs for cardiac applications.

5.2.4. Skeletal Muscle Tissue. Muscle tissue consists of organized bundles of muscle cells capable of contraction that are supported by nerves, blood vessels, and ECM.[588] Blood vessels are important in supplying muscle cells with oxygen and nutrients and removing waste created following muscle contractions. Therefore, for proper engineering of muscle tissues with thicknesses greater than 100−200 μm, a functional vascular system must be engineered into constructs.[568]

Tissue-derived bioinks have been shown to be viable options for the treatment of volumetric muscle loss (VML), as shown by Choi et al. (Figure 39D).[438] The group's approach induced extensive endothelial vessel network. Following implantation in VML space, the group found red blood cells in the lumens of implanted areas and high colocalization of human CD31 and mouse CD31 structures, indicating anastomoses between the implanted bioprinted microvasculature and host vasculature. The coaxial nozzle printing was successful in recapitulating the hierarchical architecture of the muscle and led to 85% of functional recovery.

5.2.5. Skin Tissue and Wound Healing. In clinical therapies for wounds, rapid wound treatment and the promotion of tissue regeneration is vital to prevent excess scaring and the worsening of wounds with time.[230] Strategies for treatment of wounds in the clinical setting include split thickness autografts and skin substitutes with or without cells.[230,589,590] However, several limitations in these methods persist, and improved therapies are needed. Tissue engineering has become an increasingly attractive technique for the fabrication of skin tissue and for wound healing therapies. However, one major challenge that faces the development of tissue engineered constructs is that to create full-thickness constructs, vasculature must be present. Without sufficient vasculature, problems may occur such as lack of integration of the skin substitute, presence of infection, and necrosis of the tissue.[591] Fortunately, bioprinting has emerged as a useful technique in the fabrication of full thickness tissue constructs due to the ability to generate organized microvasculature[591] and recapitulate the architecture of native skin.[590]

One application of bioprinting consisted of fabrication of a multilayered skin equivalents consisting of fibroblasts and keratinocytes on top of Matriderm.[279] These constructs were then implanted into full thickness wounds to fill the defect site and promote the infiltration of native vasculature. Additionally, in situ bioprinting methods have been used to induce microvascular infiltration into wound sites (Figure 39E).[230] A fibrin and collagen bioink laden with dermal fibroblasts and keratinocytes was used to deliver cells directly to wound sites based on the topography of a patient's wound. This study showed promise in healing full thickness wounds and demonstrated a robust technique for delivering cells in a manner unique to a patient's wounds. However, these methods did not specifically print microvasculature but only harnessed the ability of the bioinks to promote vascular infiltration into the wound site.[498,510]

6. CONCLUSIONS AND OUTLOOK

Bioprinting has tremendous potential for on-demand fabrication of human replacement tissues and organs. However, its clinical translation remains impeded by the inability to print vasculature that recapitulates the multiscale nature and function of human vascular systems. Most studies to date have focused on bioprinting tubular structures and millimeter-scale vascular constructs with simple cylindrical or branched geometry. While these structures are useful as replacements for large and medium diameter vessels, more delicate capillary networks and intraorgan vasculature are necessary for fabricating functional tissues and organs. With the development of advanced bioinks and innovative bioprinting techniques, there has been a surge in progress toward bioprinting vascularized tissues and organs with physiologically accurate architectures. In this review, we have evaluated the performance and potential of these techniques and bioinks for bioprinting microvessels. In addition, we have also examined the current applications of bioprinted microvascular constructs for in vitro assays and in vivo tissue regeneration. Despite the exciting progress made so far, there are still numerous challenges remaining in the field. They include: (1) developing novel bioinks that are both proangiogenic and highly printable, (2) printing microvasculature with physiologically relevant heterogeneity and function, (3) enabling controlled organization of microvascular networks in 3D printed tissues, and (4) developing novel printing techniques that fulfill appropriate speed, resolution, and biocompatibility requirements to fabricate clinically applicable vascularized tissues and organs.

The current shortage of bioinks with both good printability and high proangiogenic activity has created a major bottleneck in bioprinting systems for fabricating microvasculature. It is well-understood that a "biofabrication window" exists for most conventional bioinks wherein biocompatibility and printability are negatively correlated.[347] Most highly printable existing bioinks are often not cytocompatible. There is an urgent need for the development of novel, versatile bioinks that extend this

https://dx.doi.org/10.1021/acs.chemrev.0c00027
Chem. Rev. 2020, 120, 10887−10949

biofabrication window. Tremendous innovation has been demonstrated in the design of injectable proangiogenic hydrogels for therapeutic vascularization. It is highly feasible to adapt these hydrogels for bioprinting because the rheological requirements for injectability (e.g., shear-thinning, in situ gelation) are compatible with extrudability. Recent work has demonstrated the use of nanomaterials (e.g., nanoparticles and nanofibers) to reinforce the rheological properties of bioinks for printing vascular structures.[592,593] Bioprinted nanoparticles can also be loaded with growth factors to induce angiogenesis after printing.[594] In addition, physical and chemical cross-linking as well as blending strategies with tunable materials like PEGs could allow for further fine-tuning of the printability of proangiogenic biomaterials. Photo-cross-linkable functionalities could also render proangiogenic biomaterials suitable for light-assisted bioprinting of capillary-scale networks.

Ultimately, bioinks need to be formulated with biomaterials that closely mimic provascular microenvironments within native ECM. As discussed in section 2.4, the ECM plays a critical role in regulating physiological angiogenesis and tissue formation, and the exact mechanisms by which this occurs is still an active area of research. Therefore, novel bioink platforms should adapt to a contemporary understanding of the interplay between matrix biology and vascular morphogenesis. Extracellular matrix and growth factor engineering in designer biomaterials systems should take advantage of advances in matrix biology and materials science toward developing novel proangiogenic bioinks for bioprinting microvasculature.[216]

Another major challenge for bioprinting microvasculature is recapitulating physiologically relevant heterogeneity and maturity of microvascular networks in engineered tissues. As discussed in section 2, the biological mechanisms of vascular morphogenesis are exceptionally complex, and there are still gaps in knowledge of the basic science of developmental and adult vascular biology. While sophisticated engineering approaches have been developed to mimic the processes of vessel generation, the resultant microvascular networks still fail to recapitulate the physiological complexity of capillary beds. For example, the controlled release of single or dual growth factors (e.g., VEGF, PDGF) is a common strategy to promote angiogenesis, but it is not enough to drive the robust formation of functional microvascular networks. In addition, conventional proangiogenic hydrogels do not provide dynamic cell−matrix interactions and anisotropic microenvironments that orchestrate native vascular morphogenesis. Going forward, controlled release of multiple pro-angiogenic and pro-maturation factors in vascular-inductive matrices can enhance microvascular network formation and maturation within printed tissues.[595] This could be addressed by adjusting the physical properties of biomaterials to achieve desired release profiles matching natural cascades during wound healing. Another potential approach would be incorporating growth factor-loaded nanoparticles within functionalized microporous scaffolds to mimic native ECM components, as reviewed in ref 596. Furthermore, postprinting maturation through perfusion bioreactors and mechanical loading may be essential to develop mature microvasculature. Combining advanced release strategies for delivery of multiple growth factors in multimaterial bioink platforms along with mechanical stimulation may vastly improve the function of vascular networks and tissue morphogenesis in bioprinted constructs.

The heterogeneity of cell types involved during microvascular fabrication is another important consideration to build physiologically relevant microvessel systems. HUVECs have been used in most of the existing bioprinting studies due to their high availability and robust expansion in culture. However, they may not be an optimal cell type for engineering microvasculature. Microvascular endothelial cells may provide a more suitable alternative because their native function is to form capillaries in vivo. Notably, there are significant genotypic and phenotypic variations among microvascular endothelial cells from different organs and microvascular beds.[597] Therefore, bioprinting strategies will need to take into account the heterogeneity of microvasculature and their microenvironmental niches across different systems in the body. In addition to ECs, supporting cell types like stem cells and fibroblasts should also be included to further promote tissue formation, maturation, and establishment of an endogenous basement membrane around vessel networks, which lessens the likelihood of thrombotic events after in vivo implantation.[598] Therefore, biomaterials used in bioprinting should promote normal function of these supporting cell types, including appropriate guidance of stem cell differentiation for the desired tissue. Finally, mural cells (i.e., pericytes) will need to be included in bioink formulations to stabilize mature microvascular networks. This is especially important for tissues like the brain, where pericytes control the permeability of the blood−brain barrier.[194] More studies focused on the formation of mature, pericyte-supported capillaries surrounded by basement membrane (i.e., collagen type IV and laminin) in bioprinted tissues are necessary. For clinical translation and patient-specific applications, iPSC-derived ECs and supporting cells are ideal to promote immunotolerance of implanted constructs. Furthermore, recent developments in organoid and microtissue fabrication offer powerful new building blocks for engineering vascularized organs and microsystems with physiologically relevant cell density and 3D organization.

Controlling the 3D patterning of microvascular network formation in bioprinted constructs represents another critical challenge. In most bioprinting platforms, there is little control over the organization of developing microvessels. After printing, vascular cells are essentially left to self-assemble into networks in an unmanageable fashion. This causes poor reproducibility of microvascular network formation in bioinks, especially in biomaterials that have batch variations in their composition. While it is relatively straightforward to control the patterning of microvascular networks on 2D substrates through site-specific functionalization, manipulating their organization in 3D poses significant difficulties. Indirect bioprinting approaches can pattern 3D sacrificial networks, but subsequent endothelialization and angiogenesis from the parent vessels is difficult to control. Emerging biomaterials systems that offer 4D control over matrix properties like growth factor delivery and bioactive ligand presentation have tremendous potential for controlling microvascular network patterning in hydrogel bioinks.[519] For example, photosensitive biomaterials and growth factors can be spatiotemporally manipulated using laser-based direct writing to control site-specific ligand presentation and guide 3D endothelial cell migration in hydrogels.[312,316] These strategies could provide elegant control over the organization of microvasculature in bioprinted materials and should be further explored for building functional microvasculature.

https://dx.doi.org/10.1021/acs.chemrev.0c00027
Chem. Rev. 2020, 120, 10887−10949

Lastly, although numerous advanced modalities have been developed for vascular bioprinting, as discussed in section 3, each approach has inherent limitations, and no single technique on its own can fabricate microvascularized tissues with sufficient speed and biomimicry. Because these methods are being developed in pursuit of a common goal to fabricate human tissues and organs, it is foreseeable that next-generation bioprinting techniques would combine DBB, EBB, and LAB approaches into modular hybrid methods to complement their strengths, offset their individual limitations, and accommodate more diverse bioink formulations. For example, Ozbolat's group proposed a hybrid platform using coaxial extrusion and scaffold-free bioprinting to fabricate scalable tissues and organs with perfusable microvasculature and physiological cell density.[341] Alternatively, EBB and LAB methods could be combined to complement the speed and resolution of these approaches, respectively, toward high-throughput fabrication of scalable tissues with intricate microvasculature. Dual 3D bioprinting systems combining extrusion-based methods and stereolithography have recently been developed to fabricate perfusable small-diameter vasculature[248] and hierarchically vascularized bone biphasic constructs,[579] demonstrating proof-of-concept and the strong potential of hybrid bioprinting platforms for vascular tissue engineering. The evolution of similar hybrid platforms should unlock new possibilities for generating sophisticated microvascularized tissues and organs for clinical applications in the future. Furthermore, emergent applications of volumetric additive manufacturing in tissue engineering may massively increase build times for vascularized tissues and organs.[599−601]

Bioprinting technology is evolving rapidly and is undoubtedly poised to make major contributions to healthcare. Bioprinting microvasculature represents one of the most critical challenges in the evolution of the field. Complementary innovation in high-resolution bioprinting methods, highly printable sacrificial and proangiogenic biomaterials, and autologous sources of cells and biomaterials are necessary to bioprint microvasculature capable of mimicking native vascular physiology. Overcoming these challenges will bring the field closer to printing functional human organ-scale vasculature, which has been referred to as the "Mars mission of bioengineering".[602]

AUTHOR INFORMATION

Corresponding Author

Ying Mei − *Bioengineering Department, Clemson University, Clemson, South Carolina 29634, United States; Department of Regenerative Medicine and Cell Biology, Medical University of South Carolina, Charleston, South Carolina 29425, United States;* orcid.org/0000-0002-8508-4076; Email: mei@clemson.edu

Authors

Ryan W. Barrs − *Bioengineering Department, Clemson University, Clemson, South Carolina 29634, United States; Department of Regenerative Medicine and Cell Biology, Medical University of South Carolina, Charleston, South Carolina 29425, United States*

Jia Jia − *Bioengineering Department, Clemson University, Clemson, South Carolina 29634, United States; Department of Regenerative Medicine and Cell Biology, Medical University of South Carolina, Charleston, South Carolina 29425, United States*

Sophia E. Silver − *Bioengineering Department, Clemson University, Clemson, South Carolina 29634, United States; Department of Regenerative Medicine and Cell Biology, Medical University of South Carolina, Charleston, South Carolina 29425, United States*

Michael Yost − *Department of Surgery, Medical University of South Carolina, Charleston, South Carolina 29425, United States*

Complete contact information is available at: https://pubs.acs.org/10.1021/acs.chemrev.0c00027

Author Contributions

‖R.W.B. and J. J. contributed equally to this review.

Notes

The authors declare no competing financial interest.

Biographies

Ryan Barrs received his B.S. in biomedical engineering from the University of South Carolina in 2016. He began his Ph.D. in the Clemson−MUSC Joint Bioengineering Program under the direction of Dr. Ying Mei in 2017. As a MADE in SC Research Fellow, his current research focuses on the rational design and development of instructive biomaterials for cardiovascular tissue engineering.

Jia Jia, M.S., Ph.D., is a postdoctoral fellow working under the direction of Prof. Ying Mei on the development of vasculogenic biomaterials. He received his Bachelor of Science in chemistry and Master of Science in organic chemistry at Beijing Normal University. He earned his Ph.D. degree in Bioengineering at Clemson University in 2018. His doctoral research was about the development of the bioinspired novel ligands through high-throughput hydrogel arrays for the applications in tissue engineering and regenerative medicine.

Sophia Silver received her B.S. in Biomedical Engineering from North Carolina State University in 2018. In 2019, she joined the Clemson−MUSC Joint Bioengineering Program to pursue her Ph.D. under the direction of Dr. Ying Mei. Her current research involves the development of proangiogenic biomaterials and the applications of cardiac microtissues.

Michael J. Yost, Ph.D., is a Professor in the Surgery Department at the Medical University of South Carolina. He received his B.S. Ch.E. in chemical engineering at The Ohio State University in Columbus, Ohio (1985), his M.S. in chemical engineering from Ohio University in Athens, Ohio (1990), and his Ph.D. in chemical engineering from The University of South Carolina in Columbia, SC (1999). He completed a postdoctoral K25 training grant at the University of South Carolina and has been on the faculty at MUSC since 2012. The research in his lab has been focused on biofabrication, 3D bioprinting and the immune response to engineered tissue implants.

Ying Mei, Ph.D., is an Associate Professor in Bioengineering Department at Clemson University. He received his B.S. in polymer chemistry and Physics at Wuhan University (1994) and Ph.D. in materials chemistry from the Polytechnic University (now: New York University Tandon School of Engineering) (2003). He completed his postdoctoral training in MIT at the Langer lab and joined the Clemson Bioengineering Department as a faculty member in 2012. The research in his lab has been focused on the development of enabling technologies including 3D bioprinting and human cardiac organoids to address the key challenges in cardiovascular tissue engineering.

https://dx.doi.org/10.1021/acs.chemrev.0c00027
Chem. Rev. 2020, 120, 10887−10949

ACKNOWLEDGMENTS

This research was financially supported in part by the National Science Foundation EPSCoR Program under NSF award no. OIA-1655740, the South Carolina Research Alliance (SCRA) grant "South Carolina National Resource Center in Biomanufacturing", and the National Institutes of Health (R01 HL133308, 8P20 GM103444). Any opinions, findings, and conclusions or recommendations expressed in this material are those of the author(s) and do not necessarily reflect those of the National Science Foundation.

REFERENCES

(1) Sherwood, L. *Human Physiology: From Cells to Systems*; Cengage Learning, 2015.
(2) Fox, S. I. *Human Physiology*, 9th ed.; McGraw-Hill, New York, 2006.
(3) Murray, C. D. The Physiological Principle of Minimum Work Applied to the Angle of Branching of Arteries. *J. Gen. Physiol.* **1926**, *9*, 835−841.
(4) Sherman, T. F. On Connecting Large Vessels to Small. The Meaning of Murray's Law. *J. Gen. Physiol.* **1981**, *78*, 431−453.
(5) Barral, J.-P.; Croibier, A. In *Visceral Vascular Manipulations*; Barral, J.-P., Croibier, A., Eds.; Churchill Livingstone: Oxford, 2011.
(6) McMillan, D. B.; Harris, R. J. In *An Atlas of Comparative Vertebrate Histology*; McMillan, D. B., Harris, R. J., Eds.; Academic Press: San Diego, 2018.
(7) Tucker, W. D.; Mahajan, K. In *Statpearls [Internet]*; StatPearls Publishing, 2018.
(8) Lacolley, P.; Regnault, V.; Nicoletti, A.; Li, Z.; Michel, J.-B. The Vascular Smooth Muscle Cell in Arterial Pathology: A Cell That Can Take on Multiple Roles. *Cardiovasc. Res.* **2012**, *95*, 194−204.
(9) Cronenwett, J. L.; Johnston, K. W. *Rutherford's Vascular Surgery E-Book*; Elsevier Health Sciences, 2014.
(10) Lüscher, T.; Predel, H.; Yang, Z.; Bühler, F.; von Segesser, L.; Turina, M. Implications of Pulsatile Stretch on Growth of Saphenous Vein and Mammary Artery Smooth Muscle. *Lancet* **1992**, *340*, 878−879.
(11) Wong, A. P.; Nili, N.; Strauss, B. H. In Vitro Differences between Venous and Arterial-Derived Smooth Muscle Cells: Potential Modulatory Role of Decorin. *Cardiovasc. Res.* **2005**, *65*, 702−710.
(12) Chanakira, A.; Dutta, R.; Charboneau, R.; Barke, R.; Santilli, S. M.; Roy, S. Hypoxia Differentially Regulates Arterial and Venous Smooth Muscle Cell Proliferation Via Pdgfr-B and Vegfr-2 Expression. *Am. J. Physiol. Heart Circ. Physiol.* **2012**, *302*, H1173−H1184.
(13) Maton, A. *Human Biology and Health*; Prentice Hall, 1997.
(14) Langer, R.; Vacanti, J. P. Tissue Engineering. *Science* **1993**, *260*, 920−926.
(15) Novosel, E. C.; Kleinhans, C.; Kluger, P. J. Vascularization Is the Key Challenge in Tissue Engineering. *Adv. Drug Delivery Rev.* **2011**, *63*, 300−311.
(16) Rouwkema, J.; Koopman, B.; Blitterswijk, C.; Dhert, W.; Malda, J. Supply of Nutrients to Cells in Engineered Tissues. *Biotechnol. Genet. Eng. Rev.* **2009**, *26*, 163−178.
(17) Malda, J.; Klein, T. J.; Upton, Z. The Roles of Hypoxia in the in Vitro Engineering of Tissues. *Tissue Eng.* **2007**, *13*, 2153−2162.
(18) Radisic, M.; Park, H.; Chen, F.; Salazar-Lazzaro, J. E.; Wang, Y.; Dennis, R.; Langer, R.; Freed, L. E.; Vunjak-Novakovic, G. Biomimetic Approach to Cardiac Tissue Engineering: Oxygen Carriers and Channeled Scaffolds. *Tissue Eng.* **2006**, *12*, 2077−2091.
(19) Gale, B. K.; Jafek, A. R.; Lambert, C. J.; Goenner, B. L.; Moghimifam, H.; Nze, U. C.; Kamarapu, S. K. A Review of Current Methods in Microfluidic Device Fabrication and Future Commercialization Prospects. *Inventions* **2018**, *3*, 60.
(20) Ren, K.; Zhou, J.; Wu, H. Materials for Microfluidic Chip Fabrication. *Acc. Chem. Res.* **2013**, *46*, 2396−2406.
(21) Riahi, R.; Tamayol, A.; Shaegh, S. A. M.; Ghaemmaghami, A. M.; Dokmeci, M. R.; Khademhosseini, A. Microfluidics for Advanced Drug Delivery Systems. *Curr. Opin. Chem. Eng.* **2015**, *7*, 101−112.
(22) Au, A. K.; Huynh, W.; Horowitz, L. F.; Folch, A. 3d-Printed Microfluidics. *Angew. Chem., Int. Ed.* **2016**, *55*, 3862−3881.
(23) Hasan, A.; Paul, A.; Vrana, N. E.; Zhao, X.; Memic, A.; Hwang, Y.-S.; Dokmeci, M. R.; Khademhosseini, A. Microfluidic Techniques for Development of 3d Vascularized Tissue. *Biomaterials* **2014**, *35*, 7308−7325.
(24) Lee, K.; Silva, E. A.; Mooney, D. J. Growth Factor Delivery-Based Tissue Engineering: General Approaches and a Review of Recent Developments. *J. R. Soc., Interface* **2011**, *8*, 153−170.
(25) Patel, Z. S.; Mikos, A. G. Angiogenesis with Biomaterial-Based Drug-and Cell-Delivery Systems. *J. Biomater. Sci., Polym. Ed.* **2004**, *15*, 701−726.
(26) Richards, D.; Jia, J.; Yost, M.; Markwald, R.; Mei, Y. 3d Bioprinting for Vascularized Tissue Fabrication. *Ann. Biomed. Eng.* **2017**, *45*, 132−147.
(27) Elomaa, L.; Yang, Y. P. Additive Manufacturing of Vascular Grafts and Vascularized Tissue Constructs. *Tissue Eng., Part B* **2017**, *23*, 436−450.
(28) Datta, P.; Ayan, B.; Ozbolat, I. T. Bioprinting for Vascular and Vascularized Tissue Biofabrication. *Acta Biomater.* **2017**, *51*, 1−20.
(29) Hoch, E.; Tovar, G. E.; Borchers, K. Bioprinting of Artificial Blood Vessels: Current Approaches Towards a Demanding Goal. *Eur. J. Cardiothorac. Surg.* **2014**, *46*, 767−778.
(30) Ozbolat, I. T.; Yu, Y. Bioprinting toward Organ Fabrication: Challenges and Future Trends. *IEEE Trans. Biomed. Eng.* **2013**, *60*, 691−699.
(31) Zhang, Y. S.; Yue, K.; Aleman, J.; Mollazadeh-Moghaddam, K.; Bakht, S. M.; Yang, J.; Jia, W.; Dell'Erba, V.; Assawes, P.; Shin, S. R.; et al. 3d Bioprinting for Tissue and Organ Fabrication. *Ann. Biomed. Eng.* **2017**, *45*, 148−163.
(32) Miri, A. K.; Khalilpour, A.; Cecen, B.; Maharjan, S.; Shin, S. R.; Khademhosseini, A. Multiscale Bioprinting of Vascularized Models. *Biomaterials* **2019**, *198*, 204−216.
(33) Lee, M.; Wu, B. M. Recent Advances in 3d Printing of Tissue Engineering Scaffolds. *Methods Mol. Biol.* **2012**, *868*, 257−267.
(34) Mandrycky, C.; Wang, Z.; Kim, K.; Kim, D. H. 3d Bioprinting for Engineering Complex Tissues. *Biotechnol. Adv.* **2016**, *34*, 422−434.
(35) Mironov, V.; Kasyanov, V.; Markwald, R. R. Organ Printing: From Bioprinter to Organ Biofabrication Line. *Curr. Opin. Biotechnol.* **2011**, *22*, 667−673.
(36) Murphy, S. V.; Atala, A. 3d Bioprinting of Tissues and Organs. *Nat. Biotechnol.* **2014**, *32*, 773−785.
(37) Ke, D.; Murphy, S. V. Current Challenges of Bioprinted Tissues toward Clinical Translation. *Tissue Eng., Part B* **2019**, *25*, 1−13.
(38) Bogorad, M. I.; DeStefano, J.; Karlsson, J.; Wong, A. D.; Gerecht, S.; Searson, P. C. In Vitro Microvessel Models. *Lab Chip* **2015**, *15*, 4242−4255.
(39) Zheng, Y.; Chen, J.; López, J. A. Flow-Driven Assembly of Vwf Fibres and Webs in in Vitro Microvessels. *Nat. Commun.* **2015**, *6*, 7858.
(40) Zheng, Y.; Chen, J.; Craven, M.; Choi, N. W.; Totorica, S.; Diaz-Santana, A.; Kermani, P.; Hempstead, B.; Fischbach-Teschl, C.; López, J. A.; Stroock, A. D. In Vitro Microvessels for the Study of Angiogenesis and Thrombosis. *Proc. Natl. Acad. Sci. U. S. A.* **2012**, *109*, 9342−9347.
(41) Carmeliet, P.; Jain, R. K. Molecular Mechanisms and Clinical Applications of Angiogenesis. *Nature* **2011**, *473*, 298.
(42) Carmeliet, P. Mechanisms of Angiogenesis and Arteriogenesis. *Nat. Med.* **2000**, *6*, 389.
(43) Patan, S. Vasculogenesis and Angiogenesis. *Cancer Treat. Res.* **2004**, *117*, 3−32.
(44) Poole, T. J.; Coffin, J. D. Vasculogenesis and Angiogenesis: Two Distinct Morphogenetic Mechanisms Establish Embryonic Vascular Pattern. *J. Exp. Zool.* **1989**, *251*, 224−231.
(45) Risau, W. Mechanisms of Angiogenesis. *Nature* **1997**, *386*, 671.

https://dx.doi.org/10.1021/acs.chemrev.0c00027
Chem. Rev. 2020, 120, 10887−10949

(46) Carmeliet, P.; Jain, R. K. Angiogenesis in Cancer and Other Diseases. *Nature* **2000**, *407*, 249−257.
(47) Welti, J.; Loges, S.; Dimmeler, S.; Carmeliet, P. Recent Molecular Discoveries in Angiogenesis and Antiangiogenic Therapies in Cancer. *J. Clin. Invest.* **2013**, *123*, 3190−3200.
(48) Morin, K. T.; Dries-Devlin, J. L.; Tranquillo, R. T. Engineered Microvessels with Strong Alignment and High Lumen Density Via Cell-Induced Fibrin Gel Compaction and Interstitial Flow. *Tissue Eng., Part A* **2013**, *20*, 553−565.
(49) Morin, K. T.; Smith, A. O.; Davis, G. E.; Tranquillo, R. T. Aligned Human Microvessels Formed in 3d Fibrin Gel by Constraint of Gel Contraction. *Microvasc. Res.* **2013**, *90*, 12−22.
(50) Lesman, A.; Koffler, J.; Atlas, R.; Blinder, Y. J.; Kam, Z.; Levenberg, S. Engineering Vessel-Like Networks within Multicellular Fibrin-Based Constructs. *Biomaterials* **2011**, *32*, 7856−7869.
(51) Blinder, Y. J.; Freiman, A.; Raindel, N.; Mooney, D. J.; Levenberg, S. Vasculogenic Dynamics in 3d Engineered Tissue Constructs. *Sci. Rep.* **2016**, *5*, 17840.
(52) Michiels, C. Physiological and Pathological Responses to Hypoxia. *Am. J. Pathol.* **2004**, *164*, 1875−1882.
(53) Herbert, S. P.; Stainier, D. Y. Molecular Control of Endothelial Cell Behaviour During Blood Vessel Morphogenesis. *Nat. Rev. Mol. Cell Biol.* **2011**, *12*, 551.
(54) Li, X.; Eriksson, U. Novel Pdgf Family Members: Pdgf-C and Pdgf-D. *Cytokine Growth Factor Rev.* **2003**, *14*, 91−98.
(55) Lafleur, M. A.; Handsley, M. M.; Knäuper, V.; Murphy, G.; Edwards, D. R. Endothelial Tubulogenesis within Fibrin Gels Specifically Requires the Activity of Membrane-Type-Matrix Metalloproteinases (Mt-Mmps). *J. Cell Sci.* **2002**, *115*, 3427−3438.
(56) Frerich, B.; Lindemann, N.; Kurtz-Hoffmann, J.; Oertel, K. Vitro Model of a Vascular Stroma for the Engineering of Vascularized Tissues. *Int. J. Oral Maxillofac. Surg.* **2001**, *30*, 414−420.
(57) Rao, R. R.; Peterson, A. W.; Ceccarelli, J.; Putnam, A. J.; Stegemann, J. P. Matrix Composition Regulates Three-Dimensional Network Formation by Endothelial Cells and Mesenchymal Stem Cells in Collagen/Fibrin Materials. *Angiogenesis* **2012**, *15*, 253−264.
(58) Montaño, I.; Schiestl, C.; Schneider, J.; Pontiggia, L.; Luginbühl, J.; Biedermann, T.; Böttcher-Haberzeth, S.; Braziulis, E.; Meuli, M.; Reichmann, E. Formation of Human Capillaries in Vitro: The Engineering of Prevascularized Matrices. *Tissue Eng., Part A* **2010**, *16*, 269−282.
(59) Chen, X.; Aledia, A. S.; Popson, S. A.; Him, L.; Hughes, C. C.; George, S. C. Rapid Anastomosis of Endothelial Progenitor Cell−Derived Vessels with Host Vasculature Is Promoted by a High Density of Cotransplanted Fibroblasts. *Tissue Eng., Part A* **2010**, *16*, 585−594.
(60) Tallquist, M.; Kazlauskas, A. Pdgf Signaling in Cells and Mice. *Cytokine Growth Factor Rev.* **2004**, *15*, 205−213.
(61) Andrae, J.; Gallini, R.; Betsholtz, C. Role of Platelet-Derived Growth Factors in Physiology and Medicine. *Genes Dev.* **2008**, *22*, 1276−1312.
(62) Robson, M. C.; Phillips, L. G.; Robson, L.; Thomason, A.; Pierce, G. Platelet-Derived Growth Factor Bb for the Treatment of Chronic Pressure Ulcers. *Lancet* **1992**, *339*, 23−25.
(63) Smiell, J. M.; Wieman, T. J.; Steed, D. L.; Perry, B. H.; Sampson, A. R.; Schwab, B. H. Efficacy and Safety of Becaplermin (Recombinant Human Platelet-Derived Growth Factor-Bb) in Patients with Nonhealing, Lower Extremity Diabetic Ulcers: A Combined Analysis of Four Randomized Studies. *Wound Repair Regen* **1999**, *7*, 335−346.
(64) Lindahl, P.; Karlsson, L.; Hellstrom, M.; Gebre-Medhin, S.; Willetts, K.; Heath, J. K.; Betsholtz, C. Alveogenesis Failure in Pdgf-a-Deficient Mice Is Coupled to Lack of Distal Spreading of Alveolar Smooth Muscle Cell Progenitors During Lung Development. *Development* **1997**, *124*, 3943−3953.
(65) Boström, H.; Willetts, K.; Pekny, M.; Levéen, P.; Lindahl, P.; Hedstrand, H.; Pekna, M.; Hellström, M.; Gebre-Medhin, S.; Schalling, M.; et al. Pdgf-a Signaling Is a Critical Event in Lung Alveolar Myofibroblast Development and Alveogenesis. *Cell* **1996**, *85*, 863−873.
(66) Shih, A. H.; Holland, E. C. Platelet-Derived Growth Factor (Pdgf) and Glial Tumorigenesis. *Cancer Lett.* **2006**, *232*, 139−147.
(67) Hellstrom, M.; Lindahl, P.; Abramsson, A.; Betsholtz, C. Role of Pdgf-B and Pdgfr-Beta in Recruitment of Vascular Smooth Muscle Cells and Pericytes During Embryonic Blood Vessel Formation in the Mouse. *Development* **1999**, *126*, 3047−3055.
(68) Board, R.; Jayson, G. C. Platelet-Derived Growth Factor Receptor (Pdgfr): A Target for Anticancer Therapeutics. *Drug Resist. Updates* **2005**, *8*, 75−83.
(69) Vempati, P.; Popel, A. S.; Mac Gabhann, F. Extracellular Regulation of Vegf: Isoforms, Proteolysis, and Vascular Patterning. *Cytokine Growth Factor Rev.* **2014**, *25*, 1−19.
(70) Autiero, M.; Waltenberger, J.; Communi, D.; Kranz, A.; Moons, L.; Lambrechts, D.; Kroll, J.; Plaisance, S.; De Mol, M.; Bono, F.; et al. Role of Plgf in the Intra-and Intermolecular Cross Talk between the Vegf Receptors Flt1 and Flk1. *Nat. Med.* **2003**, *9*, 936−943.
(71) Mac Gabhann, F.; Popel, A. S. Model of Competitive Binding of Vascular Endothelial Growth Factor and Placental Growth Factor to Vegf Receptors on Endothelial Cells. *Am. J. Physiol. Heart Circ. Physiol.* **2004**, *286*, H153−H164.
(72) Ruhrberg, C.; Gerhardt, H.; Golding, M.; Watson, R.; Ioannidou, S.; Fujisawa, H.; Betsholtz, C.; Shima, D. T. Spatially Restricted Patterning Cues Provided by Heparin-Binding Vegf-a Control Blood Vessel Branching Morphogenesis. *Genes Dev.* **2002**, *16*, 2684−2698.
(73) Nagel, M.; Tahinci, E.; Symes, K.; Winklbauer, R. Guidance of Mesoderm Cell Migration in the Xenopus Gastrula Requires Pdgf Signaling. *Development* **2004**, *131*, 2727−2736.
(74) Gerhardt, H.; Golding, M.; Fruttiger, M.; Ruhrberg, C.; Lundkvist, A.; Abramsson, A.; Jeltsch, M.; Mitchell, C.; Alitalo, K.; Shima, D.; Betsholtz, C. Vegf Guides Angiogenic Sprouting Utilizing Endothelial Tip Cell Filopodia. *J. Cell Biol.* **2003**, *161*, 1163−1177.
(75) Song, J. W.; Munn, L. L. Fluid Forces Control Endothelial Sprouting. *Proc. Natl. Acad. Sci. U. S. A.* **2011**, *108*, 15342−15347.
(76) Iruela-Arispe, M. L.; Davis, G. E. Cellular and Molecular Mechanisms of Vascular Lumen Formation. *Dev. Cell* **2009**, *16*, 222−231.
(77) Carmeliet, P.; Ferreira, V.; Breier, G.; Pollefeyt, S.; Kieckens, L.; Gertsenstein, M.; Fahrig, M.; Vandenhoeck, A.; Harpal, K.; Eberhardt, C. Abnormal Blood Vessel Development and Lethality in Embryos Lacking a Single Vegf Allele. *Nature* **1996**, *380*, 435−439.
(78) Ferrara, N. Role of Vascular Endothelial Growth Factor in the Regulation of Angiogenesis. *Kidney Int.* **1999**, *56*, 794−814.
(79) Shalaby, F.; Ho, J.; Stanford, W. L.; Fischer, K.-D.; Schuh, A. C.; Schwartz, L.; Bernstein, A.; Rossant, J. A Requirement for Flk1 in Primitive and Definitive Hematopoiesis and Vasculogenesis. *Cell* **1997**, *89*, 981−990.
(80) Fong, G.-H.; Zhang, L.; Bryce, D.-M.; Peng, J. Increased Hemangioblast Commitment, Not Vascular Disorganization, Is the Primary Defect in Flt-1 Knock-out Mice. *Development* **1999**, *126*, 3015−3025.
(81) Peichev, M.; Naiyer, A. J.; Pereira, D.; Zhu, Z.; Lane, W. J.; Williams, M.; Oz, M. C.; Hicklin, D. J.; Witte, L.; Moore, M. A.; Rafil, S. Expression of Vegfr-2 and Ac133 by Circulating Human Cd34+ Cells Identifies a Population of Functional Endothelial Precursors. *Blood* **2000**, *95*, 952−958.
(82) Ferrara, N.; Gerber, H.-P.; LeCouter, J. The Biology of Vegf and Its Receptors. *Nat. Med.* **2003**, *9*, 669−676.
(83) Shing, Y.; Folkman, J.; Sullivan, R.; Butterfield, C.; Murray, J.; Klagsbrun, M. Heparin Affinity: Purification of a Tumor-Derived Capillary Endothelial Cell Growth Factor. *Science* **1984**, *223*, 1296−1299.
(84) Cross, M. J.; Claesson-Welsh, L. Fgf and Vegf Function in Angiogenesis: Signalling Pathways, Biological Responses and Therapeutic Inhibition. *Trends Pharmacol. Sci.* **2001**, *22*, 201−207.

https://dx.doi.org/10.1021/acs.chemrev.0c00027
Chem. Rev. 2020, 120, 10887−10949

(85) Lee, S. H.; Schloss, D. J.; Swain, J. L. Maintenance of Vascular Integrity in the Embryo Requires Signaling through the Fibroblast Growth Factor Receptor. *J. Biol. Chem.* **2000**, *275*, 33679−33687.
(86) Colvin, J. S.; Bohne, B. A.; Harding, G. W.; McEwen, D. G.; Ornitz, D. M. Skeletal Overgrowth and Deafness in Mice Lacking Fibroblast Growth Factor Receptor 3. *Nat. Genet.* **1996**, *12*, 390.
(87) Larsson, H.; Klint, P.; Landgren, E.; Claesson-Welsh, L. Fibroblast Growth Factor Receptor-1-Mediated Endothelial Cell Proliferation Is Dependent on the Src Homology (Sh) 2/Sh3 Domain-Containing Adaptor Protein Crk. *J. Biol. Chem.* **1999**, *274*, 25726−25734.
(88) Mohammadi, M.; Honegger, A.; Rotin, D.; Fischer, R.; Bellot, F.; Li, W.; Dionne, C.; Jaye, M.; Rubinstein, M.; Schlessinger, J. A Tyrosine-Phosphorylated Carboxy-Terminal Peptide of the Fibroblast Growth Factor Receptor (Flg) Is a Binding Site for the Sh2 Domain of Phospholipase C-Gamma 1. *Mol. Cell. Biol.* **1991**, *11*, 5068−5078.
(89) Cross, M. J.; Hodgkin, M. N.; Roberts, S.; Landgren, E.; Wakelam, M.; Claesson-Welsh, L. Tyrosine 766 in the Fibroblast Growth Factor Receptor-1 Is Required for Fgf-Stimulation of Phospholipase C, Phospholipase D, Phospholipase a (2), Phosphoinositide 3-Kinase and Cytoskeletal Reorganisation in Porcine Aortic Endothelial Cells. *J. Cell Sci.* **2000**, *113*, 643−651.
(90) Landgren, E.; Klint, P.; Yokote, K.; Claesson-Welsh, L. Fibroblast Growth Factor Receptor-1 Mediates Chemotaxis Independently of Direct Sh2-Domain Protein Binding. *Oncogene* **1998**, *17*, 283.
(91) Zieris, A.; Prokoph, S.; Levental, K. R.; Welzel, P. B.; Grimmer, M.; Freudenberg, U.; Werner, C. Fgf-2 and Vegf Functionalization of Starpeg−Heparin Hydrogels to Modulate Biomolecular and Physical Cues of Angiogenesis. *Biomaterials* **2010**, *31*, 7985−7994.
(92) Zieris, A.; Chwalek, K.; Prokoph, S.; Levental, K.; Welzel, P.; Freudenberg, U.; Werner, C. Dual Independent Delivery of Pro-Angiogenic Growth Factors from Starpeg-Heparin Hydrogels. *J. Controlled Release* **2011**, *156*, 28−36.
(93) Sakiyama-Elbert, S. E. Incorporation of Heparin into Biomaterials. *Acta Biomater.* **2014**, *10*, 1581−1587.
(94) Beenken, A.; Mohammadi, M. The Fgf Family: Biology, Pathophysiology and Therapy. *Nat. Rev. Drug Discovery* **2009**, *8*, 235−253.
(95) Massagué, J. Tgf*β* Signalling in Context. *Nat. Rev. Mol. Cell Biol.* **2012**, *13*, 616.
(96) McCarty, J. H. Integrin-Mediated Regulation of Neurovascular Development, Physiology and Disease. *Cell Adh. Migr.* **2009**, *3*, 211−215.
(97) Mu, D.; Cambier, S.; Fjellbirkeland, L.; Baron, J. L.; Munger, J. S.; Kawakatsu, H.; Sheppard, D.; Broaddus, V. C.; Nishimura, S. L. The Integrin Av*β*8 Mediates Epithelial Homeostasis through Mt1-Mmp−Dependent Activation of Tgf-B1. *J. Cell Biol.* **2002**, *157*, 493−507.
(98) Edwards, J. P.; Thornton, A. M.; Shevach, E. M. Release of Active Tgf-B1 from the Latent Tgf-B1/Garp Complex on T Regulatory Cells Is Mediated by Integrin B8. *J. Immunol.* **2014**, *193*, 2843−2849.
(99) Tian, M.; Neil, J. R.; Schiemann, W. P. Transforming Growth Factor-B and the Hallmarks of Cancer. *Cell. Signalling* **2011**, *23*, 951−962.
(100) Li, C.; Guo, B.; Bernabeu, C.; Kumar, S. Angiogenesis in Breast Cancer: The Role of Transforming Growth Factor B and Cd105. *Microsc. Res. Tech.* **2001**, *52*, 437−449.
(101) Hofer, E.; Schweighofer, B. Signal Transduction Induced in Endothelial Cells by Growth Factor Receptors Involved in Angiogenesis. *Thromb. Haemostasis* **2007**, *97*, 355−363.
(102) Krupinski, J.; Kumar, P.; Kumar, S.; Kaluza, J. Increased Expression of Tgf-B1 in Brain Tissue after Ischemic Stroke in Humans. *Stroke* **1996**, *27*, 852−857.
(103) Dissen, G.; Lara, H.; Fahrenbach, W.; Costa, M.; Ojeda, S. Immature Rat Ovaries Become Revascularized Rapidly after Autotransplantation and Show a Gonadotropin-Dependent Increase in Angiogenic Factor Gene Expression. *Endocrinology* **1994**, *134*, 1146−1154.
(104) Mallet, C.; Vittet, D.; Feige, J. J.; Bailly, S. Tgf*β*1 Induces Vasculogenesis and Inhibits Angiogenic Sprouting in an Embryonic Stem Cell Differentiation Model: Respective Contribution of Alk1 and Alk5. *Stem Cells* **2006**, *24*, 2420−2427.
(105) Pepper, M. S. Transforming Growth Factor-Beta: Vasculogenesis, Angiogenesis, and Vessel Wall Integrity. *Cytokine Growth Factor Rev.* **1997**, *8*, 21−43.
(106) Ferrari, G.; Pintucci, G.; Seghezzi, G.; Hyman, K.; Galloway, A. C.; Mignatti, P. Vegf, a Prosurvival Factor, Acts in Concert with Tgf-B1 to Induce Endothelial Cell Apoptosis. *Proc. Natl. Acad. Sci. U. S. A.* **2006**, *103*, 17260−17265.
(107) Ten Dijke, P.; Arthur, H. M. Extracellular Control of Tgf*β* Signalling in Vascular Development and Disease. *Nat. Rev. Mol. Cell Biol.* **2007**, *8*, 857.
(108) Wang, X.-J.; Dong, Z.; Zhong, X.-H.; Shi, R.-Z.; Huang, S.-H.; Lou, Y.; Li, Q.-P. Transforming Growth Factor-B1 Enhanced Vascular Endothelial Growth Factor Synthesis in Mesenchymal Stem Cells. *Biochem. Biophys. Res. Commun.* **2008**, *365*, 548−554.
(109) Stowers, R. S.; Drinnan, C. T.; Chung, E.; Suggs, L. J. Mesenchymal Stem Cell Response to Tgf-B1 in Both 2d and 3d Environments. *Biomater. Sci.* **2013**, *1*, 860−869.
(110) Sato, T. N.; Qin, Y.; Kozak, C. A.; Audus, K. L. Tie-1 and Tie-2 Define Another Class of Putative Receptor Tyrosine Kinase Genes Expressed in Early Embryonic Vascular System. *Proc. Natl. Acad. Sci. U. S. A.* **1993**, *90*, 9355−9358.
(111) Augustin, H. G.; Koh, G. Y.; Thurston, G.; Alitalo, K. Control of Vascular Morphogenesis and Homeostasis through the Angiopoietin−Tie System. *Nat. Rev. Mol. Cell Biol.* **2009**, *10*, 165−177.
(112) Valenzuela, D. M.; Griffiths, J. A.; Rojas, J.; Aldrich, T. H.; Jones, P. F.; Zhou, H.; McClain, J.; Copeland, N. G.; Gilbert, D. J.; Jenkins, N. A.; et al. Angiopoietins 3 and 4: Diverging Gene Counterparts in Mice and Humans. *Proc. Natl. Acad. Sci. U. S. A.* **1999**, *96*, 1904−1909.
(113) Davis, S.; Aldrich, T. H.; Jones, P. F.; Acheson, A.; Compton, D. L.; Jain, V.; Ryan, T. E.; Bruno, J.; Radziejewski, C.; Maisonpierre, P. C.; Yancopoulos, G. D. Isolation of Angiopoietin-1, a Ligand for the Tie2 Receptor, by Secretion-Trap Expression Cloning. *Cell* **1996**, *87*, 1161−1169.
(114) Maisonpierre, P. C.; Suri, C.; Jones, P. F.; Bartunkova, S.; Wiegand, S. J.; Radziejewski, C.; Compton, D.; McClain, J.; Aldrich, T. H.; Papadopoulos, N.; et al. Angiopoietin-2, a Natural Antagonist for Tie2 That Disrupts in Vivo Angiogenesis. *Science* **1997**, *277*, 55−60.
(115) Gale, N. W.; Thurston, G.; Hackett, S. F.; Renard, R.; Wang, Q.; McClain, J.; Martin, C.; Witte, C.; Witte, M. H.; Jackson, D.; et al. Angiopoietin-2 Is Required for Postnatal Angiogenesis and Lymphatic Patterning, and Only the Latter Role Is Rescued by Angiopoietin-1. *Dev. Cell* **2002**, *3*, 411−423.
(116) Huang, X.; Wu, J.; Ferrando, R.; Lee, J.; Wang, Y.; Farese, R.; Sheppard, D. Fatal Bilateral Chylothorax in Mice Lacking the Integrin A9*β*1. *Mol. Cell. Biol.* **2000**, *20*, 5208−5215.
(117) Fiedler, U.; Reiss, Y.; Scharpfenecker, M.; Grunow, V.; Koidl, S.; Thurston, G.; Gale, N. W.; Witzenrath, M.; Rosseau, S.; Suttorp, N. Angiopoietin-2 Sensitizes Endothelial Cells to Tnf-A and Has a Crucial Role in the Induction of Inflammation. *Nat. Med.* **2006**, *12*, 235−239.
(118) Holash, J.; Maisonpierre, P.; Compton, D.; Boland, P.; Alexander, C.; Zagzag, D.; Yancopoulos, G.; Wiegand, S. Vessel Cooption, Regression, and Growth in Tumors Mediated by Angiopoietins and Vegf. *Science* **1999**, *284*, 1994−1998.
(119) Li, X.; Stankovic, M.; Bonder, C. S.; Hahn, C. N.; Parsons, M.; Pitson, S. M.; Xia, P.; Proia, R. L.; Vadas, M. A.; Gamble, J. R. Basal and Angiopoietin-1−Mediated Endothelial Permeability Is Regulated by Sphingosine Kinase-1. *Blood* **2008**, *111*, 3489−3497.
(120) Fagiani, E.; Christofori, G. Angiopoietins in Angiogenesis. *Cancer Lett.* **2013**, *328*, 18−26.

https://dx.doi.org/10.1021/acs.chemrev.0c00027
Chem. Rev. 2020, 120, 10887−10949

(121) Daly, C.; Pasnikowski, E.; Burova, E.; Wong, V.; Aldrich, T. H.; Griffiths, J.; Ioffe, E.; Daly, T. J.; Fandl, J. P.; Papadopoulos, N.; et al. Angiopoietin-2 Functions as an Autocrine Protective Factor in Stressed Endothelial Cells. *Proc. Natl. Acad. Sci. U. S. A.* **2006**, *103*, 15491−15496.
(122) Reiss, Y.; Droste, J.; Heil, M.; Tribulova, S.; Schmidt, M. H.; Schaper, W.; Dumont, D. J.; Plate, K. H. Angiopoietin-2 Impairs Revascularization after Limb Ischemia. *Circ. Res.* **2007**, *101*, 88−96.
(123) Sato, T. N.; Tozawa, Y.; Deutsch, U.; Wolburg-Buchholz, K.; Fujiwara, Y.; Gendron-Maguire, M.; Gridley, T.; Wolburg, H.; Risau, W.; Qin, Y. Distinct Roles of the Receptor Tyrosine Kinases Tie-1 and Tie-2 in Blood Vessel Formation. *Nature* **1995**, *376*, 70−74.
(124) Iivanainen, E.; Nelimarkka, L.; Elenius, V.; Heikkinen, S. M.; Junttila, T. T.; Sihombing, L.; Sundvall, M.; Maatta, J. A.; Laine, V. J.; Yla-Herttuala, S.; et al. Angiopoietin-Regulated Recruitment of Vascular Smooth Muscle Cells by Endothelial-Derived Heparin Binding Egf-Like Growth Factor. *FASEB J.* **2003**, *17*, 1609−1621.
(125) Lobov, I. B.; Brooks, P. C.; Lang, R. A. Angiopoietin-2 Displays Vegf-Dependent Modulation of Capillary Structure and Endothelial Cell Survival in Vivo. *Proc. Natl. Acad. Sci. U. S. A.* **2002**, *99*, 11205−11210.
(126) Oshima, Y.; Deering, T.; Oshima, S.; Nambu, H.; Reddy, P. S.; Kaleko, M.; Connelly, S.; Hackett, S. F.; Campochiaro, P. A. Angiopoietin-2 Enhances Retinal Vessel Sensitivity to Vascular Endothelial Growth Factor. *J. Cell. Physiol.* **2004**, *199*, 412−417.
(127) Oshima, Y.; Oshima, S.; Nambu, H.; Kachi, S.; Takahashi, K.; Umeda, N.; Shen, J.; Dong, A.; Apte, R. S.; Duh, E.; et al. Different Effects of Angiopoietin-2 in Different Vascular Beds in the Eye: New Vessels Are Most Sensitive. *FASEB J.* **2005**, *19*, 963−965.
(128) Kayakabe, K.; Kuroiwa, T.; Sakurai, N.; Ikeuchi, H.; Kadiombo, A. T.; Sakairi, T.; Matsumoto, T.; Maeshima, A.; Hiromura, K.; Nojima, Y. Interleukin-6 Promotes Destabilized Angiogenesis by Modulating Angiopoietin Expression in Rheumatoid Arthritis. *Rheumatology* **2012**, *51*, 1571−1579.
(129) Hirata, A.; Ogawa, S.-i.; Kometani, T.; Kuwano, T.; Naito, S.; Kuwano, M.; Ono, M. Zd1839 (Iressa) Induces Antiangiogenic Effects through Inhibition of Epidermal Growth Factor Receptor Tyrosine Kinase. *Cancer Res.* **2002**, *62*, 2554−2560.
(130) van Cruijsen, H.; Giaccone, G.; Hoekman, K. Epidermal Growth Factor Receptor and Angiogenesis: Opportunities for Combined Anticancer Strategies. *Int. J. Cancer* **2005**, *117*, 883−888.
(131) Beets, K.; Huylebroeck, D.; Moya, I. M.; Umans, L.; Zwijsen, A. Robustness in Angiogenesis: Notch and Bmp Shaping Waves. *Trends Genet.* **2013**, *29*, 140−149.
(132) Neufeld, G.; Kessler, O. Pro-Angiogenic Cytokines and Their Role in Tumor Angiogenesis. *Cancer Metastasis Rev.* **2006**, *25*, 373.
(133) Schraufstatter, I. U.; Chung, J.; Burger, M. Il-8 Activates Endothelial Cell Cxcr1 and Cxcr2 through Rho and Rac Signaling Pathways. *Am. J. Physiol. Lung Cell Mol. Physiol.* **2001**, *280*, L1094−L1103.
(134) Li, A.; Dubey, S.; Varney, M. L.; Dave, B. J.; Singh, R. K. Il-8 Directly Enhanced Endothelial Cell Survival, Proliferation, and Matrix Metalloproteinases Production and Regulated Angiogenesis. *J. Immunol.* **2003**, *170*, 3369−3376.
(135) Kryczek, I.; Lange, A.; Mottram, P.; Alvarez, X.; Cheng, P.; Hogan, M.; Moons, L.; Wei, S.; Zou, L.; Machelon, V. Cxcl12 and Vascular Endothelial Growth Factor Synergistically Induce Neoangiogenesis in Human Ovarian Cancers. *Cancer Res.* **2005**, *65*, 465−472.
(136) Petit, I.; Jin, D.; Rafii, S. The Sdf-1-Cxcr4 Signaling Pathway: A Molecular Hub Modulating Neo-Angiogenesis. *Trends Immunol.* **2007**, *28*, 299−307.
(137) Fujisawa, N.; Hayashi, S.; Kurdowska, A.; Carr, F. K.; Miller, E. J. Inhibition of Groα-Induced Human Endothelial Cell Proliferation by the A-Chemokine Inhibitor Antileukinate. *Cytokine + **1999**, *11*, 231−238.
(138) Fajardo, L. F. Special Report the Complexity of Endothelial Cells: A Review. *Am. J. Clin. Pathol.* **1989**, *92*, 241−250.
(139) Swartz, D. D.; Andreadis, S. T. Animal Models for Vascular Tissue-Engineering. *Curr. Opin. Biotechnol.* **2013**, *24*, 916−925.
(140) Chi, J.-T.; Chang, H. Y.; Haraldsen, G.; Jahnsen, F. L.; Troyanskaya, O. G.; Chang, D. S.; Wang, Z.; Rockson, S. G.; Van De Rijn, M.; Botstein, D.; Brown, P. O. Endothelial Cell Diversity Revealed by Global Expression Profiling. *Proc. Natl. Acad. Sci. U. S. A.* **2003**, *100*, 10623−10628.
(141) Bouïs, D.; Hospers, G. A.; Meijer, C.; Molema, G.; Mulder, N. H. Endothelium in Vitro: A Review of Human Vascular Endothelial Cell Lines for Blood Vessel-Related Research. *Angiogenesis* **2001**, *4*, 91−102.
(142) Goldberger, A.; Middleton, K. A.; Oliver, J. A.; Paddock, C.; Yan, H.-C.; DeLisser, H. M.; Albelda, S. M.; Newman, P. J. Biosynthesis and Processing of the Cell Adhesion Molecule Pecam-1 Includes Production of a Soluble Form. *J. Biol. Chem.* **1994**, *269*, 17183−17191.
(143) Nozawa, F.; Hirota, M.; Okabe, A.; Shibata, M.; Iwamura, T.; Haga, Y.; Ogawa, M. Tumor Necrosis Factor A Acts on Cultured Human Vascular Endothelial Cells to Increase the Adhesion of Pancreatic Cancer Cells. *Pancreas* **2000**, *21*, 392−398.
(144) Muscella, A.; Marsigliante, S.; Carluccio, M.; Vinson, G.; Storelli, C. Angiotensin Ii At1 Receptors and Na^+/K^+ Atpase in Human Umbilical Vein Endothelial Cells. *J. Endocrinol.* **1997**, *155*, 587−593.
(145) Mou, Y.; Yue, Z.; Zhang, H.; Shi, X.; Zhang, M.; Chang, X.; Gao, H.; Li, R.; Wang, Z. High Quality in Vitro Expansion of Human Endothelial Progenitor Cells of Human Umbilical Vein Origin. *Int. J. Med. Sci.* **2017**, *14*, 294.
(146) Nakatsu, M. N.; Sainson, R. C.; Aoto, J. N.; Taylor, K. L.; Aitkenhead, M.; Perez-del-Pulgar, S.; Carpenter, P. M.; Hughes, C. C. Angiogenic Sprouting and Capillary Lumen Formation Modeled by Human Umbilical Vein Endothelial Cells (Huvec) in Fibrin Gels: The Role of Fibroblasts and Angiopoietin-1. *Microvasc. Res.* **2003**, *66*, 102−112.
(147) Pi, Q.; Maharjan, S.; Yan, X.; Liu, X.; Singh, B.; van Genderen, A. M.; Robledo-Padilla, F.; Parra-Saldivar, R.; Hu, N.; Jia, W.; et al. Digitally Tunable Microfluidic Bioprinting of Multilayered Cannular Tissues. *Adv. Mater.* **2018**, *30*, 1706913.
(148) Kolesky, D. B.; Homan, K. A.; Skylar-Scott, M. A.; Lewis, J. A. Three-Dimensional Bioprinting of Thick Vascularized Tissues. *Proc. Natl. Acad. Sci. U. S. A.* **2016**, *113*, 3179−3184.
(149) Colosi, C.; Shin, S. R.; Manoharan, V.; Massa, S.; Costantini, M.; Barbetta, A.; Dokmeci, M. R.; Dentini, M.; Khademhosseini, A. Microfluidic Bioprinting of Heterogeneous 3d Tissue Constructs Using Low-Viscosity Bioink. *Adv. Mater.* **2016**, *28*, 677−684.
(150) Chen, Y. W.; Shen, Y. F.; Ho, C. C.; Yu, J.; Wu, Y. A.; Wang, K.; Shih, C. T.; Shie, M. Y. Osteogenic and Angiogenic Potentials of the Cell-Laden Hydrogel/Mussel-Inspired Calcium Silicate Complex Hierarchical Porous Scaffold Fabricated by 3d Bioprinting. *Mater. Sci. Eng., C* **2018**, *91*, 679−687.
(151) Park, H.-J.; Zhang, Y.; Georgescu, S. P.; Johnson, K. L.; Kong, D.; Galper, J. B. Human Umbilical Vein Endothelial Cells and Human Dermal Microvascular Endothelial Cells Offer New Insights into the Relationship between Lipid Metabolism and Angiogenesis. *Stem Cell Rev.* **2006**, *2*, 93−101.
(152) Chen, Z.; Htay, A.; Dos Santos, W.; Gillies, G. T.; Fillmore, H. L.; Sholley, M. M.; Broaddus, W. C. Vitro Angiogenesis by Human Umbilical Vein Endothelial Cells (Huvec) Induced by Three-Dimensional Co-Culture with Glioblastoma Cells. *J. Neuro-Oncol.* **2009**, *92*, 121−128.
(153) Mazur, M., *Primary Human Liver Co-Culture With Flow and Kupffer Cell Integration On Microfluidic Liver-On-A-Chip*. Senior Thesis, Brandeis University, Waltham, MA, 2015.
(154) Zhang, B.; Korolj, A.; Lai, B. F. L.; Radisic, M. Advances in Organ-on-a-Chip Engineering. *Nat. Rev. Mater.* **2018**, *3*, 257.
(155) Wang, Z.; Wen, F.; Lim, P. N.; Zhang, Q.; Konishi, T.; Wang, D.; Teoh, S. H.; Thian, E. S. Nanomaterial Scaffolds to Regenerate Musculoskeletal Tissue: Signals from within for Neovessel Formation. *Drug Discovery Today* **2017**, *22*, 1385−1391.
(156) Rufaihah, A. J.; Huang, N. F.; Kim, J.; Herold, J.; Volz, K. S.; Park, T. S.; Lee, J. C.; Zambidis, E. T.; Reijo-Pera, R.; Cooke, J. P.

https://dx.doi.org/10.1021/acs.chemrev.0c00027
Chem. Rev. 2020, 120, 10887−10949

Human Induced Pluripotent Stem Cell-Derived Endothelial Cells Exhibit Functional Heterogeneity. *Am. J. Transl. Res.* **2013**, *5*, 21.
(157) Choi, K. D.; Yu, J.; Smuga-Otto, K.; Salvagiotto, G.; Rehrauer, W.; Vodyanik, M.; Thomson, J.; Slukvin, I. Hematopoietic and Endothelial Differentiation of Human Induced Pluripotent Stem Cells. *Stem Cells* **2009**, *27*, 559−567.
(158) Wang, L.; Xiang, M.; Liu, Y.; Sun, N.; Lu, M.; Shi, Y.; Wang, X.; Meng, D.; Chen, S.; Qin, J. Human Induced Pluripotent Stem Cells Derived Endothelial Cells Mimicking Vascular Inflammatory Response under Flow. *Biomicrofluidics* **2016**, *10*, 014106.
(159) Adams, W. J.; Zhang, Y.; Cloutier, J.; Kuchimanchi, P.; Newton, G.; Sehrawat, S.; Aird, W. C.; Mayadas, T. N.; Luscinskas, F. W.; García-Cardeña, G. Functional Vascular Endothelium Derived from Human Induced Pluripotent Stem Cells. *Stem Cell Rep.* **2013**, *1*, 105−113.
(160) Kurokawa, Y. K.; Yin, R. T.; Shang, M. R.; Shirure, V. S.; Moya, M. L.; George, S. C. Human Induced Pluripotent Stem Cell-Derived Endothelial Cells for Three-Dimensional Microphysiological Systems. *Tissue Eng., Part C* **2017**, *23*, 474−484.
(161) Rajendran, P.; Rengarajan, T.; Thangavel, J.; Nishigaki, Y.; Sakthisekaran, D.; Sethi, G.; Nishigaki, I. The Vascular Endothelium and Human Diseases. *Int. J. Biol. Sci.* **2013**, *9*, 1057.
(162) Lacorre, D.-A.; Baekkevold, E. S.; Garrido, I.; Brandtzaeg, P.; Haraldsen, G.; Amalric, F.; Girard, J.-P. Plasticity of Endothelial Cells: Rapid Dedifferentiation of Freshly Isolated High Endothelial Venule Endothelial Cells Outside the Lymphoid Tissue Microenvironment. *Blood* **2004**, *103*, 4164−4172.
(163) Asahara, T.; Murohara, T.; Sullivan, A.; Silver, M.; van der Zee, R.; Li, T.; Witzenbichler, B.; Schatteman, G.; Isner, J. M. Isolation of Putative Progenitor Endothelial Cells for Angiogenesis. *Science* **1997**, *275*, 964−966.
(164) Risau, W.; Sariola, H.; Zerwes, H.-G.; Sasse, J.; Ekblom, P.; Kemler, R.; Doetschman, T. Vasculogenesis and Angiogenesis in Embryonic-Stem-Cell-Derived Embryoid Bodies. *Development* **1988**, *102*, 471−478.
(165) Asahara, T.; Kawamoto, A.; Masuda, H. Concise Review: Circulating Endothelial Progenitor Cells for Vascular Medicine. *Stem Cells* **2011**, *29*, 1650−1655.
(166) Chong, M. S. K.; Ng, W. K.; Chan, J. K. Y. Concise Review: Endothelial Progenitor Cells in Regenerative Medicine: Applications and Challenges. *Stem Cells Transl. Med.* **2016**, *5*, 530−538.
(167) Peters, E. B.; Christoforou, N.; Leong, K. W.; Truskey, G. A.; West, J. L. Poly(Ethylene Glycol) Hydrogel Scaffolds Containing Cell-Adhesive and Protease-Sensitive Peptides Support Microvessel Formation by Endothelial Progenitor Cells. *Cell. Mol. Bioeng.* **2016**, *9*, 38−54.
(168) Rouwkema, J.; Westerweel, P. E.; de Boer, J.; Verhaar, M. C.; van Blitterswijk, C. A. The Use of Endothelial Progenitor Cells for Prevascularized Bone Tissue Engineering. *Tissue Eng., Part A* **2009**, *15*, 2015−2027.
(169) Melero-Martin, J. M.; Khan, Z. A.; Picard, A.; Wu, X.; Paruchuri, S.; Bischoff, J. In Vivo Vasculogenic Potential of Human Blood-Derived Endothelial Progenitor Cells. *Blood* **2007**, *109*, 4761−4768.
(170) Werner, N.; Kosiol, S.; Schiegl, T.; Ahlers, P.; Walenta, K.; Link, A.; Böhm, M.; Nickenig, G. Circulating Endothelial Progenitor Cells and Cardiovascular Outcomes. *N. Engl. J. Med.* **2005**, *353*, 999−1007.
(171) Bailey, A. S.; Jiang, S.; Afentoulis, M.; Baumann, C. I.; Schroeder, D. A.; Olson, S. B.; Wong, M. H.; Fleming, W. H. Transplanted Adult Hematopoietic Stems Cells Differentiate into Functional Endothelial Cells. *Blood* **2004**, *103*, 13−19.
(172) Ingram, D. A.; Mead, L. E.; Moore, D. B.; Woodard, W.; Fenoglio, A.; Yoder, M. C. Vessel Wall−Derived Endothelial Cells Rapidly Proliferate Because They Contain a Complete Hierarchy of Endothelial Progenitor Cells. *Blood* **2005**, *105*, 2783−2786.
(173) Patel, J.; Seppanen, E.; Chong, M. S.; Yeo, J. S.; Teo, E. Y.; Chan, J. K.; Fisk, N. M.; Khosrotehrani, K. Prospective Surface Marker-Based Isolation and Expansion of Fetal Endothelial Colony-Forming Cells from Human Term Placenta. *Stem Cells Transl. Med.* **2013**, *2*, 839−847.
(174) Shi, Q.; Rafii, S.; Wu, M. H.-D.; Wijelath, E. S.; Yu, C.; Ishida, A.; Fujita, Y.; Kothari, S.; Mohle, R.; Sauvage, L. R.; et al. Evidence for Circulating Bone Marrow-Derived Endothelial Cells. *Blood* **1998**, *92*, 362−367.
(175) Timmermans, F.; Plum, J.; Yöder, M. C.; Ingram, D. A.; Vandekerckhove, B.; Case, J. Endothelial Progenitor Cells: Identity Defined? *J. Cell. Mol. Med.* **2009**, *13*, 87−102.
(176) Basile, D. P.; Yoder, M. C. Circulating and Tissue Resident Endothelial Progenitor Cells. *J. Cell. Physiol.* **2013**, *229*, 10−16.
(177) Urbich, C.; Heeschen, C.; Aicher, A.; Dernbach, E.; Zeiher, A. M.; Dimmeler, S. Relevance of Monocytic Features for Neovascularization Capacity of Circulating Endothelial Progenitor Cells. *Circulation* **2003**, *108*, 2511−2516.
(178) Lin, Y.; Weisdorf, D. J.; Solovey, A.; Hebbel, R. P. Origins of Circulating Endothelial Cells and Endothelial Outgrowth from Blood. *J. Clin. Invest.* **2000**, *105*, 71−77.
(179) Yoon, C.-H.; Hur, J.; Park, K.-W.; Kim, J.-H.; Lee, C.-S.; Oh, I.-Y.; Kim, T.-Y.; Cho, H.-J.; Kang, H.-J.; Chae, I.-H.; et al. Synergistic Neovascularization by Mixed Transplantation of Early Endothelial Progenitor Cells and Late Outgrowth Endothelial Cells: The Role of Angiogenic Cytokines and Matrix Metalloproteinases. *Circulation* **2005**, *112*, 1618−1627.
(180) Rehman, J.; Li, J.; Orschell, C. M.; March, K. L. Peripheral Blood "Endothelial Progenitor Cells" Are Derived from Monocyte/Macrophages and Secrete Angiogenic Growth Factors. *Circulation* **2003**, *107*, 1164−1169.
(181) Masuda, H.; Iwasaki, H.; Kawamoto, A.; Akimaru, H.; Ishikawa, M.; Ii, M.; Shizuno, T.; Sato, A.; Ito, R.; Horii, M.; et al. Development of Serum-Free Quality and Quantity Control Culture of Colony-Forming Endothelial Progenitor Cell for Vasculogenesis. *Stem Cells Transl. Med.* **2012**, *1*, 160−171.
(182) Boilson, B. A.; Kiernan, T. J.; Harbuzariu, A.; Nelson, R. E.; Lerman, A.; Simari, R. D. Circulating Cd34+ Cell Subsets in Patients with Coronary Endothelial Dysfunction. *Nat. Clin. Pract. Cardiovasc. Med.* **2008**, *5*, 489−496.
(183) Case, J.; Mead, L. E.; Bessler, W. K.; Prater, D.; White, H. A.; Saadatzadeh, M. R.; Bhavsar, J. R.; Yoder, M. C.; Haneline, L. S.; Ingram, D. A. Human Cd34+ Ac133+ Vegfr-2+ Cells Are Not Endothelial Progenitor Cells but Distinct, Primitive Hematopoietic Progenitors. *Exp. Hematol.* **2007**, *35*, 1109−1118.
(184) Heil, M.; Ziegelhoeffer, T.; Mees, B.; Schaper, W. A Different Outlook on the Role of Bone Marrow Stem Cells in Vascular Growth: Bone Marrow Delivers Software Not Hardware. *Circ. Res.* **2004**, *94*, 573−574.
(185) Ingram, D. A.; Mead, L. E.; Tanaka, H.; Meade, V.; Fenoglio, A.; Mortell, K.; Pollok, K.; Ferkowicz, M. J.; Gilley, D.; Yoder, M. C. Identification of a Novel Hierarchy of Endothelial Progenitor Cells Using Human Peripheral and Umbilical Cord Blood. *Blood* **2004**, *104*, 2752−2760.
(186) Masuda, H.; Alev, C.; Akimaru, H.; Ito, R.; Shizuno, T.; Kobori, M.; Horii, M.; Ishihara, T.; Isobe, K.; Isozaki, M.; et al. Methodological Development of a Clonogenic Assay to Determine Endothelial Progenitor Cell Potential. *Circ. Res.* **2011**, *109*, 20−37.
(187) Kwon, S.-M.; Eguchi, M.; Wada, M.; Iwami, Y.; Hozumi, K.; Iwaguro, H.; Masuda, H.; Kawamoto, A.; Asahara, T. Specific Jagged-1 Signal from Bone Marrow Microenvironment Is Required for Endothelial Progenitor Cell Development for Neovascularization. *Circulation* **2008**, *118*, 157.
(188) Tanaka, R.; Wada, M.; Kwon, S. M.; Masuda, H.; Carr, J.; Ito, R.; Miyasaka, M.; Warren, S. M.; Asahara, T.; Tepper, O. M. The Effects of Flap Ischemia on Normal and Diabetic Progenitor Cell Function. *Plast. Reconstr. Surg.* **2008**, *121*, 1929−1942.
(189) Mund, J. A.; Estes, M. L.; Yoder, M. C.; Ingram, D. A., Jr; Case, J. Flow Cytometric Identification and Functional Characterization of Immature and Mature Circulating Endothelial Cells. *Arterioscler., Thromb., Vasc. Biol.* **2012**, *32*, 1045−1053.

https://dx.doi.org/10.1021/acs.chemrev.0c00027
Chem. Rev. 2020, 120, 10887−10949

(190) Sieveking, D. P.; Buckle, A.; Celermajer, D. S.; Ng, M. K. Strikingly Different Angiogenic Properties of Endothelial Progenitor Cell Subpopulations: Insights from a Novel Human Angiogenesis Assay. *J. Am. Coll. Cardiol.* **2008**, *51*, 660−668.
(191) Schechner, J. S.; Nath, A. K.; Zheng, L.; Kluger, M. S.; Hughes, C. C.; Sierra-Honigmann, M. R.; Lorber, M. I.; Tellides, G.; Kashgarian, M.; Bothwell, A. L.; et al. In Vivo Formation of Complex Microvessels Lined by Human Endothelial Cells in an Immunodeficient Mouse. *Proc. Natl. Acad. Sci. U. S. A.* **2000**, *97*, 9191−9196.
(192) Bergers, G.; Song, S. The Role of Pericytes in Blood-Vessel Formation and Maintenance. *Neuro Oncol* **2005**, *7*, 452−464.
(193) Sweeney, M. D.; Ayyadurai, S.; Zlokovic, B. V. Pericytes of the Neurovascular Unit: Key Functions and Signaling Pathways. *Nat. Neurosci.* **2016**, *19*, 771.
(194) Armulik, A.; Genové, G.; Mäe, M.; Nisancioglu, M. H.; Wallgard, E.; Niaudet, C.; He, L.; Norlin, J.; Lindblom, P.; Strittmatter, K.; et al. Pericytes Regulate the Blood−Brain Barrier. *Nature* **2010**, *468*, 557−561.
(195) Attwell, D.; Mishra, A.; Hall, C. N.; O'Farrell, F. M.; Dalkara, T. What Is a Pericyte? *J. Cereb. Blood Flow Metab.* **2016**, *36*, 451−455.
(196) Kim, J.; Chung, M.; Kim, S.; Jo, D. H.; Kim, J. H.; Jeon, N. L. Engineering of a Biomimetic Pericyte-Covered 3d Microvascular Network. *PLoS One* **2015**, *10*, No. e0133880.
(197) Campisi, M.; Shin, Y.; Osaki, T.; Hajal, C.; Chiono, V.; Kamm, R. D. 3d Self-Organized Microvascular Model of the Human Blood-Brain Barrier with Endothelial Cells, Pericytes and Astrocytes. *Biomaterials* **2018**, *180*, 117−129.
(198) Caplan, A. I. All Mscs Are Pericytes? *Cell stem cell* **2008**, *3*, 229−230.
(199) Pittenger, M. F.; Mackay, A. M.; Beck, S. C.; Jaiswal, R. K.; Douglas, R.; Mosca, J. D.; Moorman, M. A.; Simonetti, D. W.; Craig, S.; Marshak, D. R. Multilineage Potential of Adult Human Mesenchymal Stem Cells. *Science* **1999**, *284*, 143−147.
(200) Pittenger, M. F.; Discher, D. E.; Peault, B. M.; Phinney, D. G.; Hare, J. M.; Caplan, A. I. Mesenchymal Stem Cell Perspective: Cell Biology to Clinical Progress. *NPJ. Regen Med.* **2019**, *4*, 22.
(201) Dominici, M.; Le Blanc, K.; Mueller, I.; Slaper-Cortenbach, I.; Marini, F.; Krause, D.; Deans, R.; Keating, A.; Prockop, D.; Horwitz, E. Minimal Criteria for Defining Multipotent Mesenchymal Stromal Cells. The International Society for Cellular Therapy Position Statement. *Cytotherapy* **2006**, *8*, 315−317.
(202) Watt, S. M.; Gullo, F.; van der Garde, M.; Markeson, D.; Camicia, R.; Khoo, C. P.; Zwaginga, J. J. The Angiogenic Properties of Mesenchymal Stem/Stromal Cells and Their Therapeutic Potential. *Br. Med. Bull.* **2013**, *108*, 25−53.
(203) Huang, N. F.; Li, S. Mesenchymal Stem Cells for Vascular Regeneration. *Regener. Med.* **2008**, *3*, 877−892.
(204) Au, P.; Tam, J.; Fukumura, D.; Jain, R. K. Bone Marrow−Derived Mesenchymal Stem Cells Facilitate Engineering of Long-Lasting Functional Vasculature. *Blood* **2008**, *111*, 4551−4558.
(205) Nassiri, S. M.; Rahbarghazi, R. Interactions of Mesenchymal Stem Cells with Endothelial Cells. *Stem Cells Dev.* **2014**, *23*, 319−332.
(206) Crisan, M.; Yap, S.; Casteilla, L.; Chen, C. W.; Corselli, M.; Park, T. S.; Andriolo, G.; Sun, B.; Zheng, B.; Zhang, L.; et al. A Perivascular Origin for Mesenchymal Stem Cells in Multiple Human Organs. *Cell Stem Cell* **2008**, *3*, 301−313.
(207) Hashi, C. K.; Zhu, Y.; Yang, G.-Y.; Young, W. L.; Hsiao, B. S.; Wang, K.; Chu, B.; Li, S. Antithrombogenic Property of Bone Marrow Mesenchymal Stem Cells in Nanofibrous Vascular Grafts. *Proc. Natl. Acad. Sci. U. S. A.* **2007**, *104*, 11915−11920.
(208) Tao, H.; Han, Z.; Han, Z. C.; Li, Z. Proangiogenic Features of Mesenchymal Stem Cells and Their Therapeutic Applications. *Stem Cells Int.* **2016**, *2016*, 1314709.
(209) Newman, A. C.; Nakatsu, M. N.; Chou, W.; Gershon, P. D.; Hughes, C. C. The Requirement for Fibroblasts in Angiogenesis: Fibroblast-Derived Matrix Proteins Are Essential for Endothelial Cell Lumen Formation. *Mol. Biol. Cell* **2011**, *22*, 3791−3800.
(210) Yang, X.; Liaw, L.; Prudovsky, I.; Brooks, P. C.; Vary, C.; Oxburgh, L.; Friesel, R. Fibroblast Growth Factor Signaling in the Vasculature. *Curr. Atheroscler. Rep.* **2015**, *17*, 31.
(211) Lermusiaux, P.; Leroux, C.; Tasse, J. C.; Castellani, L.; Martinez, R. Aortic Aneurysm: Construction of a Life-Size Model by Rapid Prototyping. *Ann. Vasc. Surg.* **2001**, *15*, 131−135.
(212) Schwartz, S. M.; Campbell, G. R.; Campbell, J. H. Replication of Smooth Muscle Cells in Vascular Disease. *Circ. Res.* **1986**, *58*, 427−444.
(213) Price, R. J.; Owens, G. K.; Skalak, T. C. Immunohistochemical Identification of Arteriolar Development Using Markers of Smooth Muscle Differentiation. Evidence That Capillary Arterialization Proceeds from Terminal Arterioles. *Circ. Res.* **1994**, *75*, 520−527.
(214) Owens, G. K. Regulation of Differentiation of Vascular Smooth Muscle Cells. *Physiol. Rev.* **1995**, *75*, 487−517.
(215) Scotti, L.; Abramovich, D.; Pascuali, N.; Durand, L. H.; Irusta, G.; de Zuniga, I.; Tesone, M.; Parborell, F. Inhibition of Angiopoietin-1 (Angpt1) Affects Vascular Integrity in Ovarian Hyperstimulation Syndrome (Ohss). *Reprod., Fertil. Dev.* **2016**, *28*, 690−699.
(216) Martino, M. M.; Brkic, S.; Bovo, E.; Burger, M.; Schaefer, D. J.; Wolff, T.; Gürke, L.; Briquez, P. S.; Larsson, H. M.; Gianni-Barrera, R.; et al. Extracellular Matrix and Growth Factor Engineering for Controlled Angiogenesis in Regenerative Medicine. *Front. Bioeng. Biotechnol.* **2015**, *3*, 45.
(217) Briquez, P. S.; Clegg, L. E.; Martino, M. M.; Gabhann, F. M.; Hubbell, J. A. Design Principles for Therapeutic Angiogenic Materials. *Nat. Rev. Mater.* **2016**, *1*, 15006.
(218) Hospodiuk, M.; Dey, M.; Sosnoski, D.; Ozbolat, I. T. The Bioink: A Comprehensive Review on Bioprintable Materials. *Biotechnol. Adv.* **2017**, *35*, 217−239.
(219) Zhang, Y. S.; Oklu, R.; Dokmeci, M. R.; Khademhosseini, A. Three-Dimensional Bioprinting Strategies for Tissue Engineering. *Cold Spring Harbor Perspect. Med.* **2018**, *8*, a025718.
(220) Gudapati, H.; Dey, M.; Ozbolat, I. A Comprehensive Review on Droplet-Based Bioprinting: Past, Present and Future. *Biomaterials* **2016**, *102*, 20−42.
(221) Xu, C.; Zhang, M.; Huang, Y.; Ogale, A.; Fu, J.; Markwald, R. R. Study of Droplet Formation Process During Drop-on-Demand Inkjetting of Living Cell-Laden Bioink. *Langmuir* **2014**, *30*, 9130−9138.
(222) Benning, L.; Gutzweiler, L.; Trondle, K.; Riba, J.; Zengerle, R.; Koltay, P.; Zimmermann, S.; Stark, G. B.; Finkenzeller, G. Assessment of Hydrogels for Bioprinting of Endothelial Cells. *J. Biomed. Mater. Res., Part A* **2018**, *106*, 935−947.
(223) Wilson, W. C., Jr.; Boland, T. Cell and Organ Printing 1: Protein and Cell Printers. *Anat. Rec.* **2003**, *272A*, 491−496.
(224) Nakamura, M.; Kobayashi, A.; Takagi, F.; Watanabe, A.; Hiruma, Y.; Ohuchi, K.; Iwasaki, Y.; Horie, M.; Morita, I.; Takatani, S. Biocompatible Inkjet Printing Technique for Designed Seeding of Individual Living Cells. *Tissue Eng.* **2005**, *11*, 1658−1666.
(225) Kesari, P.; Xu, T.; Boland, T. Layer-by-Layer Printing of Cells and Its Application to Tissue Engineering. *Mater. Res. Soc. Symp.* **2004**, *845*, AA4.5.
(226) Boland, T.; Tao, X.; Damon, B. J.; Manley, B.; Kesari, P.; Jalota, S.; Bhaduri, S. Drop-on-Demand Printing of Cells and Materials for Designer Tissue Constructs. *Mater. Sci. Eng., C* **2007**, *27*, 372−376.
(227) Yanez, M.; Rincon, J.; Dones, A.; De Maria, C.; Gonzales, R.; Boland, T. In Vivo Assessment of Printed Microvasculature in a Bilayer Skin Graft to Treat Full-Thickness Wounds. *Tissue Eng., Part A* **2015**, *21*, 224−233.
(228) Xu, T.; Zhao, W.; Zhu, J. M.; Albanna, M. Z.; Yoo, J. J.; Atala, A. Complex Heterogeneous Tissue Constructs Containing Multiple Cell Types Prepared by Inkjet Printing Technology. *Biomaterials* **2013**, *34*, 130−139.
(229) Xu, C.; Zhang, Z.; Christensen, K.; Huang, Y.; Fu, J.; Markwald, R. R. Freeform Vertical and Horizontal Fabrication of Alginate-Based Vascular-Like Tubular Constructs Using Inkjetting. *J. Manuf. Sci. Eng.* **2014**, *136*, 061010.

https://dx.doi.org/10.1021/acs.chemrev.0c00027
Chem. Rev. 2020, 120, 10887−10949

(230) Albanna, M.; Binder, K. W.; Murphy, S. V.; Kim, J.; Qasem, S. A.; Zhao, W.; Tan, J.; El-Amin, I. B.; Dice, D. D.; Marco, J.; et al. In Situ Bioprinting of Autologous Skin Cells Accelerates Wound Healing of Extensive Excisional Full-Thickness Wounds. *Sci. Rep.* **2019**, *9*, 1856.
(231) Skardal, A.; Mack, D.; Kapetanovic, E.; Atala, A.; Jackson, J. D.; Yoo, J.; Soker, S. Bioprinted Amniotic Fluid-Derived Stem Cells Accelerate Healing of Large Skin Wounds. *Stem Cells Transl. Med.* **2012**, *1*, 792−802.
(232) Solis, L. H.; Ayala, Y.; Portillo, S.; Varela-Ramirez, A.; Aguilera, R.; Boland, T. Thermal Inkjet Bioprinting Triggers the Activation of the Vegf Pathway in Human Microvascular Endothelial Cells in Vitro. *Biofabrication* **2019**, *11*, 045005.
(233) Boland, T.; Xu, T.; Damon, B.; Cui, X. Application of Inkjet Printing to Tissue Engineering. *Biotechnol. J.* **2006**, *1*, 910−917.
(234) Hansen, C. J.; Saksena, R.; Kolesky, D. B.; Vericella, J. J.; Kranz, S. J.; Muldowney, G. P.; Christensen, K. T.; Lewis, J. A. High-Throughput Printing Via Microvascular Multinozzle Arrays. *Adv. Mater.* **2013**, *25*, 96−102.
(235) Skylar-Scott, M. A.; Mueller, J.; Visser, C. W.; Lewis, J. A. Voxelated Soft Matter Via Multimaterial Multinozzle 3d Printing. *Nature* **2019**, *575*, 330−335.
(236) Yu, Y.; Zhang, Y.; Martin, J. A.; Ozbolat, I. T. Evaluation of Cell Viability and Functionality in Vessel-Like Bioprintable Cell-Laden Tubular Channels. *J. Biomech. Eng.* **2013**, *135*, 091011.
(237) Duan, B.; Hockaday, L. A.; Kang, K. H.; Butcher, J. T. 3d Bioprinting of Heterogeneous Aortic Valve Conduits with Alginate/Gelatin Hydrogels. *J. Biomed. Mater. Res., Part A* **2013**, *101*, 1255−1264.
(238) Bertassoni, L. E.; Cardoso, J. C.; Manoharan, V.; Cristino, A. L.; Bhise, N. S.; Araujo, W. A.; Zorlutuna, P.; Vrana, N. E.; Ghaemmaghami, A. M.; Dokmeci, M. R.; et al. Direct-Write Bioprinting of Cell-Laden Methacrylated Gelatin Hydrogels. *Biofabrication* **2014**, *6*, 024105.
(239) Bertassoni, L. E.; Cecconi, M.; Manoharan, V.; Nikkhah, M.; Hjortnaes, J.; Cristino, A. L.; Barabaschi, G.; Demarchi, D.; Dokmeci, M. R.; Yang, Y.; et al. Hydrogel Bioprinted Microchannel Networks for Vascularization of Tissue Engineering Constructs. *Lab Chip* **2014**, *14*, 2202−2211.
(240) Zhao, L.; Lee, V. K.; Yoo, S. S.; Dai, G.; Intes, X. The Integration of 3-D Cell Printing and Mesoscopic Fluorescence Molecular Tomography of Vascular Constructs within Thick Hydrogel Scaffolds. *Biomaterials* **2012**, *33*, 5325−5332.
(241) Wu, W.; DeConinck, A.; Lewis, J. A. Omnidirectional Printing of 3d Microvascular Networks. *Adv. Mater.* **2011**, *23*, H178−183.
(242) Miller, J. S.; Stevens, K. R.; Yang, M. T.; Baker, B. M.; Nguyen, D. H.; Cohen, D. M.; Toro, E.; Chen, A. A.; Galie, P. A.; Yu, X.; et al. Rapid Casting of Patterned Vascular Networks for Perfusable Engineered Three-Dimensional Tissues. *Nat. Mater.* **2012**, *11*, 768−774.
(243) Lee, V. K.; Lanzi, A. M.; Ngo, H.; Yoo, S. S.; Vincent, P. A.; Dai, G. Generation of Multi-Scale Vascular Network System within 3d Hydrogel Using 3d Bio-Printing Technology. *Cell. Mol. Bioeng.* **2014**, *7*, 460−472.
(244) Song, K. H.; Highley, C. B.; Rouff, A.; Burdick, J. A. Complex 3d-Printed Microchannels within Cell-Degradable Hydrogels. *Adv. Funct. Mater.* **2018**, *28*, 1801331.
(245) Sheng, W.; Ogunwobi, O. O.; Chen, T.; Zhang, J.; George, T. J.; Liu, C.; Fan, Z. H. Capture, Release and Culture of Circulating Tumor Cells from Pancreatic Cancer Patients Using an Enhanced Mixing Chip. *Lab Chip* **2014**, *14*, 89−98.
(246) Chung, S.; Sudo, R.; Mack, P. J.; Wan, C.-R.; Vickerman, V.; Kamm, R. D. Cell Migration into Scaffolds under Co-Culture Conditions in a Microfluidic Platform. *Lab Chip* **2009**, *9*, 269−275.
(247) Gao, Q.; He, Y.; Fu, J.-z.; Liu, A.; Ma, L. Coaxial Nozzle-Assisted 3d Bioprinting with Built-in Microchannels for Nutrients Delivery. *Biomaterials* **2015**, *61*, 203−215.
(248) Cui, H.; Zhu, W.; Huang, Y.; Liu, C.; Yu, Z. X.; Nowicki, M.; Miao, S.; Cheng, Y.; Zhou, X.; Lee, S. J.; et al. In Vitro and in Vivo Evaluation of 3d Bioprinted Small-Diameter Vasculature with Smooth Muscle and Endothelium. *Biofabrication* **2020**, *12*, 015004.
(249) Norotte, C.; Marga, F. S.; Niklason, L. E.; Forgacs, G. Scaffold-Free Vascular Tissue Engineering Using Bioprinting. *Biomaterials* **2009**, *30*, 5910−5917.
(250) Ozbolat, I. T.; Hospodiuk, M. Current Advances and Future Perspectives in Extrusion-Based Bioprinting. *Biomaterials* **2016**, *76*, 321−343.
(251) Costantini, M.; Colosi, C.; Swieszkowski, W.; Barbetta, A. Co-Axial Wet-Spinning in 3d Bioprinting: State of the Art and Future Perspective of Microfluidic Integration. *Biofabrication* **2019**, *11*, 012001.
(252) Liu, X.; Carter, S.-S. D.; Renes, M. J.; Kim, J.; Rojas-Canales, D. M.; Penko, D.; Angus, C.; Beirne, S.; Drogemuller, C. J.; Yue, Z.; et al. Development of a Coaxial 3d Printing Platform for Biofabrication of Implantable Islet-Containing Constructs. *Adv. Healthcare Mater.* **2019**, *8*, No. 1801181.
(253) Millik, S. C.; Dostie, A. M.; Karis, D. G.; Smith, P. T.; McKenna, M.; Chan, N.; Curtis, C. D.; Nance, E.; Theberge, A. B.; Nelson, A. 3d Printed Coaxial Nozzles for the Extrusion of Hydrogel Tubes toward Modeling Vascular Endothelium. *Biofabrication* **2019**, *11*, 045009.
(254) Zhang, X.; Zhang, Y. Tissue Engineering Applications of Three-Dimensional Bioprinting. *Cell Biochem. Biophys.* **2015**, *72*, 777−782.
(255) Colosi, C.; Shin, S. R.; Manoharan, V.; Massa, S.; Costantini, M.; Barbetta, A.; Dokmeci, M. R.; Dentini, M.; Khademhosseini, A. Microfluidic Bioprinting of Heterogeneous 3d Tissue Constructs Using Low-Viscosity Bioink. *Adv. Mater.* **2016**, *28*, 677−684.
(256) Rutz, A. L.; Hyland, K. E.; Jakus, A. E.; Burghardt, W. R.; Shah, R. N. A Multimaterial Bioink Method for 3d Printing Tunable, Cell-Compatible Hydrogels. *Adv. Mater.* **2015**, *27*, 1607−1614.
(257) Kang, H. W.; Lee, S. J.; Ko, I. K.; Kengla, C.; Yoo, J. J.; Atala, A. A 3d Bioprinting System to Produce Human-Scale Tissue Constructs with Structural Integrity. *Nat. Biotechnol.* **2016**, *34*, 312−319.
(258) Oxman, N. Variable Property Rapid Prototyping. *Virtual Phys. Prototyp.* **2011**, *6*, 3−31.
(259) Hardin, J. O.; Ober, T. J.; Valentine, A. D.; Lewis, J. A. Microfluidic Printheads for Multimaterial 3d Printing of Viscoelastic Inks. *Adv. Mater.* **2015**, *27*, 3279−3284.
(260) Ober, T. J.; Foresti, D.; Lewis, J. A. Active Mixing of Complex Fluids at the Microscale. *Proc. Natl. Acad. Sci. U. S. A.* **2015**, *112*, 12293−12298.
(261) Liu, W.; Zhang, Y. S.; Heinrich, M. A.; De Ferrari, F.; Jang, H. L.; Bakht, S. M.; Alvarez, M. M.; Yang, J.; Li, Y. C.; Trujillo-de Santiago, G. Rapid Continuous Multimaterial Extrusion Bioprinting. *Adv. Mater.* **2017**, *29*, 1604630.
(262) Grosskopf, A. K.; Truby, R. L.; Kim, H.; Perazzo, A.; Lewis, J. A.; Stone, H. A. Viscoplastic Matrix Materials for Embedded 3d Printing. *ACS Appl. Mater. Interfaces* **2018**, *10*, 23353−23361.
(263) Wehner, M.; Truby, R. L.; Fitzgerald, D. J.; Mosadegh, B.; Whitesides, G. M.; Lewis, J. A.; Wood, R. J. An Integrated Design and Fabrication Strategy for Entirely Soft, Autonomous Robots. *Nature* **2016**, *536*, 451−455.
(264) Muth, J. T.; Vogt, D. M.; Truby, R. L.; Menguc, Y.; Kolesky, D. B.; Wood, R. J.; Lewis, J. A. Embedded 3d Printing of Strain Sensors within Highly Stretchable Elastomers. *Adv. Mater.* **2014**, *26*, 6307−6312.
(265) Jin, Y.; Compaan, A.; Bhattacharjee, T.; Huang, Y. Granular Gel Support-Enabled Extrusion of Three-Dimensional Alginate and Cellular Structures. *Biofabrication* **2016**, *8*, 025016.
(266) Bhattacharjee, T.; Zehnder, S. M.; Rowe, K. G.; Jain, S.; Nixon, R. M.; Sawyer, W. G.; Angelini, T. E. Writing in the Granular Gel Medium. *Sci. Adv.* **2015**, *1*, No. e1500655.
(267) Riley, L.; Schirmer, L.; Segura, T. Granular Hydrogels: Emergent Properties of Jammed Hydrogel Microparticles and Their Applications in Tissue Repair and Regeneration. *Curr. Opin. Biotechnol.* **2019**, *60*, 1−8.

https://dx.doi.org/10.1021/acs.chemrev.0c00027
Chem. Rev. 2020, 120, 10887−10949

(268) McCormack, A.; Highley, C. B.; Leslie, N. R.; Melchels, F. P. W. 3d Printing in Suspension Baths: Keeping the Promises of Bioprinting Afloat. *Trends Biotechnol.* **2020**, *38*, 584−593.
(269) Lee, A.; Hudson, A. R.; Shiwarski, D. J.; Tashman, J. W.; Hinton, T. J.; Yerneni, S.; Bliley, J. M.; Campbell, P. G.; Feinberg, A. W. 3d Bioprinting of Collagen to Rebuild Components of the Human Heart. *Science* **2019**, *365*, 482−487.
(270) Hinton, T. J.; Jallerat, Q.; Palchesko, R. N.; Park, J. H.; Grodzicki, M. S.; Shue, H. J.; Ramadan, M. H.; Hudson, A. R.; Feinberg, A. W. Three-Dimensional Printing of Complex Biological Structures by Freeform Reversible Embedding of Suspended Hydrogels. *Sci. Adv.* **2015**, *1*, No. e1500758.
(271) Highley, C. B.; Rodell, C. B.; Burdick, J. A. Direct 3d Printing of Shear-Thinning Hydrogels into Self-Healing Hydrogels. *Adv. Mater.* **2015**, *27*, 5075−5079.
(272) Skylar-Scott, M. A.; Uzel, S. G.; Nam, L. L.; Ahrens, J. H.; Truby, R. L.; Damaraju, S.; Lewis, J. A. Biomanufacturing of Organ-Specific Tissues with High Cellular Density and Embedded Vascular Channels. *Sci. Adv.* **2019**, *5*, No. eaaw2459.
(273) Noor, N.; Shapira, A.; Edri, R.; Gal, I.; Wertheim, L.; Dvir, T. 3d Printing of Personalized Thick and Perfusable Cardiac Patches and Hearts. *Adv. Sci.* **2019**, *6*, 1900344.
(274) Stumberger, G.; Vihar, B. Freeform Perfusable Microfluidics Embedded in Hydrogel Matrices. *Materials* **2018**, *11*, 2529.
(275) Hinton, T. J.; Hudson, A.; Pusch, K.; Lee, A.; Feinberg, A. W. 3d Printing Pdms Elastomer in a Hydrophilic Support Bath Via Freeform Reversible Embedding. *ACS Biomater. Sci. Eng.* **2016**, *2*, 1781−1786.
(276) Kawata, S.; Sun, H. B.; Tanaka, T.; Takada, K. Finer Features for Functional Microdevices. *Nature* **2001**, *412*, 697−698.
(277) Kerouredan, O.; Hakobyan, D.; Remy, M.; Ziane, S.; Dusserre, N.; Fricain, J. C.; Delmond, S.; Thebaud, N. B.; Devillard, R. In Situ Prevascularization Designed by Laser-Assisted Bioprinting: Effect on Bone Regeneration. *Biofabrication* **2019**, *11*, 045002.
(278) Kérourédan, O.; Bourget, J.-M.; Rémy, M.; Crauste-Manciet, S.; Kalisky, J.; Catros, S.; Thébaud, N. B.; Devillard, R. Micropatterning of Endothelial Cells to Create a Capillary-Like Network with Defined Architecture by Laser-Assisted Bioprinting. *J. Mater. Sci.: Mater. Med.* **2019**, *30*, 28.
(279) Michael, S.; Sorg, H.; Peck, C. T.; Koch, L.; Deiwick, A.; Chichkov, B.; Vogt, P. M.; Reimers, K. Tissue Engineered Skin Substitutes Created by Laser-Assisted Bioprinting Form Skin-Like Structures in the Dorsal Skin Fold Chamber in Mice. *PLoS One* **2013**, *8*, No. e57741.
(280) Koch, L.; Deiwick, A.; Schlie, S.; Michael, S.; Gruene, M.; Coger, V.; Zychlinski, D.; Schambach, A.; Reimers, K.; Vogt, P. M.; et al. Skin Tissue Generation by Laser Cell Printing. *Biotechnol. Bioeng.* **2012**, *109*, 1855−1863.
(281) Gaebel, R.; Ma, N.; Liu, J.; Guan, J.; Koch, L.; Klopsch, C.; Gruene, M.; Toelk, A.; Wang, W.; Mark, P.; et al. Patterning Human Stem Cells and Endothelial Cells with Laser Printing for Cardiac Regeneration. *Biomaterials* **2011**, *32*, 9218−9230.
(282) Gruene, M.; Pflaum, M.; Hess, C.; Diamantouros, S.; Schlie, S.; Deiwick, A.; Koch, L.; Wilhelmi, M.; Jockenhoevel, S.; Haverich, A.; et al. Laser Printing of Three-Dimensional Multicellular Arrays for Studies of Cell-Cell and Cell-Environment Interactions. *Tissue Eng., Part C* **2011**, *17*, 973−982.
(283) You, S.; Li, J.; Zhu, W.; Yu, C.; Mei, D.; Chen, S. Nanoscale 3d Printing of Hydrogels for Cellular Tissue Engineering. *J. Mater. Chem. B* **2018**, *6*, 2187−2197.
(284) Hribar, K. C.; Soman, P.; Warner, J.; Chung, P.; Chen, S. Light-Assisted Direct-Write of 3d Functional Biomaterials. *Lab Chip* **2014**, *14*, 268−275.
(285) Ifkovits, J. L.; Burdick, J. A. Review: Photopolymerizable and Degradable Biomaterials for Tissue Engineering Applications. *Tissue Eng.* **2007**, *13*, 2369−2385.
(286) Nguyen, K. T.; West, J. L. Photopolymerizable Hydrogels for Tissue Engineering Applications. *Biomaterials* **2002**, *23*, 4307−4314.
(287) Schiele, N. R.; Corr, D. T.; Huang, Y.; Raof, N. A.; Xie, Y.; Chrisey, D. B. Laser-Based Direct-Write Techniques for Cell Printing. *Biofabrication* **2010**, *2*, 032001.
(288) Barron, J. A.; Wu, P.; Ladouceur, H. D.; Ringeisen, B. R. Biological Laser Printing: A Novel Technique for Creating Heterogeneous 3-Dimensional Cell Patterns. *Biomed. Biomed. Microdevices* **2004**, *6*, 139−147.
(289) Wu, P. K.; Ringeisen, B. R.; Callahan, J.; Brooks, M.; Bubb, D. M.; Wu, H. D.; Piqué, A.; Spargo, B.; McGill, R. A.; Chrisey, D. B. The Deposition, Structure, Pattern Deposition, and Activity of Biomaterial Thin-Films by Matrix-Assisted Pulsed-Laser Evaporation (Maple) and Maple Direct Write. *Thin Solid Films* **2001**, *398*−*399*, 607−614.
(290) Duocastella, M.; Colina, M.; Fernández-Pradas, J. M.; Serra, P.; Morenza, J. L. Study of the Laser-Induced Forward Transfer of Liquids for Laser Bioprinting. *Appl. Surf. Sci.* **2007**, *253*, 7855−7859.
(291) Guillemot, F.; Souquet, A.; Catros, S.; Guillotin, B. Laser-Assisted Cell Printing: Principle, Physical Parameters Versus Cell Fate and Perspectives in Tissue Engineering. *Nanomedicine (London, U. K.)* **2010**, *5*, 507−515.
(292) Hopp, B.; Smausz, T.; Kresz, N.; Barna, N.; Bor, Z.; Kolozsvári, L.; Chrisey, D. B.; Szabó, A.; Nógrádi, A. Survival and Proliferative Ability of Various Living Cell Types after Laser-Induced Forward Transfer. *Tissue Eng.* **2005**, *11*, 1817−1823.
(293) Guillotin, B.; Souquet, A.; Catros, S.; Duocastella, M.; Pippenger, B.; Bellance, S.; Bareille, R.; Remy, M.; Bordenave, L.; Amedee, J.; et al. Laser Assisted Bioprinting of Engineered Tissue with High Cell Density and Microscale Organization. *Biomaterials* **2010**, *31*, 7250−7256.
(294) Wu, P. K.; Ringeisen, B. R. Development of Human Umbilical Vein Endothelial Cell (Huvec) and Human Umbilical Vein Smooth Muscle Cell (Huvsmc) Branch/Stem Structures on Hydrogel Layers Via Biological Laser Printing (Biolp). *Biofabrication* **2010**, *2*, 014111.
(295) Nishiguchi, A.; Mourran, A.; Zhang, H.; Möller, M. In-Gel Direct Laser Writing for 3d-Designed Hydrogel Composites That Undergo Complex Self-Shaping. *Adv. Sci.* **2018**, *5*, 1700038.
(296) Gittard, S. D.; Narayan, R. J. Laser Direct Writing of Micro- and Nano-Scale Medical Devices. *Expert Rev. Med. Devices* **2010**, *7*, 343−356.
(297) Kaihara, S.; Borenstein, J.; Koka, R.; Lalan, S.; Ochoa, E. R.; Ravens, M.; Pien, H.; Cunningham, B.; Vacanti, J. P. Silicon Micromachining to Tissue Engineer Branched Vascular Channels for Liver Fabrication. *Tissue Eng.* **2000**, *6*, 105−117.
(298) Lim, D.; Kamotani, Y.; Cho, B.; Mazumder, J.; Takayama, S. Fabrication of Microfluidic Mixers and Artificial Vasculatures Using a High-Brightness Diode-Pumped Nd:Yag Laser Direct Write Method. *Lab Chip* **2003**, *3*, 318−323.
(299) Kloxin, A. M.; Kasko, A. M.; Salinas, C. N.; Anseth, K. S. Photodegradable Hydrogels for Dynamic Tuning of Physical and Chemical Properties. *Science* **2009**, *324*, 59−63.
(300) Brandenberg, N.; Lutolf, M. P. In Situ Patterning of Microfluidic Networks in 3d Cell-Laden Hydrogels. *Adv. Mater.* **2016**, *28*, 7450−7456.
(301) Mondy, W. L.; Cameron, D.; Timmermans, J. P.; De Clerck, N.; Sasov, A.; Casteleyn, C.; Piegl, L. A. Micro-Ct of Corrosion Casts for Use in the Computer-Aided Design of Microvasculature. *Tissue Eng., Part C* **2009**, *15*, 729−738.
(302) Melchels, F. P.; Feijen, J.; Grijpma, D. W. A Review on Stereolithography and Its Applications in Biomedical Engineering. *Biomaterials* **2010**, *31*, 6121−6130.
(303) Mapili, G.; Lu, Y.; Chen, S.; Roy, K. Laser-Layered Microfabrication of Spatially Patterned Functionalized Tissue-Engineering Scaffolds. *J. Biomed. Mater. Res., Part B* **2005**, *75B*, 414−424.
(304) Williams, C. G.; Malik, A. N.; Kim, T. K.; Manson, P. N.; Elisseeff, J. H. Variable Cytocompatibility of Six Cell Lines with Photoinitiators Used for Polymerizing Hydrogels and Cell Encapsulation. *Biomaterials* **2005**, *26*, 1211−1218.

https://dx.doi.org/10.1021/acs.chemrev.0c00027
Chem. Rev. 2020, 120, 10887−10949

(305) Bryant, S. J.; Nuttelman, C. R.; Anseth, K. S. Cytocompatibility of Uv and Visible Light Photoinitiating Systems on Cultured Nih/3t3 Fibroblasts in Vitro. *J. Biomater. Sci., Polym. Ed.* **2000**, *11*, 439−457.
(306) Chartrain, N. A.; Williams, C. B.; Whittington, A. R. A Review on Fabricating Tissue Scaffolds Using Vat Photopolymerization. *Acta Biomater.* **2018**, *74*, 90−111.
(307) Knox, K.; Kerber, C. W.; Singel, S. A.; Bailey, M. J.; Imbesi, S. G. Stereolithographic Vascular Replicas from Ct Scans: Choosing Treatment Strategies, Teaching, and Research from Live Patient Scan Data. *AJNR Am. J. Neuroradiol.* **2005**, *26*, 1428−1431.
(308) Ovsianikov, A.; Deiwick, A.; Van Vlierberghe, S.; Dubruel, P.; M?ller, L.; Drager, G.; Chichkov, B. Laser Fabrication of Three-Dimensional Cad Scaffolds from Photosensitive Gelatin for Applications in Tissue Engineering. *Biomacromolecules* **2011**, *12*, 851−858.
(309) Ovsianikov, A.; Malinauskas, M.; Schlie, S.; Chichkov, B.; Gittard, S.; Narayan, R.; Löbler, M.; Sternberg, K.; Schmitz, K. P.; Haverich, A. Three-Dimensional Laser Micro- and Nano-Structuring of Acrylated Poly(Ethylene Glycol) Materials and Evaluation of Their Cytoxicity for Tissue Engineering Applications. *Acta Biomater.* **2011**, *7*, 967−974.
(310) Kufelt, O.; El-Tamer, A.; Sehring, C.; Schlie-Wolter, S.; Chichkov, B. N. Hyaluronic Acid Based Materials for Scaffolding Via Two-Photon Polymerization. *Biomacromolecules* **2014**, *15*, 650−659.
(311) Meyer, W.; Engelhardt, S.; Novosel, E.; Elling, B.; Wegener, M.; Kruger, H. Soft Polymers for Building up Small and Smallest Blood Supplying Systems by Stereolithography. *J. Funct. Biomater.* **2012**, *3*, 257−268.
(312) Shadish, J. A.; Benuska, G. M.; DeForest, C. A. Bioactive Site-Specifically Modified Proteins for 4d Patterning of Gel Biomaterials. *Nat. Mater.* **2019**, *18*, 1005−1014.
(313) Gawade, P. M.; Shadish, J. A.; Badeau, B. A.; DeForest, C. A. Logic-Based Delivery of Site-Specifically Modified Proteins from Environmentally Responsive Hydrogel Biomaterials. *Adv. Mater.* **2019**, *31*, 1902462.
(314) Shadish, J. A.; DeForest, C. A. Site-Selective Protein Modification: From Functionalized Proteins to Functional Biomaterials. *Matter* **2020**, *2*, 50−77.
(315) Lee, S. H.; Moon, J. J.; West, J. L. Three-Dimensional Micropatterning of Bioactive Hydrogels Via Two-Photon Laser Scanning Photolithography for Guided 3d Cell Migration. *Biomaterials* **2008**, *29*, 2962−2968.
(316) Arakawa, C. K.; Badeau, B. A.; Zheng, Y.; DeForest, C. A. Multicellular Vascularized Engineered Tissues through User-Programmable Biomaterial Photodegradation. *Adv. Mater.* **2017**, *29*, 1703156.
(317) Arakawa, C.; Gunnarsson, C.; Howard, C.; Bernabeu, M.; Phong, K.; Yang, E.; DeForest, C. A.; Smith, J. D.; Zheng, Y. Biophysical and Biomolecular Interactions of Malaria-Infected Erythrocytes in Engineered Human Capillaries. *Sci. Adv.* **2020**, *6*, No. eaay7243.
(318) Matheu, M. P.; Busby, E.; Borglin, J. *Human Organ and Tissue Engineering: Advances and Challenges in Addressing the Medical Crisis of the 21st Century*, 2018.
(319) Zhang, A. P.; Qu, X.; Soman, P.; Hribar, K. C.; Lee, J. W.; Chen, S.; He, S. Rapid Fabrication of Complex 3d Extracellular Microenvironments by Dynamic Optical Projection Stereolithography. *Adv. Mater.* **2012**, *24*, 4266−4270.
(320) Xue, D.; Wang, Y.; Zhang, J.; Mei, D.; Wang, Y.; Chen, S. Projection-Based 3d Printing of Cell Patterning Scaffolds with Multiscale Channels. *ACS Appl. Mater. Interfaces* **2018**, *10*, 19428−19435.
(321) Zhu, W.; Qu, X.; Zhu, J.; Ma, X.; Patel, S.; Liu, J.; Wang, P.; Lai, C. S.; Gou, M.; Xu, Y.; et al. Direct 3d Bioprinting of Prevascularized Tissue Constructs with Complex Microarchitecture. *Biomaterials* **2017**, *124*, 106−115.
(322) Yu, C.; Ma, X.; Zhu, W.; Wang, P.; Miller, K. L.; Stupin, J.; Koroleva-Maharajh, A.; Hairabedian, A.; Chen, S. Scanningless and Continuous 3d Bioprinting of Human Tissues with Decellularized Extracellular Matrix. *Biomaterials* **2019**, *194*, 1−13.
(323) Wang, P.; Berry, D.; Moran, A.; He, F.; Tam, T.; Chen, L.; Chen, S. Controlled Growth Factor Release in 3d-Printed Hydrogels. *Adv. Healthcare Mater.* **2020**, *9*, 1900977.
(324) Roos, W. P.; Kaina, B. DNA Damage-Induced Cell Death by Apoptosis. *Trends Mol. Med.* **2006**, *12*, 440−450.
(325) Wang, Z.; Abdulla, R.; Parker, B.; Samanipour, R.; Ghosh, S.; Kim, K. A Simple and High-Resolution Stereolithography-Based 3d Bioprinting System Using Visible Light Crosslinkable Bioinks. *Biofabrication* **2015**, *7*, 045009.
(326) Wang, Z.; Kumar, H.; Tian, Z.; Jin, X.; Holzman, J. F.; Menard, F.; Kim, K. Visible Light Photoinitiation of Cell-Adhesive Gelatin Methacryloyl Hydrogels for Stereolithography 3d Bioprinting. *ACS Appl. Mater. Interfaces* **2018**, *10*, 26859−26869.
(327) Grigoryan, B.; Paulsen, S. J.; Corbett, D. C.; Sazer, D. W.; Fortin, C. L.; Zaita, A. J.; Greenfield, P. T.; Calafat, N. J.; Gounley, J. P.; Ta, A. H.; et al. Multivascular Networks and Functional Intravascular Topologies within Biocompatible Hydrogels. *Science* **2019**, *364*, 458−464.
(328) Foty, R. A Simple Hanging Drop Cell Culture Protocol for Generation of 3d Spheroids. *J. Visualized Exp.* **2011**, 2720.
(329) Bernard, A. B.; Lin, C.-C.; Anseth, K. S. A Microwell Cell Culture Platform for the Aggregation of Pancreatic B-Cells. *Tissue Eng., Part C* **2012**, *18*, 583−592.
(330) Gentile, C.; Fleming, P. A.; Mironov, V.; Argraves, K. M.; Argraves, W. S.; Drake, C. J. Vegf-Mediated Fusion in the Generation of Uniluminal Vascular Spheroids. *Dev. Dyn.* **2008**, *237*, 2918−2925.
(331) Fleming, P. A.; Argraves, W. S.; Gentile, C.; Neagu, A.; Forgacs, G.; Drake, C. J. Fusion of Uniluminal Vascular Spheroids: A Model for Assembly of Blood Vessels. *Dev. Dyn.* **2010**, *239*, 398−406.
(332) Kelm, J. M.; Djonov, V.; Ittner, L. M.; Fluri, D.; Born, W.; Hoerstrup, S. P.; Fussenegger, M. Design of Custom-Shaped Vascularized Tissues Using Microtissue Spheroids as Minimal Building Units. *Tissue Eng.* **2006**, *12*, 2151−2160.
(333) Alajati, A.; Laib, A. M.; Weber, H.; Boos, A. M.; Bartol, A.; Ikenberg, K.; Korff, T.; Zentgraf, H.; Obodozie, C.; Graeser, R.; et al. Spheroid-Based Engineering of a Human Vasculature in Mice. *Nat. Methods* **2008**, *5*, 439−445.
(334) Pattanaik, S.; Arbra, C.; Bainbridge, H.; Dennis, S. G.; Fann, S. A.; Yost, M. J. Vascular Tissue Engineering Using Scaffold-Free Prevascular Endothelial-Fibroblast Constructs. *BioRes. Open Access* **2019**, *8*, 1−15.
(335) Jakab, K.; Neagu, A.; Mironov, V.; Markwald, R. R.; Forgacs, G. Engineering Biological Structures of Prescribed Shape Using Self-Assembling Multicellular Systems. *Proc. Natl. Acad. Sci. U. S. A.* **2004**, *101*, 2864−2869.
(336) Jakab, K.; Norotte, C.; Damon, B.; Marga, F.; Neagu, A.; Besch-Williford, C. L.; Kachurin, A.; Church, K. H.; Park, H.; Mironov, V.; et al. Tissue Engineering by Self-Assembly of Cells Printed into Topologically Defined Structures. *Tissue Eng., Part A* **2008**, *14*, 413−421.
(337) Tan, Y.; Richards, D. J.; Trusk, T. C.; Visconti, R. P.; Yost, M. J.; Kindy, M. S.; Drake, C. J.; Argraves, W. S.; Markwald, R. R.; Mei, Y. 3d Printing Facilitated Scaffold-Free Tissue Unit Fabrication. *Biofabrication* **2014**, *6*, 024111.
(338) Xu, C.; Chai, W.; Huang, Y.; Markwald, R. R. Scaffold-Free Inkjet Printing of Three-Dimensional Zigzag Cellular Tubes. *Biotechnol. Bioeng.* **2012**, *109*, 3152−3160.
(339) Yang, X.; Mironov, V.; Wang, Q. Modeling Fusion of Cellular Aggregates in Biofabrication Using Phase Field Theories. *J. Theor. Biol.* **2012**, *303*, 110−118.
(340) Shafiee, A.; McCune, M.; Forgacs, G.; Kosztin, I. Post-Deposition Bioink Self-Assembly: A Quantitative Study. *Biofabrication* **2015**, *7*, 045005.
(341) Yu, Y.; Zhang, Y.; Ozbolat, I. T. A Hybrid Bioprinting Approach for Scale-up Tissue Fabrication. *J. Manuf. Sci. Eng.* **2014**, *136*, 061013.

https://dx.doi.org/10.1021/acs.chemrev.0c00027
Chem. Rev. 2020, 120, 10887−10949

(342) Yu, Y.; Moncal, K. K.; Li, J.; Peng, W.; Rivero, I.; Martin, J. A.; Ozbolat, I. T. Three-Dimensional Bioprinting Using Self-Assembling Scalable Scaffold-Free "Tissue Strands" as a New Bioink. *Sci. Rep.* **2016**, *6*, 28714.
(343) De Moor, L.; Merovci, I.; Baetens, S.; Verstraeten, J.; Kowalska, P.; Krysko, D. V.; De Vos, W. H.; Declercq, H. High-Throughput Fabrication of Vascularized Spheroids for Bioprinting. *Biofabrication* **2018**, *10*, 035009.
(344) Mironov, V.; Visconti, R. P.; Kasyanov, V.; Forgacs, G.; Drake, C. J.; Markwald, R. R. Organ Printing: Tissue Spheroids as Building Blocks. *Biomaterials* **2009**, *30*, 2164−2174.
(345) Visconti, R. P.; Kasyanov, V.; Gentile, C.; Zhang, J.; Markwald, R. R.; Mironov, V. Towards Organ Printing: Engineering an Intra-Organ Branched Vascular Tree. *Expert Opin. Biol. Ther.* **2010**, *10*, 409−420.
(346) Drury, J. L.; Mooney, D. J. Hydrogels for Tissue Engineering: Scaffold Design Variables and Applications. *Biomaterials* **2003**, *24*, 4337−4351.
(347) Malda, J.; Visser, J.; Melchels, F. P.; Jungst, T.; Hennink, W. E.; Dhert, W. J.; Groll, J.; Hutmacher, D. W. 25th Anniversary Article: Engineering Hydrogels for Biofabrication. *Adv. Mater.* **2013**, *25*, 5011−5028.
(348) Lee, K. Y.; Mooney, D. J. Hydrogels for Tissue Engineering. *Chem. Rev.* **2001**, *101*, 1869−1879.
(349) Khademhosseini, A.; Langer, R. Microengineered Hydrogels for Tissue Engineering. *Biomaterials* **2007**, *28*, 5087−5092.
(350) Bao Ha, T. L.; Minh, T.; Nguyen, D.; Minh, D. In *Regenerative Medicine and Tissue Engineering*, 2013; DOI: 10.5772/55668.
(351) Singh, M. R.; Patel, S.; Singh, D. In *Nanobiomaterials in Soft Tissue Engineering*; Grumezescu, A. M., Ed.; William Andrew Publishing, 2016; DOI: 10.1016/B978-0-323-42865-1.00009-X.
(352) Liu, F.; Chen, Q.; Liu, C.; Ao, Q.; Tian, X.; Fan, J.; Tong, H.; Wang, X. Natural Polymers for Organ 3d Bioprinting. *Polymers* **2018**, *10*, 1278.
(353) Poschl, E.; Schlotzer-Schrehardt, U.; Brachvogel, B.; Saito, K.; Ninomiya, Y.; Mayer, U. Collagen Iv Is Essential for Basement Membrane Stability but Dispensable for Initiation of Its Assembly During Early Development. *Development* **2004**, *131*, 1619−1628.
(354) van der Rest, M.; Garrone, R. Collagen Family of Proteins. *FASEB J.* **1991**, *5*, 2814−2823.
(355) Prockop, D. J.; Kivirikko, K. I. Collagens: Molecular Biology, Diseases, and Potentials for Therapy. *Annu. Rev. Biochem.* **1995**, *64*, 403−434.
(356) Parenteau-Bareil, R.; Gauvin, R.; Berthod, F. Collagen-Based Biomaterials for Tissue Engineering Applications. *Materials* **2010**, *3*, 1863−1887.
(357) Twardowski, T.; Fertala, A.; Orgel, J. P.; San Antonio, J. D. Type I Collagen and Collagen Mimetics as Angiogenesis Promoting Superpolymers. *Curr. Pharm. Des.* **2007**, *13*, 3608−3621.
(358) Knight, C. G.; Morton, L. F.; Onley, D. J.; Peachey, A. R.; Messent, A. J.; Smethurst, P. A.; Tuckwell, D. S.; Farndale, R. W.; Barnes, M. J. Identification in Collagen Type I of an Integrin Alpha2 Beta1-Binding Site Containing an Essential Ger Sequence. *J. Biol. Chem.* **1998**, *273*, 33287−33294.
(359) Seandel, M.; Noack-Kunnmann, K.; Zhu, D.; Aimes, R. T.; Quigley, J. P. Growth Factor-Induced Angiogenesis in Vivo Requires Specific Cleavage of Fibrillar Type I Collagen. *Blood* **2001**, *97*, 2323−2332.
(360) Liu, Y.; Senger, D. R. Matrix-Specific Activation of Src and Rho Initiates Capillary Morphogenesis of Endothelial Cells. *FASEB J.* **2004**, *18*, 457−468.
(361) Mason, B. N.; Starchenko, A.; Williams, R. M.; Bonassar, L. J.; Reinhart-King, C. A. Tuning Three-Dimensional Collagen Matrix Stiffness Independently of Collagen Concentration Modulates Endothelial Cell Behavior. *Acta Biomater.* **2013**, *9*, 4635−4644.
(362) Lee, P. F.; Bai, Y.; Smith, R. L.; Bayless, K. J.; Yeh, A. T. Angiogenic Responses Are Enhanced in Mechanically and Microscopically Characterized, Microbial Transglutaminase Crosslinked Collagen Matrices with Increased Stiffness. *Acta Biomater.* **2013**, *9*, 7178−7190.
(363) Yamamura, N.; Sudo, R.; Ikeda, M.; Tanishita, K. Effects of the Mechanical Properties of Collagen Gel on the in Vitro Formation of Microvessel Networks by Endothelial Cells. *Tissue Eng.* **2007**, *13*, 1443−1453.
(364) Davis, G. E.; Senger, D. R. Endothelial Extracellular Matrix: Biosynthesis, Remodeling, and Functions During Vascular Morphogenesis and Neovessel Stabilization. *Circ. Res.* **2005**, *97*, 1093−1107.
(365) Diamantides, N.; Wang, L.; Pruiksma, T.; Siemiatkoski, J.; Dugopolski, C.; Shortkroff, S.; Kennedy, S.; Bonassar, L. J. Correlating Rheological Properties and Printability of Collagen Bioinks: The Effects of Riboflavin Photocrosslinking and Ph. *Biofabrication* **2017**, *9*, 034102.
(366) Lai, G.; Li, Y.; Li, G. Effect of Concentration and Temperature on the Rheological Behavior of Collagen Solution. *Int. J. Biol. Macromol.* **2008**, *42*, 285−291.
(367) Diamantides, N.; Dugopolski, C.; Blahut, E.; Kennedy, S.; Bonassar, L. J. High Density Cell Seeding Affects the Rheology and Printability of Collagen Bioinks. *Biofabrication* **2019**, *11*, 045016.
(368) Lee, J. W.; Choi, Y. J.; Yong, W. J.; Pati, F.; Shim, J. H.; Kang, K. S.; Kang, I. H.; Park, J.; Cho, D. W. Development of a 3d Cell Printed Construct Considering Angiogenesis for Liver Tissue Engineering. *Biofabrication* **2016**, *8*, 015007.
(369) Davidenko, N.; Schuster, C. F.; Bax, D. V.; Raynal, N.; Farndale, R. W.; Best, S. M.; Cameron, R. E. Control of Crosslinking for Tailoring Collagen-Based Scaffolds Stability and Mechanics. *Acta Biomater.* **2015**, *25*, 131−142.
(370) Perez-Puyana, V.; Romero, A.; Guerrero, A. Influence of Collagen Concentration and Glutaraldehyde on Collagen-Based Scaffold Properties. *J. Biomed. Mater. Res., Part A* **2016**, *104*, 1462−1468.
(371) Kim, Y. B.; Lee, H.; Kim, G. H. Strategy to Achieve Highly Porous/Biocompatible Macroscale Cell Blocks, Using a Collagen/Genipin-Bioink and an Optimal 3d Printing Process. *ACS Appl. Mater. Interfaces* **2016**, *8*, 32230−32240.
(372) Lee, J.; Yeo, M.; Kim, W.; Koo, Y.; Kim, G. H. Development of a Tannic Acid Cross-Linking Process for Obtaining 3d Porous Cell-Laden Collagen Structure. *Int. J. Biol. Macromol.* **2018**, *110*, 497−503.
(373) Natarajan, V.; Krithica, N.; Madhan, B.; Sehgal, P. K. Preparation and Properties of Tannic Acid Cross-Linked Collagen Scaffold and Its Application in Wound Healing. *J. Biomed. Mater. Res., Part B* **2013**, *101B*, 560−567.
(374) Kim, W.; Kim, G. Intestinal Villi Model with Blood Capillaries Fabricated Using Collagen-Based Bioink and Dual-Cell-Printing Process. *ACS Appl. Mater. Interfaces* **2018**, *10*, 41185−41196.
(375) Kang, D.; Ahn, G.; Kim, D.; Kang, H. W.; Yun, S.; Yun, W. S.; Shim, J. H.; Jin, S. Pre-Set Extrusion Bioprinting for Multiscale Heterogeneous Tissue Structure Fabrication. *Biofabrication* **2018**, *10*, 035008.
(376) Pataky, K.; Braschler, T.; Negro, A.; Renaud, P.; Lutolf, M. P.; Brugger, J. Microdrop Printing of Hydrogel Bioinks into 3d Tissue-Like Geometries. *Adv. Mater.* **2012**, *24*, 391−396.
(377) Gettler, B. C.; Zakhari, J. S.; Gandhi, P. S.; Williams, S. K. Formation of Adipose Stromal Vascular Fraction Cell-Laden Spheroids Using a Three-Dimensional Bioprinter and Superhydrophobic Surfaces. *Tissue Eng., Part C* **2017**, *23*, 516−524.
(378) Liu, Y.; Sun, S.; Singha, S.; Cho, M. R.; Gordon, R. J. 3d Femtosecond Laser Patterning of Collagen for Directed Cell Attachment. *Biomaterials* **2005**, *26*, 4597−4605.
(379) Hribar, K. C.; Meggs, K.; Liu, J.; Zhu, W.; Qu, X.; Chen, S. Three-Dimensional Direct Cell Patterning in Collagen Hydrogels with near-Infrared Femtosecond Laser. *Sci. Rep.* **2015**, *5*, 17203.
(380) Drzewiecki, K. E.; Malavade, J. N.; Ahmed, I.; Lowe, C. J.; Shreiber, D. I. A Thermoreversible, Photocrosslinkable Collagen Bio-Ink for Free-Form Fabrication of Scaffolds for Regenerative Medicine. *Technology (Singap World Sci)* **2017**, *5*, 185−195.
(381) Lotz, C.; Schmid, F. F.; Oechsle, E.; Monaghan, M. G.; Walles, H.; Groeber-Becker, F. Cross-Linked Collagen Hydrogel

Matrix Resisting Contraction to Facilitate Full-Thickness Skin Equivalents. *ACS Appl. Mater. Interfaces* **2017**, *9*, 20417−20425.
(382) An, B.; Kaplan, D. L.; Brodsky, B. Engineered Recombinant Bacterial Collagen as an Alternative Collagen-Based Biomaterial for Tissue Engineering. *Front. Chem.* **2014**, *2*, 40.
(383) Pratt, K. P.; Cote, H. C.; Chung, D. W.; Stenkamp, R. E.; Davie, E. W. The Primary Fibrin Polymerization Pocket: Three-Dimensional Structure of a 30-Kda C-Terminal Gamma Chain Fragment Complexed with the Peptide Gly-Pro-Arg-Pro. *Proc. Natl. Acad. Sci. U. S. A.* **1997**, *94*, 7176−7181.
(384) Yang, Z.; Mochalkin, I.; Doolittle, R. F. A Model of Fibrin Formation Based on Crystal Structures of Fibrinogen and Fibrin Fragments Complexed with Synthetic Peptides. *Proc. Natl. Acad. Sci. U. S. A.* **2000**, *97*, 14156−14161.
(385) Clark, R. A. Fibrin and Wound Healing. *Ann. N. Y. Acad. Sci.* **2001**, *936*, 355−367.
(386) Storm, C.; Pastore, J. J.; MacKintosh, F. C.; Lubensky, T. C.; Janmey, P. A. Nonlinear Elasticity in Biological Gels. *Nature* **2005**, *435*, 191−194.
(387) Weisel, J. W. Structure of Fibrin: Impact on Clot Stability. *J. Thromb. Haemostasis* **2007**, *5*, 116−124.
(388) Clark, R. A.; Tonnesen, M. G.; Gailit, J.; Cheresh, D. A. Transient Functional Expression of Alphavbeta 3 on Vascular Cells During Wound Repair. *Am. J. Pathol.* **1996**, *148*, 1407−1421.
(389) Brooks, P. C.; Clark, R. A.; Cheresh, D. A. Requirement of Vascular Integrin Alpha V Beta 3 for Angiogenesis. *Science* **1994**, *264*, 569−571.
(390) Davis, G. E.; Bayless, K. J. An Integrin and Rho Gtpase-Dependent Pinocytic Vacuole Mechanism Controls Capillary Lumen Formation in Collagen and Fibrin Matrices. *Microcirculation* **2003**, *10*, 27−44.
(391) Sahni, A.; Francis, C. W. Vascular Endothelial Growth Factor Binds to Fibrinogen and Fibrin and Stimulates Endothelial Cell Proliferation. *Blood* **2000**, *96*, 3772−3778.
(392) Sahni, A.; Sporn, L. A.; Francis, C. W. Potentiation of Endothelial Cell Proliferation by Fibrin(Ogen)-Bound Fibroblast Growth Factor-2. *J. Biol. Chem.* **1999**, *274*, 14936−14941.
(393) Chen, X.; Aledia, A. S.; Ghajar, C. M.; Griffith, C. K.; Putnam, A. J.; Hughes, C. C.; George, S. C. Prevascularization of a Fibrin-Based Tissue Construct Accelerates the Formation of Functional Anastomosis with Host Vasculature. *Tissue Eng., Part A* **2009**, *15*, 1363−1371.
(394) Park, C. H.; Woo, K. M. Fibrin-Based Biomaterial Applications in Tissue Engineering and Regenerative Medicine. *Adv. Exp. Med. Biol.* **2018**, *1064*, 253−261.
(395) Janmey, P. A.; Winer, J. P.; Weisel, J. W. Fibrin Gels and Their Clinical and Bioengineering Applications. *J. R. Soc., Interface* **2009**, *6*, 1−10.
(396) Cui, X.; Boland, T. Human Microvasculature Fabrication Using Thermal Inkjet Printing Technology. *Biomaterials* **2009**, *30*, 6221−6227.
(397) Xu, T.; Gregory, C. A.; Molnar, P.; Cui, X.; Jalota, S.; Bhaduri, S. B.; Boland, T. Viability and Electrophysiology of Neural Cell Structures Generated by the Inkjet Printing Method. *Biomaterials* **2006**, *27*, 3580−3588.
(398) Piard, C.; Baker, H.; Kamalitdinov, T.; Fisher, J. Bioprinted Osteon-Like Scaffolds Enhance in Vivo Neovascularization. *Biofabrication* **2019**, *11*, 025013.
(399) Wang, Z.; Lee, S. J.; Cheng, H. J.; Yoo, J. J.; Atala, A. 3d Bioprinted Functional and Contractile Cardiac Tissue Constructs. *Acta Biomater.* **2018**, *70*, 48−56.
(400) Meinhart, J.; Fussenegger, M.; Hobling, W. Stabilization of Fibrin-Chondrocyte Constructs for Cartilage Reconstruction. *Ann. Plast. Surg.* **1999**, *42*, 673−678.
(401) Carlson, M. A.; Calcaterra, J.; Johanning, J. M.; Pipinos, II; Cordes, C. M.; Velander, W. H. A Totally Recombinant Human Fibrin Sealant. *J. Surg. Res.* **2014**, *187*, 334−342.
(402) Van den Steen, P. E.; Dubois, B.; Nelissen, I.; Rudd, P. M.; Dwek, R. A.; Opdenakker, G. Biochemistry and Molecular Biology of Gelatinase B or Matrix Metalloproteinase-9 (Mmp-9). *Crit. Rev. Biochem. Mol. Biol.* **2002**, *37*, 375−536.
(403) Galis, Z. S.; Khatri, J. J. Matrix Metalloproteinases in Vascular Remodeling and Atherogenesis: The Good, the Bad, and the Ugly. *Circ. Res.* **2002**, *90*, 251−262.
(404) Devillard, C. D.; Mandon, C. A.; Lambert, S. A.; Blum, L. J.; Marquette, C. A. Bioinspired Multi-Activities 4d Printing Objects: A New Approach toward Complex Tissue Engineering. *Biotechnol. J.* **2018**, *13*, No. 1800098.
(405) Gao, D.; Kumar, G.; Co, C.; Ho, C. C. Formation of Capillary Tube-Like Structures on Micropatterned Biomaterials. *Adv. Exp. Med. Biol.* **2008**, *614*, 199−205.
(406) Sakai, S.; Hirose, K.; Taguchi, K.; Ogushi, Y.; Kawakami, K. An Injectable, in Situ Enzymatically Gellable, Gelatin Derivative for Drug Delivery and Tissue Engineering. *Biomaterials* **2009**, *30*, 3371−3377.
(407) Yang, G.; Xiao, Z.; Ren, X.; Long, H.; Qian, H.; Ma, K.; Guo, Y. Enzymatically Crosslinked Gelatin Hydrogel Promotes the Proliferation of Adipose Tissue-Derived Stromal Cells. *PeerJ* **2016**, *4*, No. e2497.
(408) Lee, V. K.; Kim, D. Y.; Ngo, H.; Lee, Y.; Seo, L.; Yoo, S.-S.; Vincent, P. A.; Dai, G. Creating Perfused Functional Vascular Channels Using 3d Bio-Printing Technology. *Biomaterials* **2014**, *35*, 8092−8102.
(409) Benton, J. A.; DeForest, C. A.; Vivekanandan, V.; Anseth, K. S. Photocrosslinking of Gelatin Macromers to Synthesize Porous Hydrogels That Promote Valvular Interstitial Cell Function. *Tissue Eng., Part A* **2009**, *15*, 3221−3230.
(410) Ramon-Azcon, J.; Ahadian, S.; Obregon, R.; Camci-Unal, G.; Ostrovidov, S.; Hosseini, V.; Kaji, H.; Ino, K.; Shiku, H.; Khademhosseini, A.; et al. Gelatin Methacrylate as a Promising Hydrogel for 3d Microscale Organization and Proliferation of Dielectrophoretically Patterned Cells. *Lab Chip* **2012**, *12*, 2959−2969.
(411) Yue, K.; Trujillo-de Santiago, G.; Alvarez, M. M.; Tamayol, A.; Annabi, N.; Khademhosseini, A. Synthesis, Properties, and Biomedical Applications of Gelatin Methacryloyl (Gelma) Hydrogels. *Biomaterials* **2015**, *73*, 254−271.
(412) Aubin, H.; Nichol, J. W.; Hutson, C. B.; Bae, H.; Sieminski, A. L.; Cropek, D. M.; Akhyari, P.; Khademhosseini, A. Directed 3d Cell Alignment and Elongation in Microengineered Hydrogels. *Biomaterials* **2010**, *31*, 6941−6951.
(413) Bae, H.; Ahari, A. F.; Shin, H.; Nichol, J. W.; Hutson, C. B.; Masaeli, M.; Kim, S. H.; Aubin, H.; Yamanlar, S.; Khademhosseini, A. Cell-Laden Microengineered Pullulan Methacrylate Hydrogels Promote Cell Proliferation and 3d Cluster Formation. *Soft Matter* **2011**, *7*, 1903−1911.
(414) Nichol, J. W.; Koshy, S. T.; Bae, H.; Hwang, C. M.; Yamanlar, S.; Khademhosseini, A. Cell-Laden Microengineered Gelatin Methacrylate Hydrogels. *Biomaterials* **2010**, *31*, 5536−5544.
(415) Zhang, Y. S.; Pi, Q.; van Genderen, A. M. Microfluidic Bioprinting for Engineering Vascularized Tissues and Organoids. *J. Visualized Exp.* **2017**, *126*, 55957.
(416) Shao, L.; Gao, Q.; Zhao, H.; Xie, C.; Fu, J.; Liu, Z.; Xiang, M.; He, Y. Fiber-Based Mini Tissue with Morphology-Controllable Gelma Microfibers. *Small* **2018**, *14*, 1802187.
(417) Jia, W.; Gungor-Ozkerim, P. S.; Zhang, Y. S.; Yue, K.; Zhu, K.; Liu, W.; Pi, Q.; Byambaa, B.; Dokmeci, M. R.; Shin, S. R.; Khademhosseini, A. Direct 3d Bioprinting of Perfusable Vascular Constructs Using a Blend Bioink. *Biomaterials* **2016**, *106*, 58−68.
(418) Byambaa, B.; Annabi, N.; Yue, K.; Trujillo-de Santiago, G.; Alvarez, M. M.; Jia, W.; Kazemzadeh-Narbat, M.; Shin, S. R.; Tamayol, A.; Khademhosseini, A. Bioprinted Osteogenic and Vasculogenic Patterns for Engineering 3d Bone Tissue. *Adv. Healthcare Mater.* **2017**, *6*, 1700015.
(419) D'Andrea, L. D.; Iaccarino, G.; Fattorusso, R.; Sorriento, D.; Carannante, C.; Capasso, D.; Trimarco, B.; Pedone, C. Targeting Angiogenesis: Structural Characterization and Biological Properties of

https://dx.doi.org/10.1021/acs.chemrev.0c00027
Chem. Rev. 2020, 120, 10887−10949

a De Novo Engineered Vegf Mimicking Peptide. *Proc. Natl. Acad. Sci. U. S. A.* **2005**, *102*, 14215−14220.
(420) Prakash Parthiban, S.; Rana, D.; Jabbari, E.; Benkirane-Jessel, N.; Ramalingam, M. Covalently Immobilized Vegf-Mimicking Peptide with Gelatin Methacrylate Enhances Microvascularization of Endothelial Cells. *Acta Biomater.* **2017**, *51*, 330−340.
(421) Quan, W.-Y.; Hu, Z.; Liu, H.-Z.; Ouyang, Q.-Q.; Zhang, D.-Y.; Li, S.-D.; Li, P.-W.; Yang, Z.-M. Mussel-Inspired Catechol-Functionalized Hydrogels and Their Medical Applications. *Molecules* **2019**, *24*, 2586.
(422) Jia, J.; Coyle, R. C.; Richards, D. J.; Berry, C. L.; Barrs, R. W.; Biggs, J.; James Chou, C.; Trusk, T. C.; Mei, Y. Development of Peptide-Functionalized Synthetic Hydrogel Microarrays for Stem Cell and Tissue Engineering Applications. *Acta Biomater.* **2016**, *45*, 110−120.
(423) Wenz, A.; Tjoeng, I.; Schneider, I.; Kluger, P. J.; Borchers, K. Improved Vasculogenesis and Bone Matrix Formation through Coculture of Endothelial Cells and Stem Cells in Tissue-Specific Methacryloyl Gelatin-Based Hydrogels. *Biotechnol. Bioeng.* **2018**, *115*, 2643−2653.
(424) Stratesteffen, H.; Kopf, M.; Kreimendahl, F.; Blaeser, A.; Jockenhoevel, S.; Fischer, H. Gelma-Collagen Blends Enable Drop-on-Demand 3d Printablility and Promote Angiogenesis. *Biofabrication* **2017**, *9*, 045002.
(425) Noshadi, I.; Hong, S.; Sullivan, K. E.; Shirzaei Sani, E.; Portillo-Lara, R.; Tamayol, A.; Shin, S. R.; Gao, A. E.; Stoppel, W. L.; Black, L. D., III; et al. In Vitro and in Vivo Analysis of Visible Light Crosslinkable Gelatin Methacryloyl (Gelma) Hydrogels. *Biomater. Sci.* **2017**, *5*, 2093−2105.
(426) AnilKumar, S.; Allen, S. C.; Tasnim, N.; Akter, T.; Park, S.; Kumar, A.; Chattopadhyay, M.; Ito, Y.; Suggs, L. J.; Joddar, B. The Applicability of Furfuryl-Gelatin as a Novel Bioink for Tissue Engineering Applications. *J. Biomed. Mater. Res., Part B* **2019**, *107*, 314−323.
(427) Gilpin, A.; Yang, Y. Decellularization Strategies for Regenerative Medicine: From Processing Techniques to Applications. *BioMed Res. Int.* **2017**, *2017*, 9831534.
(428) Crapo, P. M.; Gilbert, T. W.; Badylak, S. F. An Overview of Tissue and Whole Organ Decellularization Processes. *Biomaterials* **2011**, *32*, 3233−3243.
(429) Nakamura, N.; Kimura, T.; Kishida, A. Overview of the Development, Applications, and Future Perspectives of Decellularized Tissues and Organs. *ACS Biomater. Sci. Eng.* **2017**, *3*, 1236−1244.
(430) Ott, H. C.; Clippinger, B.; Conrad, C.; Schuetz, C.; Pomerantseva, I.; Ikonomou, L.; Kotton, D.; Vacanti, J. P. Regeneration and Orthotopic Transplantation of a Bioartificial Lung. *Nat. Med.* **2010**, *16*, 927−933.
(431) Petersen, T. H.; Calle, E. A.; Zhao, L.; Lee, E. J.; Gui, L.; Raredon, M. B.; Gavrilov, K.; Yi, T.; Zhuang, Z. W.; Breuer, C.; et al. Tissue-Engineered Lungs for in Vivo Implantation. *Science* **2010**, *329*, 538−541.
(432) Pati, F.; Jang, J.; Ha, D. H.; Won Kim, S.; Rhie, J. W.; Shim, J. H.; Kim, D. H.; Cho, D. W. Printing Three-Dimensional Tissue Analogues with Decellularized Extracellular Matrix Bioink. *Nat. Commun.* **2014**, *5*, 3935.
(433) Jang, J.; Kim, T. G.; Kim, B. S.; Kim, S. W.; Kwon, S. M.; Cho, D. W. Tailoring Mechanical Properties of Decellularized Extracellular Matrix Bioink by Vitamin B2-Induced Photo-Crosslinking. *Acta Biomater.* **2016**, *33*, 88−95.
(434) Skardal, A.; Devarasetty, M.; Kang, H. W.; Mead, I.; Bishop, C.; Shupe, T.; Lee, S. J.; Jackson, J.; Yoo, J.; Soker, S.; et al. A Hydrogel Bioink Toolkit for Mimicking Native Tissue Biochemical and Mechanical Properties in Bioprinted Tissue Constructs. *Acta Biomater.* **2015**, *25*, 24−34.
(435) Ali, M.; Pr, A. K.; Yoo, J. J.; Zahran, F.; Atala, A.; Lee, S. J. A Photo-Crosslinkable Kidney Ecm-Derived Bioink Accelerates Renal Tissue Formation. *Adv. Healthcare Mater.* **2019**, *8*, 1800992.
(436) Park, J. Y.; Ryu, H.; Lee, B.; Ha, D. H.; Ahn, M.; Kim, S.; Kim, J. Y.; Jeon, N. L.; Cho, D. W. Development of a Functional Airway-on-a-Chip by 3d Cell Printing. *Biofabrication* **2019**, *11*, 015002.
(437) Gao, G.; Lee, J. H.; Jang, J.; Lee, D. H.; Kong, J.-S.; Kim, B. S.; Choi, Y.-J.; Jang, W. B.; Hong, Y. J.; Kwon, S.-M.; Cho, D. W. Tissue Engineered Bio-Blood-Vessels Constructed Using a Tissue-Specific Bioink and 3d Coaxial Cell Printing Technique: A Novel Therapy for Ischemic Disease. *Adv. Funct. Mater.* **2017**, *27*, 1700798.
(438) Choi, Y.-J.; Jun, Y.-J.; Kim, D. Y.; Yi, H.-G.; Chae, S.-H.; Kang, J.; Lee, J.; Gao, G.; Kong, J.-S.; Jang, J.; et al. A 3d Cell Printed Muscle Construct with Tissue-Derived Bioink for the Treatment of Volumetric Muscle Loss. *Biomaterials* **2019**, *206*, 160−169.
(439) Gao, G.; Park, J. Y.; Kim, B. S.; Jang, J.; Cho, D. W. Coaxial Cell Printing of Freestanding, Perfusable, and Functional in Vitro Vascular Models for Recapitulation of Native Vascular Endothelium Pathophysiology. *Adv. Healthcare Mater.* **2018**, *7*, No. 1801102.
(440) Edri, R.; Gal, I.; Noor, N.; Harel, T.; Fleischer, S.; Adadi, N.; Green, O.; Shabat, D.; Heller, L.; Shapira, A.; et al. Personalized Hydrogels for Engineering Diverse Fully Autologous Tissue Implants. *Adv. Mater.* **2019**, *31*, No. 1803895.
(441) Normand, V.; Lootens, D. L.; Amici, E.; Plucknett, K. P.; Aymard, P. New Insight into Agarose Gel Mechanical Properties. *Biomacromolecules* **2000**, *1*, 730−738.
(442) Xiong, J. Y.; Narayanan, J.; Liu, X. Y.; Chong, T. K.; Chen, S. B.; Chung, T. S. Topology Evolution and Gelation Mechanism of Agarose Gel. *J. Phys. Chem. B* **2005**, *109*, 5638−5643.
(443) Dai, B.; Matsukawa, S. Elucidation of Gelation Mechanism and Molecular Interactions of Agarose in Solution by 1h Nmr. *Carbohydr. Res.* **2013**, *365*, 38−45.
(444) Zarrintaj, P.; Manouchehri, S.; Ahmadi, Z.; Saeb, M. R.; Urbanska, A. M.; Kaplan, D. L.; Mozafari, M. Agarose-Based Biomaterials for Tissue Engineering. *Carbohydr. Polym.* **2018**, *187*, 66−84.
(445) López-Marcial, G. R.; Zeng, A. Y.; Osuna, C.; Dennis, J.; García, J. M.; O'Connell, G. D. Agarose-Based Hydrogels as Suitable Bioprinting Materials for Tissue Engineering. *ACS Biomater. Sci. Eng.* **2018**, *4*, 3610−3616.
(446) Koch, L.; Kuhn, S.; Sorg, H.; Gruene, M.; Schlie, S.; Gaebel, R.; Polchow, B.; Reimers, K.; Stoelting, S.; Ma, N.; et al. Laser Printing of Skin Cells and Human Stem Cells. *Tissue Eng., Part C* **2010**, *16*, 847−854.
(447) Fedorovich, N. E.; De Wijn, J. R.; Verbout, A. J.; Alblas, J.; Dhert, W. J. Three-Dimensional Fiber Deposition of Cell-Laden, Viable, Patterned Constructs for Bone Tissue Printing. *Tissue Eng., Part A* **2008**, *14*, 127−133.
(448) Fan, R.; Piou, M.; Darling, E.; Cormier, D.; Sun, J.; Wan, J. Bio-Printing Cell-Laden Matrigel-Agarose Constructs. *J. Biomater. Appl.* **2016**, *31*, 684−692.
(449) Kopf, M.; Campos, D. F.; Blaeser, A.; Sen, K. S.; Fischer, H. A Tailored Three-Dimensionally Printable Agarose-Collagen Blend Allows Encapsulation, Spreading, and Attachment of Human Umbilical Artery Smooth Muscle Cells. *Biofabrication* **2016**, *8*, 025011.
(450) Kreimendahl, F.; Kopf, M.; Thiebes, A. L.; Duarte Campos, D. F.; Blaeser, A.; Schmitz-Rode, T.; Apel, C.; Jockenhoevel, S.; Fischer, H. Three-Dimensional Printing and Angiogenesis: Tailored Agarose-Type I Collagen Blends Comprise Three-Dimensional Printability and Angiogenesis Potential for Tissue-Engineered Substitutes. *Tissue Eng., Part C* **2017**, *23*, 604−615.
(451) Forget, A.; Christensen, J.; Ludeke, S.; Kohler, E.; Tobias, S.; Matloubi, M.; Thomann, R.; Shastri, V. P. Polysaccharide Hydrogels with Tunable Stiffness and Provasculogenic Properties Via Alpha-Helix to Beta-Sheet Switch in Secondary Structure. *Proc. Natl. Acad. Sci. U. S. A.* **2013**, *110*, 12887−12892.
(452) Forget, A.; Derme, T.; Mitterberger, D.; Heiny, M.; Sweeney, C.; Mudili, L.; Dargaville, T. R.; Shastri, V. P. Architecture-Inspired Paradigm for 3d Bioprinting of Vessel-Like Structures Using Extrudable Carboxylated Agarose Hydrogels. *Emergent Mater.* **2019**, *2*, 233−243.

https://dx.doi.org/10.1021/acs.chemrev.0c00027
Chem. Rev. 2020, 120, 10887−10949

(453) Forget, A.; Blaeser, A.; Miessmer, F.; Kopf, M.; Campos, D. F. D.; Voelcker, N. H.; Blencowe, A.; Fischer, H.; Shastri, V. P. Mechanically Tunable Bioink for 3d Bioprinting of Human Cells. *Adv. Healthcare Mater.* **2017**, *6*, 1700255.
(454) Luo, Y.; Shoichet, M. S. A Photolabile Hydrogel for Guided Three-Dimensional Cell Growth and Migration. *Nat. Mater.* **2004**, *3*, 249−253.
(455) Grant, G. T.; Morris, E. R.; Rees, D. A.; Smith, P. J. C.; Thom, D. Biological Interactions between Polysaccharides and Divalent Cations: The Egg-Box Model. *FEBS Lett.* **1973**, *32*, 195−198.
(456) Tonnesen, H. H.; Karlsen, J. Alginate in Drug Delivery Systems. *Drug Dev. Ind. Pharm.* **2002**, *28*, 621−630.
(457) Lee, K. Y.; Mooney, D. J. Alginate: Properties and Biomedical Applications. *Prog. Polym. Sci.* **2012**, *37*, 106−126.
(458) Axpe, E.; Oyen, M. L. Applications of Alginate-Based Bioinks in 3d Bioprinting. *Int. J. Mol. Sci.* **2016**, *17*, 1976.
(459) Rezende, R. A.; Bártolo, P. J.; Mendes, A.; Filho, R. M. Rheological Behavior of Alginate Solutions for Biomanufacturing. *J. Appl. Polym. Sci.* **2009**, *113*, 3866−3871.
(460) Ma, J.; Lin, Y.; Chen, X.; Zhao, B.; Zhang, J. Flow Behavior, Thixotropy and Dynamical Viscoelasticity of Sodium Alginate Aqueous Solutions. *Food Hydrocolloids* **2014**, *38*, 119−128.
(461) Bouhadir, K. H.; Lee, K. Y.; Alsberg, E.; Damm, K. L.; Anderson, K. W.; Mooney, D. J. Degradation of Partially Oxidized Alginate and Its Potential Application for Tissue Engineering. *Biotechnol. Prog.* **2001**, *17*, 945−950.
(462) Kong, H. J.; Kaigler, D.; Kim, K.; Mooney, D. J. Controlling Rigidity and Degradation of Alginate Hydrogels Via Molecular Weight Distribution. *Biomacromolecules* **2004**, *5*, 1720−1727.
(463) Jia, J.; Richards, D. J.; Pollard, S.; Tan, Y.; Rodriguez, J.; Visconti, R. P.; Trusk, T. C.; Yost, M. J.; Yao, H.; Markwald, R. R.; et al. Engineering Alginate as Bioink for Bioprinting. *Acta Biomater.* **2014**, *10*, 4323−4331.
(464) Khalil, S.; Sun, W. Bioprinting Endothelial Cells with Alginate for 3d Tissue Constructs. *J. Biomech. Eng.* **2009**, *131*, 111002.
(465) Chung, J. H. Y.; Naficy, S.; Yue, Z.; Kapsa, R.; Quigley, A.; Moulton, S. E.; Wallace, G. G. Bio-Ink Properties and Printability for Extrusion Printing Living Cells. *Biomater. Sci.* **2013**, *1*, 763−773.
(466) Gao, T.; Gillispie, G. J.; Copus, J. S.; Pr, A. K.; Seol, Y. J.; Atala, A.; Yoo, J. J.; Lee, S. J. Optimization of Gelatin-Alginate Composite Bioink Printability Using Rheological Parameters: A Systematic Approach. *Biofabrication* **2018**, *10*, 034106.
(467) Wang, Y.; Huang, X.; Shen, Y.; Hang, R.; Zhang, X.; Wang, Y.; Yao, X.; Tang, B. Direct Writing Alginate Bioink inside Pre-Polymers of Hydrogels to Create Patterned Vascular Networks. *J. Mater. Sci.* **2019**, *54*, 7883−7892.
(468) Peters, M. C.; Isenberg, B. C.; Rowley, J. A.; Mooney, D. J. Release from Alginate Enhances the Biological Activity of Vascular Endothelial Growth Factor. *J. Biomater. Sci., Polym. Ed.* **1998**, *9*, 1267−1278.
(469) Ahlfeld, T.; Cidonio, G.; Kilian, D.; Duin, S.; Akkineni, A. R.; Dawson, J. I.; Yang, S.; Lode, A.; Oreffo, R. O. C.; Gelinsky, M. Development of a Clay Based Bioink for 3d Cell Printing for Skeletal Application. *Biofabrication* **2017**, *9*, 034103.
(470) Faramarzi, N.; Yazdi, I. K.; Nabavinia, M.; Gemma, A.; Fanelli, A.; Caizzone, A.; Ptaszek, L. M.; Sinha, I.; Khademhosseini, A.; Ruskin, J. N.; et al. Patient-Specific Bioinks for 3d Bioprinting of Tissue Engineering Scaffolds. *Adv. Healthcare Mater.* **2018**, *7*, No. e1701347.
(471) Yu, J.; Gu, Y.; Du, K. T.; Mihardja, S.; Sievers, R. E.; Lee, R. J. The Effect of Injected Rgd Modified Alginate on Angiogenesis and Left Ventricular Function in a Chronic Rat Infarct Model. *Biomaterials* **2009**, *30*, 751−756.
(472) Bidarra, S. J.; Barrias, C. C.; Fonseca, K. B.; Barbosa, M. A.; Soares, R. A.; Granja, P. L. Injectable in Situ Crosslinkable Rgd-Modified Alginate Matrix for Endothelial Cells Delivery. *Biomaterials* **2011**, *32*, 7897−7904.
(473) Torres, A. L.; Bidarra, S. J.; Pinto, M. T.; Aguiar, P. C.; Silva, E. A.; Barrias, C. C. Guiding Morphogenesis in Cell-Instructive Microgels for Therapeutic Angiogenesis. *Biomaterials* **2018**, *154*, 34−47.
(474) Valentin, T. M.; Leggett, S. E.; Chen, P.-Y.; Sodhi, J. K.; Stephens, L. H.; McClintock, H. D.; Sim, J. Y.; Wong, I. Y. Stereolithographic Printing of Ionically-Crosslinked Alginate Hydrogels for Degradable Biomaterials and Microfluidics. *Lab Chip* **2017**, *17*, 3474−3488.
(475) Bellan, L. M.; Singh, S. P.; Henderson, P. W.; Porri, T. J.; Craighead, H. G.; Spector, J. A. Fabrication of an Artificial 3-Dimensional Vascular Network Using Sacrificial Sugar Structures. *Soft Matter* **2009**, *5*, 1354.
(476) Gelber, M. K.; Hurst, G.; Comi, T. J.; Bhargava, R. Model-Guided Design and Characterization of a High-Precision 3d Printing Process for Carbohydrate Glass. *Addit. Manuf.* **2018**, *22*, 38−50.
(477) Gelber, M. K.; Bhargava, R. Monolithic Multilayer Microfluidics Via Sacrificial Molding of 3d-Printed Isomalt. *Lab Chip* **2015**, *15*, 1736−1741.
(478) Mirabella, T.; MacArthur, J. W.; Cheng, D.; Ozaki, C. K.; Woo, Y. J.; Yang, M.; Chen, C. S. 3d-Printed Vascular Networks Direct Therapeutic Angiogenesis in Ischaemia. *Nat. Biomed Eng.* **2017**, *1*, 0083.
(479) Sooppan, R.; Paulsen, S. J.; Han, J.; Ta, A. H.; Dinh, P.; Gaffey, A. C.; Venkataraman, C.; Trubelja, A.; Hung, G.; Miller, J. S.; et al. In Vivo Anastomosis and Perfusion of a Three-Dimensionally-Printed Construct Containing Microchannel Networks. *Tissue Eng., Part C* **2016**, *22*, 1−7.
(480) Gauvin-Rossignol, G.; Legros, P.; Ruel, J.; Fortin, M. A.; Begin-Drolet, A. Sugar Glass Fugitive Ink Loaded with Calcium Chloride for the Rapid Casting of Alginate Scaffold Designs. *Heliyon* **2018**, *4*, No. e00680.
(481) Fraser, J. R.; Laurent, T. C.; Laurent, U. B. Hyaluronan: Its Nature, Distribution, Functions and Turnover. *J. Intern. Med.* **1997**, *242*, 27−33.
(482) Day, A. J.; Prestwich, G. D. Hyaluronan-Binding Proteins: Tying up the Giant. *J. Biol. Chem.* **2002**, *277*, 4585−4588.
(483) Toole, B. P. Hyaluronan: From Extracellular Glue to Pericellular Cue. *Nat. Rev. Cancer* **2004**, *4*, 528−539.
(484) Genasetti, A.; Vigetti, D.; Viola, M.; Karousou, E.; Moretto, P.; Rizzi, M.; Bartolini, B.; Clerici, M.; Pallotti, F.; De Luca, G.; et al. Hyaluronan and Human Endothelial Cell Behavior. *Connect. Tissue Res.* **2008**, *49*, 120−123.
(485) Toole, B. P. Hyaluronan and Its Binding Proteins, the Hyaladherins. *Curr. Opin. Cell Biol.* **1990**, *2*, 839−844.
(486) Khunmanee, S.; Jeong, Y.; Park, H. Crosslinking Method of Hyaluronic-Based Hydrogel for Biomedical Applications. *J. Tissue Eng.* **2017**, *8*, 2041731417726464.
(487) Schanté, C. E.; Zuber, G.; Herlin, C.; Vandamme, T. F. Chemical Modifications of Hyaluronic Acid for the Synthesis of Derivatives for a Broad Range of Biomedical Applications. *Carbohydr. Polym.* **2011**, *85*, 469−489.
(488) Burdick, J. A.; Chung, C.; Jia, X.; Randolph, M. A.; Langer, R. Controlled Degradation and Mechanical Behavior of Photopolymerized Hyaluronic Acid Networks. *Biomacromolecules* **2005**, *6*, 386−391.
(489) Gerecht, S.; Burdick, J. A.; Ferreira, L. S.; Townsend, S. A.; Langer, R.; Vunjak-Novakovic, G. Hyaluronic Acid Hydrogel for Controlled Self-Renewal and Differentiation of Human Embryonic Stem Cells. *Proc. Natl. Acad. Sci. U. S. A.* **2007**, *104*, 11298−11303.
(490) Khetan, S.; Katz, J. S.; Burdick, J. A. Sequential Crosslinking to Control Cellular Spreading in 3-Dimensional Hydrogels. *Soft Matter* **2009**, *5*, 1601−1606.
(491) Khetan, S.; Burdick, J. A. Patterning Network Structure to Spatially Control Cellular Remodeling and Stem Cell Fate within 3-Dimensional Hydrogels. *Biomaterials* **2010**, *31*, 8228−8234.
(492) Hanjaya-Putra, D.; Bose, V.; Shen, Y. I.; Yee, J.; Khetan, S.; Fox-Talbot, K.; Steenbergen, C.; Burdick, J. A.; Gerecht, S. Controlled Activation of Morphogenesis to Generate a Functional Human Microvasculature in a Synthetic Matrix. *Blood* **2011**, *118*, 804−815.
(493) Hanjaya-Putra, D.; Wong, K. T.; Hirotsu, K.; Khetan, S.; Burdick, J. A.; Gerecht, S. Spatial Control of Cell-Mediated

https://dx.doi.org/10.1021/acs.chemrev.0c00027
Chem. Rev. 2020, 120, 10887−10949

Degradation to Regulate Vasculogenesis and Angiogenesis in Hyaluronan Hydrogels. *Biomaterials* **2012**, *33*, 6123−6131.
(494) Kusuma, S.; Shen, Y. I.; Hanjaya-Putra, D.; Mali, P.; Cheng, L.; Gerecht, S. Self-Organized Vascular Networks from Human Pluripotent Stem Cells in a Synthetic Matrix. *Proc. Natl. Acad. Sci. U. S. A.* **2013**, *110*, 12601−12606.
(495) Yee, D.; Hanjaya-Putra, D.; Bose, V.; Luong, E.; Gerecht, S. Hyaluronic Acid Hydrogels Support Cord-Like Structures from Endothelial Colony-Forming Cells. *Tissue Eng., Part A* **2011**, *17*, 1351−1361.
(496) Park, K. M.; Gerecht, S. Harnessing Developmental Processes for Vascular Engineering and Regeneration. *Development* **2014**, *141*, 2760−2769.
(497) Kiyotake, E. A.; Douglas, A. W.; Thomas, E. E.; Nimmo, S. L.; Detamore, M. S. Development and Quantitative Characterization of the Precursor Rheology of Hyaluronic Acid Hydrogels for Bioprinting. *Acta Biomater.* **2019**, *95*, 176.
(498) Noh, I.; Kim, N.; Tran, H. N.; Lee, J.; Lee, C. 3d Printable Hyaluronic Acid-Based Hydrogel for Its Potential Application as a Bioink in Tissue Engineering. *Biomater. Res.* **2019**, *23*, 3.
(499) Mazzocchi, A.; Devarasetty, M.; Huntwork, R.; Soker, S.; Skardal, A. Optimization of Collagen Type I-Hyaluronan Hybrid Bioink for 3d Bioprinted Liver Microenvironments. *Biofabrication* **2019**, *11*, 015003.
(500) Skardal, A.; Zhang, J.; McCoard, L.; Xu, X.; Oottamasathien, S.; Prestwich, G. D. Photocrosslinkable Hyaluronan-Gelatin Hydrogels for Two-Step Bioprinting. *Tissue Eng., Part A* **2010**, *16*, 2675−2685.
(501) Skardal, A.; Zhang, J.; Prestwich, G. D. Bioprinting Vessel-Like Constructs Using Hyaluronan Hydrogels Crosslinked with Tetrahedral Polyethylene Glycol Tetracrylates. *Biomaterials* **2010**, *31*, 6173−6181.
(502) Loebel, C.; Rodell, C. B.; Chen, M. H.; Burdick, J. A. Shear-Thinning and Self-Healing Hydrogels as Injectable Therapeutics and for 3d-Printing. *Nat. Protoc.* **2017**, *12*, 1521−1541.
(503) Ma, X.; Qu, X.; Zhu, W.; Li, Y. S.; Yuan, S.; Zhang, H.; Liu, J.; Wang, P.; Lai, C. S.; Zanella, F.; et al. Deterministically Patterned Biomimetic Human Ipsc-Derived Hepatic Model Via Rapid 3d Bioprinting. *Proc. Natl. Acad. Sci. U. S. A.* **2016**, *113*, 2206−2211.
(504) Fu, L. L.; Pang, B. Y.; Zhu, Y.; Wang, L.; Leng, A. J.; Chen, H. L. Yi Guan Jian Decoction May Enhance Hepatic Differentiation of Bone Marrowderived Mesenchymal Stem Cells Via Sdf1 in Vitro. *Mol. Med. Rep.* **2017**, *16*, 2511−2521.
(505) Lutolf, M. P.; Raeber, G. P.; Zisch, A. H.; Tirelli, N.; Hubbell, J. A. Cell-Responsive Synthetic Hydrogels. *Adv. Mater.* **2003**, *15*, 888−892.
(506) Lutolf, M. P.; Hubbell, J. A. Synthetic Biomaterials as Instructive Extracellular Microenvironments for Morphogenesis in Tissue Engineering. *Nat. Biotechnol.* **2005**, *23*, 47−55.
(507) Yang, Q.; Lai, S. K. Anti-Peg Immunity: Emergence, Characteristics, and Unaddressed Questions. *WIREs Nanomed. Nanobiotechnol.* **2015**, *7*, 655−677.
(508) Leslie-Barbick, J. E.; Moon, J. J.; West, J. L. Covalently-Immobilized Vascular Endothelial Growth Factor Promotes Endothelial Cell Tubulogenesis in Poly(Ethylene Glycol) Diacrylate Hydrogels. *J. Biomater. Sci., Polym. Ed.* **2009**, *20*, 1763−1779.
(509) DeLong, S. A.; Moon, J. J.; West, J. L. Covalently Immobilized Gradients of Bfgf on Hydrogel Scaffolds for Directed Cell Migration. *Biomaterials* **2005**, *26*, 3227−3234.
(510) Saik, J. E.; Gould, D. J.; Keswani, A. H.; Dickinson, M. E.; West, J. L. Biomimetic Hydrogels with Immobilized Ephrina1 for Therapeutic Angiogenesis. *Biomacromolecules* **2011**, *12*, 2715−2722.
(511) West, J. L.; Hubbell, J. A. Polymeric Biomaterials with Degradation Sites for Proteases Involved in Cell Migration. *Macromolecules* **1999**, *32*, 241−244.
(512) Gobin, A. S.; West, J. L. Cell Migration through Defined, Synthetic Ecm Analogs. *FASEB J.* **2002**, *16*, 751−753.
(513) Moon, J. J.; Saik, J. E.; Poche, R. A.; Leslie-Barbick, J. E.; Lee, S. H.; Smith, A. A.; Dickinson, M. E.; West, J. L. Biomimetic Hydrogels with Pro-Angiogenic Properties. *Biomaterials* **2010**, *31*, 3840−3847.
(514) Leslie-Barbick, J. E.; Saik, J. E.; Gould, D. J.; Dickinson, M. E.; West, J. L. The Promotion of Microvasculature Formation in Poly(Ethylene Glycol) Diacrylate Hydrogels by an Immobilized Vegf-Mimetic Peptide. *Biomaterials* **2011**, *32*, 5782−5789.
(515) Qi, D.; Wu, S.; Kuss, M. A.; Shi, W.; Chung, S.; Deegan, P. T.; Kamenskiy, A.; He, Y.; Duan, B. Mechanically Robust Cryogels with Injectability and Bioprinting Supportability for Adipose Tissue Engineering. *Acta Biomater.* **2018**, *74*, 131−142.
(516) Maiullari, F.; Costantini, M.; Milan, M.; Pace, V.; Chirivi, M.; Maiullari, S.; Rainer, A.; Baci, D.; Marei, H. E.; Seliktar, D.; et al. A Multi-Cellular 3d Bioprinting Approach for Vascularized Heart Tissue Engineering Based on Huvecs and Ipsc-Derived Cardiomyocytes. *Sci. Rep.* **2018**, *8*, 13532.
(517) Bertassoni, L. E.; Cecconi, M.; Manoharan, V.; Nikkhah, M.; Hjortnaes, J.; Cristino, A. L.; Barabaschi, G.; Demarchi, D.; Dokmeci, M. R.; Yang, Y.; et al. Hydrogel Bioprinted Microchannel Networks for Vascularization of Tissue Engineering Constructs. *Lab Chip* **2014**, *14*, 2202−2211.
(518) Rutz, A. L.; Gargus, E. S.; Hyland, K. E.; Lewis, P. L.; Setty, A.; Burghardt, W. R.; Shah, R. N. Employing Peg Crosslinkers to Optimize Cell Viability in Gel Phase Bioinks and Tailor Post Printing Mechanical Properties. *Acta Biomater.* **2019**, *99*, 121.
(519) Culver, J. C.; Hoffmann, J. C.; Poché, R. A.; Slater, J. H.; West, J. L.; Dickinson, M. E. Three-Dimensional Biomimetic Patterning in Hydrogels to Guide Cellular Organization. *Adv. Mater.* **2012**, *24*, 2344−2348.
(520) Malmsten, M.; Lindman, B. Self-Assembly in Aqueous Block Copolymer Solutions. *Macromolecules* **1992**, *25*, 5440−5445.
(521) Fakhari, A.; Corcoran, M.; Schwarz, A. Thermogelling Properties of Purified Poloxamer 407. *Heliyon* **2017**, *3*, No. e00390.
(522) Batrakova, E. V.; Kabanov, A. V. Pluronic Block Copolymers: Evolution of Drug Delivery Concept from Inert Nanocarriers to Biological Response Modifiers. *J. Controlled Release* **2008**, *130*, 98−106.
(523) Nalbandian, R. M.; Henry, R. L.; Balko, K. W.; Adams, D. V.; Neuman, N. R. Pluronic F-127 Gel Preparation as an Artificial Skin in the Treatment of Third-Degree Burns in Pigs. *J. Biomed. Mater. Res.* **1987**, *21*, 1135−1148.
(524) Khattak, S. F.; Bhatia, S. R.; Roberts, S. C. Pluronic F127 as a Cell Encapsulation Material: Utilization of Membrane-Stabilizing Agents. *Tissue Eng.* **2005**, *11*, 974−983.
(525) Matthew, J. E.; Nazario, Y. L.; Roberts, S. C.; Bhatia, S. R. Effect of Mammalian Cell Culture Medium on the Gelation Properties of Pluronic F127. *Biomaterials* **2002**, *23*, 4615−4619.
(526) Kolesky, D. B.; Truby, R. L.; Gladman, A. S.; Busbee, T. A.; Homan, K. A.; Lewis, J. A. 3d Bioprinting of Vascularized, Heterogeneous Cell-Laden Tissue Constructs. *Adv. Mater.* **2014**, *26*, 3124−3130.
(527) Jacoby, A.; Morrison, K. A.; Hooper, R. C.; Asanbe, O.; Joyce, J.; Bleecker, R.; Weinreb, R. H.; Osoria, H. L.; Mukherjee, S.; Spector, J. A. Fabrication of Capillary-Like Structures with Pluronic F127(R) and Kerria Lacca Resin (Shellac) in Biocompatible Tissue-Engineered Constructs. *J. Tissue Eng. Regener. Med.* **2017**, *11*, 2388−2397.
(528) Esch, E. W.; Bahinski, A.; Huh, D. Organs-on-Chips at the Frontiers of Drug Discovery. *Nat. Rev. Drug Discovery* **2015**, *14*, 248−260.
(529) Lee, H.; Cho, D. W. One-Step Fabrication of an Organ-on-a-Chip with Spatial Heterogeneity Using a 3d Bioprinting Technology. *Lab Chip* **2016**, *16*, 2618−2625.
(530) Tissue-Engineered Disease Models. *Nat. Biomed. Eng.* **2018**, *2*, 879−880.
(531) Memic, A.; Navaei, A.; Mirani, B.; Cordova, J. A. V.; Aldhahri, M.; Dolatshahi-Pirouz, A.; Akbari, M.; Nikkhah, M. Bioprinting Technologies for Disease Modeling. *Biotechnol. Lett.* **2017**, *39*, 1279−1290.

https://dx.doi.org/10.1021/acs.chemrev.0c00027
Chem. Rev. 2020, 120, 10887−10949

(532) Bugrim, A.; Nikolskaya, T.; Nikolsky, Y. Early Prediction of Drug Metabolism and Toxicity: Systems Biology Approach and Modeling. *Drug Discovery Today* **2004**, *9*, 127−135.
(533) van Midwoud, P. M.; Merema, M. T.; Verpoorte, E.; Groothuis, G. M. Microfluidics Enables Small-Scale Tissue-Based Drug Metabolism Studies with Scarce Human Tissue. *J. Lab Autom* **2011**, *16*, 468−476.
(534) Massa, S.; Sakr, M. A.; Seo, J.; Bandaru, P.; Arneri, A.; Bersini, S.; Zare-Eelanjegh, E.; Jalilian, E.; Cha, B. H.; Antona, S.; et al. Bioprinted 3d Vascularized Tissue Model for Drug Toxicity Analysis. *Biomicrofluidics* **2017**, *11*, 044109.
(535) Bian, W.; Jackman, C. P.; Bursac, N. Controlling the Structural and Functional Anisotropy of Engineered Cardiac Tissues. *Biofabrication* **2014**, *6*, 024109.
(536) Zhang, Y. S.; Aleman, J.; Arneri, A.; Bersini, S.; Piraino, F.; Shin, S. R.; Dokmeci, M. R.; Khademhosseini, A. From Cardiac Tissue Engineering to Heart-on-a-Chip: Beating Challenges. *Biomed. Mater.* **2015**, *10*, 034006.
(537) Rouwkema, J.; Rivron, N. C.; van Blitterswijk, C. A. Vascularization in Tissue Engineering. *Trends Biotechnol.* **2008**, *26*, 434−441.
(538) Alonzo, M.; AnilKumar, S.; Roman, B.; Tasnim, N.; Joddar, B. 3d Bioprinting of Cardiac Tissue and Cardiac Stem Cell Therapy. *Transl. Res.* **2019**, *211*, 64−83.
(539) Zhang, Y. S.; Arneri, A.; Bersini, S.; Shin, S. R.; Zhu, K.; Goli-Malekabadi, Z.; Aleman, J.; Colosi, C.; Busignani, F.; Dell'Erba, V.; et al. Bioprinting 3d Microfibrous Scaffolds for Engineering Endothelialized Myocardium and Heart-on-a-Chip. *Biomaterials* **2016**, *110*, 45−59.
(540) Piccini, J. P.; Whellan, D. J.; Berridge, B. R.; Finkle, J. K.; Pettit, S. D.; Stockbridge, N.; Valentin, J. P.; Vargas, H. M.; Krucoff, M. W. Current Challenges in the Evaluation of Cardiac Safety During Drug Development: Translational Medicine Meets the Critical Path Initiative. *Am. Heart J.* **2009**, *158*, 317−326.
(541) Zhao, L.; Zhang, B. Doxorubicin Induces Cardiotoxicity through Upregulation of Death Receptors Mediated Apoptosis in Cardiomyocytes. *Sci. Rep.* **2017**, *7*, 44735.
(542) Alvarado, A.; Arce, I. Metabolic Functions of the Lung, Disorders and Associated Pathologies. *J. Clin. Med. Res.* **2016**, *8*, 689−700.
(543) Orfanos, S. E.; Mavrommati, I.; Korovesi, I.; Roussos, C. Pulmonary Endothelium in Acute Lung Injury: From Basic Science to the Critically Ill. *Intensive Care Med.* **2004**, *30*, 1702−1714.
(544) Miller, A. J.; Spence, J. R. In Vitro Models to Study Human Lung Development, Disease and Homeostasis. *Physiology* **2017**, *32*, 246−260.
(545) Horvath, L.; Umehara, Y.; Jud, C.; Blank, F.; Petri-Fink, A.; Rothen-Rutishauser, B. Engineering an in Vitro Air-Blood Barrier by 3d Bioprinting. *Sci. Rep.* **2015**, *5*, 7974.
(546) Lin, N. Y. C.; Homan, K. A.; Robinson, S. S.; Kolesky, D. B.; Duarte, N.; Moisan, A.; Lewis, J. A. Renal Reabsorption in 3d Vascularized Proximal Tubule Models. *Proc. Natl. Acad. Sci. U. S. A.* **2019**, *116*, 5399−5404.
(547) Kuo, C. Y.; Shevchuk, M.; Opfermann, J.; Guo, T.; Santoro, M.; Fisher, J. P.; Kim, P. C. Trophoblast-Endothelium Signaling Involves Angiogenesis and Apoptosis in a Dynamic Bioprinted Placenta Model. *Biotechnol. Bioeng.* **2019**, *116*, 181−192.
(548) Meng, F.; Meyer, C. M.; Joung, D.; Vallera, D. A.; McAlpine, M. C.; Panoskaltsis-Mortari, A. 3d Bioprinted in Vitro Metastatic Models Via Reconstruction of Tumor Microenvironments. *Adv. Mater.* **2019**, *31*, No. 1806899.
(549) Lauschke, V. M.; Hendriks, D. F.; Bell, C. C.; Andersson, T. B.; Ingelman-Sundberg, M. Novel 3d Culture Systems for Studies of Human Liver Function and Assessments of the Hepatotoxicity of Drugs and Drug Candidates. *Chem. Res. Toxicol.* **2016**, *29*, 1936−1955.
(550) Matsusaki, M.; Sakaue, K.; Kadowaki, K.; Akashi, M. Three-Dimensional Human Tissue Chips Fabricated by Rapid and Automatic Inkjet Cell Printing. *Adv. Healthcare Mater.* **2013**, *2*, 534−539.
(551) Homan, K. A.; Gupta, N.; Kroll, K. T.; Kolesky, D. B.; Skylar-Scott, M.; Miyoshi, T.; Mau, D.; Valerius, M. T.; Ferrante, T.; Bonventre, J. V.; et al. Flow-Enhanced Vascularization and Maturation of Kidney Organoids in Vitro. *Nat. Methods* **2019**, *16*, 255−262.
(552) Hasegawa, S.; Tanaka, T.; Nangaku, M. Recent Advances in Renal Regeneration. *F1000Research* **2019**, *8*, 216.
(553) Nicholson, J. K.; Holmes, E.; Wilson, I. D. Gut Microorganisms, Mammalian Metabolism and Personalized Health Care. *Nat. Rev. Microbiol.* **2005**, *3*, 431−438.
(554) Du, P.; O'Grady, G.; Davidson, J. B.; Cheng, L. K.; Pullan, A. J. Multiscale Modeling of Gastrointestinal Electrophysiology and Experimental Validation. *Crit. Rev. Biomed. Eng.* **2010**, *38*, 225−254.
(555) Kim, S. H.; Chi, M.; Yi, B.; Kim, S. H.; Oh, S.; Kim, Y.; Park, S.; Sung, J. H. Three-Dimensional Intestinal Villi Epithelium Enhances Protection of Human Intestinal Cells from Bacterial Infection by Inducing Mucin Expression. *Integr. Biol. (Camb.)* **2014**, *6*, 1122−1131.
(556) Pappenheimer, J. R.; Michel, C. C. Role of Villus Microcirculation in Intestinal Absorption of Glucose: Coupling of Epithelial with Endothelial Transport. *J. Physiol.* **2003**, *553*, 561−574.
(557) Fraser, H. M.; Lunn, S. F. Angiogenesis and Its Control in the Female Reproductive System. *Br. Med. Bull.* **2000**, *56*, 787−797.
(558) Demir, R.; Yaba, A.; Huppertz, B. Vasculogenesis and Angiogenesis in the Endometrium During Menstrual Cycle and Implantation. *Acta Histochem.* **2010**, *112*, 203−214.
(559) Plitman Mayo, R. Advances in Human Placental Biomechanics. *Comput. Struct. Biotechnol. J.* **2018**, *16*, 298−306.
(560) Mehta, D.; Malik, A. B. Signaling Mechanisms Regulating Endothelial Permeability. *Physiol. Rev.* **2006**, *86*, 279−367.
(561) Sasmal, P.; Datta, P.; Wu, Y.; Ozbolat, I. T. 3d Bioprinting for Modelling Vasculature. *Microphysiol. Syst.* **2018**, *2*, 1.
(562) Qiu, Y.; Ahn, B.; Sakurai, Y.; Hansen, C. E.; Tran, R.; Mimche, P. N.; Mannino, R. G.; Ciciliano, J. C.; Lamb, T. J.; Joiner, C. H.; et al. Microvasculature-on-a-Chip for the Long-Term Study of Endothelial Barrier Dysfunction and Microvascular Obstruction in Disease. *Nat. Biomed. Eng.* **2018**, *2*, 453−463.
(563) Yang, L.; Shridhar, S. V.; Gerwitz, M.; Soman, P. An in Vitro Vascular Chip Using 3d Printing-Enabled Hydrogel Casting. *Biofabrication* **2016**, *8*, 035015.
(564) Sun, Y.; Yang, X.; Wang, Q. In-Silico Analysis on Biofabricating Vascular Networks Using Kinetic Monte Carlo Simulations. *Biofabrication* **2014**, *6*, 015008.
(565) Zhang, Y. S.; Duchamp, M.; Oklu, R.; Ellisen, L. W.; Langer, R.; Khademhosseini, A. Bioprinting the Cancer Microenvironment. *ACS Biomater. Sci. Eng.* **2016**, *2*, 1710−1721.
(566) Cao, Y. Tumor Angiogenesis and Therapy. *Biomed. Pharmacother.* **2005**, *59*, S340−5343.
(567) Wang, X.; Li, X.; Dai, X.; Zhang, X.; Zhang, J.; Xu, T.; Lan, Q. Bioprinting of Glioma Stem Cells Improves Their Endotheliogenic Potential. *Colloids Surf., B* **2018**, *171*, 629−637.
(568) Jain, R. K.; Au, P.; Tam, J.; Duda, D. G.; Fukumura, D. Engineering Vascularized Tissue. *Nat. Biotechnol.* **2005**, *23*, 821−823.
(569) Chang, W. G.; Niklason, L. E. A Short Discourse on Vascular Tissue Engineering. *NPJ. Regen Med.* **2017**, *2*, 7.
(570) Bersini, S.; Yazdi, I. K.; Talo, G.; Shin, S. R.; Moretti, M.; Khademhosseini, A. Cell-Microenvironment Interactions and Architectures in Microvascular Systems. *Biotechnol. Adv.* **2016**, *34*, 1113−1130.
(571) Paulsen, S. J.; Miller, J. S. Tissue Vascularization through 3d Printing: Will Technology Bring Us Flow? *Dev. Dyn.* **2015**, *244*, 629−640.
(572) Clarke, B. Normal Bone Anatomy and Physiology. *Clin. J. Am. Soc. Nephrol.* **2008**, *3*, S131.
(573) Nguyen, L. H.; Annabi, N.; Nikkhah, M.; Bae, H.; Binan, L.; Park, S.; Kang, Y.; Yang, Y.; Khademhosseini, A. Vascularized Bone Tissue Engineering: Approaches for Potential Improvement. *Tissue Eng., Part B* **2012**, *18*, 363−382.

https://dx.doi.org/10.1021/acs.chemrev.0c00027
Chem. Rev. 2020, 120, 10887−10949

(574) Filipowska, J.; Tomaszewski, K. A.; Niedzwiedzki, L.; Walocha, J. A.; Niedzwiedzki, T. The Role of Vasculature in Bone Development, Regeneration and Proper Systemic Functioning. *Angiogenesis* **2017**, *20*, 291−302.
(575) Midha, S.; Dalela, M.; Sybil, D.; Patra, P.; Mohanty, S. Advances in Three-Dimensional Bioprinting of Bone: Progress and Challenges. *J. Tissue Eng. Regener. Med.* **2019**, *13*, 925−945.
(576) Anada, T.; Pan, C. C.; Stahl, A. M.; Mori, S.; Fukuda, J.; Suzuki, O.; Yang, Y. Vascularized Bone-Mimetic Hydrogel Constructs by 3d Bioprinting to Promote Osteogenesis and Angiogenesis. *Int. J. Mol. Sci.* **2019**, *20*, 1096.
(577) Liu, X.; Jakus, A. E.; Kural, M.; Qian, H.; Engler, A.; Ghaedi, M.; Shah, R.; Steinbacher, D. M.; Niklason, L. E. Vascularization of Natural and Synthetic Bone Scaffolds. *Cell Transplant* **2018**, *27*, 1269−1280.
(578) Ahlfeld, T.; Schuster, F. P.; Forster, Y.; Quade, M.; Akkineni, A. R.; Rentsch, C.; Rammelt, S.; Gelinsky, M.; Lode, A. 3d Plotted Biphasic Bone Scaffolds for Growth Factor Delivery: Biological Characterization in Vitro and in Vivo. *Adv. Healthcare Mater.* **2019**, *8*, No. 1801512.
(579) Cui, H.; Zhu, W.; Nowicki, M.; Zhou, X.; Khademhosseini, A.; Zhang, L. G. Hierarchical Fabrication of Engineered Vascularized Bone Biphasic Constructs Via Dual 3d Bioprinting: Integrating Regional Bioactive Factors into Architectural Design. *Adv. Healthcare Mater.* **2016**, *5*, 2174−2181.
(580) Duarte Campos, D. F.; Zhang, S.; Kreimendahl, F.; Kopf, M.; Fischer, H.; Vogt, M.; Blaeser, A.; Apel, C.; Esteves-Oliveira, M. Hand-Held Bioprinting for De Novo Vascular Formation Applicable to Dental Pulp Regeneration. *Connect. Connect. Tissue Res.* **2020**, *61*, 205−215.
(581) Ma, Y.; Xie, L.; Yang, B.; Tian, W. Three-Dimensional Printing Biotechnology for the Regeneration of the Tooth and Tooth-Supporting Tissues. *Biotechnol. Bioeng.* **2019**, *116*, 452−468.
(582) Huang, C. C.; Narayanan, R.; Warshawsky, N.; Ravindran, S. Dual Ecm Biomimetic Scaffolds for Dental Pulp Regenerative Applications. *Front. Physiol.* **2018**, *9*, 495.
(583) Benjamin, E. J.; Muntner, P.; Alonso, A.; Bittencourt, M. S.; Callaway, C. W.; Carson, A. P.; Chamberlain, A. M.; Chang, A. R.; Cheng, S.; Das, S. R.; et al. Heart Disease and Stroke Statistics-2019 Update: A Report from the American Heart Association. *Circulation* **2019**, *139*, e56−e528.
(584) Carrier, R. L.; Papadaki, M.; Rupnick, M.; Schoen, F. J.; Bursac, N.; Langer, R.; Freed, L. E.; Vunjak-Novakovic, G. Cardiac Tissue Engineering: Cell Seeding, Cultivation Parameters, and Tissue Construct Characterization. *Biotechnol. Bioeng.* **1999**, *64*, 580−589.
(585) Izadifar, M.; Chapman, D.; Babyn, P.; Chen, X.; Kelly, M. E. Uv-Assisted 3d Bioprinting of Nanoreinforced Hybrid Cardiac Patch for Myocardial Tissue Engineering. *Tissue Eng., Part C* **2018**, *24*, 74−88.
(586) Huang, N. F.; Serpooshan, V.; Morris, V. B.; Sayed, N.; Pardon, G.; Abilez, O. J.; Nakayama, K. H.; Pruitt, B. L.; Wu, S. M.; Yoon, Y. S.; et al. Big Bottlenecks in Cardiovascular Tissue Engineering. *Commun. Biol.* **2018**, *1*, 199.
(587) Fang, Y.; Zhang, T.; Zhang, L.; Gong, W.; Sun, W. Biomimetic Design and Fabrication of Scaffolds Integrating Oriented Micro-Pores with Branched Channel Networks for Myocardial Tissue Engineering. *Biofabrication* **2019**, *11*, 035004.
(588) Juhas, M.; Bursac, N. Engineering Skeletal Muscle Repair. *Curr. Opin. Biotechnol.* **2013**, *24*, 880−886.
(589) Augustine, R. Skin Bioprinting: A Novel Approach for Creating Artificial Skin from Synthetic and Natural Building Blocks. *Prog. Biomater* **2018**, *7*, 77−92.
(590) Tarassoli, S. P.; Jessop, Z. M.; Al-Sabah, A.; Gao, N.; Whitaker, S.; Doak, S.; Whitaker, I. S. Skin Tissue Engineering Using 3d Bioprinting: An Evolving Research Field. *J. Plast. Reconstr. Aesthet. Surg.* **2018**, *71*, 615−623.
(591) Frueh, F. S.; Menger, M. D.; Lindenblatt, N.; Giovanoli, P.; Laschke, M. W. Current and Emerging Vascularization Strategies in Skin Tissue Engineering. *Crit. Rev. Biotechnol.* **2017**, *37*, 613−625.
(592) Peak, C. W.; Singh, K. A.; Adlouni, M.; Chen, J.; Gaharwar, A. K. Printing Therapeutic Proteins in 3d Using Nanoengineered Bioink to Control and Direct Cell Migration. *Adv. Healthcare Mater.* **2019**, *8*, No. 1801553.
(593) Samfors, S.; Karlsson, K.; Sundberg, J.; Markstedt, K.; Gatenholm, P. Biofabrication of Bacterial Nanocellulose Scaffolds with Complex Vascular Structure. *Biofabrication* **2019**, *11*, 045010.
(594) Moghassemi, S.; Hadjizadeh, A.; Hakamivala, A.; Omidfar, K. Growth Factor-Loaded Nano-Niosomal Gel Formulation and Characterization. *AAPS PharmSciTech* **2017**, *18*, 34−41.
(595) Brudno, Y.; Ennett-Shepard, A. B.; Chen, R. R.; Aizenberg, M.; Mooney, D. J. Enhancing Microvascular Formation and Vessel Maturation through Temporal Control over Multiple Pro-Angiogenic and Pro-Maturation Factors. *Biomaterials* **2013**, *34*, 9201−9209.
(596) Wang, Z.; Wang, Z.; Lu, W. W.; Zhen, W.; Yang, D.; Peng, S. Novel Biomaterial Strategies for Controlled Growth Factor Delivery for Biomedical Applications. *NPG Asia Mater.* **2017**, *9*, No. e435.
(597) Langenkamp, E.; Molema, G. Microvascular Endothelial Cell Heterogeneity: General Concepts and Pharmacological Consequences for Anti-Angiogenic Therapy of Cancer. *Cell Tissue Res.* **2009**, *335*, 205−222.
(598) Ben-Shaul, S.; Landau, S.; Merdler, U.; Levenberg, S. Mature Vessel Networks in Engineered Tissue Promote Graft−Host Anastomosis and Prevent Graft Thrombosis. *Proc. Natl. Acad. Sci. U. S. A.* **2019**, *116*, 2955−2960.
(599) Kelly, B. E.; Bhattacharya, I.; Heidari, H.; Shusteff, M.; Spadaccini, C. M.; Taylor, H. K. Volumetric Additive Manufacturing Via Tomographic Reconstruction. *Science* **2019**, *363*, 1075.
(600) Loterie, D.; Delrot, P.; Moser, C. High-Resolution Tomographic Volumetric Additive Manufacturing. *Nat. Commun.* **2020**, *11*, 852.
(601) Bernal, P. N.; Delrot, P.; Loterie, D.; Li, Y.; Malda, J.; Moser, C.; Levato, R. Volumetric Bioprinting of Complex Living-Tissue Constructs within Seconds. *Adv. Mater.* **2019**, *31*, No. 1904209.
(602) Zhang, B.; Radisic, M. Organ-Level Vascularization: The Mars Mission of Bioengineering. *J. Thorac. Cardiovasc. Surg.* **2020**, *159*, P2003.

https://dx.doi.org/10.1021/acs.chemrev.0c00027
Chem. Rev. 2020, 120, 10887−10949